Potential for Recycled Concrete Aggregate Stabilisation with Bitumen Emulsion and Foamed Bitumen.

by

Nokuthula Mandy Antonia Mazibuko

Thesis presented in fulfilment of the requirements for the degree of Master of Engineering in the Faculty of Civil Engineering at Stellenbosch University

Supervisor:

Dr Chantal E. Rudman

Co-supervisor:

Professor Kim J. Jenkins

SANRAL Chair in Pavement Engineering

March 2020

Declaration

By submitting this thesis electronically, I declare that the entirety of the work contained therein is my own, original work, that I am the sole author thereof (save to the extent explicitly otherwise stated), that reproduction and publication thereof by Stellenbosch University will not infringe any third party rights and that I have not previously in its entirety or in part submitted it for obtaining any qualification.

March 2020

Abstract

Bitumen stabilisation is a technology used to improve the strength properties of any aggregate, which is also environmentally friendly. The method of stabilisation requires less energy in comparison to hot asphalt mixes and it causes less pollution when compared to cement stabilisation. The sustainability benefit of BSMs can be improved when recycled materials from construction demolition waste such as recycled concrete is used.

The existing TG2 outlines the process to determine whether an aggregate is suitable to be stabilised with foamed bitumen or bitumen emulsion. This research aims to use the same process to determine whether RCA is a suitable aggregate for stabilisation with bitumen emulsion or foamed bitumen. In addition, the BSM classification of the resultant BSM with RCA is determined along with the performance properties of the mix design.

The indirect tensile strength (ITS) was used to determine the suitable active filler for RCA stabilised with bitumen emulsion and foamed bitumen. Active fillers considered included 1% lime and 1% cement. Furthermore, the optimum bitumen content for the aggregate was determined and found to be 2.2% for both bitumen emulsion and foamed bitumen. The shear strength parameters and resilient moduli of the optimum mix designs made from foamed bitumen and bitumen emulsion were tested with the monotonic and dynamic triaxial test.

The preliminary results indicate that RCA is a suitable aggregate for stabilisation with low viscosity bitumen. Moreover, the ITS results suggest that no active filler is required and a potential BSM 1 layer can be produced with 2.2% bitumen content. This indicates the potential of using this material considering economical relevance. Furthermore, the shear parameters obtained for both binders (bitumen emulsion and foamed bitumen) also indicates that the mix designs can be classified as a BSM 1. Additionally, a high resistance to moisture damage was achieved as shown by the retained cohesion ranging from 88.2 to 90%. Moreover, the resilient modulus analysis indicates a stress dependent behaviour, which can be modelled by existing models used for unbound granular materials. However, care should be taken when stabilisation is done with bitumen emulsion due to the high absorptivity of the mortar, which causes early breaking of the emulsion. Pre-soaking of the aggregate was required to manage this challenge.

The pavement life analysis shows that, if the layer is used in the base layer with a G5 subbase a pavement life suitable for a Category B road is obtained. Therefore, the addition of bitumen improves the behaviour and performance of RCA and the results indicate that it

can be successfully used in a base layer. Therefore, there is potential for the stabilisation of RCA with either foamed bitumen or bitumen emulsion.

Opsomming

Stabilisasie van bitumen is 'n manier om die sterkte-eienskappe van enige aggregaat, wat ook omgewingsvriendelik is, te verbeter. Die metode van stabilisering benodig minder energie in vergelyking met warm asfaltmengsels en dit veroorsaak minder besoedeling in vergelyking met sementstabilisering. Die volhoubaarheidsvoordeel van bitumen gestabiliseerde material (BSMs) kan verder verbeter word wanneer herwinde materiale van konstruksie-afvalafval, soos herwinde beton (RCA), gebruik word.

Die bestaande TG2 beskryf die proses hoe om te bepaal of 'n aggregaat geskik is om met bitumen-skuim of bitumen-emulsie gestabiliseer te word. Die doel van hierdie navorsing is om dieselfde proses te gebruik om te bepaal of RCA 'n geskikte aggregaat is vir stabilisering met bitumenemulsie of bitumenskuim. Gevolglik kan 'n mens ook die BSM-klassifikasie verkry wanneer RCA gebruik word. Verder was die gedrageienskappe van die materiaal ook in hierdie navorsing ondersoek.

Die indirekte treksterkte (ITS) is gebruik om die geskikte aktiewe vulstof vir RCA te bepaal, gestabiliseer met bitumenemulsie en bitumenskuim. Beide kalk en sement was oorweeg as aktiewe vullers Verder is bepaal dat die optimale bitumeninhoud vir die aggregaat 2,2% was vir beide emulsie en skuimbitumen. Die skuifsterkte-eienskappe en veerkragmodulus modulus van die optimale mengsels gemaak van bitumenskuim en bitumenemulsie is deur monotoniese en triaksiale toetse ondersoek.

Die voorlopige resultate dui daarop dat RCA, behandel met 'n lae viskositeit bitumen vir stabilisering, wel geskik is. Volgens die ITS-resultate is geen aktiewe vulstof nodig nie en kan 'n moontlike BSM 1-laag met 2,2% bitumeninhoud geproduseer word. Die skuifparameters wat vir beide binders verkry word, dui ook op 'n moontlike BSM 1-laag wat bestand is teen vogskade, soos aangetoon deur die behoue kohesie wat wissel van 88,2 tot 90%. Daarbenewens dui die veerkragmodulus-analise op spanningsafhanklike gedrag wat deur bestaande ongebonde granulere materiaalmodelle gemodelleer kan word. Daar moet egter voorsorg geneem word wanneer met bitumenemulsie gestabiliseer word as gevolg van die hoe absorptiewe eienskappe van RCA. Om hierdie aspek te bestuur is dit noodsaaklik om die materiaal vogtig te maak voor die finale meng.

'n Ontleding van die falingseienskappe van die materiaal dui op aanvaarbare padlewe (as Kategorie B geanaliseer) wanneer dit as kroonlaag samehangende 'n redelike stutlaag soos 'n G5 toegepas word. Die gevolgtrekking is dat RCA, met die toevoeging van bitumen, die gedrag van RCA kan verbeter.

Daar is dus potensiaal vir verdere gebruik van RCA met skuim- of bitumen-emulsie in padlae en moet dus verder ondersoek word.

Acknowledgements

"You only need 5 people to help you reach your full potential and be happy in a specific chosen journey and these are:
Cheerleader: *To cheer you on and believe in you when you do not believe in yourself*
Mentor*: To point you in the right direction*
Coach: *To make you feel uncomfortable so that you can grow and reach your full potential*
Friend*: To remind you of your hearts desires and make sure you are actually happy doing what you have chosen to do.*
Peer*: Someone in the same field who has gone through a similar journey and help you keep your head in the game."*

Stacy Flowers

For this journey, I would like to show appreciation to the following five people:

My Cheerleader. Dr Chantal Rudman, thank you for seeing my potential when I did not even recognise it and for believing in me when I did not believe in myself.

My Mentor, Prof Kim Jenkins, thank you Prof for pointing me in the right direction at every meeting I got to have with you even when it had nothing to do with my thesis but needing a good mechanic.

My Coach, Dr Bianca Brandt, thank you for coaching and sometimes pushed me to overcome my fear of writing this thesis.

My Friend, Thato Muso, thank you for ensuring that I remembered what I wanted to do with my life in the mist of hard times I faced with this project.

My Peers, Ricky-Lee Beardmore and Elaine Goosen, thank you so much for reminding me that it is a tough journey but very doable with a little patience and love.

Thank you to my family that provided food, security, assistance, love, kindness and laughter

My Office family: Riaan Briedenhann, Ntate Gavin Williams, Ntate Colline, Ntate Eric and Rosie Sardien.

Mum and Dad, Andrina and Vusi Mazibuko, for their support. My brother (MJ) and sisters (Lungi, Dumi, Hlengi) for helping in all ways you could to make this project come together even spending your school holidays to help me in the lab.

Thank you to my Sponsors

SuperPave and Colas for the bitumen. Finally, thank you to SANRAL for providing me with the funds to complete my studies, which would have not been possible without.

Table of Contents

List of Tables

List of Equations

List of Figures

List of Symbols and Abbreviations

Symbols

φ	-	Internal angle of friction
τ	-	Shear stress
C	-	Cohesion
σ	-	Stress
ε	-	Strain
M_r	-	Resilient Modulus
θ	-	Bulk stress

Abbreviations

BSM	-	Bitumen Stabilised Materials
CDW	-	Construction demolition waste
RCA	-	Recycled Concrete Aggregate
TG2	-	Technical Guideline for Bitumen Stabilised Materials
FWD	-	Falling weight deflectometer
OMC	-	Optimum moisture content
MDD	-	Maximum dry density
OFC	-	Optimum fluid contents
PI	-	Plasticity index
GM	-	Grading Modulus
PI	-	Plasticity index
LL	-	Liquid limit
PL	-	Plastic limit
CBR	-	California bearing ratio
ITS	-	Indirect tensile strength

ITSM	-	Indirect tensile stiffness modulus
UCS	-	Unconfined compression strength
MTS	-	Material Testing System
LVDT	-	Linear variable differential transducer
DSR	-	Deviator stress ratio
PSR	-	Principal stress ratio

Chapter 1: Introduction

1.1 Background

Over the past 20 years, the construction of road infrastructure worldwide has moved towards recycling existing materials and construction methods that are expeditious because of high traffic volumes. This shift has been influenced by the Rio summit held in 1992 on sustainable development and most recently, the sustainable development goals for 2030 set by the United Nations (Kisku *et al.*, 2017). Sustainability in construction can be defined as construction materials and methods which reduce carbon emissions, conserve natural resources and preserve the environment (Schultz, 2015). As large quantities of construction and demolition waste (CDW) is dumped on landfill areas and with limited amounts of natural aggregates, recycling is the best means for sustainability. At the end of life of a typical structure, waste generated include a mixture of ceramic, masonry, reinforced concrete, wood and steel. Figure 1-1 illustrates the general estimated quantities of each waste material (Oikonomou, 2005). As a result, previous research has shown that CDW is suitable for reuse in the construction of pavement structures (Poon & Chan, 2006).

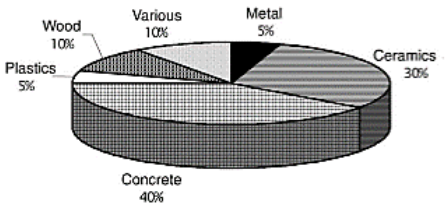

Figure 1-1 Basic Components of Construction and Demolition Wastes (Oikonomou, 2005)

The increase in the volume of heavy vehicles and loading, requires pavement structures to have a high resilience to repetitive loading. Therefore, the pavement materials currently used require improvement in quality, an increase in strength and stiffness in order to accommodate the increases in traffic volumes (Sharma *et al.*, 2016). At the end of a pavement life, materials such as old asphalt, seals, granular layers, cement stabilised layers and concrete are reused in the rehabilitation of existing roads or the construction of new roads. Aggregates produced from CDW have been used around the world for the construction of pavement layers, mostly in low volume traffic roads and has shown good performance. Moreover, CDW with higher contents of aggregates produced from old concrete, referred to as recycled concrete aggregate (RCA), have resulted in superior performance properties as investigated by Poon and Chan (2005).

1.1.1 What is recycled concrete aggregate?

Old concrete structures such as floors, columns, beams and concrete slabs from the road are crushed and processed into different sized fractions for use as aggregate, which is generally referred to as recycled concrete aggregate (RCA). The crushed concrete aggregate consists of cement mortar attached to natural aggregate (Kisku *et al.*, 2017). Recycled concrete aggregate has been used with success in fresh concrete and for the construction of unbound pavement layers (Kisku *et al.*, 2017). Previous feasibility studies have primarily concentrated on the use of CDW in pavement structures, with a few focused on the use of RCA alone. Higher contents of RCA in a mixture of CDW exhibits better performance properties (Van Niekerk, 2002). Several developed countries around the world such as the Netherlands and United States of America use RCA and masonry in the construction of roads. In these countries, the infrastructure to crush and process old concrete is well established and the proper use of the aggregate is outlined in guideline documents, all based on extensive research (Saeed & Hammons, 2008).

These developed countries use RCA due to the high cost of limited crushed stone and heavy penalties on the disposal of CDW. Similarly, developing countries particularly South Africa, Brazil and India are also in the preliminary implementing phases to use CDW and RCA. As a result of strict mining legislations and pressure from the rising cost of virgin materials (Leite *et al.*, 2011a). The use of RCA is however hindered by the absence of specifications to guide the appropriate use of the aggregate and the lack of infrastructure to produce RCA (Barnes & Rudman, 2016). Research is currently being performed in these countries to understand the performance of the aggregate in indigenous climates and to update guideline documents for the overall use of CDW, signalling some progress towards the use of RCA.

Research undertaken at the University of Sao Paulo in Brazil, studied the feasibility of the use of CDW in the pavement structure (Leite *et al.*, 2011a). The research outcomes show that despite the breakage of the material during compaction, the bearing capacity, resilient modulus and resistance to permanent deformation qualified the recycled material for use in the base and subbase layers of low-volume traffic roads (Leite *et al.*, 2011a). Furthermore, a study done at the University of Stellenbosch in South Africa considered the effect of the crushing method, compaction and mix compositions of CDW, with RCA and masonry, on the performance properties (Barisanga, 2014). The performance properties of the CDW were mainly influenced by the mix compositions with higher contents of RCA followed by compaction. The study concluded that the mix can be used in pavement structures for low to moderate traffic volume roads (Barisanga, 2014).

Numerous authors have investigated the potential for self-cementation of RCA due to the active latent cement present in the mortar. The self-cementation can be beneficial as it strengthens the material over time, however if it becomes too rigid it can be detrimental to the performance properties. The behaviour of RCA and masonry changed over time, due to increases of the stiffness in the material (Rudman & Jenkins, 2015). The self-cementation phenomenon was also observed in a study done at the University of Pisa on the performance of RCA stabilised with cement. The challenge experienced on the study was the unknown content of the active latent cement which made it difficult to determine the optimum cement content for the required design compressive strength (Marradi & Lancieri, 2008). The cement added resulted in high variable compressive strengths which caused excessive shrinkage cracking. However, a study done by Bredenkamp (2018) found that the active latent cement can be reduced by soaking the RCA in water. Therefore, the quality of the aggregate can be improved by reducing the high variability that is introduced by the active latent cement. Even though research has shown good results regarding the performance as an unbound alternative aggregate, the material has its limits. It is therefore expedient to explore other applications that could broaden the use of the materials.

The improvement of marginal and recycled pavement materials has conventionally been done by cement stabilisation. Marradi and Lancieri, (2006) looked at how the performance properties of RCA could be enhanced when it is stabilised with cement. It was found that shrinkage cracking resulted in the poor performance of the mix. Therefore, it is critical to use suitable stabilising agents to change the chemical and physical properties of an aggregate to be used in the pavement structure (Patel, 2012). Other typical stabilisers used are lime and fly ash; however, much research and construction has been done on stabilisation with bitumen in the form of foam or emulsion to produce bitumen-stabilised materials (BSM). A feasibility study was done were a mixture of RCA and masonry was stabilised with foamed bitumen, which found an improvement in the performance properties (Saleh, 2000). Furthermore, research on the behaviour of CDW stabilised with bitumen emulsion showed that the material was more flexible and resisted permanent deformation without cracking. (Gómez-Meijide *et al.*, 2015).

1.1.2 **What is a bitumen-stabilised material?**

A bitumen stabilised material (BSM) is a mixture of aggregate, water, active filler and low viscosity bitumen in the form of foam or emulsion (Asphalt Academy, 2009). The low viscosity bitumen spreads to the fine particles with which it makes a mortar that binds the

uncoated larger aggregates. The resultant mix has been defined as a non-continuously bound material (Collings & Jenkins, 2011). The mixture is currently used to construct base or subbase pavement layers. The layers constructed behave similar to a stress dependent unbound granular layer but with improved strength and durability properties (Collings & Jenkins, 2011). Moreover, the behaviour has been described to exist between a hot mix asphalt and a cement stabilised layer, depending on the bitumen and active filler content. Therefore, the mix can be slightly visco-elastic and rigid as demonstrated by Figure 1-2 (Asphalt Academy, 2009). Stabilisation with bitumen is currently used to recycle existing pavement materials, as it has a low carbon footprint and reduces the construction period compared to conventional rehabilitation methods (Jenkins & Yu, 2009a). Although BSMs are mostly used for rehabilitation projects to improve the existing pavement materials, it has also been used for new road construction (Lynch & Jenkins, 2013).

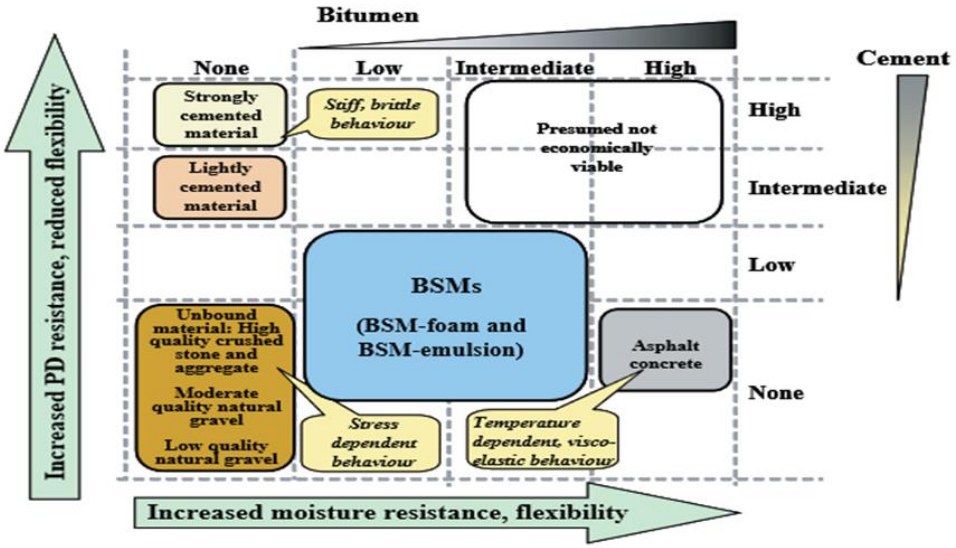

Figure 1-2 Conceptual Behaviour of Pavement materials

(Asphalt Academy, 2009)

A considerable amount of literature has been published on the performance of BSMs from pavement field studies. A few of the many benefits of the use of a BSM in a pavement structure are highlighted below:

- The material has an increased shear strength and a higher resistance to permanent deformation when compared to an unbound granular crushed material (Jenkins *et al.*, 2002).
- The layer is less sensitive to water damage because the fine particles are coated with bitumen hence more durable (Asphalt Academy, 2009).

- The existing pavement layers can be recycled in-situ or in plant. As a result, there is no wastage, no need for new aggregate and low haulage costs (Jenkins & Yu, 2009a)
- The quality of a large variety of natural and recycled aggregates are improved. These include crushed stone, natural gravel, reclaimed asphalt and previously cement stabilised materials (Wirtgen Group, 2012)

However, CDW such as recycled concrete aggregate (RCA) and masonry have not been listed as options for aggregate selection in specifications, such as the Technical Guideline for bitumen stabilised materials (TG2), used in South Africa. A study done to assess the durability and long term performance of CDW stabilised with bitumen emulsion found an increase in the resistance to permanent deformation (Gomez-Meijide & Perez, 2016). However, weak bonds between the binder and aggregate were observed after the mix was immersed in boiling water and mechanically agitated. It is possible based on the study that the weak bonds might be due to the weaker components of CDW such as ceramics and masonry. To improve the performance properties of RCA and reduce the inherent detrimental potential to self-cement, bitumen stabilisation could be a better option over cement stabilisation. Consequently, the improved RCA stabilised with bitumen could be used in the pavement structure of higher traffic roads as a more sustainable alternative to natural aggregate.

1.2 Problem Statement

In the TG2 and the Wirtgen Cold recycling technology manual, which are both used to design and construct BSM pavement layers, both CDW and RCA are currently not listed as potential aggregates for a BSM. This is due to the lack of research on the behaviour and understanding of the long-term performance of the resultant BSM with RCA stabilised with foamed bitumen or bitumen emulsion. The central question in this dissertation asks, is it feasible to stabilise recycled concrete aggregate (RCA) with foamed bitumen or bitumen emulsion and use as a secondary material for pavement construction? The research also seeks to address the following questions:

- Would the mix design with the current optimised bitumen contents for crushed stone in the Wirtgen cold recycling technology be suitable to stabilise RCA?
- Would the laboratory evaluation of the performance properties of the mix qualify the material as suitable for use in BSM?
- Which binder would be more suitable for RCA, bitumen foam or bitumen emulsion?

Recycled concrete aggregate could be used as an aggregate for BSMs with foamed bitumen and bitumen emulsion for a sustainable alternative to natural aggregate. This is based on previous research which has reported that RCA behaves in a similar manner to natural aggregate. The performance properties of the material will therefore be enhanced, and it could be suitable for use in roads with higher traffic volumes. This research will lay the foundation in the acquisition of knowledge to determine the performance aspects of RCA stabilised with bitumen and the practicality of such an application toward future addition to the TG2 and Wirtgen Cold recycling technology manual.

1.3 Research Goal and Objectives

The main purpose of the study is to develop an understanding and gain insight into the engineering properties of RCA stabilised with foamed bitumen or bitumen emulsion. This will assist in gaining a reliable understanding of the key performance properties and sustainable design models for BSM with RCA.

In order to achieve the abovementioned research goal and to address the problem statement the following objectives form the basis of this study:

a) Characterise RCA to determine whether it is suitable for use in a BSM layer. The physical properties of the aggregate will be tested and classified according to the TG2.

b) Determine the optimum mix design of RCA by varying the binder contents for foamed bitumen and bitumen emulsion. The suitable active filler will be determined from two types of active fillers with the same content to the dry mass of the RCA namely: Cement and lime. The indirect tensile strength of the different mixes will be tested and used as the measurement of influence.

c) Investigate the mix designs resistance to moisture susceptibility by testing the soaked tensile strength of the mixes. This will allow for an understanding of the durability properties of the BSM with RCA.

d) Evaluate the performance properties of the optimum mix designs with foamed bitumen and bitumen emulsion for use in a pavement layer. Test the shear strength and resilient modulus by using the triaxial machine.

e) Verify the feasible use of RCA stabilised with foamed bitumen and bitumen emulsion through classification of the BSM according to the TG2 specification.

f) Evaluate the resilient modulus of the BSM with RCA stabilised with foamed bitumen and bitumen emulsion to gain an understanding of the dynamic response of the material.

g) Perform a pavement design analysis with the mix properties to compare and benchmark against traditional materials in order to determine feasibility of its use.

1.4 Significance of the Research and Limitation

The current study contributes to our knowledge by addressing the performance of RCA stabilised with foamed bitumen or bitumen emulsion. This knowledge can lead to more research done on foamed bitumen and bitumen emulsion stabilisation of RCA. The outcomes will build confidence in the use of RCA in the construction industry and encourage sustainable construction methods. The findings of this research may also be used in the development of best practice industry guideline manuals, such as Technical Guideline for Bitumen Stabilised Materials (TG2) and the Wirtgen cold recycling technology manual.

The limitations of the study are as follows:

a) The type, age and treatment of the RCA has a significant influence on the behaviour of the material as previous research has shown. However, for this project it will not be considered because the aggregate used is obtained from one source.

b) The bitumen content used for the project is based on the current limits for crushed stone in the Wirtgen cold recycling technology. This is to establish whether the range would be suitable for RCA.

c) The combination of RCA with other recycled pavement aggregates as typically done on site to produce a BSM layer will not be investigated in this research due to time constraints.

Therefore, the scope of the study focuses on testing and the analysis of the mix design properties of RCA stabilised with foamed bitumen or bitumen emulsion, with lime and cement as active fillers. The optimum mix design will be used to investigate the performance properties with triaxial testing. These tests and investigations are critical to the research project because the results will validate whether RCA can be used for BSM layers according to the TG2 specification guideline.

1.5 Brief Chapter Overviews

The overall structure of the study takes the form of seven chapters, including this introductory chapter.

Chapter 1 presents the introduction to the research project with a brief background on the development of sustainable road construction with construction demolition waste particularly recycled concrete aggregate and bitumen-stabilised materials. The problem statement, research goal and objectives that will address the research question are outlined. Finally, the chapter concludes with the significance of the research and limitations to the scope of the project.

Chapter 2 includes the literature review regarding the physical and performance properties of RCA and BSM. The chapter also gives an overview of the research that validates the use of recycled concrete aggregate. The components of bitumen-stabilised materials have also been discussed in the literature review along with the factors that influence the performance of the mix. A brief overview on the testing methods are presented along with the models used to predict the resilient modules of BSM mixes.

Chapter 3 demonstrates the experimental plan and methodology for the research project. The material preparation is discussed along with the test methods that are used for the aggregate characterisation, mix design strength testing and the performance evaluation.

Chapter 4 presents the results obtained from Phase 1 and 2 of the research project where the aggregate preliminary characterisation was conducted. The results obtained from phase 2 where the BSM_RCA mix design optimisation with the ITS was done. The suitable active filler is determined along with the optimum bitumen content for RCA. A comprehensive discussion of the results is done to interpretate the obtained results.

Chapter 5 presents the results obtained from phase 3 of the experiment where the shear parameters and the resilient modulus of the optimum mix design were measured with the triaxial machine. A discussion and interpretation of the results is done with various models to predict the properties.

Chapter 6 presents the pavement design and analysis of the optimum mix design. The aim of the design is to determine the maximum load repetitions the BSM layer with RCA can resist prior to failure in various typical pavement structures. Additionally an outline of the practical considerations regarding the use of the aggregate in a BSM mix.

Chapter 7 outlines the research conclusions and recommendations for further research on the use of the material.

Chapter 2: Literature Review

Understanding the fundamentals of RCA and BSM separately, allows for preliminary insight into what can be expected if these two materials are used in combination. This literature review briefly describes the typical pavement structures used in South Africa. Then focuses on the performance properties of an unbound granular layer that can be improved to a non-continuously bound layer such as a bitumen-stabilised material (BSM). A detailed discussion is conducted on the important aspects that affect the shear strength, resilient modulus and durability which result in the permanent deformation of these layers. This is followed by a discussion on the physical properties and characteristics of recycled concrete aggregates (RCA) which influences the performance properties as well as how RCA can be used to make a BSM. The required components of a BSM are briefly highlighted along with the laboratory methods used to test the performance properties of the optimum mix design. An overview of the models used to "predict" the resilient modulus of unbound granular layers and BSMs is presented.

2.1 Pavement Structure and Performance Properties

2.1.1 Typical Pavement Structures

The functional and structural requirements of a pavement structure are to protect the weak natural ground and provide the road user with a safe comfortable roadway for the design speed of the road. These functions are achieved through a pavement structure that can support the design traffic and withstand climatic deterioration (Yang, 1972). A pavement structure is a multilayer system, which is composed of layers with a specific thickness and built from aggregates with properties to provide the required strength (Huang, 2003). The pavement structure can be surfaced or unsurfaced. A surfaced road has a top layer, which is water resistant to protect the supporting layers from moisture. On the other hand, an unsurfaced road has no top layer and constructed for low traffic volumes, referred to as gravel road. The most economical pavement structure is a balanced combination of low strength to high strength aggregates built from the bottom up in order to meet the functional requirements of the road (Croney & Croney, 1998).

The functional requirements for roads with different levels of traffic, dictate the most suitable and economical pavement structure. For example, there are three types of surfaced pavement structures used for the design of high traffic roads (Figure 2-1) namely; flexible pavements, rigid pavements and composite pavements (Thom, 2008). Flexible pavements

generally consists of a bituminous surfacing supported by a base, which can either be a bound or an unbound granular or non-continuously bound layer. The subbase layer supports the base layer which also protects the subgrade layer. Rigid pavements are made up of a concrete layer which functions as surfacing and a base supported by a subbase where the loading is mainly carried by the concrete layer (Figure 2-1). A composite pavement structure consists of a hydraulically bound layer such as concrete or cement stabilised layer as a base which is surfaced with a hot mix asphalt (Huang, 2003). The flexible pavement is the most commonly used pavement structure in South Africa for high traffic volume roads because it is the most economical (Jordaan & Kilian, 2016). As a result, the different types layers and the behaviours that make this pavement structure will be further discussed.

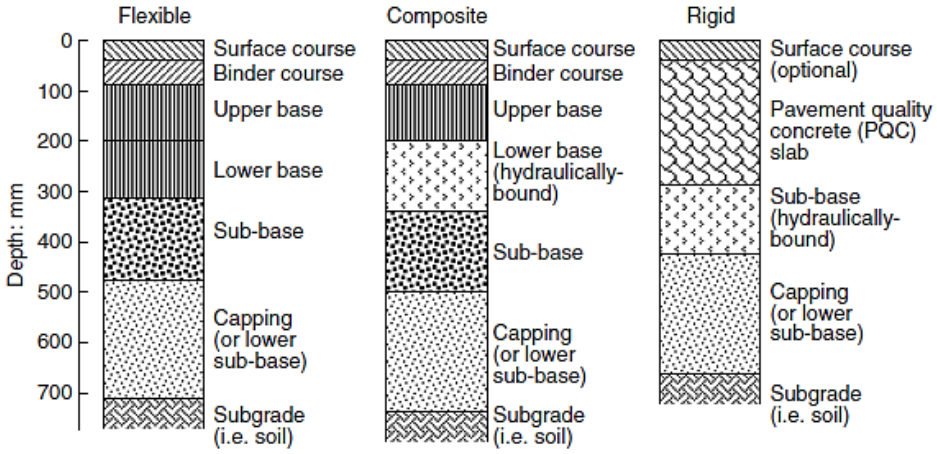

Figure 2-1: Typical surfaced pavement structures for high traffic roads (Thom, 2008)

2.1.2 **Layer Types and Behavioural Mechanisms**

Unbound granular layers are used for the construction of any layer in the pavement structure depending on the design traffic of the road. A typical unbound granular layer as illustrated in Figure 2-2(A) is composed of different sized aggregates, air voids and possible moisture from the surrounding environment (Wirtgen Group, 2012). An unbound layer is constructed from different types of granular gravel, crushed rock, soils and construction demolition waste (CDW) such as recycled concrete aggregate (RCA). These aggregates are graded and compacted in order to resist vertical compressive stresses from wheel loading (Croney & Croney, 1998). The load spreading ability of a layer, which is the response to loading, is measured as the resilient modulus. This parameter is dependent on the resistance mechanism of an unbound layer being the frictional resistance between aggregates against shear stresses induced by the vertical compressive stresses.

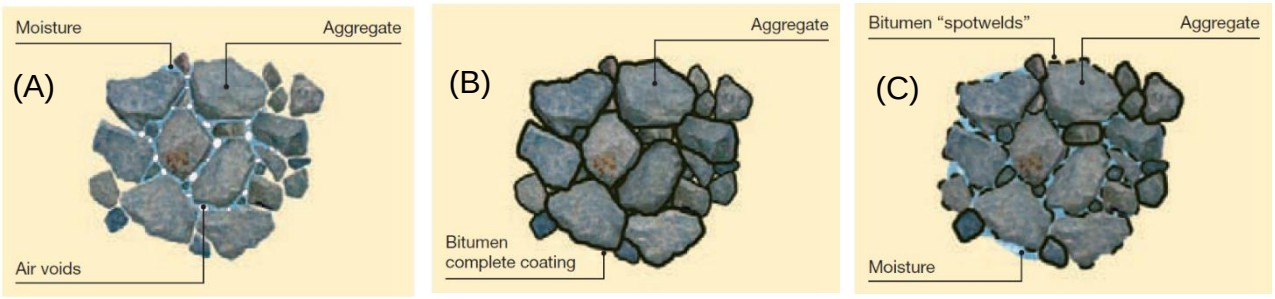

Figure 2-2: Aggregate dynamics and interaction with moisture, air, binder within (A) unbound, (B) bound and (C) non-continuously bound layers (Wirtgen Group, 2012)

The shear strength is a material property dependent on the aggregate type, layer thickness and degree of compaction (Thom, 2008). Furthermore, the unbound layer strength properties are influenced by the aggregate grading, particle shape and moisture content, which influences the edge to edge contact of the aggregates. Therefore, the performance of the layer is measured through the shear parameters and the resilient modulus, which are also dependent on the support of the layer that provides confinement. The damage parameter, plastic strain, leads to the failure mechanism of an unbound layer where permanent deformation is the result that occurs when the friction between the aggregates cannot resist the applied vertical compressive stresses (Thom, 2008).

When an unbound granular layer cannot provide enough resistance to the vertical compressive stresses caused by the traffic loading, a binding agent is added to make a bound layer. This layer has enhanced performance properties and can provide resistance to tensile stresses (Thom, 2008). Therefore, bound layers are mostly used in the upper layers of the pavement structure such as surfacing, base and subbase layers (Yoder, 1975). The most popular binders used in flexible pavements built in South Africa are cement and bitumen (Jordaan & Kilian, 2016), which completely coat the aggregates as illustrated in Figure 2-2 (B). The addition of these binders increases not only the strength of the pavement but also the cost to build the pavement. Cement produces a continuous matrix with the aggregates to form a rigid layer such as concrete and cement stabilised layer. Alternatively, bitumen makes a continuous matrix with the aggregates that forms a flexible layer with an added water proofing benefit (Jordaan & Kilian, 2016). Bound layers resist loading by bending, therefore these layers are subjected to compressive stresses at the point of loading and tensile stresses at the bottom of the layer. The layer fails when the tensile strength at the bottom cannot resist the repeated applied tensile stresses from the bending, leading to fatigue cracking (Thom, 2008). Bound layers thus must have adequate compressive strength, tensile strength and high stiffness for load spreading.

Bitumen stabilisation is another method used to improve the strength properties and moisture resistance of granular unbound materials used in the upper layers such as the base and subbase of a pavement structure (Wirtgen Group, 2012). This method produces a non-continuously bound layer, referred to as a bitumen stabilised material (BSM), where granular materials are treated with small quantities of bitumen emulsion or foamed bitumen (Asphalt Academy, 2009). The binder disperses within the filler, which when compacted forms localised bonds (spot welds) with the larger aggregates as illustrated in Figure 2-2 (C). In comparison, the aggregates are not completely coated with bitumen as seen in bound layers in Figure 2-2(B) and the layer does not form a continuous element (Collings & Jenkins, 2011). The bonds between the aggregates improve the edge to edge contact and increase the resistance against vertical compressive stresses. These types of layers behave similarly to unbound layers however, the difference is the increased cohesion resulting in resistance of higher stresses. The performance properties of these materials are shear strength, resilient modulus and resistance to permanent deformation. The failure mechanism is shearing from vertical compressive stresses which lead to deformation of the layer (Wirtgen Group, 2012). Given the benefits of non-continuously bound layers such as bitumen-stabilised materials, there is ongoing research into the performance characteristics of these layers towards cost effective and environmentally sustainable practises.

2.1.3 **Performance Characteristics of Non-Continuously Bound Layers**

The functional requirements of a road are to provide a safe and comfortable platform, as such, the performance indicators of the road are based on these functional requirements. Riding quality and the skid resistance is used as performance indicators to measure the functional condition of the road. This indicates the structural integrity of the underlying pavement structure (Thom, 2008). The performance of a flexible pavement structure will be affected when the road does not provide a comfortable riding quality and eventually unsafe to drive on at the design speed. These performance indicators are mostly affected by cracking and deformation of the road surface, which are caused by traffic loading and disintegration due to water penetration (Molenaar, 2007). Each layer in the pavement structure whether it is unbound, bound or non-continuously bound, contributes towards the deterioration of the pavement structure when it cannot resist the stresses induced by the traffic loading. Focus will be drawn to the performance properties; shear strength, resilient modulus, durability aspects and permanent deformation of an unbound granular layer. The influence of these properties on the permanent deformation of the layer and how it can be improved with bitumen stabilisation.

2.1.3.1 Shear Strength

Shear strength of a material is characterised by the angle of internal friction and cohesion, referred to as shear parameters. In a layer constructed of a graded material with different sized aggregates, the shear stress acts along the weak plane in the layer which is dependent on the internal angle of friction and cohesion of the aggregates against each other (Thom, 2008). Shear stresses along the weak plane results in permanent deformation. In this plane, the aggregates slipping over each other when the applied vertical compressive stresses exceed the friction force between the aggregates (Thorn & Brown, 1989). The friction force which resists inter particle slip is mainly influenced by the aggregate shape, surface texture, particle size distribution and moisture content of aggregates at mixing, compaction and in-service.

The shape of the aggregates after crushing is important because it influences the level of interlock within the matrix and therefore its resistance to the applied loading. Aggregate shapes range from rectangular, cubic, spherical, flat, elongated and irregular as illustrated by Figure 2-3. The shape and surface texture are influenced by the origin, mineral composition of the parent rock and crushing method (Alexander *et al.*, 2009). Crushed rocks such as dolerite generate aggregates that are long and cubic shaped whereas spherical aggregates such as sandstone originate from transportation of rocks through wind or water. In recycled demolition wastes, the harder materials such as recycled concrete generate cubic and angular fractured faced aggregates in comparison to softer materials such as masonry which tend to produce elongated aggregates when crushed (Leite *et al.*, 2011a). Cubical aggregates with rough surface textures, provide better interlocking between aggregates. This increases the compressive strength of the material and therefore higher shear stress can be resisted (Polat *et al.*, 2013).

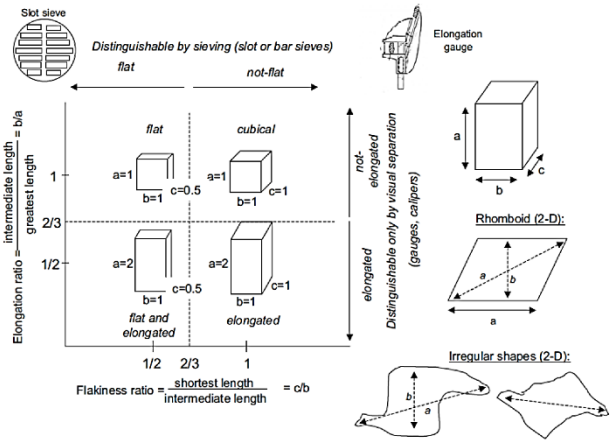

Figure 2-3: Aggregate Particle shapes (Van Niekerk, 2002)

The particle size distribution enhances the angle of internal friction by reducing the occurrence of weak shear planes. Particle size distribution is obtained by sieve analysis of a sample of natural or crushed aggregates where the aggregate sizes can range from 75 mm to 0.075 mm (Alexander *et al.*, 2009). The coarse aggregates are retained on the 4.75 mm sieve. These particles act as an internal support structure (skeleton) whereby the edges are in contact and interlock in order to provide strength (Molenaar, 2010). The fine aggregates pass the 4.75 mm sieve and retained on the 0.075 mm sieve. The particles passing the 0.075 mm sieve are referred to as the filler. These particles together with the fine aggregates improve cohesion and provide surface friction by filling the gaps between the coarse aggregates (Araya, 2011). The optimum angle of internal friction is achieved with a well-balanced filler content, coarse and fine aggregates as illustrated in Figure 2-4. Samples with excess fines reduce edge to edge contact between coarse aggregates as seen in Figure 2-4 (c). This reduces the internal angle of friction and increases the occurrence of weak shear planes. No fines leads to no cohesion between the coarse aggregates and low surface friction (Araya, 2011).

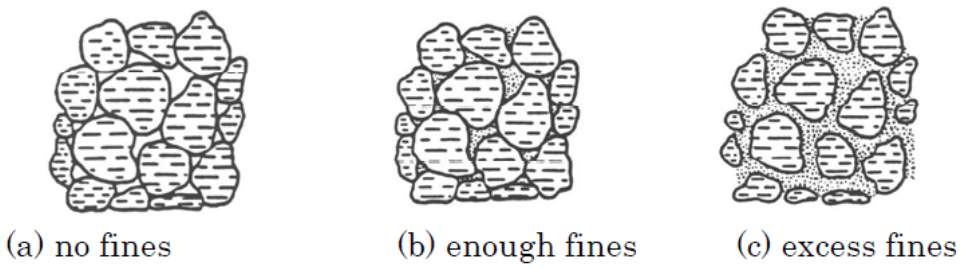

Figure 2-4: Example of the particle size distribution with different fine contents(Araya, 2011)

Various types of aggregates with variable gradations behave differently depending on the moisture content of the material. The moisture content of the aggregate mix at mixing, compaction and in service is an important factor to the shear strength of the layer. Lower cohesion results from low moisture content during mixing and compaction leading to lower dense packing of the aggregates (Yoder, 1975). The moisture content directly influences the dry density achieved from compaction i.e. improved shear strength. However, high moisture content during compaction and traffic loading results in a reduction in edge to edge contact of the coarse aggregates due to moisture lubricating the aggregates reducing the surface friction (Molenaar, 2010). Furthermore, excess moisture leads to the drainage of the fines from the aggregate mix. The drainage occurs during compaction and pumping as a result of pore pressure induced by traffic loading which changes the particle size distribution. Thus,

the change in particle size distribution reduces the angle of internal friction resulting in measured decreased shear strength of the material (Thom, 2008). Therefore, a high moisture content in a mix or layer will have an adverse effect on the resistance of the layer to loading.

Stabilisation with bitumen emulsion or foamed bitumen reduces the influence of moisture on the shear strength as it improves the cohesion of the aggregate mix due to the high viscosity of the bitumen at ambient temperatures. The mastic, made from the filler with low viscosity bitumen emulsion or foamed bitumen, hardens once the water evaporates. This mortar binds the coarse aggregates, which increases the cohesion between the particles (Asphalt Academy, 2009). However, a slight decrease was seen in the internal angle of friction with increasing bitumen contents due to increased lubrication between the particles (Jenkins *et al.*, 2007). Therefore, BSM layers have higher shear strength, due to the increased cohesion, which can resist higher compressive stresses from traffic loading.

In a laboratory, the angle of internal friction (ϕ) and cohesion C, (kPa) of a non-continuously bound material can be measured with a monotonic triaxial test. The triaxial simulates the stress conditions of a layer in the road pavement structure subjected to traffic loading by applying lateral and axial compressive stresses on the material to induce shear failure in the layer (Yoder, 1975). These shear parameters are used to calculate the shear strength of the material using the general Mohr – Coulomb failure criteria as illustrated in Equation 2-1 at a predetermined compressive stress (σ) in the specimen induced by air pressure. Therefore, the shear parameters are material specific and are determined from the shear failure envelope as illustrated in Figure 2-5. The shear failure envelope is constructed from Mohr's circles determined from triaxial test results of the specimen (Huang, 2003). This also indicates the maximum allowable compressive stresses the material can resist before failure in shear.

$$\tau = C + \sigma \tan \phi \qquad \text{Equation 2-1}$$

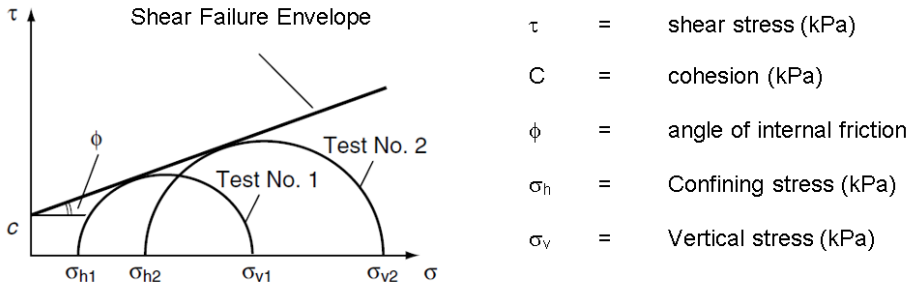

Figure 2-5: Mohr's failure envelope (Adapted from Thom, 2008)

2.1.3.2 Resilient Modulus

The elastic stiffness of a material is the ratio between the applied stress and the measured induced strain on the material. This ratio is linear for homogenous elastic materials such as steel, therefore an increase in the stress results in an increase in the induced strain (Thom, 2008). However, the resilient modulus (M_R) refers to the elastic stiffness of layers such as unbound granular layers and non-continuously bound layers, which are not homogenous and non-linear elastic, under repeated loading. The resilient modulus of these layers is a response parameter indicating the load spreading ability which is stress dependent, whereby the resilient modulus increases with an increase in confinement stress of the layer (Huang, 2003). The confinement stress increases the contact between the coarse aggregates therefore an increase in the frictional force occurs. The predominant factors which affect the resilient modulus within a layer are density, stress condition and degree of saturation (Theyse, 2002). Table 1 presents a summary of the factors which predominately influence the resilient modulus of unbound aggregates such as crushed stone and natural gravel.

Table 1: Factors affecting Resilient Modulus of an unbound aggregate (Adapted from, Theyse, 2002)

FACTOR	CHANGE IN FACTOR	INFLUENCE ON M_R
NUMBER OF LOAD CYCLES	Increase in load cycles	Up to a 20% increase
CONFINING PRESSURE	Constant vs pulsed	Constant pressure slightly overestimates M_R
SAMPLE DENSITY	Increase from 82.6 to 87.5% of apparent density	10% increase
PERCENTAGE MATERIAL < 0.075 MM	Increase in fines	Optimum at 9% fines
PARTICLE SHAPE	Increase in angularity	Slight increase
SURFACE TEXTURE	More course	Slight increase
DEGREE OF SATURATION	Increase from 20 to 90%	Up to 60% decrease

A densely packed layer results in a high resilient modulus because of an increased number of edge to edge contact between the coarse aggregates. A higher stiffness can be measured along with less deformation (Lekarp *et al.*, 2000). The packing of the aggregates i.e. density, is determined by the degree of compaction which is limited by the inherent stiffness of the aggregate (Theyse, 2002). The density is also influenced by the following aggregate characteristics: type, shape, surface texture, particle size distribution and filler content. The level of influence these aggregate characteristics have on the resilient modulus is as summarised in Table 1. For instance, a high fine particle content reduces the density of the layer due to the reduction in the edge to edge contact between the course aggregates

(Lekarp *et al.*, 2000). Alternatively, a well-balanced particle size distribution increases the packing of the aggregates during compaction consequently increases the resilient modulus (Van Aswegen, 2013). The maximum density of a layer is required in order to achieve the highest resilient modulus under traffic loading.

The confinement stress is an important factor for the resilient modulus because it influences the stiffness of the material i.e. loading spreading. The confining stress on a layer in the pavement structure is the lateral compressive stresses from the surrounding material induced by the traffic loading and the supporting layers. In a triaxial test, the confinement stress is simulated for laboratory testing with air pressure applied on the specimen in a membrane inducing lateral stresses which can be controlled (Barksdale *et al.*, 1997). Unbound granular materials are stress dependent as a result, the resilient modulus is determined from a number of different confining stresses. The increase in confining stress increases the frictional forces between the coarse aggregates at the same applied vertical stress therefore less deformation occurs (Thom, 2008). Researchers have found that an increase in the confining stress on a specimen from 20 kPa to 200 kPa resulted in a 500% increase in the resilient modulus of the layer (Van Aswegen, 2013). In summary, the higher the confinement stress, the higher the resilient modulus of the material therefore less deformation.

The presence of moisture reduces the resilient modulus of a layer/specimen due to the decrease in the contact of the aggregate edges causing a reduction of the frictional forces. In addition, moisture lubricates the aggregates resulting in slippage which leads to increased strain i.e. deformation, therefore lower resilient modulus (Cary & Zapata, 2011). The degree of saturation of a layer is the ratio between the volume of water to the total volume of the aggregates. A fully saturated material is made up of only aggregates and water in the pores whereas a partially saturated layer includes air in the voids (Craig, 2013). A fully saturated layer will experience positive pore water pressure and partially saturated will undergo negative pore water pressure (suction) due to loading depending on the type of fines. This pore water pressure affects the adhesion between the particles and reduces the effect of the confinement pressure on the layer or specimen (Sweere, 1990). Degree of saturation is important for the design of a layer to determine the sensitivity of a material at various degrees of saturation. Therefore, material behaviour is dependent on various degrees of saturation, which are brought about by changes in climate, or for layers built in areas with high water tables.

The stabilisation of an unbound granular layer with bitumen introduces localised bonds improving cohesion between the aggregates therefore a higher resilient modulus is measured from the specimen (Valentin *et al.*, 2016). These localised bonds are a result of the high stiffness of the bitumen at ambient temperatures. Furthermore, bitumen reduces the influence of moisture on the density of the material therefore the resilient modulus is retained through various degrees of saturation (Collings & Jenkins, 2011). A long term analyses on the performance of a foamed BSM found a reduction in deflections over a period of two years after construction and exposed to heavy traffic volumes. An increased back calculated resilient modulus was determined from the measured deflections of the pavement therefore the bitumen stabilisation increased the resilient modulus (Loizos, 2007).

The resilient modulus (M_R) of a non-continuously bound layer in a laboratory is measured by cyclic load triaxial tests with dynamic repeated loading. The resilient modulus is calculated (Equation 2-2) from the peak dynamic deviator stress (σ_d) in a triaxial compression test that results in a recoverable/resilient strain (ε_r) (Huang, 2003), as illustrated in Figure 2-6.

$$M_R = \frac{\sigma_d}{\varepsilon_r} \qquad \text{Equation 2-2}$$

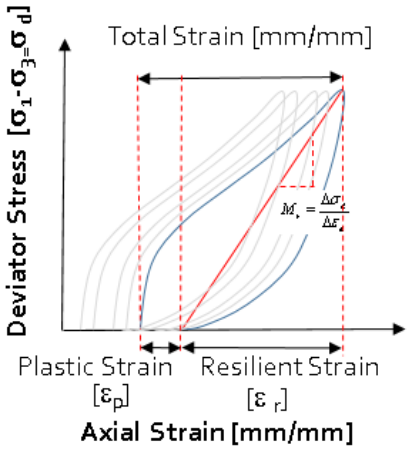

Figure 2-6: Resilient Modulus (Mr) determined from the deviator stress and recoverable strain ratio (Rudman, 2019a)

Other laboratory scale methods used to evaluate the resilient modulus are the repeated indirect tensile stress test and the true triaxial cell (Barksdale *et al.*, 1997). The triaxial cell measures the resilient modulus of specimens exposed to dynamic forces in the horizontal and vertical plane of the specimens as water is used to induce a dynamic pressure around the specimen. In the field, data measured from the falling weight deflectometer (FWD) is

used to back calculate the resilient modulus of the layers (Boateng *et al.*, 2009). The accelerated pavement testing (ATP) and heavy vehicle simulator (HVS) are other methods used to estimate the resilient modulus of the layer in the pavement structure. This value is dependent on the stress conditions, the temperature and moisture condition of the layer during testing due to seasonal influences (Valentin *et al.*, 2016). The shear strength and resilient modulus of the layer in the long-term use are dependent on the durability of the aggregates and bitumen used.

2.1.3.3 Durability

The durability of a layer in a pavement structure is the measurement of resistance to degradation leading to a longer design life. Durability is a time dependent variable influenced by the intrinsic material properties and external destructive factors resulting in degradation of a pavement structure (Twagira, 2010). The main external factors leading to degradation are repeated excessive traffic loading and climate (Sweere, 1990). Damage caused by traffic loading occurs when the design load of the pavement structure is exceeded. Climatic factors such as water and ultra violet radiation from the sun causes disintegration and decomposition of the aggregates resulting in a decrease of strength (Wirtgen Group, 2012). Pavement layers exposed to relatively high moisture content under excessive repeated loading undergo rapid deterioration due to induced high pore pressures, which reduces the adhesion between the aggregates. Consequently, the forced movement of trapped water results in the fracture of bonds between the aggregates (Thom, 2008). In addition, as previously discussed, water reduces the shear strength of the material due to excess lubrication. This reduces the response of the layers to loading i.e. resilient modulus. A particular layer with specific properties can only withstand a certain amount of repeated loading i.e. stresses and strains. In other words, a layer exposed to stresses higher than the design stress and with high moisture content would rapidly deteriorate (Twagira, 2010). Thus, a limit is placed on the applied loading for a pavement structure. Other factors affecting the durability of a layer are the type of aggregate and mix properties the aggregate produces.

The parent material of the crushed aggregates has an influence on the durability of a layer due to the inevitable natural weathering and crushing of the aggregates under repeated loading. The type of aggregate influences the intrinsic stiffness, shape and grading which are important for the resistance of the layer against loading (Weinert, 1980). A cubic or irregular shaped aggregate resists crushing better than a long flat aggregate and packs better for a higher density than rounded aggregates (Weinert, 1980). Furthermore, a well balanced grading contributes towards the interlock of the aggregates when compacted. A

higher density results in minimum voids which reduces the permeability of the layer for better resistance to loading in wet conditions (Brown & Chan, 1996). Other factors that plays a role on the durability of an aggregate are chemical reactions caused by the environment.

A reduction or an increase in the durability of the mix results from chemical reactions due to changes of the aggregate properties. Such chemical reactions include carbonation, particularly for recycled aggregates such as recycled concrete. Carbonation occurs when carbon dioxide reacts with the hardened hydration products of the cementation process in recycled concrete, producing an increase in the density and reduction in porosity of the RCA (Zhang et al., 2015). However, this reaction reduces the self-cementation benefit of RCA and the aggregates behaves similar to natural aggregates. Moreover, no increase in stiffness occurs with curing resulting in a reduction of the pavement life (Beardmore, 2018). Therefore, aggregate properties are important for the durability of the mix as influenced by properties such as density and thickness of the layer. These durability aspects can be improved with bitumen stabilisation.

The stabilisation of an unbound layer with bitumen further improves the bond between the aggregates especially under moist conditions. The mastic, made from bitumen and filler, bonds the aggregates resulting in resistance to loss in strength due to lubrication from high moisture content in the layer (Twagira & Jenkins, 2009). In addition, the dispersion of the bitumen to the filler encapsulates and immobilises these particles which results in less pumping under loading when the layer is saturated (Valentin *et al.*, 2016). However, durability issues with bitumen stabilisation include the ageing of the bitumen due to heating before mixing, oxidation and stripping off the aggregates with time. The oxidation occurs when the aggregates absorb the softer fractions of the bitumen and the bonds become brittle and sensitive to loading (Twagira, 2010).

The resistance of a BSM to moisture damage can be tested by soaking an ITS specimen in water for 24 hrs and testing the tensile strength of the saturated specimen. Other laboratory methods used to test how bitumen stabilisation improves the durability of a layer are: wet-dry brush, the moisture induction simulation test (MIST) and the model mobile load simulator (MMLS) (Twagira, 2010). Standard aggregate durability tests against loading can be empirically evaluated with the following methods: Los Angeles abrasion test, aggregate impact value test and the 10% fines value test (Sweere, 1990). In summary, the permanent deformation of an unbound or non-continuously bound layer is a result of the durability of the aggregates, which influences the shear strength and the resilient modulus of the layer.

2.1.3.4 Permanent Deformation

The ultimate failure mechanism for unbound or non-continuously bound layers is permanent deformation. This failure mechanism manifests into rutting in the wheel path for flexible pavement structures. The width of a rut indicates the depth of the failed supporting layer in the pavement structure (Huang, 2003). Furthermore, the deformation in the rut is due to the movement and crushing of the aggregates resulting in a reduction of the layer thickness leading to a lower response to loading i.e. loss of stiffness. Factors that induce the deformation include the imposed confining stress, shear strength, relative density of the layer and degree of saturation of the material (Theyse, 2002).

In the laboratory, the permanent deformation of a specimen is measured with a triaxial subjected to repeated loading. The plastic strain is the measured variable of a specimen with an increase in the cumulative repeated loading (Arnold *et al.*, 2002). The plastic strain predicts the behaviour of the aggregates which indicates the suitable traffic volumes and climatic conditions for optimum performance of the mix (Arnold & Arnold, 2008). Additionally, the results provide information on how the applied stress ratio influences different materials. Ultimately dictating the stability of the material as illustrated on Figure 2-7 by the relationship between an increase in loading and the measured plastic strain. In the case the material is unstable, deformation occurs at an exponential rate. Instability occurs at high-applied stress ratio as exemplified on Figure 2-7 B (Thom, 2008). While, this study does not analyse the plastic strain of the BSM mixes made with RCA, it is important to understand the concept. In brief, the causes and prediction of permanent deformation of an unbound or non-continuously bound layer can lead to the efficient use of material for suitable traffic and climate conditions for the design life of the pavement.

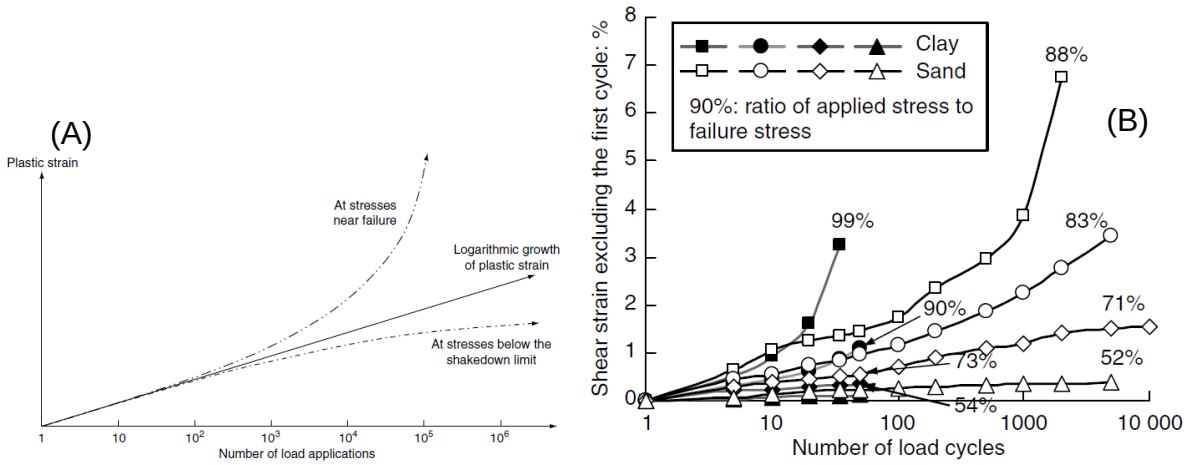

Figure 2-7 (A) Stability of the material with increasing cumulative load applications (B) Higher deviator stress ratios result to the occurrence of unstable materials at low cumulative load cycles(Thom, 2008)

2.2 Recycled Concrete Aggregate Properties and Characteristics

Recycled concrete aggregate (RCA) is an aggregate crushed from old concrete obtained from construction and demolition waste (CDW) of structures such as concrete pavements, bridges, building floor slabs, beams and columns. The aggregate is generally composed of natural aggregate covered in mortar which is made from cement, sand and water, as illustrated in Figure 2-8 (Pasandín & Pérez, 2015).

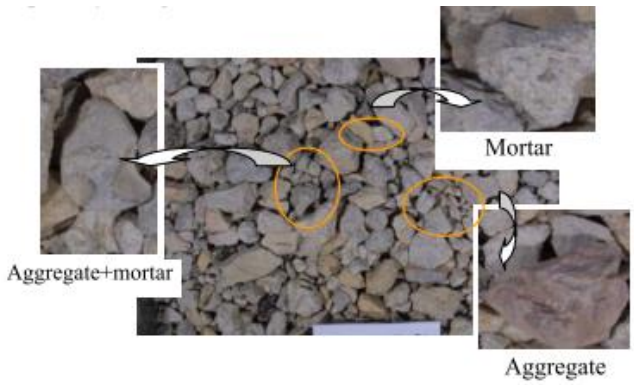

Figure 2-8: Recycled concrete aggregate (Sánchez De Juan & Gutierrez, 2009)

Numerous studies have been done on the feasible use of RCA and masonry as an alternative to natural crushed aggregate or as a secondary material for pavement construction (Yang *et al.*, 2010, Ardalan *et al.*, 2016; mahdi, 2017). Similarities were found between the physical properties of RCA in comparison to typical natural aggregates. However, RCA has a higher water requirement due to the high absorption of the mortar (Poon & Chan, 2006). Consequently, understanding the original concrete characteristics

and the composition of RCA are important factors for the efficient use of the aggregate in the pavement structure.

The strength and performance properties of an aggregate used in pavement structures are dependent on the physical properties and characteristics of the aggregates. Recycled concrete aggregate is generally composed of 65-70% natural aggregate and 30-35% cement mortar by volume (Zhang, et al., 2015). The properties of these components directly influence the strength and performance of RCA used in an unbound layer or non-continuously bound layer. This section outlines the main properties and characteristics of RCA that have the most influence on the response of the aggregate when subjected to loading. These properties include the aggregate composition, particle shape and texture, particle size distribution and moisture-density relationship. In other words, the goal is to have an understanding of the RCA properties for use in pavement structures as an unbound granular layer and potential for stabilisation with bitumen.

2.2.1 **Aggregate Composition**

Recycled concrete aggregate is highly variable as it originates from different types of concrete ranging in strengths emanating from various structural elements. The basic compositions of RCA are natural aggregate, sand and hydrated cement. These components form the mortar and in some cases active latent cement (Pasandín & Pérez, 2015). The type of natural aggregate and chemical composition of the aggregate will have a direct influence on the RCA properties. Natural aggregates commonly used in concrete are categorised into two forms: coarse or stone and fine or sand. The stone types vary from quartzite, sandstone, dolerite, andesite and granite (Alexander *et al.*, 2009). Varies types of non-cohesive sands from weathered rocks are suitable for use in concrete. These sands originate from rivers, beaches, dunes or quarries (Alexander *et al.*, 2009). The most important aspect regarding the type of aggregate is that it must be chemically inert and not react with water or the cement.

There are numerous types of cements available in the market, however, the most common type of cement for general use concrete is Portland cement (Alexander *et al.*, 2009). This basic form of cement is mainly composed of 63-69% calcium (CaC), 19-24% silicon dioxide (SiO_2), 4-7% aluminium oxide (Al_2O_3) and 1-6% ferric oxide (Fe_2O_3) (Alexander *et al.*, 2009). The mixing of cement with water results in a chemical reaction known as hydration. The products of the reaction are calcium silicate hydrate ($C_3S_2H_3$) and calcium hydroxide ($Ca(OH)_2$) along with residual unhydrated cement (Alexander *et al.*, 2009). These products

were found in three different commercially produced RCA in a study conducted by Limbachiya *et al.*, (2007). An X-ray fluorescence analysis of the RCA found components of 63-70% silica (SiO_2), 11-17% calcium oxide (CaO) and 3-5% alumina (Al_2O_3). The study concludes that similar chemical composition can be found in RCAs from different sources due to the generic mortar composition (Limbachiya *et al.*, 2007). However, users should be mindful of the chemical composition of RCA due to additives added to the concrete to improve the strength. In such cases, a complex chemical composition should be expected from the RCA.

Not only is it important to be aware of the chemical composition of RCA but the mortar content also plays an important role in the performance properties. The mortar content was found to have an adverse effect on the aggregate properties as studied by Sánchez De Juan and Gutierrez (2009). The study found that the higher the mortar content of RCA, the lower the bulk density, the higher the moisture absorption and Los Angeles abrasion as illustrated in Figure 2-9. The authors observed that the trend was mainly seen in the finer aggregates (Sánchez De Juan & Gutierrez, 2009).

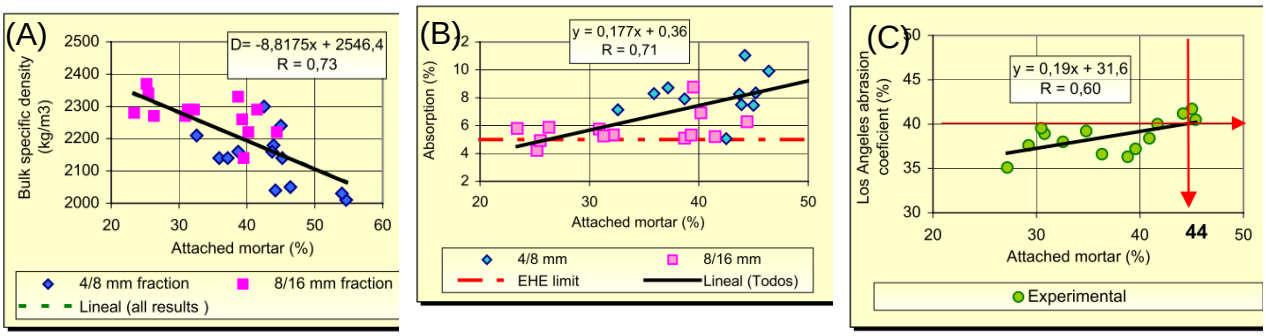

Figure 2-9: (A) Bulk specific density vs attached mortar content (B) water absorption vs attached mortar content (C) Los Angeles abrasion vs mortar (Sánchez De Juan & Gutierrez, 2009)

A similar study by Zhao *et al.*(2013) measured the mortar content of different RCA fraction sizes with a method they developed called salicylic acid dissolution. The authors found that the finer aggregates contained a higher mortar content than the coarse aggregates. This resulted from the breakdown of the mortar, which mainly constitutes of sand and cement breaking down to their original sizes during crushing therefore ending up in the finer aggregates. Consequently, an increase in water absorption and reduction in density occurs with a decrease in aggregate size due to the higher mortar content. However, the absorbency of the mortar on coarse aggregates could be improved with carbonation of the RCA as shown in a study done by Zhang *et al.* (2015). The study found that the production

of $CaCO_3$ and silica gel filled the pores in the attached mortar on the large aggregates. Which reduced water absorption and increased the dry density of the material. This means, a 4.7-5.6% increase in bulk density, a decrease in water absorption of 7.6-9.6% and 22.6-28.3% decrease in the crushing value occurred in comparison to un-carbonated RCA. In contrast, the study by Rudman (2019b) indicated that permeability of RCA decreases with carbonation. The important conclusions based on these studies include: carbonation does not necessarily improve the performance properties and it is clear that the type and content of mortar determines the quality of the RCA.

2.2.1.1 Cement Activity

The crushing of concrete breaks the bonds formed by the calcium silicate hydrate and exposes the unhydrated cement which forms as a component of the RCA (Addis, 1998). Once the RCA is exposed to moisture, secondary hydration occurs with the residual unhydrated cement resulting in cementation (Alexander *et al.*, 2009). Previous studies have reported on the improvement of strength with an increase in curing time of RCA specimens thus the RCA self-cemented (Cleghorn, 2015; Marradi & Lancieri, 2008; Paige-Green, 2010; Rudman & Jenkins, 2015). Paige-Green (2010) found that the residual latent cement resides in the mortar and the finer aggregates of the RCA. The residual latent cement content in RCA is dependent on the treatment of the aggregate prior to use. However, reactions such as carbonation and pre-soaking of the aggregates result in the reduction of the latent cement content (Bredenkamp, 2018). The potential to self-cement can be measured indirectly by the change in pH. A reduction in the pH indicates a low latent cement content in the RCA to react with water for hydration.

The measurement of the pH of a solution with RCA is one method that can be used to determine the presence of residual latent cement. Paige-Green (2010) states that a pH between 9 and 13, of a solution made from various types of RCA with different ages, indicated cement activity however not the extent. The findings presented in Figure 2-10 (A) show the measured pH and the increase in the unconfined compressive strength (UCS) from a comparison between specimens cured for 28 and 56 days as illustrated by Figure 2-10 (B). For this reason, the high pH indicates a high content of latent cement in the samples resulting in self-cementation. Therefore, it is of importance to test for the presence of the residual latent cement in RCA prior to use.

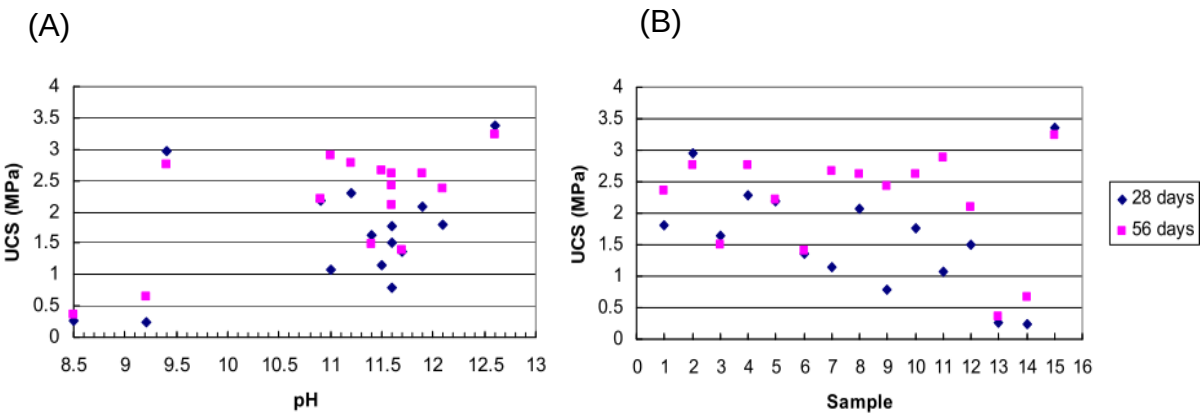

Figure 2-10: (A) Plot of UCS versus pH and (B) UCS for each sample tested after curing for 28 and 56 days in humid room (Paige-Green, 2010)

Other potential indicators that can be used to test the residual latent cement are: phenolphthalein alcohol solution and hydrochloric acid. These methods indicate the potential for self-cementation by reacting with the calcium silicate (Cleghorn, 2015). The phenolphthalein causes the RCA aggregate to turn pink when there is active cement and the colour gets darker with higher contents of cement as illustrated in Figure 2-11. Cleghorn (2015) reported the higher the content of cement the greater the increase in shear properties. Unfortunately, no studies have been carried out on the degree of influence self-cementation has on the performance properties such as shear moreover the addition of cement which is typically used in BSMs.

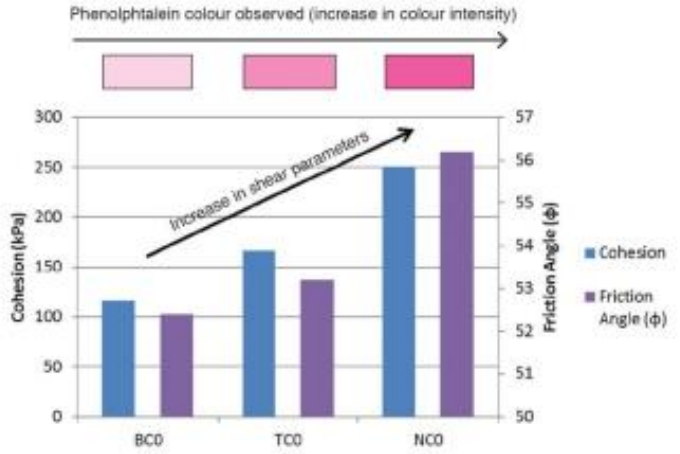

Legend

BC0: Concrete from old railway sleepers

TC0: Concrete from an old high-rise building

NC0: Fresh concrete made in the

Figure 2-11: Relationship between cement indicator and shear properties of different types of RCA. (Cleghorn, 2015)

2.2.2 **Particle Shape and Texture**

The original concrete compressive strength influences the physical properties of the crushed RCA, more specifically the shape and texture. These physical properties of any typical aggregate used in an unbound base layer, contribute to the shear strength and resistance to deformation induced by loading (Janoo, 1998). A study done by Nataatmadja and Tan (2001) found that the compressive strength of the parent concrete of RCA directly influenced the shape of the crushed RCA. A high compressive strength concrete produced aggregates with a higher flakiness index. The particle shape of RCA is inevitably expected to be either irregular, angular or elongated with a rough porous texture due to crushing and the texture of the mortar (Pickel, 2014). In addition, a study done by Koper *et al.* (2017) found that RCA produced from concrete with high compressive strength generated less fine aggregates as a result of the high crushing strength. The aggregates also had a lower moisture absorption and higher density. The compressive strength is dependent on the type of cement used and the water-cement ratio of the concrete that produced the mortar on the aggregates. This factor will have an impact on the final particle size distribution after crushing.

The type of crusher used to break down the parent aggregate plays a role on the particle shape, grading and fines generated (Alexander *et al.*, 2009). The most common methods used to crush aggregates include the jaw crusher, cone crusher and impact crusher. Other typical types of crushers used include roll crusher, gyratory crusher and rod mill. The jaw and cone crushing mechanism is based on applying compressive forces to break the aggregates against a stationary plate with a set gap for the required maximum aggregate. This type of crushing breaks the aggregate along the weak plane hence for softer aggregates, flat and elongated particle shapes are produced (Brown & Marek, 1996). The impact crusher throws the aggregates against each other and to the sides of the crusher at a high speed which produces cubical shaped particles (Van Dam *et al.*, 2011).

Research done by Van Niekerk (2002) found no relationship between the mechanical behaviour of RCA mixed with masonry when crushed with an impact crusher versus jaw crusher. This result is due to the similarity of the crushing mechanism where the crushing breaks the aggregate along the weaker plane therefore, similar particle shapes were generated. Leite *et al.* (2011) found that RCA particle shapes were cubic while, ceramic material such as bricks and roof tiles formed flat particles when crushed with a jaw crusher. A study by Arshad and Ahmed (2017) explains that a combination of crushers work well to produce the required particle size distribution and optimum shape for reclaimed asphalt pavement (RAP). The impact crusher works better on its own whereas in other cases, a

combination of the jaw crusher and roll crusher is used to reduce the particle size and obtained the required particle size distribution for CDW (Arshad & Ahmed, 2017). The compressive strength of the recycled concrete will determine the final aggregate shape as crushing occurs on the weak plane, therefore, for RCA it will be in the mortar between the aggregates.

The shape and texture of aggregates also influences the density, which affects the resilient modulus and resistance to deformation under loading. Naturally cubic shaped aggregates with rounded corners and smooth surfaces, decrease the aggregate packing reducing the density of the material (Barksdale & Itani, 1989). A study by Nataatmadja and Tan (2001b) showed that recycled aggregates with flakier shapes resulted in a lower resilient modulus and higher deformation due to breakage of the aggregates under repeated loading. The compressive strength of the original concrete influenced the shape of the particles, measured with the flakiness index, as demonstrated in Figure 2-12 . Therefore, the higher the compressive strength of the original concrete the flakier the aggregates generated which result in a lower resilient modulus under repeated loading.

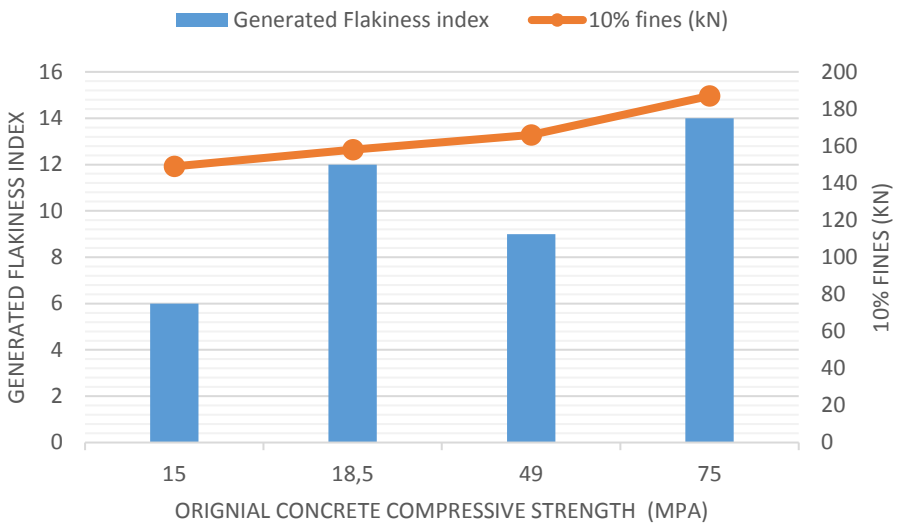

Figure 2-12: Influence of the original concrete compressive strength on the flakiness index of the aggregates and the 10% fines (Nataatmadja and Tan, 2001b)

Furthermore, the study by Leite *et al.* (2011) found that cubic shaped RCA with a rough surface texture provide an enhanced resistance to breakage during compaction and superior strength due to the high density achieved during compaction. In contrast, the crushing of ceramic materials, such as bricks, produced flat elongated aggregates, which further broke down during compaction and loading. However, a study done by Cook (2015) focused on how the particle shape effected the performance of a base layer. The result of the study

showed that the particle shape had a major effect on open graded layers and a minor effect on the performance of dense graded layers. Therefore, the shape of the RCA will not have a major effect for a continuous grading. However, the flakier RCA will affect durability of the layer due to the breakage of the aggregate during compaction and under loading.

2.2.3 **Particle Size Distribution**

The particle size distribution commonly referred to as grading, influences the packing of the aggregates during compaction. This affects the required performance for any unbound or non-continuously bound layer as discussed in Section 2.1.3.1. The grading specifies the maximum particle size, relative distribution of the particle sizes and the filler content (<0.075 mm) of an aggregate mix (SANRAL, 2014). The grading can be categorised as coarse or fine with methods such as the grading modulus, grading coefficient, median size and uniformity coefficient (Paige-Green, 1999). Moreover, classifications of the grading include gap graded, uniformly graded or continuously/densely graded. These grading classifications are generally compared to the ideal grading curve determined from the Talbot's equation which indicates how the packing will influence the void content, as a result the density of the specimen/layer (Talbot & Richart, 1923).

The Talbot grading curve is a theoretical grading that produces minimum voids and optimum packing to achieve the maximum density with a granular material when n = 0.45 or 0.5 based on Fullers work (Richardson, 2005). Furthermore, Nijboer showed that the optimum void content for granular materials can be achieved at n = 0.45 as illustrated in Figure 2-13. The South African Pavement Engineering Manual (SAPEM) uses the Talbot grading curve with Nijboer's grading exponent (Equation 2-3) and the grading modulus (Equation 2-4) to categorise, classify and compare different sets of gradations.

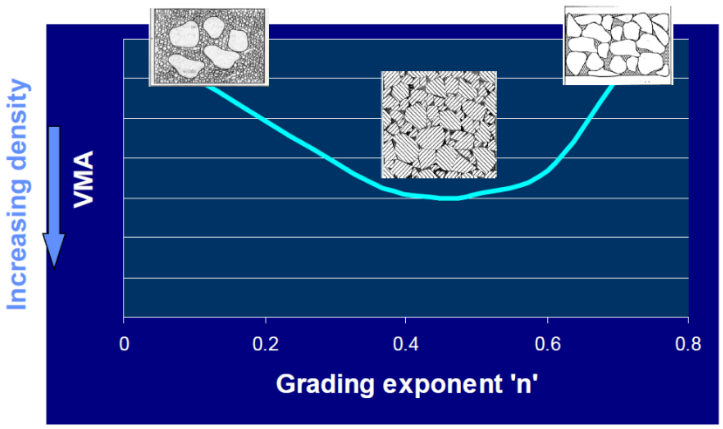

Figure 2-13: Optimum grading exponent (n) for the lowest void content in a graded material (Dr Rudman & Prof Jenkins, 2019)

The grading modulus (GM) determines the total percentage of the aggregates passing the 2.0, 0.425 and 0.075 mm sieves to the total mass of the aggregates. A GM value of 3 indicates a coarse grading which would result when no aggregates pass the 2 mm sieve (Paige-Green, 1999). Therefore, these equations (SANRAL, 2014) can be used to compare different gradations generated from different crushing methods. In Equation 2-3, p = percent passing, d = sieve size, D = maximum particles size and n = grading exponent. Whereas, Equation 2-4, P2.00, P0.425 and P0.075 mm = aggregate percentage passing the indicated sieve size.

$$p = 100\left(\frac{d}{D}\right)^{n} \qquad \text{Equation 2-3}$$

$$GM = \frac{300 - (P2.00mm + P0.425mm + P0.075mm)}{100} \qquad \text{Equation 2-4}$$

The study done by Van Niekerk (2002) demonstrates the influence of grading on the mechanical response and performance properties of RCA mixed with 35% masonry. The gradations tested ranged from fine to coarse based on the Dutch specification grading curves for granular materials namely: fine grading (UL), continuously graded (CO), uniformly graded (UN), average grading of upper and lower limit (AL), coarse grading (LL) and Talbot grading curve (FL) with n = 0.45. The study determined and compared the moisture-density relationships of all the gradations as demonstrated in Figure 2-14. The resultant maximum dry density of the samples ranged from 1590 kg/m^3 to 1755 kg/m^3.

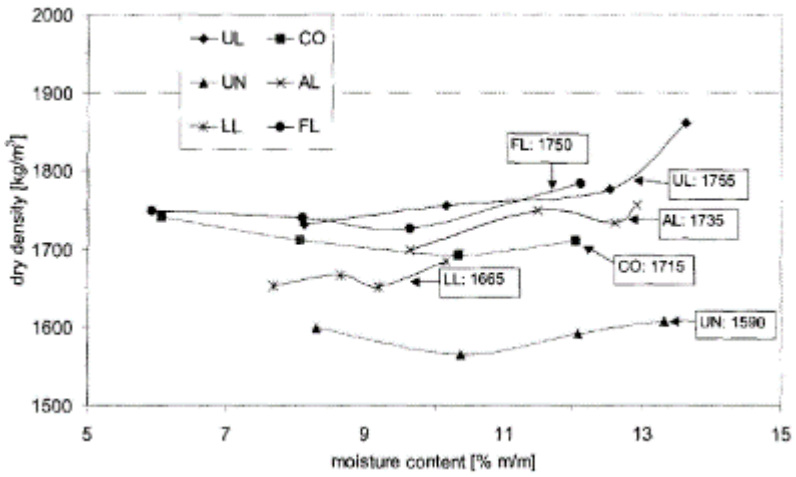

Figure 2-14: Dry density moisture relationships for 65%RCA and 35%Masonary for different gradations. (Van Niekerk, 2002)

The highest dry density was obtained for FL and UL as 1750 kg/m^3 and 1755 kg/m^3 respectively. This confirms that the Talbot grading curve, with n = 0.45 according to Fullers work, continues to produce the optimum density for recycled materials such as RCA as it

does for typical granular materials. The author noted that the high density determined for UL was as a result of good packing of the fine aggregates in the test moulds (Van Niekerk, 2002). The grading requirement for RCA corresponds to the required grading for a specific performance similar to that of natural crushed aggregate for use in an unbound granular layer.

2.2.3.1 Fine Content

Even though a fine grading, constituting mainly aggregates passing the 4.75 mm sieve, packs well when compacted resulting in a high density, there are aspects such as surface area, plasticity and type of fines that reduce the performance properties. Filler on the other hand is defined as the aggregate size smaller than 0.075 mm. This fraction size makes a paste when mixed with water. As a result an increase in the cohesion occurs which improves interlock between the coarse aggregates by filling the gaps. However, there is a limit on the filler content required due to their large surface area (Molenaar, 2010). An increase in surface area of an aggregate mix results in an increase in moisture required for mixing and compaction. Van Niekerk (2002) noted a similar behaviour where the fine grading (UL) achieved the highest density at the highest moisture content.

On the other hand, fine aggregates are sensitive to changes in moisture and this property is quantified by the plasticity index i.e. PI (Craig, 2013). Plasticity is an important aspect because it indicates how the fine particles react or to what extent they change form with variations in the moisture content. For instance, clay particles typically have a high PI subsequently, they change form at certain moisture contents. The variation in moisture content results to changes in volume of the layer where either shrinkage or swelling occurs. However, in the case of RCA, the fines have been found to be none plastic because concrete requires the use of non-cohesive sands as the fine aggregates (Alexander *et al.*, 2009). There have been reports on the fine particles of RCA sensitive to changes in moisture content. These aspects along with the type of fines affect the performance properties of the mix and the sensitivity of the layer to changes in moisture content.

A study conducted by Poon and Chan (2006) focused on how the type of recycled filler influenced the dry density and moisture content of a mix with RCA and masonry. The mixes referred to as series 1 contained filler produced from RCA, and series 2 mixes contained filler produced from masonry as demonstrated in Figure 2-15. The authors found a high correlation between the type of filler and moisture density relationship. Where filler produced from RCA (series 1) achieved higher densities at lower moisture contents.

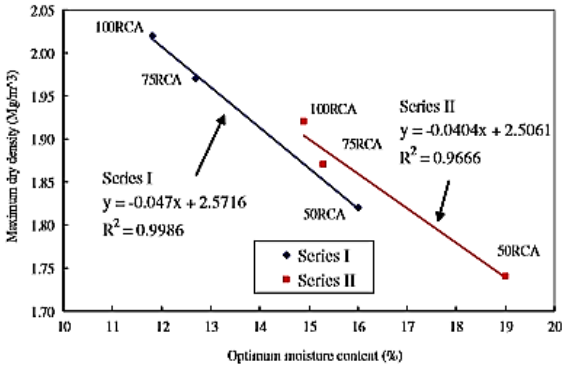

Figure 2-15: Relationship between types of fines(Poon & Chan, 2006)

Furthermore, a similar study looked at replacing the filler with either sand, cement or clay in mixes with RCA. An investigation on how the type of filler influenced the density and moisture content of the mixes with RCA showed that the type of filler played a role in the resultant density and required moisture content as demonstrated in Figure 2-16 (Boudlal & Melbouci, 2009). For that reason, the type of filler used in a grading has a significant role in the outcome properties of the mix. This is important for stabilisation with bitumen because a high filler content results to a higher bitumen content. As previously discussed in Section 2.1.3, a low-density results in a lower resistance to loading due to less contact between the coarse aggregates therefore a reduction in the performance properties.

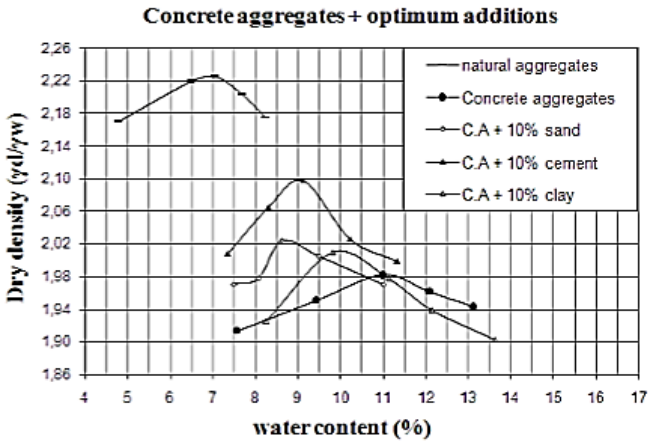

Figure 2-16 Influence of type of fines on the density and water content of RCA.(Boudlal & Melbouci, 2009)

Van Niekerk (2002) measured the internal angle of friction, on mixes with the different gradations (UL, CO, UN, AL, LL, FL) previously mentioned. The highest internal angles of friction measured were 46º, 45.2º and 43.4º for the following gradations: AL, CO and FL as illustrated in Figure 2-17(A). The author concluded that the internal angle of friction is dependent on a balanced content of the coarse and fine aggregates. However, the cohesion

was dependent on the fine content and the curing time of the mixes. This is evident from an analysis of the results obtained for UL and AL which are gradations containing a higher filler content. The specimens achieved an increased cohesion from 49 to 94 kPa and 46.4 to 81.8 kPa after 28 days of curing as demonstrated on Figure 2-17(B). A well-graded sample is the best option for RCA to be used in an unbound granular layer because grading plays an important role in the density and performance properties of the material (Van Niekerk, 2002). The next section gives a detailed discussion on the moisture density relationship of RCA in comparison to typical granular aggregates and other factors that influence this relationship.

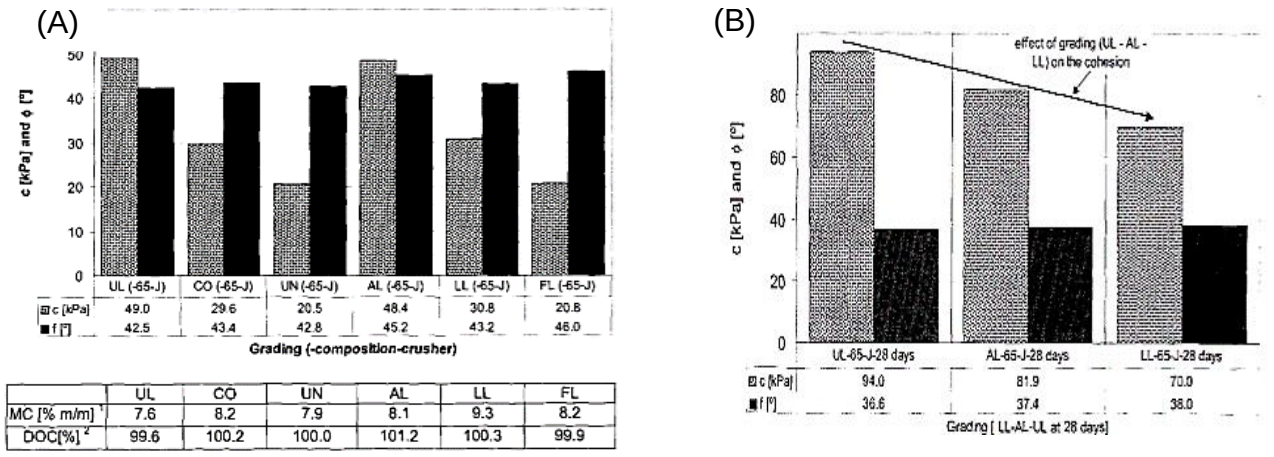

	UL	CO	UN	AL	LL	FL
MC [% m/m] [1]	7.6	8.2	7.9	8.1	9.3	8.2
DOC[%] [2]	99.6	100.2	100.0	101.2	100.3	99.9

Figure 2-17 Shear properties of 65% RCA and 35% Masonry at different grading tested immediately after compaction (A) and 28 days after compaction (B) (Van Niekerk, 2002).

2.2.4 **Moisture content and maximum dry density**

Natural crushed aggregates or gravel, depending on the grading, requires less moisture to reach the maximum dry density in comparison to recycled aggregates as illustrated in Figure 2-18 (A). Recycled aggregates, including RCA, require a higher moisture content ranging from 11 to 19% as determined by Poon and Chan (2006) and Van Niekerk (2002). Due to the higher porosity found in recycled aggregates, with increasing content of mortar and masonry, lower densities are achieved (Figure 2-18 A). Whereas, for natural aggregates the density versus moisture relationship typically described by an increases in density as the moisture content increases. Moreover, a decreasing density once the maximum dry density has been achieved at the optimum moisture content (Molenaar, 2010).

Interestingly, the density versus moisture relationship for RCA has been found to be similar to that of natural aggregates (Poon & Chan, 2006). However in some instances, the density does not decrease with increasing moisture due to the high porosity as shown by Figure 2-18 B (Van Niekerk, 2002). Van Niekerk (2002) also noted that water drained out of

specimens mixed at high moisture contents during compaction. As a result, the moisture in the specimen at compaction was less than the water added at mixing. This finding indicates that care is required during mixing and compaction for the determination of the optimum moisture content of porous RCA. The compaction method used to compact a typical crushed granular aggregate influences the resultant maximum dry density achieved at an optimum moisture content, this factor serves to be true for RCA.

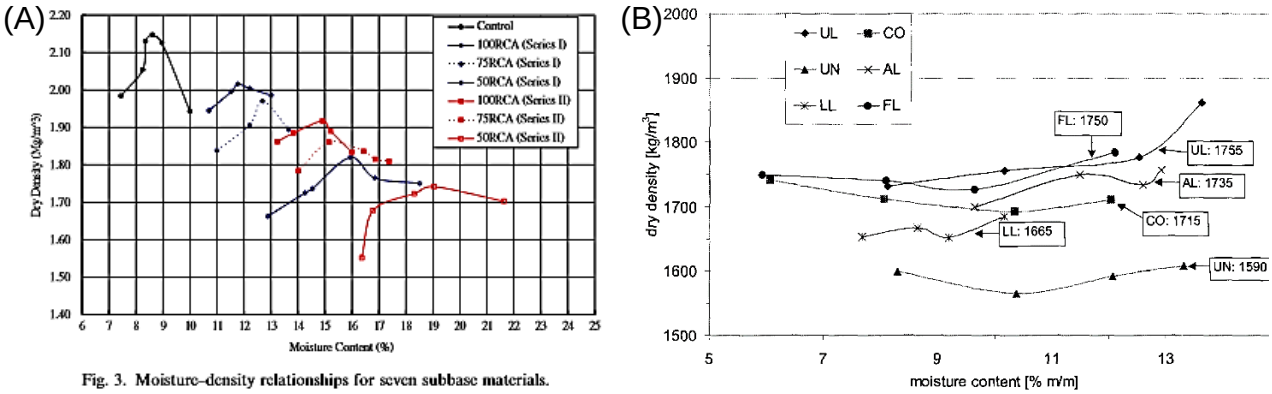

Figure 2-18: (A) Density vs Moisture relationship for recycled concrete and masonry in comparison to natural aggregate.(Poon & Chan, 2006) vs Moisture relationship for RCA and masonry at different gradings (Van Niekerk, 2002)

Different laboratory compaction methods influence the density achieved, for a given grading, due to the applied compaction effort (Molenaar, 2010). These various types of compaction methods apply varying degrees of compaction energy to the material. Methods typically used for unbound materials include the modified Proctor, vibratory hammer and the gyratory compactor. Samples compacted with a vibratory compaction method resist more deformation than specimens compacted with an impact force such as the modified Proctor (Hoff et al., 2004). The study by Leite et al. (2011) on recycled construction demolition waste (RCDW) highlighted that an increase in the degree of compaction resulted in a higher dry density at a lower moisture content as demonstrated in Figure 2-19. Additionally, the better compacted the specimen-, the lower the void content that plays a vital role towards the resistance against moisture damage. In this case, the resilient modulus of the specimen improved and the permanent strain was reduced (Leite et al, 2011).

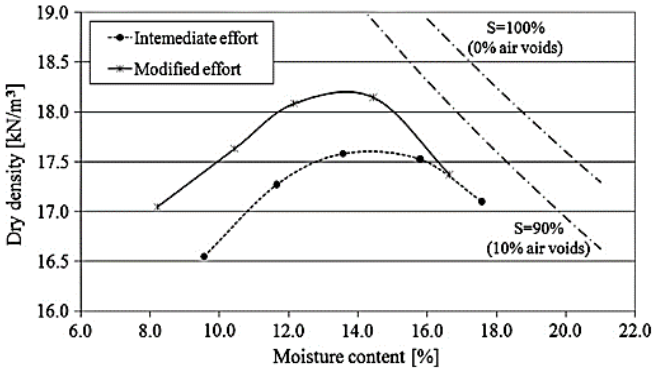

Figure 2-19: Relationship between moisture content and dry density for the RCDW aggregate compacted at two different efforts. (Leite *et al.*, 2011a)

Furthermore, Van Niekerk (2002) also showed that the maximum dry density of RCA and masonry increases as the degree of compaction increased resulting in higher shear strength, resilient modulus and reduced permanent deformation. Research findings by Barisanga (2014) also points towards an increase in the degree of compaction results in an increase of the shear properties and resilient modulus of the specimens made with RCA and masonry.

However, there is a limit on the degree of compaction that can be applied on different types of aggregates before crushing occurs (Molenaar, 2010). This proves to be true for recycled aggregates where a higher compaction energy results in crushing of the aggregates. The crushing results in a change in grading shown by the upward shift of the grading curve as illustrated in Figure 2-20. An increase in the fine contents was seen, which increased the density of the material due to better packing in the mould (Leite *et al.*, 2011a). Van Niekerk (2002) concluded that the degree of compaction had the most influence on the mechanical behaviour of RCA mixed with masonry, followed by the grading and composition of the material.

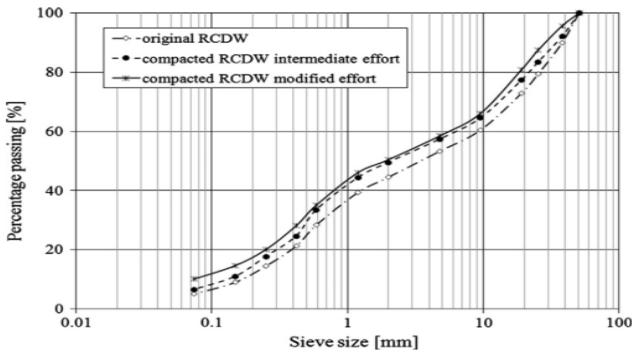

Figure 2-20: Particle size distribution curves of Recycled construction demolition waste (RCDW) before and after compaction (Leite *et al.*, 2011a)

The mechanical behaviours such as the California Bearing Ratio (CBR) is an important measured property for unbound granular materials. The CBR of an aggregate mix is an indicator of the bearing capacity to applied compressive stresses which result in the shear failure of a specimen in a steel mould (Lewis *et al.*, 2013). The CBR generally increases at higher degrees of compaction and reduces at high moisture content in the specimen. The 4 day soaked CBR of a potential aggregate for BSM is of interest and a minimum CBR of 10% is specified for a BSM 3 layer (Asphalt Academy, 2009). A BSM 3 layer is the lowest quality of the 3 BSM layers that can be produced guided by the TG2. The BSM 3 layer is made from low quality aggregate such as soil, gravel or sand and can only be used in the base layer of pavements that carry traffic loading less the 1 million equivalent standard axles (MESA).

According to Van Niekerk (2002), the 4 day soaked CBR of RCA and masonry increased with the application of higher degrees of compaction. Poon and Chan (2006) also found that no reduction occurred on the 4 day soaked CBR of RCA in comparison to the unsoaked CBR. Typical natural aggregates bearing capacity is reduced by moisture as seen in Figure 2-21 A. The above finding is consistent with the study by Behiry & El-Maaty (2013), whereby no reduction occurred on the 4 day soaked CBR of RCA in comparion to the CBR of natural aggregates (Figure 2-21 B). The CBR of RCA determined by both authors ranged from 62 to 66% which is higher than the minimum CBR required for BSM 3 layer. These findings suggest that in general, RCA is resilient to loss in strength induced by moisture and that the CBR obtained will qualify the material for use as a potential aggregate for BSM.

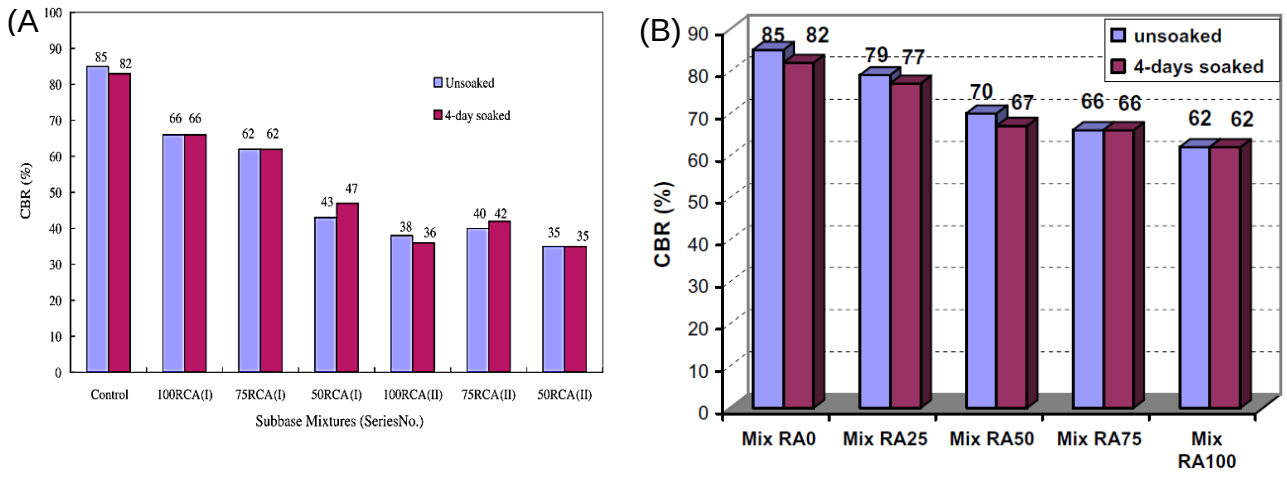

Figure 2-21: A comparison of soaked and 4 day unsoaked CBR of natural aggregates and various mixes of RCA (A) (Poon & Chan, 2006) (B) (Behiry & El-Maaty, 2013)

2.2.5 **Performance Properties of RCA Improved with Bitumen Stabilisation**

So far, the physical properties and characteristics of RCA discussed in the sections above, indicate the potential use of RCA in an unbound granular subbase layer for medium to low traffic roads (Ardalan *et al.*, 2016).

2.2.5.1 Enhancement methods

Nevertheless, an enhancement of the performance properties of RCA can potentially eradicate the limit on its use and increase the pavement life. Numerous studies have examined the various potential uses and means to treat RCA/CDW in order to improve performance. The following experiments were done: RCA stabilised with cement (Behiry & El-Maaty, 2013), use of RCA in concrete for structures or pavements (Yang *et al.*, 2010), use of RCA in hot asphalt mixes (Pasandín & Pérez, 2015), use of CDW in cold asphalt mixes (Gomez-Meijide *et al.*, 2016) and stabilisation of RCA and Masonry with foamed bitumen (Saleh, 2000). For each treatment, unique challenges manifested due to the inherent variability of RCA and the attached mortar. For this reason, further studies are required to produce suitable practical mixes with RCA for better uses. The focus of this research investigates the performance properties of RCA stabilised with bitumen emulsion or foamed bitumen to make a BSM.

Cold in-situ recycling is the common reference to construction methods such as BSMs and cold asphalt mixes. These terms are sometimes used interchangeably due to similarity in benefits (Mollenhauer *et al.*, 2016). In various countries, cold in-situ recycling is defined differently depending on the bitumen content and active filler added to the recycled aggregates. An example of such, are countries in Europe, which use different names as illustrated by Figure 2-22. These cold in-situ recycling methods typically consume less energy and, in most cases recycle existing materials. However, the TG2 describes a BSM as a mixture of aggregates stabilised with bitumen emulsion or foamed bitumen with contents not exceeding 3% of the total dry mass of the aggregate (Asphalt Academy, 2009). The aggregates can be either naturally sourced or recycled. If required, the TG2 permits the addition of an active filler such as cement or lime, with a maximum content of 1% to the dry mass of the aggregate. Due to the recycling capability of a BSM, the method is regarded as environmentally sustainable and energy efficient for road rehabilitation (Wirtgen Group, 2017).

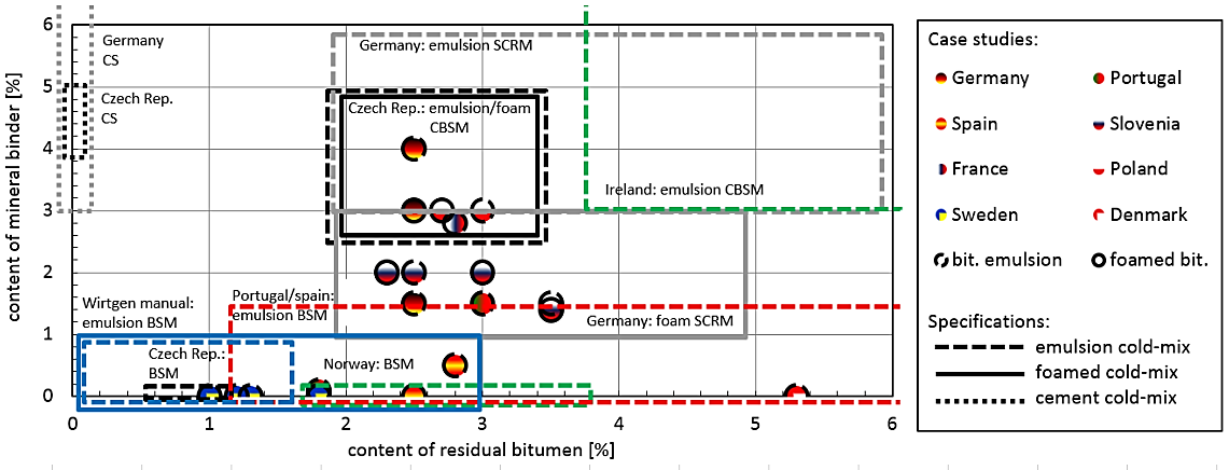

Figure 2-22: Summary of the use of bitumen stabilisation across Europe (Mollenhauer *et al.*, 2016)

Conversely, cold recycled asphalt mixes (CAM) contain a higher bitumen content in comparison to BSMs. Mollenhauer *et al.*(2016) summarizes the product produced, shown in Table 2, from different ranges of bitumen content and active fillers. A high bitumen content results in mixes with stiffness values in the range achieved by hot asphalt mixes (HAM). Consequently, the resultant behaviour differs from that of a BSM. This was also highlighted by Mollenhauer *et al.*(2016) in a comprehensive review of the various methods used in Europe to produce cold recycled asphalt mixes. The review shows each recycled mix behaviours differently. As a result, different design methods for the layers would be required. Furthermore, literature on the stabilisation of RCA to produce a BSM are limited. However, research on cold asphalt mixes on recycled aggregates give insight on the potential of RCA as a BSM.

Table 2: Cold recycling treatment methods based on bitumen and mineral binder content (Adapted from, Mollenhauer *et al.*(2016)

COLD RECYCLING MATERIAL: DEFINITION	RESIDUAL BITUMEN CONTENT ADDED (%)	CONTENT OF MINERAL BINDER (%)
CEMENT STABILIZATION (CS)	0	1 to 6
LEAN CONCRETE (LC)	0	>6
BITUMEN STABILISED MATERIAL (BSM)	1 to 3	<1
BITUMEN CEMENT STABILISED MATERIAL (BCSM)	1 to 3	1 to 3
COLD ASPHALT MIX (CAM)	>3	0
SEALING COLD RECYCLED MATERIAL (SCRM)	3 to 6	1 to 6

2.2.5.2 Strength and performance properties tested

Several studies investigated the stabilisation of CDW with bitumen emulsion ranging from 2% to 6% (Gomez-Meijide & Perez, 2013, Gomez-Meijide & Perez 2015, Gomez-Meijide *et al.*, 2016). The results show an improvement in the strength properties of the CDW, composed of 70% RCA, 25% natural aggregate and 5% impurities. The addition of bitumen increased the UCS, ITS and moisture susceptibility of the stabilised CDW. However, higher bitumen and water contents were required for CDW in comparison to hornfel as illustrated by Figure 2-23. The study also highlights that a slight change in the grading of CDW occurred during compaction, which supports the brief review previously discussed on the physical properties of RCA in Section 2.2.3. Furthermore, Gómez-Meijide and Pérez (2013) showed that the water at mixing was an important aspect due to the high absorption of CDW resulting in premature breaking of the bitumen emulsion therefore reducing the resultant strength properties.

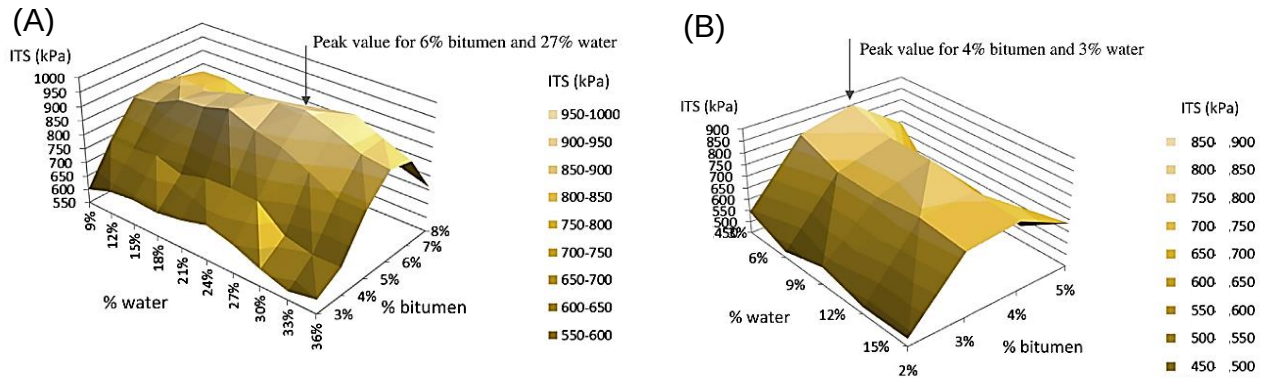

Figure 2-23: Indirect Tensile Strength (kPa) of cold asphalt mixes with (A)100% CDW and (B) 100% hornfel at different bitumen and water contents (Gómez-Meijide & Pérez, 2013)

In another study, Gomez-Meijide *et al.*(2016) examined how the curing period influenced the stiffness of mixes with construction demolition waste aggregate (CDWA) stabilised with bitumen emulsion at contents ranging from 3% to 8%. The results show that the longer the curing period, an increase in the indirect tensile strength modulus (ITSM) of the specimen occurred (Figure 2-24). Moreover, higher ITSM occurred for mixes made with CDWA when compared to mixes made with natural aggregate (NA) hornfel. These ITSM values are extremely high for a bitumen-stabilised material. Therefore, these mixes would be similar to a bound layer with a high load spreading ability such as HSM.

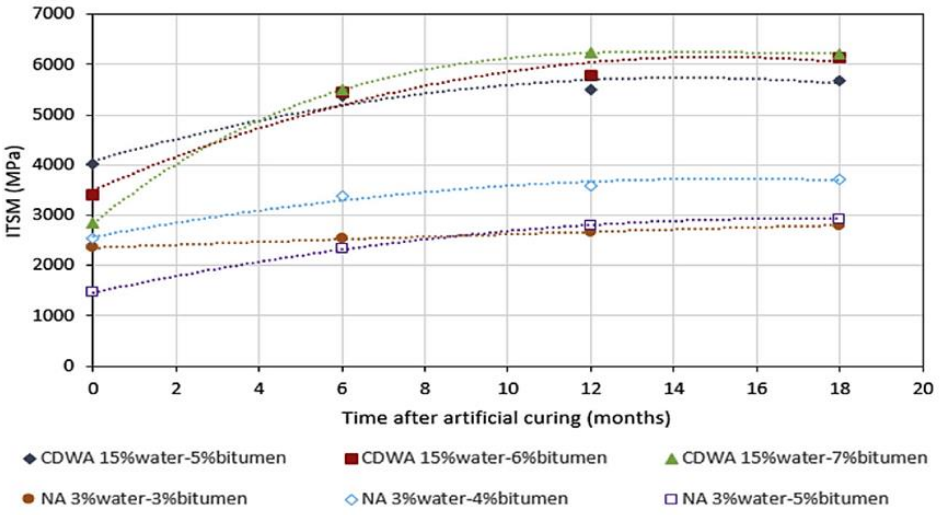

Figure 2-24: Indirect tensile strength modulus (ITSM) increase for six mixes measured a varying curing periods(Gomez-Meijide *et al.*, 2016)

In a different study, Gómez-Meijide and Pérez (2015) further investigated the influence curing had on the shear parameters of stabilised CDWA and NA (hornfel). A comparison of the failure envelops obtained for specimens not cured from CDWA stabilised with 6% bitumen content while, 4% was used for hornfel. The comparison shows that a better outcome was obtained for the hornfel specimens. However, after 3 days of curing, the shear parameters of CDWA improved to match those achieved by NA cured for the same period as demonstrated in Figure 2-25. In addition, the CDWA specimens resulted in an approximately 100% increase in the cohesion from 219.27 kPa to 388.71 kPa. This demonstrates the speculated presence of latent cement in CDWA. However, no pH test was done for this material to provide evidence. The use of CDWA proves to be a suitable replacement for NA as the shear parameters increased with curing.

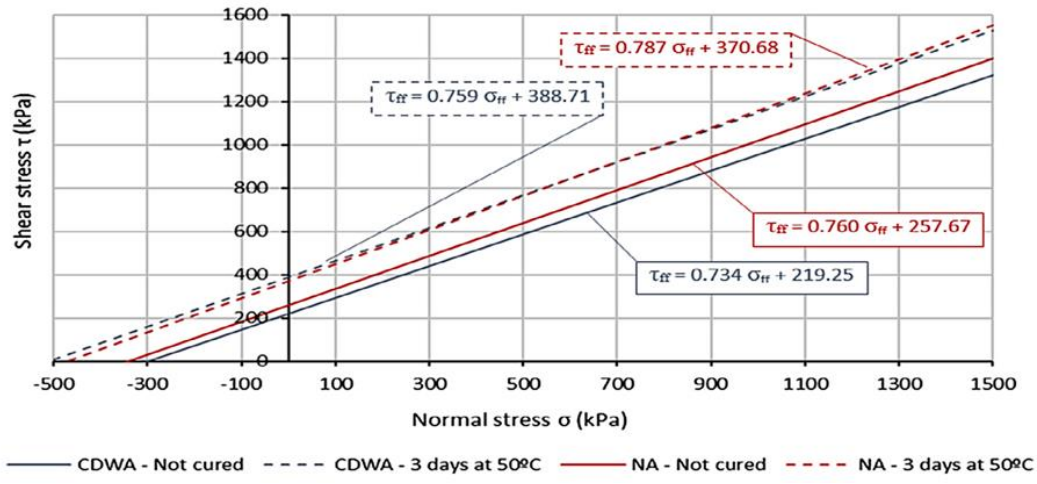

Figure 2-25: Mohr-Coulomb envelopes obtained for CDW stabilised with 6% bitumen and NA stabilised with 4% bitumen and cured for 3 days

An early study by Saleh (2000) performed an experiment focused on the stabilisation of a mixture of 78% RCA and 22% bricks (by mass) with foamed bitumen to make a BSM. The study found the optimum foamed bitumen content at 2% which resulted in an increase of the cohesion for the unbound mix from 165 kPa to 325 kPa. However, the addition of the foamed bitumen reduced the internal angle of friction of the unbound mix from 44.7º to 37º. The reduction of the internal angle of friction is a common occurrence with the addition of bitumen to aggregates. In addition, Jenkins (2000) produced a similar mix and found that a 100% increase in cohesion occurred for the mix with 78% RCA and 22% bricks stabilised with 2% foamed bitumen as illustrated in Figure 2-26 A and B. Furthermore, Saleh (2000) also revealed that stabilisation with foamed bitumen enhanced the fatigue properties of the RCA mix observed from the increase in the strain at break of the specimens.

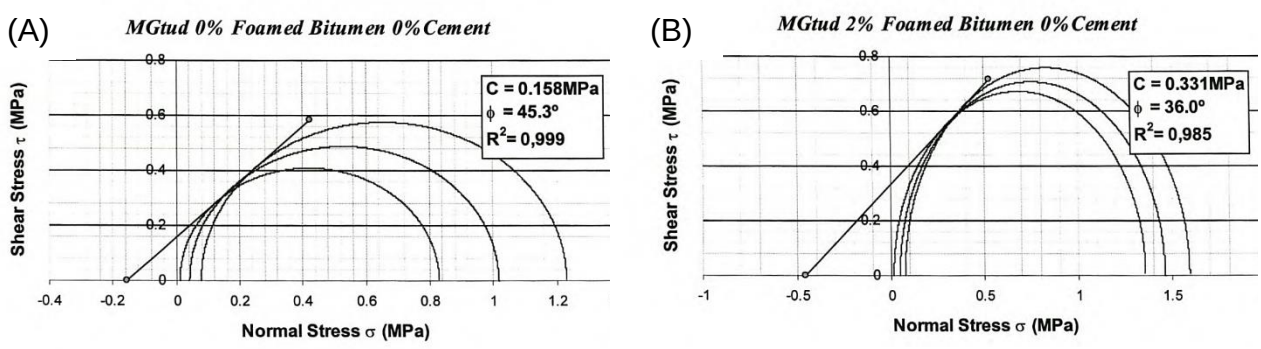

Figure 2-26: Mohr-Coloumb Plot of Monotonic Triaxial Tests on 78%RCA and 22% Bricks (A) Unbound and (B) 2% foamed bitumen stabilisation (Jenkins, 2000)

The resilient modulus of a CDWA stabilised with 6% bitumen emulsion was analysed and demonstrated a stress dependent behaviour as illustrated by Figure 2-27. As a result, the mix was not a bound layer due to the high bitumen content. Instead, this provides an indication of the absorption of the bitumen by the CDWA (Gómez-Meijide & Pérez, 2015). It appears from the aforementioned investigations that numerous studies focused on the stabilisation of CDWA with bitumen emulsion at high bitumen contents. However, the mixes based on the resilient modulus would behaviour similarly to BSMs but are sensitive to variation in temperature (Gómez-Meijide *et al.*, 2015). Therefore, the studies indicate potential to stabilise RCA with bitumen emulsion at lower bitumen contents excluding masonry.

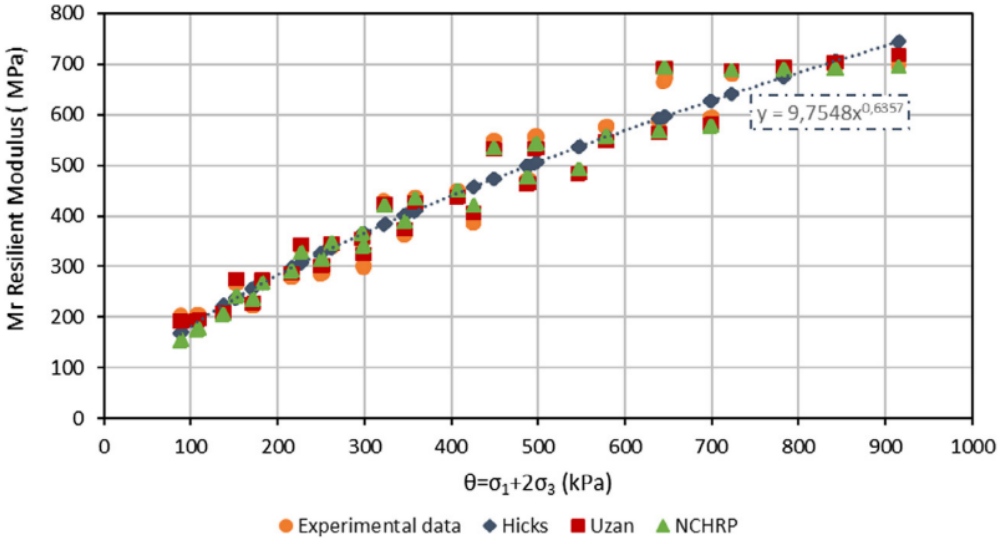

Figure 2-27: Resilient modulus model for CDWA stabilised with 6% bitumen emulsion (Gómez-Meijide & Pérez, 2015)

The life (load cycles) of a pavement layer is dependent on the shear parameters of the material which are linked to the rate of deformation under repeated loading . The typical deviator stress ratio (DSR) determined from the shear parameters for BSMs, produced from aggregates such as hornfels used in base layer of high traffic roads, ranges between 55% to 60% (Jenkins *et al.*, 2002). This parameter indicates the degree of distortion the aggregates can endure prior to shear failure (Rudman, 2019a). The study be Rudman, (2019b) analysed the permanent deformation from specimens produced from 100% RCA exposed to moisture and not exposed to moisture. The study aimed to determine the influence of moisture on the resilience of the aggregate to repeated loading. Therefore, the higher the DSR the more resilient the material is to repeated loading. RCA tested after 1 day of compaction destabilised at a DSR of 45% as shown in Figure 2-28 (A). In the case RCA is exposed to moisture for an extended period of time, the DSR was obtained as 27%; see Figure 2-28 (B). These studies highlight that although the durability of the RCA is affected by moisture, there is potential to improve the performance properties with bitumen stabilisation.

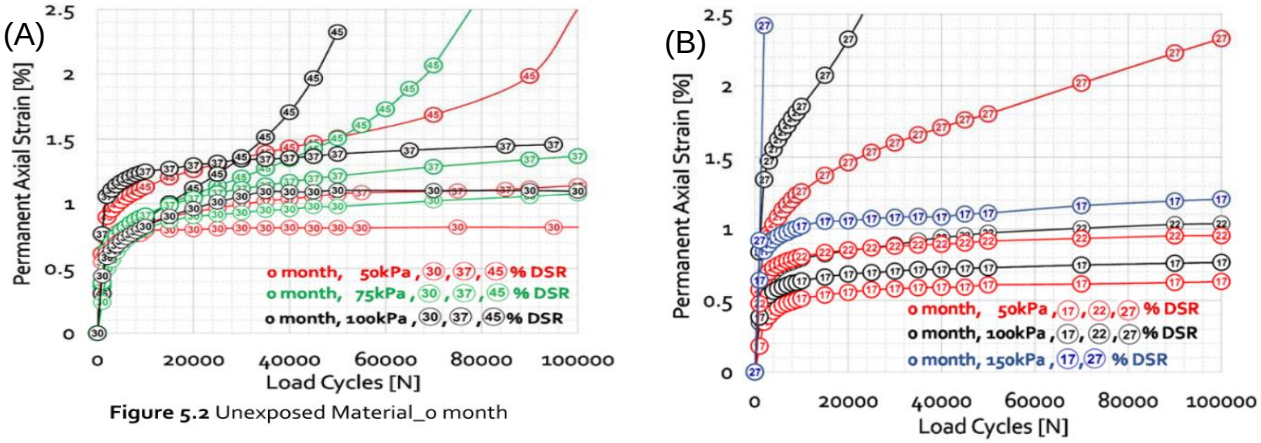

Figure 5.2 Unexposed Material_0 month

Figure 2-28: The influence changes in DSR with increasing confinement pressure on the permanent axial strain of RCA tested a day after compaction (A) Unexposed (B) Exposed (Rudman, 2019b)

The DSR for CDWA stabilised with 6% residual bitumen emulsion destabilied at 50% (Gómez-Meijide & Pérez, 2015). This investigation indicates that the addition of bitumen to the CDWA enhanced the resistence against deformation under repeated loading as illustrated on Figure 2-29. Consequently, the addition of bitumen increased the pavement life of CDWA to dynamic loading. The study concludes that the mix can be used in low to medium traffic roads

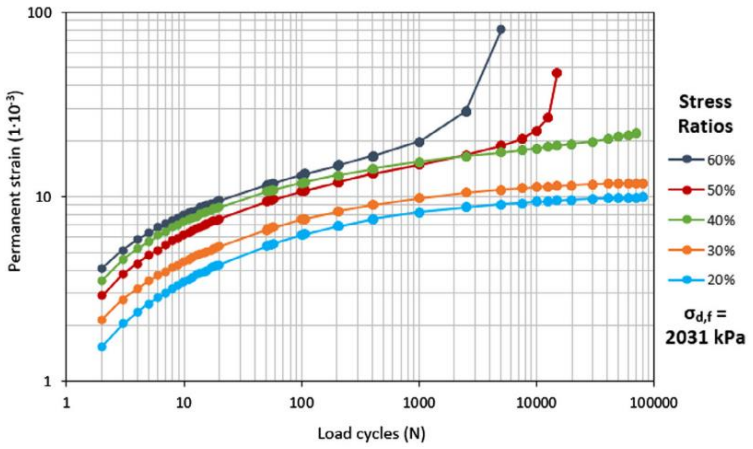

Figure 2-29:The influence of increasing stress ratio on the permanent strain of stabilised CDWA with an increase in the load cycles. (Gómez-Meijide & Pérez, 2015)

In summary, the studies discussed above indicate the potential to stabilise RCA with bitumen emulsion and foamed bitumen for use in pavement structures with high traffic volumes. Although the investigation examined the stabilisation of a mixture of RCA and Masonry, to the best of author's knowledge, no literature systematically describes the effect of foamed bitumen and bitumen emulsion stabilisation with RCA. For that reason, this served

as motivation for the present study and therefore general components of BSMs are further discussed.

2.3 Bitumen Stabilised Materials

Bitumen stabilisation is one method used to enhance the performance of weak pavement materials by increasing the load carrying capacity and durability of the aggregate mix (Marais & Tait, 1989). The mix is produced from the addition of bitumen up to a maximum content of 3% to the total dry mass of the aggregates and when required, active filler to a maximum content of 1% is added (Asphalt Academy, 2009). Because the bitumen does not completely cover the aggregates, the resultant product is a non-continuously bound material. This method has gained popularity in the pavement industry due to the demand to recycle existing aggregates and unlike hot asphalt mixes, the construction process requires less energy (Yan *et al.*, 2010). The main components of the mix include the binding agent, graded aggregates and active filler. Further details on the role of these components and the influence of variations on the behaviour of the mix are discussed.

2.3.1 **Binder Components and Characteristics**

The bitumen-stabilised materials (BSMs) made in Southern Africa, as guided by the TG2, are produced from two types of binders based on the most suitable for the available aggregate (Asphalt Academy, 2009). The binders used are bitumen emulsion and foamed bitumen mixed with aggregates at ambient temperatures. This section will briefly discuss the manufacture, important characteristics, binding mechanism with the aggregates and a summary of the advantages and disadvantages of each binder.

2.3.1.1 Bitumen emulsion components and production

An emulsion is a product of a chemical process used to mix two liquids that would naturally not mix on their own. An example of such is a bitumen emulsion, which is a mixture of bitumen and water (Hunter, 1994). The bitumen emulsion is produced in a batch plant or a continuous plant. In the plant, the bitumen viscosity is reduced with heat and milled into a water solution with an emulsifying agent in a colloid mill as demonstrated in Figure 2-30. The milling process breaks the bitumen into small droplets which are charged with ionized emulsifier to repel each other (Meyer, 1999). The type of bitumen emulsion is classified by the charged droplets, which can either be positively charged or negatively charged. Positively charged droplets produce a cationic bitumen emulsion and negatively charged droplets produce an anionic emulsion (Meyer, 1999).

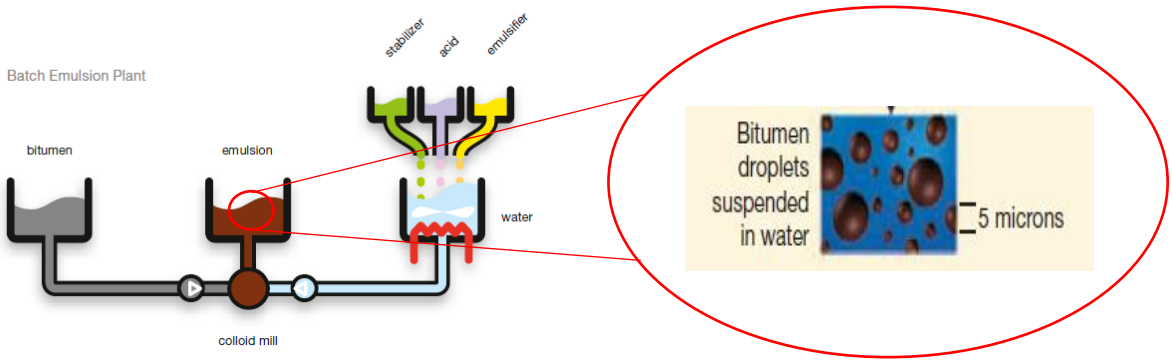

Figure 2-30: Production of bitumen emulsion and the resultant product (Adapted from, Meyer, 1999; Wirtgen Group, 2012)

The breaking rate of the bitumen droplets is a parameter used to measure the time required for the droplets to loss the charge and coalesce. The breaking of an emulsion results in the bitumen droplets returning to the original high viscosity nature at low temperatures (Asphalt Academy, 2009). A slow setting emulsion is used for mixes such as BSMs because breaking is desired after compaction. Whereas, a rapid setting emulsion is required for rapid strength gain mixes such as seals (Ebels & Jenkins, 2007b). Therefore, bitumen emulsion is a low viscosity bitumen used for road construction at ambient temperature and characterised by the charge of the droplets, the breaking time and the residual bitumen content.

In the production of a BSM, the binding between the low viscosity bitumen emulsion and aggregates occurs in various forms depending on the aggregate type and the characteristics of the bitumen emulsion. The binding process to form mastic is initiated when opposite charges attract between the finer aggregates (<0.425 mm) and the bitumen droplets (Collings & Jenkins, 2009). Furthermore, the binding process continues as the aggregates absorb the emulsifiers and water or the water evaporates into the atmosphere. Subsequently, the bitumen droplets release emulsion ions resulting in the breaking of the bitumen emulsion (Hunter, 1994). The bitumen emulsion partially coats the aggregates and acts as a lubricating agent during mixing and compaction. However, no bonds occur beside the localised bonds formed by the mastic (Wirtgen Group, 2012). The type of emulsion and residual bitumen content influences the binding process. In addition, the quality of the resultant BSM specimen is also influenced by the dispersion and breaking rate during mixing and compaction.

There are many advantages in the use of bitumen emulsion for BSM. Mainly it is cost effective and easy to access due to the variety of uses in the construction industry (Jordaan & Kilian, 2016). Another major advantage is the application at ambient temperatures on lower temperature and moist aggregates (Fazhou *et al.*, 2013). Bitumen emulsion has a long

storage life therefore it can be stocked in bulk (Wirtgen Group, 2012). However, there are a number of disadvantages in using the binder for BSM especially sensitivity to weather variations. During construction, high temperatures lead to rapid breaking and low temperatures result in slow breaking therefore slower strength gain occurs (Ebels & Jenkins, 2007b). Another disadvantage is the limit on the type of aggregates suitable for use with bitumen emulsion. Hence, an advanced knowledge on the construction material is required at all times (Asphalt Academy, 2009). In the case bitumen emulsion is not a viable binder for BSM, foamed bitumen is another option and the characteristics of the binder will be discussed.

2.3.1.2 Foam characteristics

Foamed bitumen is another temporary form of low viscosity bitumen. It is produced in an expansion chamber from a mixture of hot bitumen and water sprayed at a high air pressure as illustrated in Figure 2-31. This method uses a physical process to reduce the viscosity of the bitumen for use at cooler temperatures on moist and ambient temperature aggregates (Jenkins *et al.*, 2000). The main characteristics of a foamed bitumen include the expansion ratio (ER) and half-life ($\tau_{1/2}$), defining the decay of the foam. The expansion ratio indicates the viscosity and quality of dispersion of the foamed bitumen on the aggregates. While, the half-life represents the stability and the rate at which the foam will collapse during mixing (Iwański & Chomicz-Kowalska, 2013a). The ER is determined from the ratio of the foamed bitumen and the original bitumen volumes. The TG2 specifies a minimum ER of 10 times for mixing with aggregates at a minimum temperature of 10^{o} C. The half-life is the measured time in seconds required for the foamed bitumen to collapse to half of the expanded volume. A minimum half-life of 6 seconds is specified by the TG2 (Asphalt Academy, 2009). These characteristics are dependent on the bitumen grade, bitumen temperature, water content and air pressure.

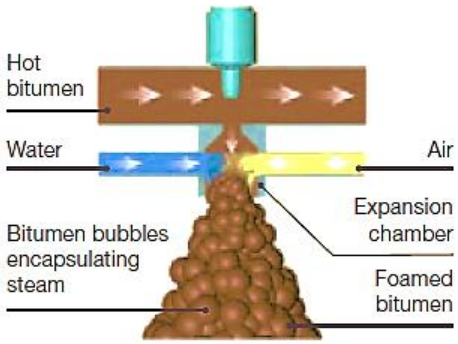

Figure 2-31: Production of foamed bitumen in expansion chamber (Wirtgen Group, 2012)

The optimum chosen expansion ratio and half-life influences the binding mechanism of the foamed bitumen with the aggregates. The binding process occurs when the high-energy bitumen droplets encapsulated in water vapour produces mastic when contact is made with the filler (Collings & Jenkins, 2009). During compaction, the mastic forms spot-welds or localised bonds between uncoated large aggregates forming a non-continually bound mix as illustrated in Figure 2-32. The quality of the bonds is dependent on the dispersion of the foamed bitumen in the aggregates during mixing (Jenkins *et al.*, 2000). Optimum dispersion is achieved at a high expansion ratio and long half-life which are dependent on the bitumen grade, temperature, water content and air pressure (Iwański & Chomicz-Kowalska, 2013b).

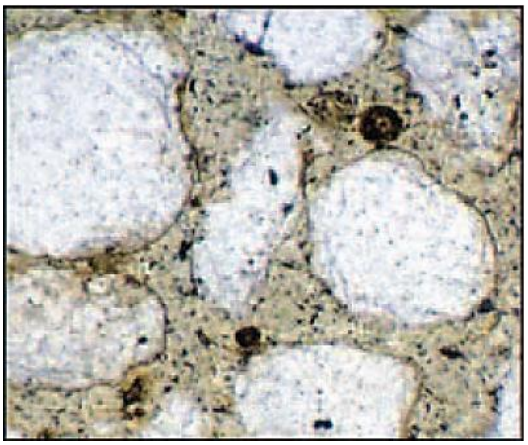

Figure 2-32: Dispersion of Foamed bitumen in aggregates (Collings & Jenkins, 2009)

The use of foamed bitumen has numerous advantages especially for the environment. Such as minimum wastage, low energy requirement and an efficient construction process (Jenkins & Yu, 2009b). Foamed bitumen is suitable for in-situ recycling or in plant mixing. These forms allows for flexibility in the quality control required for each mixes produced. Foamed bitumen mixes can also be stock pilled and used later as required (Wirtgen Group, 2012). Another advantage is that a wide variety of the aggregates can be stabilised with foamed bitumen (Iwański & Chomicz-Kowalska, 2013b). However, a major disadvantage in the use of foamed bitumen requires specialised recycling equipment and training of labour (Jenkins & Yu, 2009b).

2.3.2 **BSM Aggregate Requirements**

The aggregate is an important component in a BSM as it constitutes 97% of the total mass of the mix and dictates the suitable use of the final BSM mix. Additionally, the aggregates form the skeleton of the layer to support loading as previously discussed in 2.1.3.1. However, better performance can be achieved when stabilised with bitumen. Not all aggregates have been tested and proven suitable for stabilisation with bitumen. Most

marginal and recycled aggregates such as reclaimed asphalt pavement (RAP) can be stabilised with bitumen yet, very few studies have examined stabilising RCA with bitumen (Asphalt Academy, 2009). In order to determine suitability of an aggregate for stabilisation with bitumen, the TG2 requires a specific grading, limit on filler content, low plasticity index (PI) and for marginal aggregates the 4 day soaked CBR. A continuous grading is specified to fit between the ideal boundaries as illustrated in

Figure 2-33. A PI less than 7 is specified in order to optimise the dispersion of the low viscosity bitumen to the aggregates (Asphalt Academy, 2009).

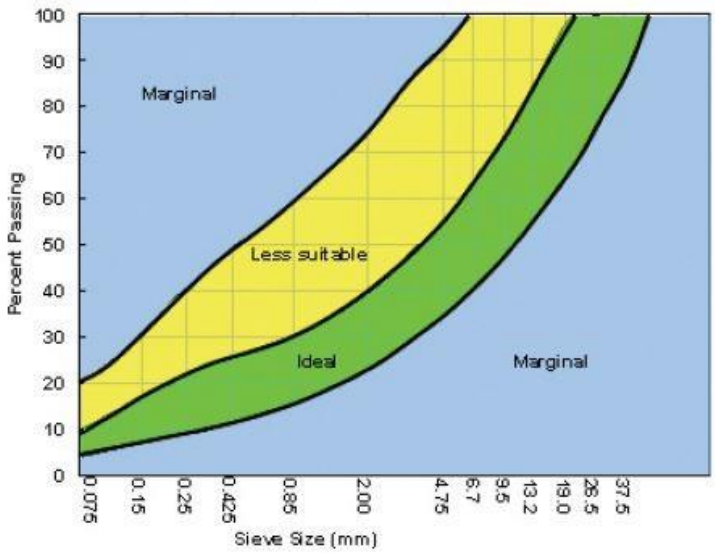

Figure 2-33: Grading boundaries for stabilisation with bitumen emulsion and foamed bitumen

A high PI generally indicates the presence of high cohesive particles such as clay which tends to retain moisture and form lumps (Wirtgen Group, 2012). The formation of lumps results in the reduction of the available filler particles used for the dispersion of the bitumen in the mix. However, the PI of the aggregates can be modified with the addition of lime. On the other hand, a minimum soaked CBR of 10% is required for a BSM 3 layer. This indicates the bearing capacity of marginal aggregates and provides insight on the susceptibility of the aggregates to weathering due to an increase of the moisture content (Asphalt Academy, 2009). The grading, filler content, PI and CBR are critical towards the quality of bitumen dispersion on the aggregates, which is key to the performance of the mix under loading. Therefore, it is important to adhere to these limits in order to produce the required BSM for intended use.

Kendall *et al.*(1999) presented a summary obtained from Bowering and Martin (1976) showing that a well graded aggregate generally requires less bitumen content to achieve its

optimum performance. In addition, Saleh (2006) demonstrated that a coarser grading resulted in a higher resilient modulus in comparison to a mix made with a finer grading with the same filler content. Therefore, a balanced grading is critical for the loading spreading ability of the aggregates.

In general, a well graded aggregate results in an optimum mix for stabilisation with bitumen. Yet, bitumen emulsion and foamed bitumen are essentially different products with different aggregate requirements. A mix with bitumen emulsion is sensitive to the charge of the aggregates. Alternatively, foamed bitumen is sensitive to the temperature of the aggregate prior to mixing (Jenkins, 2000). The charge of the aggregates determines the type of bitumen emulsion suitable for use in the mix (Asphalt Academy, 2009). In addition, the aggregate charge is determined by the mineralogy such as silicate or carbonate which influence the reaction between the aggregates and the bitumen emulsion (Asphalt Academy, 2009). Mixes with foamed bitumen require the temperature of the aggregates to be a minimum of 10^{o}C (Wirtgen Group, 2012). The sensitivity to the temperature of the aggregate, is a result of the rapid change in energy that occurs when the bitumen droplets come into contact with the filler (Jenkins, 2000). Stringers are lumps of bitumen which form as a result of a low filler content or cold aggregates leading to a low quality mix with weak bitumen rich spots in the layer (Jenkins, 2000). Therefore, in such cases, active filler is added in order to improve the quality of the mix.

2.3.3 **Active filler effect on mixes**

In a BSM mix, the active filler can fulfil various roles such as increasing the filler content to improve the quality of dispersion of the bitumen (Asphalt Academy, 2009). There are 3 types of active fillers that can be used for stabilisation with bitumen as specified by the TG2 which include: cement, fly ash and hydrated lime (Asphalt Academy, 2009). The different types of fillers increase strength properties such as the indirect tensile strength (ITS) of mixes as shown in Figure 2-34. The ITS increases as the cement content is increased along with the resistance to moisture damage (Nwando, 2013; Saleh, 2006). Another important use of the active filler is the reduction of the PI of a natural aggregate with hydrated lime (Asphalt Academy, 2009).

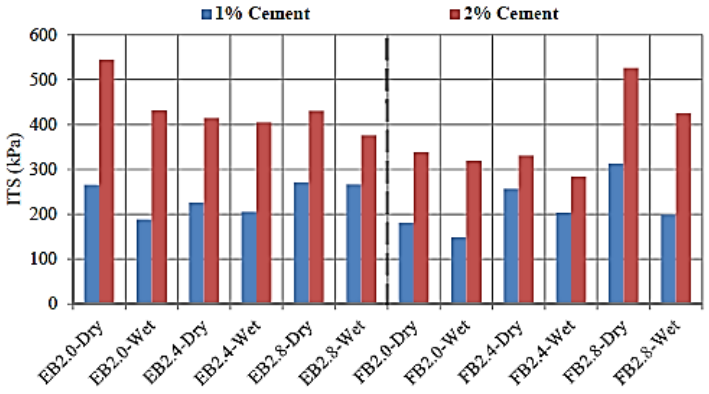

Figure 2-34: Comparison of ITS of bitumen emulsion (EB) and foamed bitumen (FB) with varying contents (2-2.8%) tested in dry and wet conditions (Nwando, 2013)

The active filler interacts differently when mixed with bitumen emulsion or foamed bitumen. In a bitumen emulsion mix, active filler accelerates the breaking rate to induce strength gain (Jordaan & Kilian, 2016). The accelerated breaking of the emulsion is due to the hydration process of cement that absorbs the water in the emulsion. Whereas, in foamed bitumen mixes the droplets bond to the active filler for dispersion (Fazhou *et al.*, 2013). In general, active filler has been proven to improve dispersion and adhesion between bitumen and aggregates. However, the content has been limited to 1% of the total dry mass of the aggregates (Asphalt Academy, 2009).

The limit on the active filler content is specified in order to avoid reduction of the flexibility introduced by the addition of bitumen to the mixes (Jenkins & Collings, 2017). The flexibility of a mix can be estimated by the fracture energy required to induce failure of a specimen. The fracture energy is determined from the area under the force versus deformation graph as demonstrated in Figure 2-35 (A). The higher the fracture energy required to cause the failure of the specimen, the more flexible and durable the mix would be under repeated loading as a result of the ductile behaviour. For example, Saleh (2006) showed that a higher fracture energy was required to break specimens made from hot mix asphalt (HMA) in comparison to a foam stabilised mix with fly ash and 1% cement (FA1C) as illustrated in Figure 2-35 (B). Therefore, higher contents of bitumen produce durable flexible mixes and this property indicates the fatigue life of the layer.

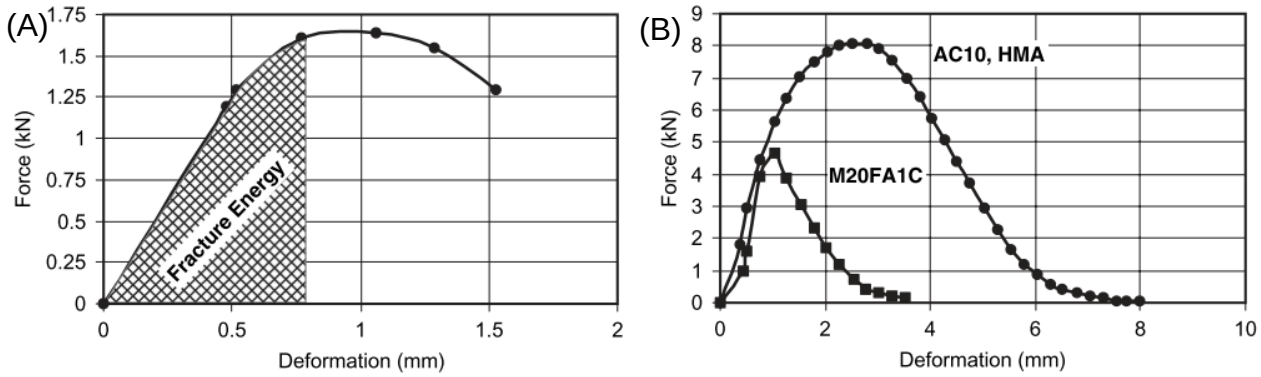

Figure 2-35: (A) Fracture energy determined from force and deformation measured with ITS and (B) comparison of fracture energy of a bitumen foam mix with 1 % fly ash and hot asphalt mix (Saleh, 2006)

Furthermore, Nwando (2013) focused on how high cement contents influenced the flexibility of BMS mixes with bitumen emulsion (EB) and foamed bitumen (FB). The fracture energy decreased with an increase in cement content indicating a brittle mix. The findings highlight that an increase in the cement content produced brittle mixes regardless of an increase in the bitumen content, demonstrated in Figure 2-36.

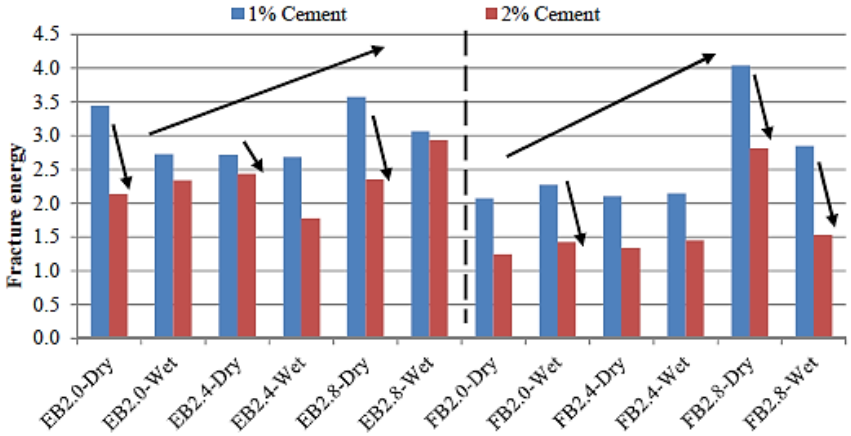

Figure 2-36: Comparison of fracture energy of BSM mixes with varying bitumen content and 1% or 2% cement (Nwando, 2013)

In another study by Campher (2015), the flexibility of the BSM mixes were analysed using the stiffness of the mix, dissipated energy and strain at break. An increase in the cement content (1% to 2%) resulted in an increase in stiffness, along with a decrease in the strain at break and fracture energy as shown in Figure 2-37. Consequently, these results indicate brittle mixes. However, an increase in the bitumen content (0.9 to 2.4%) resulted in an increase in the dissipated energy and strain at break. Therefore, the higher strain at break and higher fracture energy indicates a ductile mix.

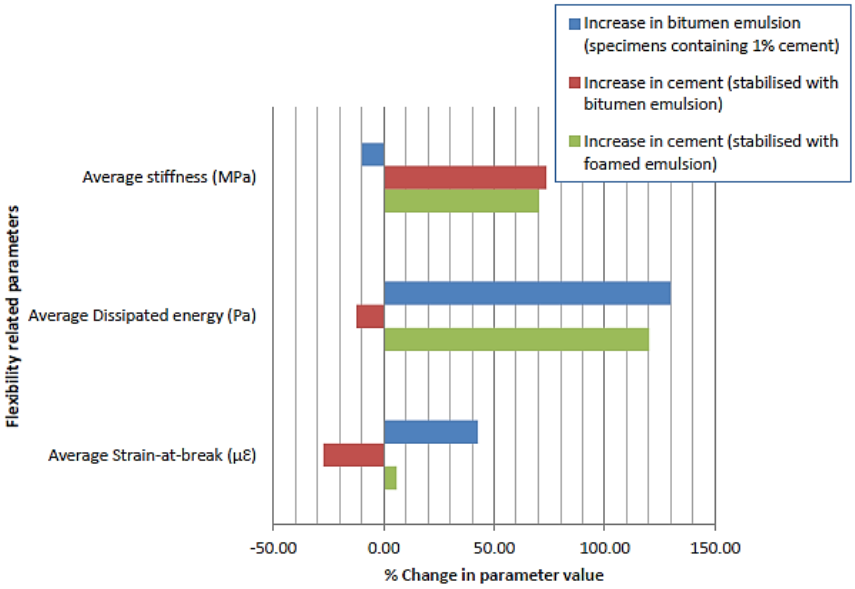

Figure 2-37: Parameters related to flexibility and change based on an increase in cement content in BSM mixes(Campher, 2015)

A study by Fenton (2013) suggests that the confining pressure, maximum dry density and moisture content at break have the most significant influence on the flexibility of a BSM mix. For that reason, the parameters should be kept constant in order to accurately measure how the addition of active filler affects the flexibility of the BSM mix. This is important for RCA, which has residual latent cement. The addition of too much cement would result in an increase in stiffness over the long term that would reduce the flexibility introduced by the addition of bitumen.

2.3.4 **Other factors that influence BSM performance properties**

Numerous factors have an influence on the resultant BSM mix. For the purpose of the research project, factors such as moisture in the aggregates prior to mixing, compaction method and the laboratory curing methods are discussed. The moisture content in the aggregates prior to the addition of bitumen is critical in different manners for stabilisation with bitumen emulsion and foamed bitumen (Jenkins, 2000). Furthermore, the vibratory hammer is currently the specified compaction method in the TG2 for the production of BSM specimens. Thus, it is important to understand the impact of the method on the performance of the mixes. Finally, a brief discussion is presented on how accelerated curing methods influence the measured properties of mixes stabilised with bitumen emulsion and foamed bitumen (Asphalt Academy, 2009). Therefore, a good understanding of these factors is required to better interpret the results.

2.3.4.1 Mixing moisture influence on BSM quality

The moisture content of the aggregates prior to the addition of foamed bitumen or bitumen emulsion is critical. This is to avoid premature breaking of the bitumen emulsion and provide good dispersion of the foamed bitumen to the aggregates (Jenkins, 2000). In a foamed bitumen mix, the optimum moisture content for mixing to produce the maximum bulk volume of the aggregates is referred to as the fluff point (Jenkins, 2000). The fluff point loosens the filler from the larger aggregates for mixing with the foamed bitumen droplets. The water added to achieve the fluff point is determined as a percentage of the OMC and ranges between 65 to 85% depending on the sensitivity of the aggregates to moisture (Asphalt Academy, 2009). The remaining portion of the OMC is added after spraying the foamed bitumen. However, the moisture added in the production of foamed bitumen in the foam plant does not contribute towards the total required OMC.

On the other hand, the residual bitumen and emulsifier in bitumen emulsion contributes towards the total required OMC of the untreated aggregates (Asphalt Academy, 2009). As a result, the total moisture content in the aggregates is referred to as the optimum mixing moisture content (OMMC). The OMMC is a sum of the added bitumen emulsion and the remaining moisture to achieve the required OMC (Wirtgen Group, 2012). The OMMC lubricates the aggregates during mixing and compaction. It should be noted that stabilisation with bitumen emulsion is highly sensitive to variations in moisture content of the aggregates. A low moisture content in the aggregates results to the absorption of water in the bitumen emulsion leading to premature breaking (Wirtgen Group, 2012). Consequently, high porous aggregates such as RCA should be treated with care and accuracy is required when adding the mixing moisture. (Gomez-Meijide *et al.*, 2016). Therefore, it is important to ensure the correct moisture is added to the aggregates prior to mixing with both bitumen emulsion and foamed bitumen.

2.3.4.2 Compaction influence on BSM quality

Subsequent to mixing, the compaction of the BSM specimens is performed with a vibratory hammer as specified by the TG2. The compaction method orients and packs the aggregates to reduce voids and for a BSM mix, assists the mastic to adhere to the larger aggregates (Ebels & Jenkins, 2007c). As discussed in Section 2.2.4, high energy compaction methods such as a vibratory hammer results in a higher maximum dry density at lower OMC. Kelfkens, (2008) demonstrated that compaction with a vibratory hammer, of untreated and bitumen stabilised aggregates, provides optimum packing of the aggregates at lower

moisture contents as presented in Figure 2-38. Kelfkens, (2008) also noted that in cases of mixes stabilised with bitumen emulsion, the bitumen contributes towards the compaction moisture hence a reduction in the mixing moisture is not observed in Figure 2-38(A). Furthermore, the vibratory hammer simulates the vibratory rollers used on a site as a result, target densities can be achieved (Jenkins *et al.*, 2012). The TG2 recommends that a reduction of the OMC can be done due to the high energy applied by the vibratory compaction method used on a typical site.

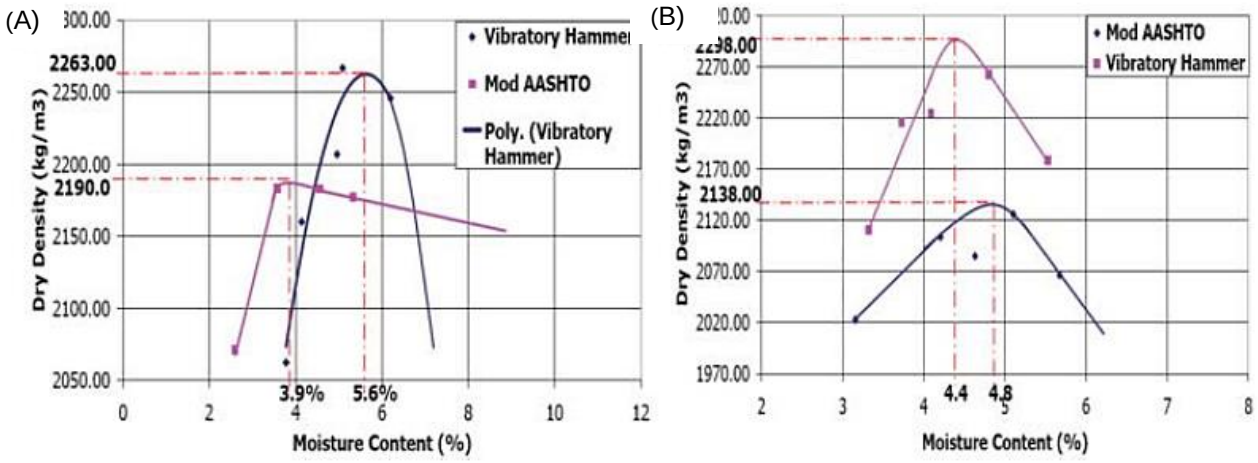

Figure 2-38: The comparison of moisture-density relationship of crushed hornfels compacted with vibratory hammer and Mod AASHTO (G2) stabilised with (A) bitumen emulsion and (B) foamed bitumen

2.3.4.3 Curing influence on BSM quality

The final step in the preparation of a BSM specimen prior to loading is the curing of the mix to gain strength. Jenkins *et al.*,(2012) defined the curing process as the loss of moisture from the specimen through evaporation, particle charge repulsion and pore pressure induced flow paths during compaction or traffic loading. The curing process results in an increase in the tensile strength, compressive strength and stiffness. In addition, the longer the curing period after compaction the higher the strength of the mix. Therefore, in order to evaluate the expected performance of a mix under traffic loading, realistic curing laboratory simulations are required.

Alexander *et al.*(2009) defined accelerated curing as a method used in the laboratory to simulate the curing that would occur on site. The simulation is a creation of the expected conditions, where the moisture and temperature are kept constant or the release of moisture is accelerated to allow the material to bond in order to gain strength. There are different forms of accelerated curing methods based on the climatic conditions of the environment the road is to be built (Asphalt Academy, 2009). The TG2 specifies different curing

procedures at the different levels of the mix design process as illustrated by Figure 2-39. This is based on the different specimen sizes and the curing temperature. The specified curing hours aim to represent 12 to 24 months curing period on site as validated by Moloto (2010).

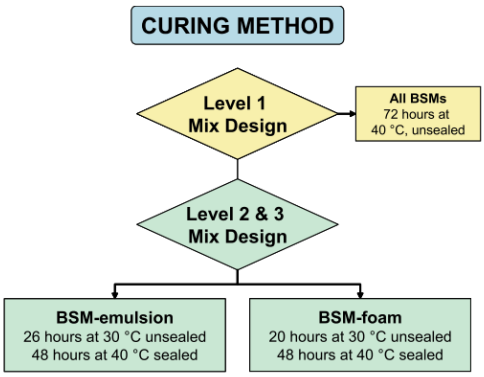

Figure 2-39: Curing regimes for BSMs (Asphalt Academy, 2009)

Triaxial specimens produced at level 3 are cured to represent long term strength attainable on site (DalBen & Jenkins, 2014). The breaking rate of the bitumen emulsion is influenced by the temperature and humidity of the environment. Consequently, mixes with bitumen emulsion require a longer curing period to acquire the desired strength prior to loading (Jenkins *et al.*, 2012). Due to the high moisture content in a BSM mix with RCA, a longer curing period would be required to gain strength as noted in Section 2.2.4

The above-mentioned curing methods do not encourage hydration of cement. This was shown in a study by Nwando (2013) where the benefit of cement was obtained or measured from a long term curing method relatively to a rapid curing method (see Figure 2-40). Specimens cured for 28 days (long term curing) achieved an ITS of 600 kPa with 2% cement with bitumen emulsion which is higher than the 420kPa achieved with rapid curing (3days in oven at 40^0C).Therefore, the self-cementation property of RCA will not be realized from the specimens cured according to the TG2.

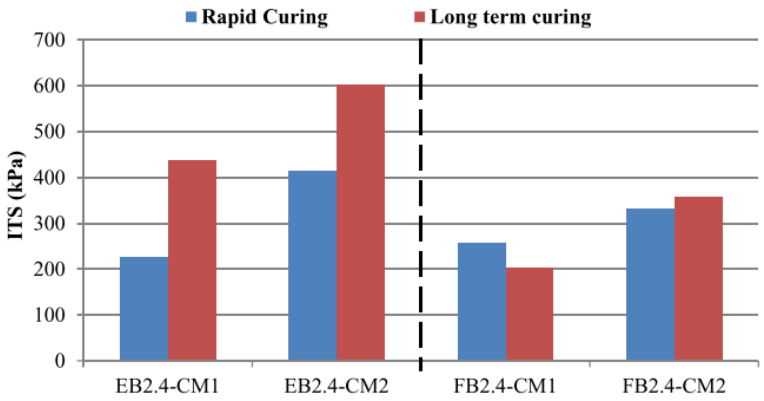

Figure 2-40: The influence of curing method on the ITS measured for mixes with 2.4% Bitumen Emulsion (EB2.4) and 1%cement (CM1) or 2%cement (CM2) (Nwando, 2013)

2.4 Laboratory Evaluation of BSM Mix Designs and Performance Properties

In general, BSM mixes are produced from recycled aggregates with an optimum combination of bitumen and active filler to support a given design traffic. An economical pavement design is specified based on an accurate understanding of the material performance properties (Jenkins & Collings, 2017). Recently, the pavement design process of BSMs was revised to provide understanding of the material as illustrated in Figure 2-41. The process requires testing of the indirect tensile strength (ITS) of various potential mixes. These ITS results are used as an indicator for the most suitable mix, which is further tested for, shear properties with the triaxial monotonic test. The basic principles of the tests and interpretation of the results are discussed in this section. In addition, the factors that influence the results obtained from the tests will be highlighted. Therefore, users should be aware of possible variables that will influence the results, especially testing new materials such as RCA.

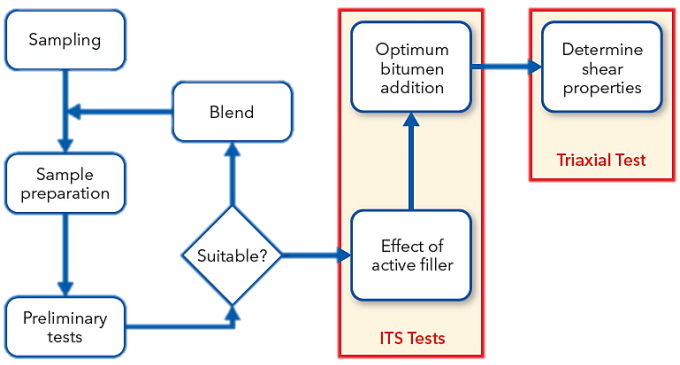

Figure 2-41: BSM mix design flowchart (Wirtgen Group, 2017)

2.4.1 **ITS Testing**

The ITS test is used to determine the optimum mix design by eliminating unsuitable mixes produced from different types and varying contents of active filler and bitumen (Asphalt Academy, 2009). The most suitable BSM mix is determined from an optimum combination of graded aggregates, bitumen type and content and active filler as discussed in Section 2.3. The ITS results are not a direct measure of the tensile strength of the mixes due to the size of the specimens. However, the results provide an indication on how the addition of bitumen and active filler influences the response of the mix to the applied force (Ebels & Jenkins, 2007c). In addition, the durability of the potential mixes against moisture damage is measured on the ITS specimens soaked in water for 24 hours. The mix which retains most of the measured ITS is regarded as moisture resistant (Asphalt Academy, 2009). The tensile strength retained (TSR), calculated from the ratio between the wet and dry ITS is used as a measure of the mix durability.

The ITS test is a relatively simple and cost effective manner to estimate the indirect tensile strength of a material (Ronald *et al.*, 1968). A compressive force is applied along two points on the circumference of a cylindrical specimen as shown in Figure 2-42. The force causes tensile stresses at the centre of the specimen resulting in a split along the loading plate (Ronald *et al.*, 1968). The width of the loading strip, testing temperature, loading rate and specimen size are the main factors which influence the ITS results. Due to these influential factors, the ITS results are not repeatable and do not resemble field loading. However, a low coefficient of variation (COV) is obtained from a set of specimens tested. Ben and Jenkins (2014) found that the higher the testing temperature of the specimen, the lowered the measured ITS. Therefore, this proves that BSM mixes are temperature dependent. For consistent results, BSM specimens are loaded at a constant deformation rate of 50.8 mm/min along the height of the specimen at a temperature of 25^{o}C (Wirtgen Group, 2017).

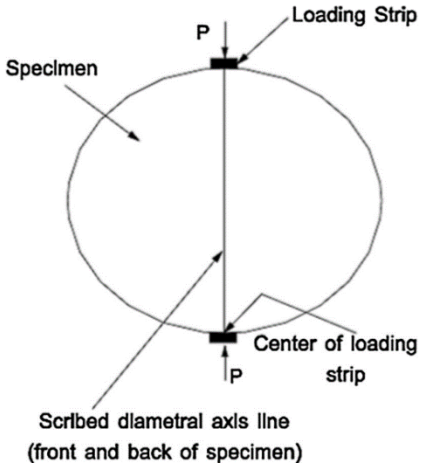

(Fatemi & Imaninasab, 2016)

(Wirtgen Group, 2012)

Figure 2-42: ITS specimen testing schematics

The data obtained from the ITS test serve as an indirect measure of flexibility of a BSM mix design during loading. Additionally, the data can be used to estimate the resilience of a mix against deformation as discussed in Section 2.3.3. The TG2 provides limits on the calculated ITS and TSR to estimate the most likely attainable BSM class and indicate unsuitable and uneconomical mixes. Other methods previously used as indicators to determine a suitable mix design include the UCS. However, Nwando (2013) obtained a good correlation between the results obtained from the ITS and UCS of a bitumen emulsion mix as demonstrated in Figure 2-43. Consequently, either tests essentially indicates a similar optimum mix design. Therefore, the ITS is the prescribe method to determine the optimum BSM mix design for the available aggregate.

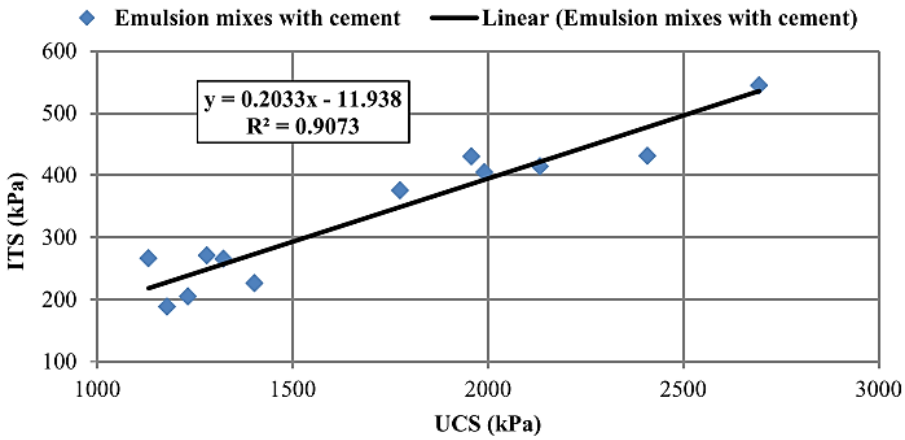

Figure 2-43: Comparison between ITS and UCS of a bitumen emulsion mix. (Nwando, 2013)

2.4.2 **Monotonic Triaxial Test**

The optimum BSM mix design determined from the ITS results as described in Section 2.4.1 is further evaluated to determine the shear strength as guided by the process illustrated in Figure 2-41. The specified method used to determine the shear strength is the monotonic triaxial test (Ebels & Jenkins, 2007c). This test was developed and validated at the University of Stellenbosch as the simple triaxial test (STT) (Mulusa, 2009). The TG2 specifies a specimen with a height of 300 mm and a diameter of 150 mm in order to accommodate the large aggregates used in the pavement layers (Asphalt Academy, 2009). Furthermore, a rubber bladder is used to apply a given confinement pressure (σ_3) with air as depicted in Figure 2-44. Then, the test applies a constant impact load to achieve a given principle stress (σ_1) on the specimen. This method has since been simplified for commercial use and standardized for consistent results (Jenkins & Collings, 2017).

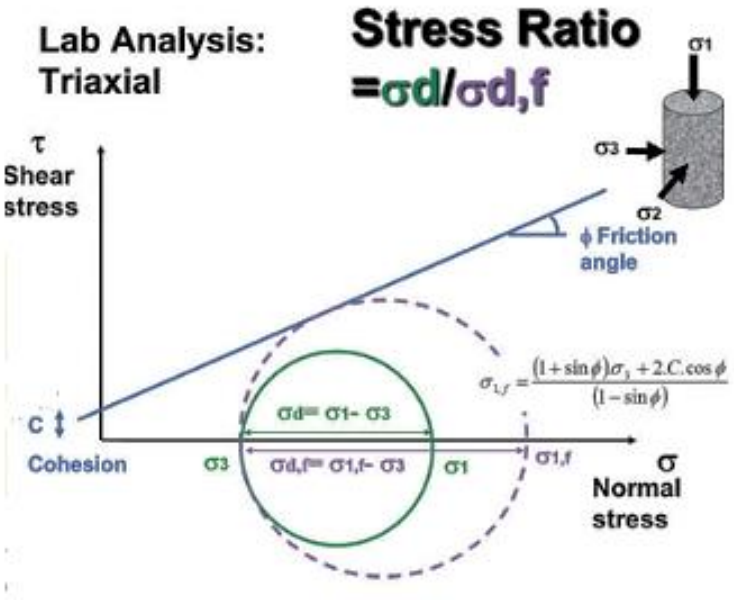

Figure 2-44: Shear parameters measured from triaxial monotonic testing (Jenkins & Collings, 2017)

The shear strength of a mix is characterised by the calculated cohesion (C) and the internal angle of friction (ϕ) as discussed in Section 2.1.3.1 and shown in Figure 2-44. The shear parameters are material properties dependent on the density, moisture content and curing period of the specimen tested as discussed in Section 2.1.3.1. In addition, the durability of a mix against moisture damage under static loading is measured from the retained cohesion (RC) of a specimen soaked in water for 24 hours prior to testing (Asphalt Academy, 2009).The RC gives an indication on how moisture loosens the mastic bond between the

larger aggregates. The processing and modelling of the data obtained from the test is discussed in the following section.

2.4.2.1 Shear parameters analysis and interpretation

The data generated by the monotonic triaxial test is modelled with the Mohr-Coulomb failure envelope to determine the cohesion and angle of internal friction (Jenkins *et al.*, 2002). The addition of bitumen increases the cohesion of the unbound granular aggregates. In addition, the increased cohesion results in an upward shift of the failure envelop. As a result, an increase in the principle failure stress ($\sigma_{1,f}$) occurs i.e. increase in shear strength of the mix (Ebels & Jenkins, 2007b). On the other hand, the type of aggregate stabilised influences the internal angle of friction which represents the slope of the failure envelop as illustrated in Figure 2-45. The addition of the bitumen results in a decrease of the slope i.e. decrease in principle failure stress and shear strength of the mix design.

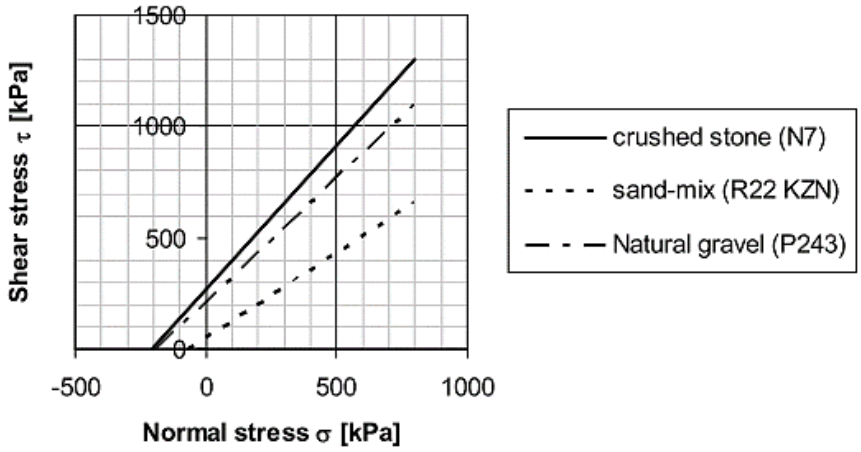

Figure 2-45: Examples of Mohr-Coulomb Failure lines of BSM made with strong and weak aggregates(Ebels & Jenkins, 2007b)

The quality of the BSM mix produced declines based on the type of natural gravel and natural sands used in the mix. Ebels & Jenkins,(2007a) reports on a cohesion as high as 400 kPa and an internal angle of 55^{o} measured from specimens made with crushed rock. Alternatively, RCA is a mixture of crushed rock, natural sands, cement and for that reason, a good quality BSM can be expected when stabilised with bitumen. Furthermore, the higher the shear parameters of a mix, the higher the maximum principal stress at failure (Jenkins *et al.*, 2002). Consequently, an increase of the principle stress results in an increase of the deviator stress ratio (DSR) shown in Figure 2-44. Therefore, shear parameters are generally used to define the mode of failure of the mix design and predict the life of the material with

a transfer function. In addition, the shear parameters are used to determine the resilient modulus of the material under dynamic loading which is discussed below.

2.4.3 **Dynamic Triaxial test**

In pavement engineering, the resilient modulus (Mr) quantifies the response parameter of the material to loading. Whereas, the damage parameter is quantified by the permanent deformation (ε). These parameters are measured with the dynamic triaxial test otherwise known was the cyclic loaded triaxial test (DalBen & Jenkins, 2014; Ebels & Jenkins, 2007b). The triaxial testing of BSM mix designs is not specified in the TG2. However, for research purposes of new materials, the response to loading and damage parameter provide a good understanding of a material under repeated loading. As discussed in Section 2.1.3.2, the resilient modulus is mainly used to determine the load spreading capability of a mix under simulated repeated traffic loading. Additionally, the resilient modulus is an input parameter in the mechanistic-empirical structural design of a layer (Boateng *et al.*, 2009). Therefore, the resilient modulus and permanent deformation are essential measures regarding the appropriate use of a mix in a road pavement structure.

A typical test setup for the resilient modulus requires a loading frame, triaxial cell, load cells, linear variable displacement transducers (LVDTs), a control and data acquisition system (Boateng *et al.*, 2009). The cyclic triaxial test applies an impact load (σ_1) followed by a rest period to simulate traffic loading. At different constant confinement pressures (σ_3), a variety of impact loads are applied on the specimen to induce a range of predetermined deviator stress ratios (DSR) as illustrated in Figure 2-46. This is done to simulate various traffic loadings on the potential mix design placed in different positions in the pavement structure (Boateng *et al.*, 2009). Prior to testing the resilient modulus, conditioning is done to stabilise the specimen which has an influence on the response of the material subsequently to also obtain representative results (Jenkins *et al.*, 2002). In order to prevent permanent deformation of a specimen, the DSR is controlled by applying stresses that will not result in failure (Boateng *et al.*, 2009). Therefore, testing the resilient modulus of a material requires specialised skills and an understanding of the critical input parameters for the test which include the deviator stress ratios (DSR), and other influential factors.

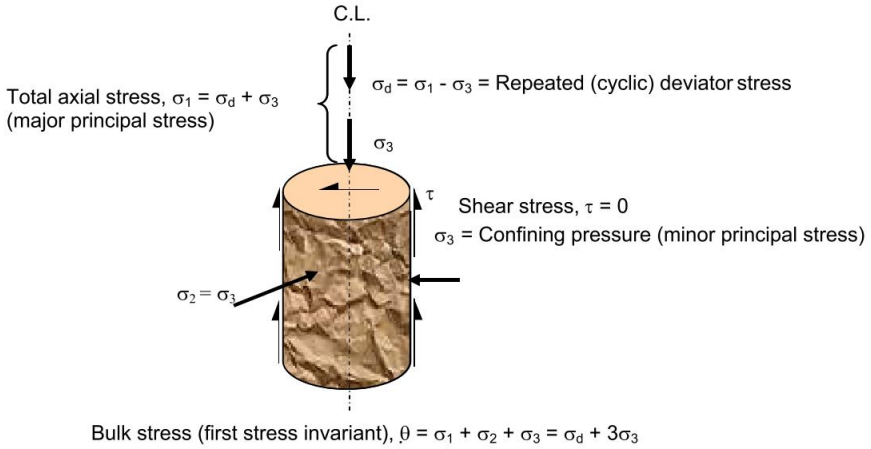

Figure 2-46: Resilient modulus test setup (Boateng *et al.*, 2009)

The deviator stress ratio (DSR) is calculated from the shear parameters of the material obtained from the monotonic triaxial test. Typical granular materials and BSMs have a limit on the DSR which ranges between 40-60%. A DSR value higher than the limit leads to a rapid deformation of a specimen resulting in premature failure (Long & Theyse, 2004). The higher the DSR required for failure of the specimen, the higher the loading the material can support. However, a reduction in loading results in a longer pavement life (Ebels & Jenkins, 2006). Other factors that have an influence on the measured Mr prior to testing include the density and moisture content of the specimen. These factors measure how the condition of the specimen affects the measured Mr. On the other hand, factors external to the specimen which influence the measured resilient modulus include the stress levels i.e. DSR, stress history, number of load repetitions and the conditioning sequences (Boateng *et al.*, 2009). Therefore, care is required when assessing the Mr of a specimen in order to obtain reliable results.

2.4.3.1 Resilient modulus analysis and interpretation

The relationship between the bulk stress (= $\sigma_1 + \sigma_2 + \sigma_3$) and the calculated Mr demonstrates the behaviour of a material under repeated loading. In general, an increase in the bulk stress results to an increased Mr for coarse granular materials, referred to as stress stiffening. Alternatively, stress softening has been observed in fine grained materials where an increase in the bulk stress results in a decreased Mr (Boateng *et al.*, 2009). The stress dependent behaviours of the materials can be modelled to relate the confining stress, DSR and how the applied loading influences the measured Mr (Van Niekerk, 2002). Additionally, the models are also used to predict the Mr for any given bulk stress. There are four types of

models commonly used to describe the resilient behaviour of a stress dependent granular material which can also be used for BSMs (Jenkins, 2000). The models and the variables are presented in Table 3.

Table 3: Mr Models and variables (adapted from Van Niekerk, 2002)

MR- MODEL	VARIABLES
K-θ MODEL $M_r = k_1(\frac{\theta}{\theta_0})^{k_2}$	k_1, k_2, k_3, k_4, k_5 = Model coefficients θ = sum of principal stresses/bulk stress ($\sigma_1+\sigma_2+\sigma_3$) [kPa] σ_3 = minor principal/confining stress [kPa] σ_d =deviator stress ($\sigma_1-\sigma_3$) [kPa] $\sigma_{d.f}$ = maximum allowable deviator stress based on the shear parameters ($\sigma_{d.f} = \sigma_{1.f} - \sigma_3$) [kPa] $\sigma_{3.0}$, $\sigma_{d.0}$ = reference stresses
M_R-σ_3-σ_D UZAN AND WITZACK MODEL $M_r = k_1(\frac{\sigma_3}{\sigma_{3.0}})^{k_2} \times (\frac{\sigma_d}{\sigma_{d.0}})^{k_3}$	
PARABOLIC M_R-σ_3-σ_D MODEL $M_r = k_1(\frac{\sigma_3}{\sigma_{3.0}})^{k_2} \times (-k_3\left(\frac{\sigma_d}{\sigma_{d.f}}\right)^2 + k_4\left(\frac{\sigma_d}{\sigma_{d.f}}\right)^2 + k_5$	
M_R-θ-σ_D /$\sigma_{D,F}$ MODEL $M_r = k_1(\frac{\theta}{\theta_0})^{k_2} \times (1 - k_4\left(\frac{\sigma_d}{\sigma_{d.f}}\right)^{k_5}$	

The models are fitted to the measured data using a non-linear regression analysis method. The characteristics of each model are summarised in Table 4. The K-θ model has been used for its simplicity to describe the stiffening stage of the material. However, it does not incorporate the effect of the confining stress (σ_3) and the deviator stress (σ_d) on the Mr as a result, the Mr-σ_3-σ_d model was developed (Ebels, 2008). Conversely, the Mr-σ_3-σ_d model does not consider the individual effect of σ_3 and σ_d on the Mr. Subsequently, Van Niekerk (2002) modified the model to consider both the stress stiffening and stress softening as the bulk stress increases. Therefore, this is the most used model for unbound and foamed bitumen granular mixes (Jenkins, 2000).

Table 4: A summary of the characteristics for each Mr-model and coefficient interpretation (Ebels, 2008; Jenkins, 2000; Van Niekerk, 2002)

MR-MODEL	CHARACTERISTICS	COEFFICIENT INTERPRETATION
K-θ MODEL	• Simple to use • Describes stiffening • Does not measure the influence of the confining stress and deviator stress separately	k_1- Directly proportional to Mr k_2- Indicates the slope of the line

	• Cannot describe stress stiffening or stress softening	
M_R-σ_3-σ_D	• Considers the effect of the confining stress and deviator stress on the Mr • Physically correct in comparison to k-θ model • Cannot differentiate between stress stiffening and stress softening.	
M_R-σ_3-σ_D	• Models the stress stiffening and softening • Considers the effect of σ_3 and σ_d on the Mr separately	
M_R-θ-σ_D /$\sigma_{D,F}$	• Describes the influence of stress stiffening or softening • Physically incorrect • Doesn't not consider the influence of σ_3 and σ_d on the Mr separately.	First term– describes the stress stiffening of the material Second term- describes the decrease of Mr and stress increases to failure stress k_3–Describes the relative decrease of Mr at high stresses k_4-Decribes the shape of the Mr decrease

2.5 Chapter Summary

The chapter begins with a brief overview on the typical types of pavement structures used in South Africa. The discussion covers the main differences between a flexible, composite and rigid pavement structures. Then, focus is drawn to the different types of layers used to construct a flexible pavement structure. This includes a summary of the characteristics of a bound, unbound and non-continuously bound layer. The design of any pavement layer requires knowledge on the behaviour of each layer under repeated loading. Therefore, an in-depth overview is conducted on the behaviour and performance properties of a non-continuously bound layer in comparison to an unbound layer. In addition, factors that influence the performance properties such as shear strength, resilient modulus, durability and permanent deformation are discussed. Therefore, the use of a new material, such as recycled concrete aggregate, in a pavement layer requires an understanding of the holistic pavement structure.

Recycled concrete aggregates are currently used in the pavement structure as an unbound layer. In order to improve the performance properties of RCA, bitumen stabilisation is one method that can be used which produces a non-continuously bound layer. Therefore, an

understanding of the aggregate composition, shape, texture, grading, moisture content and maximum dry density are required prior to the addition of bitumen. These aspects are discussed in depth to provide understanding to produce BSM mixes suitable for use. The chapter also covers the main components of a BSM and the effectiveness of the method to enhance an unbound granular layer.

The main BSM components are binder composition, aggregate requirements and types of active fillers. The types of binders such as foamed bitumen and bitumen emulsion are discussed including the characteristics of the binders. This is followed by an analysis on literature conducted on how the aggregate influences the resultant BSM mix. The types and uses of active fillers in a BSM mix are examined to provide a better understanding of their influence on a BSM mix. Finally, the section briefly highlights how the mixing moisture, compaction and curing of a specimen influences the BMS strength properties.

Once a BSM specimen is mixed, compacted and cured the following strength properties are tested in the laboratory: indirect tensile strength, shear strength and resilient modulus. The test methods are discussed followed by the data analysis and modelling methods typically used. Therefore, based on this background on RCA, BSMs and laboratory tests, there is potential for RCA to be stabilised with bitumen to determine whether it is suitable for use in the pavement structure.

Chapter 3: Experimental Design and Methodology

The experimental design consists of four phases, which aim to explore the feasibility to stabilise recycled concrete aggregate (RCA) with foamed bitumen or bitumen emulsion. Phase 1 characterises the aggregate properties to verify suitability for stabilisation and determines the bitumen foaming characteristics. Phase 2 assesses the suitable active filler and optimum bitumen content to stabilise RCA. In Phase 3 the shear parameters of the mix design, with the optimum bitumen content and suitable active filler determined in Phase 2, are measured. The shear parameters are then used to evaluate the resilient modulus of the resultant specimens to determine the dynamic response of the mixes to repeated loading. Furthermore, the resilient modulus results obtained are further used to model the resilient behaviour of the mixes in Phase 3. Finally, the pavement analysis of the mixes is conducted in Phase 4 of the study. The experimental design is outlined in Figure 3-1.

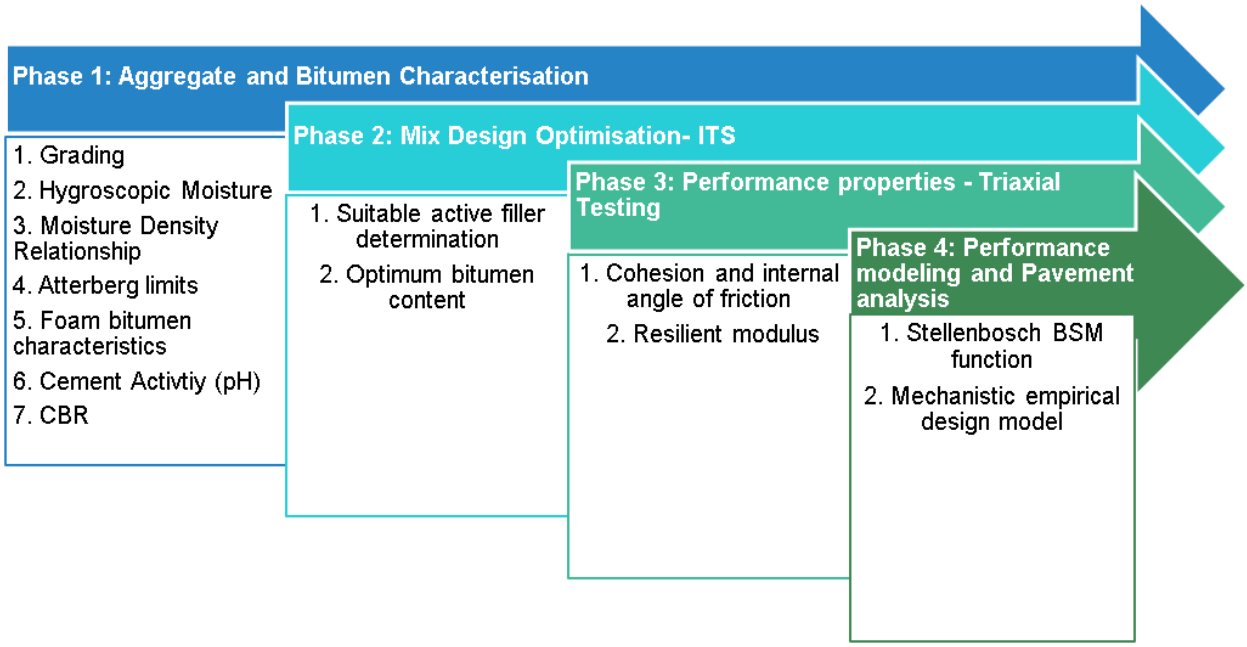

Figure 3-1: Experimental Design Outline

3.1 Materials

The raw materials used for the research project include aggregates from recycled concrete, 70/100 penetration grade bitumen, bitumen emulsion, lime and cement. Further details on each material are discussed in the section.

Recycled concrete aggregate (RCA)

The recycled concrete used in the project originates from a jointed concrete road built in 1971 on the N2 between Borcherds Quarry Road (M22) and Swartklip Interchange (R300) in the Western Cape, South Africa. The concrete slabs retrieved from the road slightly differed in appearance due to the alkali silica reaction (ASR) which occurred on some sections of the road resulting to the formation of cracks. ASR occurs due to the presence of silica on the aggregates used for the concrete mix (Addis, 1998). The silica on the aggregates reacts with the alkalis in the cement resulting to the expansion of the concrete which causes cracking. The cracks were penetrated by water which lead to the weakening of the supporting granular layers (Strauss & Van der Walt, 1989). The road was immediately repaired with overlays which were removed and separated from the concrete when the road was due for a heavy rehabilitation and realignment. The concrete slabs were transported and stored in covered concrete storages at the Civil Engineering building, Stellenbosch University.

Stabilising agents

Two types of stabilising agents are used for the project namely: foamed bitumen and bitumen emulsion. The foamed bitumen is produced from a 70/100 penetration grade bitumen which was supplied by COLAS received from Much Asphalt. The bitumen was received from Much Asphalt in 20 five litre tins and stored at room temperature. The grade of bitumen used was selected because it is a softer bitumen grade which provides a greater distribution of the bitumen on the aggregates (Asphalt Academy, 2009)

An anionic stable grade 60% (SS60) bitumen emulsion supplied by Spray Pave is used. The bitumen emulsion contains 60% residual bitumen, 40% water and emulsifier. The bitumen emulsion was received from the supplier in 5 x 5l plastic bottles which were stored at ambient temperature.

Active fillers

Two types of active fillers are used for the mix design optimisation phase namely: cement and hydrated lime. The general purpose cement IDM CEM II 32.5 N manufactured by PPC was sourced from Builder Warehouse. Due to the role of active filler to increase dispersion of the bitumen in the aggregate mix, a low strength and slow setting cement is preferred for bitumen stabilisation. The Rotalym hydrated lime manufactured by PPC is used.

3.2 Phase 1 – Aggregate and Bitumen Characterisation

Phase 1 of the laboratory experiments focuses on the physical properties of recycled concrete aggregate (RCA) and the foaming characteristics of the bitumen. The physical properties of RCA tested include: the grading obtained from crushing the concrete segments, hygroscopic moisture of the RCA, maximum dry density at optimum moisture content, plasticity index (PI) and cement activity i.e. pH. The 4-day soaked CBR of the graded RCA is tested on specimens compacted with the Modified AASHTO hammer and vibratory hammer. The methods followed are discussed in this section.

3.2.1 **Aggregate Grading**

The goal of the research project is to study the feasibility of stabilising RCA with foamed bitumen and bitumen emulsion. Recycled concrete aggregate (RCA) is a relatively new material in the construction industry especially in South Africa. Therefore, it is likely to be used as a secondary material due to the lack of guideline documents as research on its long-term performance is ongoing. For the same reason, there is currently no specified grading for specific uses of RCA except that good performance has been seen from well-balanced continuous gradations (Van Niekerk, 2002). The process followed to determine the grading used for the research project aims to produce the most economical continuous grading that can be achieved on a typical construction site. However, the grading is required to fit the grading limits specified in the technical guideline document for bitumen stabilised materials (TG2) for stabilisation with foamed bitumen and bitumen emulsion.

Broken concrete slabs are crushed into smaller segments (Figure 3-2 A) with a jackhammer in order to fit into the jaw crusher (Figure 3-2 B) used in the laboratory. Prior to crushing, the material is moistened with water to reduce the loss of fine particles during crushing. Three different samples (designated S1, S2, and S3) are all initially crushed through a 20 mm gap set on the jaw crusher thereafter processed differently which produces different particle size distributions.

Figure 3-2: (A) Recycled Concrete segments and (B) Laboratory Jaw crusher

The grading for sample 1 (S1) is determined as obtained from the primary crushing of the concrete segments with the jaw crusher set with a 20 mm gap. The wet sieve analysis Method A1 (a) outlined in the Technical Methods for Highways (TMH 1) is used to evaluate the particle size distribution of the sample after crushing. The crushing method for S1 represents the most economical method that can be used on a typical construction site to produce aggregate grading with a maximum particle size of 20 mm. The crusher gap was limited to 20 mm due to the mould sizes used to produce the specimens in the laboratory. The ratio between the specimen diameter and maximum particle size of the aggregates dictates the maximum particle size of the aggregates. This is done in order to eliminate segregation during compaction of the specimen and the influence of individual aggregates on the measured behaviour of the material under loading (Van Zyl, 2015).

A two stage crushing process of the concrete segments is done to produce sample 2 (S2). Initial crushing through a 20 mm gap set on the jaw crusher produces the same grading as S1. Secondary crushing is conducted by setting the jaw crusher gap to the smallest possible size which is 2 mm where the whole sample is crushed again. Sample 2 is sieved using the wet sieve analysis method and a fine grading is obtained as illustrated in Figure 3-3. This method of crushing would be uneconomical in practice because the whole stockpile would require double crushing.

Figure 3-3: Crushed Concrete Sample 1 (S1) 1st crushing at 20 mm and Sample 2 (S2) 1st crushing at 20 mm + 2nd crushing at 2 mm

Sample 3 (S3) is produced from a two stage crushing process of the concrete segments i.e. 1st crushing at 20 mm + 2nd crushing of ½ the sample at 2 mm. Primary crushing of the sample is done through the 20 mm gap set on the jaw crusher. This crushed sample is separated into two equal batches with a riffler with 25 mm openings. A secondary crushing is done on one batch through a 2 mm gap set on the jaw crusher and then mixed with the second batch containing the primary crushed aggregates. Based on the gradations obtained for S1 and S2, presented in Chapter 4, the filler content for S3 would lie between the filler content obtained for S1 and S2. Therefore, the grading of S3 is determined using the dry sieving method and found to be the most appropriate and practical grading for BSMs based on reasons explained in Chapter 4.

A stockpile of crushed concrete aggregates is air dried and dry sieved to separate the aggregates according to size and packed in bags. Thereafter, the bags of the same sized aggregates are mixed in order to reduce the inherent variability of RCA. A distinct difference in the colour of the mortar on the 14 mm aggregates is observed therefore this constitutes to two slightly different types of aggregates (Figure 3-4) produced from the old concrete slabs. The physical properties of these two aggregates are tested and the results led to the need to separate the aggregates in order to produce consistent mixes with the foamed bitumen and bitumen emulsion. RCA 1 is used as the 14 mm aggregate for the research project to make a BSM. The crushed aggregates sizes smaller than 14 mm consists of less mortar and the distinct difference seen on the mortar of RCA 1 and RCA 2 is not observed therefore these fractions are not separated

Figure 3-4: Two types of 14 mm aggregate produced from the recycled concrete

The different fraction sizes are reconstituted to produce the final grading for test specimens to determine the maximum dry density and optimum moisture content of the grading. Furthermore, the final grading is reconstituted for each mix manufactured for test specimens used in the mix design optimisation and performance properties testing phases.

Wet Sieve Analysis

The wet sieve analysis method is used to separate the aggregates according to size in order to determine the mass of the aggregates retained on each sieve size (mm). The mass of each aggregate size is used to determine the percentage in the mix to compile the grading curve of the material. This method allows for an accurate determination of the aggregates smaller than 0.075 mm generated from crushing, by separating the finer aggregates from the larger aggregates. Method A1 (a) from TMH1 is adapted because a smaller sample size of 2500 g is used to produce grading S1 and S2. The smaller sample size is chosen to make it easy to wash the sample and sieve, consequently the following steps are taken:

1. After crushing, the sample is quartered with a riffler with 25 mm openings and the quarters are mixed and the whole sample is oven dried at 110^{o}C overnight.
2. The riffler is used to evenly separate the oven dried crushed sample and only 2500g of the total crushed aggregates is soaked in water over night at room temperature to loosen and remove the fines attached to the larger aggregates.
3. The sample is washed through a 0.075 mm sieve until the water is clear in colour and only particles larger than 0.075 mm remain.
4. The aggregates retained on 0.075 mm sieve are oven dried overnight at 110^{o}C and sieved the next day through the following sieve sizes: 28, 20, 14, 10, 7.1, 5, 2, 1, 0.6, 0.425, 0.3, 0.15 and 0.075 mm.

5. The masses of aggregates retained on each sieve are weighed in grams and summed to determine the total weight of the remaining sample.
6. The original total mass of the sample is 2500 g and it is used to determine the mass of the finer fraction. The mass of the finer fraction is the difference between the remaining total of the aggregates determined in step 5 and the original total 2500g.
7. The cumulative retained mass on each sieve is used to determine the percentage passing of the aggregates through each sieve which produces the grading curve of the aggregates.

Dry Sieve Analysis

The dry sieve analysis method is used to separate the aggregates according to size and determine the mass of each aggregate retained on the sieve. This method is mainly used for larger crushed samples of crushed rock or granular material. A sample size of 5172.2 g is used for S3 and Method A1 (b) from TMH1 is adapted and the following steps are followed to compile the grading for S3.

1. After crushing the sample is oven dried at 110^{o}C overnight.
2. Prior to sieving, the sample is weighed and then sieved through the following sieve sizes: 28, 20, 14, 10, 7.1, 5, 2, 1, 0.6, 0.425, 0.3, 0.15 and 0.075 mm.
3. The steps that follow are identical to step 5 to step 7 of the wet sieve analysis method previously discussed.

3.2.2 Hygroscopic moisture

The hygroscopic moisture or moisture content of a sample of aggregates is the mass of water in the aggregates expressed as a percentage to the total dry mass of the aggregates. The moisture in the aggregates is due to the surrounding humidity which is absorbed by the aggregates. Recycled concrete aggregate is a porous material which easily absorbs and retains moisture from the surrounding environment and has been found to have a higher hygroscopic moisture in comparison to natural aggregates (Poon & Chan, 2006). Therefore, the hygroscopic moisture of the aggregates is an important primary input parameter for the required mixing moisture and it is determined prior to all mixing activities. The process to determine the moisture content of RCA by oven-drying is adapted from SANS 3001-GR20:2010 Edition 1.

1. In order to achieve consistent readings, the method specified is adapted by reconstituting the final grading obtained for the project into four 1 kg samples of RCA for analysis.

2. The masses (Cm) of four steel containers are weighed before the 1 kg aggregates (Mw) are reconstituted. Thereafter, the containers with the reconstituted aggregates as illustrated in Figure 3-5 (Cm + Mw) are weighed and placed in the oven.
3. The 1 kg samples of RCA are oven dried at 110°C overnight.
4. After drying, the containers with the oven-dried aggregates (Cm + Md) are weighed and the difference in the weight of the container before it was placed in the oven and after quantified the mass of the hygroscopic moisture in the aggregates. The moisture content (W) calculated from Equation 3-1 is expressed as a percentage of the dry mass (Md) of the aggregates.
5. The average of the four calculated hygroscopic moistures is used as input for the optimum moisture determination for mixing.

$$W = \frac{M_w - M_d}{M_d} \times 100 \qquad \text{Equation 3-1}$$

Figure 3-5: Reconstituted RCA fractions

3.2.3 **Maximum dry density and Optimum moisture content**

The maximum dry density and optimum moisture content of the final grading is determined from the moisture-density relationship of RCA 1 and RCA 2 compacted at the Modified AASHTO compaction effort at different moisture contents as specified in the SANS 3001-GR30:2015 Edition 1.2. This method is chosen because it is the common method used to determine the moisture-density relationship of a granular material in the South African construction industry. The process outlined in the specification is adapted and the following steps are taken to determine the maximum dry density and optimum moisture content:

1. The hygroscopic moisture of the aggregates is determined with the method described in Section 3.2.2.

2. Seven 6 kg bags of RCA are reconstituted and sealed to prevent the loss of moisture overnight prior to mixing and compaction. This is done to prevent changes to the hygroscopic moisture in the aggregates.
3. The mass of the hygroscopic moisture calculated from the percentage value W, determined with Equation 3-1, is subtracted from the mass of the aggregates in the sample bags to determine the estimated dry mass of the aggregates.
4. The dry mass of the aggregates is used to calculate the mass of the water to be added to achieve the targeted moisture contents.
5. The first two sample bags are mixed with water to achieve 11 and 13% moisture contents (Wi) and the approximate dry density achieved after compaction is determined for each mix. The water is distributed on the aggregates while the mixer rotates to evenly distribute the moisture.
6. After mixing, a small sample of the mix is taken to oven dry at 110^{o}C overnight to determine the accurate moisture content in the mix and calculate the dry density (D_{Di}) of the compacted specimen.
7. Based on approximate densities calculated in step 5, a further 3 moisture contents (10, 15 and 16%) are mixed and the approximate densities are calculated to complete the moisture content and dry density curve.
8. A steel mould (152 mm x 152 mm) is weighed before the compaction of the specimen for use in the mass calculation of the wet compacted specimen (Mswi).
9. The mix is compacted in the steel mould in 5 layers with a free falling steel tamper with a 50 mm diameter face which weighed 4500 g and 55 blows are applied to each layer.
10. The mould and the compacted specimen are weighed after compaction and the approximate dry density (D_{Di}) of the compacted sample at each moisture content is determined from the mould factor (F) and the moisture content (Wi) with Equation 3 2

$$D_{Di} = \frac{M_{swi}\, x\, F}{100 + W_i} \qquad \text{Equation 3-2.}$$

11. The relationship between the dry density and the moisture content is evaluated from a graph where the moisture content is plotted on the x-axis and the dry density on the y-axis. The peak of the graph indicates the maximum dry density (MDD) of the material at a specific moisture content read off the graph. This moisture content represents the optimum moisture content (OMC) of the aggregate mix.

3.2.4 **Atterberg limits Determination**

The Atterberg limits are tested in order to understand the behaviour of the fine aggregates to changes in moisture content. The test aims to determine the liquid limit (LL) and the plastic limit (PL) of the aggregates passing the 0.425 mm sieve in order to calculate the plasticity index (PI). The process followed to determine each Atterberg limit is as specified in SANS 3001-GR10 2013 Edition 1.2 with no adaptations. The liquid limit is determined with the liquid limit device used to separate the mixture of water and aggregates in a steel dish by tapping in the centre of the dish. The plastic limit is determined by rolling a number of 3 mm diameter threads of the aggregates mixed with a range of different moisture contents to determine the moisture content that results in the thread crumbling. The plasticity index (PI) is calculated from the difference between the liquid limit and the plastic limit and it indicates the range of moisture contents the aggregates are sensitive too.

3.2.5 **Cement Activity of RCA**

Recycled concrete aggregate has been proven to contain residual cement which results in the potential self-cementation of the aggregates (Rudman & Jenkins, 2015). The age and treatment of the aggregates prior to use in construction influences the potential to self-cement as shown by a study done by Bredenkamp (2018). Paige-Green (2010) recommends testing the pH of the aggregates as it is done for cement stabilisation. The test measures the initial consumption of cement (ICC) which indicates the occurrence of hydration as the pH changes to alkaline. The pH test measures the hydrogen ion concentration in a soil suspension with a calibrated pH meter. The pH is tested for a graded mix with 14 mm RCA 1 and a mix with 14 mm RCA 2 as specified by the SANS 3001-GR57 2014 however, no cement is added. The aggregates are mixed with distilled water and three pH readings are measured with the calibrated pH meter (Figure 3-6). Phenolphthalein solution is also used to test the presence of active cement on a specimen produced at OMC and covered in plastic to cure for 3 days.

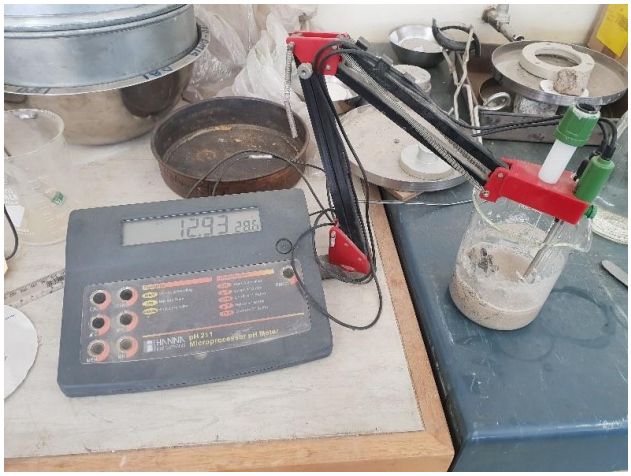

Figure 3-6: pH meter during sample testing

3.2.6 **California bearing ratio**

The TG2 requires the determination of the 4-day soaked California bearing ratio (CBR) of the untreated soil or gravel in order to understand the bearing capacity of the material with varying compaction efforts. The CBR of RCA 1 and RCA 2 are determined guided by a combination of the TMH 1 1986 Method A8 and SANS 3001 GR40 2013. Two specimens for each RCA type are reconstituted and produced at their individual OMC to achieve the MDD as determined in Section 3.2.3. For each mix, one specimen is compacted with the vibratory hammer to achieve 100% density obtained with the MOD hammer however with 93% OMC. The second sample is compacted with the MOD hammer to achieve a 100% MOD density. The specimens are soaked for 4 days after which the surface of each specimen is penetrated at 1.27 mm per minute. The CBR for each specimen is determined at a penetration depth 2.54 mm.

3.2.7 **Bitumen Foam Properties**

The foaming properties of the 70/100 grade bitumen are determined based on the Wirtgen BSM cold recycling laboratory handbook and the Wirtgen WLB 10 S laboratory foam bitumen unit manual. The foaming properties of bitumen are defined as the expansion ratio and the half-life of the foamed bitumen. These properties are critical for the optimum dispersion of the foamed bitumen within the aggregates. For this project the Wirtgen WLB 10S laboratory foam bitumen unit (Figure 3-7) is used to produce the foamed bitumen. The process aims to determine the expansion ratio and half-life at the optimum temperature of the bitumen and water content. The following steps are taken in order to determine the foaming properties:

Figure 3-7: Wirtgen WLB 10S foam plant

1. 15 litres of 70/100 penetration grade bitumen is preheated in the oven overnight at 100ºC and for a further 3 hours at 160ºC prior to the production of the foamed bitumen.
2. The foaming plant is switched on to heat up and soften the residual bitumen in the machine.
3. The bitumen spray discharge rate (g/sec) and water flow rate (l/h) calibration of the unit is done by ensuring the air pressure is at 5 bar, water pressure is at 6 bar and the pump rate (100g/sec) required as per the manual.
4. The foamed bitumen is sprayed in a heated steel drum and the height of the foam is measured with the calibrated dip stick to calculate the expansion ratio. The time is measured with a timer from end of spraying to the time the height reduces to half the original sprayed height to determine the half-life of the foamed bitumen.
5. The foamed bitumen is produced at a range of water contents (2%, 3%, and 4%) at two bitumen temperatures (165ºC and 175ºC) to formulate a graph that represents a relationship between the water content and temperature of the bitumen with the foaming properties of the bitumen.

The optimum foamed bitumen characteristics obtained are a half-life of 12 secs and an expansion ratio of 11.7 times. These properties were achieved with 2% water content at 165ºC bitumen temperature. The foam characteristics comply with the minimum required expansion ratio of 8 times the original volume and a half-life of 6 secs for the stabilisation of aggregates at a temperature greater than 15ºC (Wirtgen Group, 2012).

3.3 Phase 2 – Mix Design Optimisation

The mix design optimisation phase aims to determine whether an active filler is required to optimally disperse the bitumen binder to the aggregates and to determine the optimum required bitumen content. The effect of active filler and the optimum bitumen content are measured by testing the indirect tensile strength (ITS) of the specimens. The steps followed to produce the specimens are adapted from three SANS 3001 BSM specifications with slight adjustments to improve the quality of the BSM with RCA mixes. The subsections discuss the general preparation done before mixing, compaction and curing of the specimen. A detailed process on the mixing with bitumen emulsion, foamed bitumen and testing of the tensile strength of the resultant specimens is given in this section. A total of 12 mix designs with 6 specimens per mix are produced. Three of the six specimens are tested dry and the other three are tested wet therefore a total of 72 specimens are produced for Phase 2. Table 5 summarizes the different mix designs and the respective variables to determine the effect of active filler and optimum bitumen content with bitumen emulsion and foamed bitumen.

Table 5: Mix design optimisation variables

PURPOSE	BITUMEN TYPE + CONTENT (%)[i]	ACTIVE FILLER (%)	NO. ITS SPECIMEN	NO. MONOTONIC SPECIMEN
SUITABLE ACTIVE FILLER	Emulsion - 2.2%	no active filler	6	10
		1% cement	6	-
		1% lime	6	-
	Foam - 2.2%	no active filler	6	10
		1% cement	6	-
		1% lime	6	-
OPTIMUM BITUMEN CONTENT	Emulsion - 2.0%	no active filler	6	-
	Emulsion - 2.4%		6	-
	Emulsion - 2.8%		6	-
	Foam - 2.0%	no active filler	6	-
	Foam - 2.4%		6	-
	Foam - 2.8%		6	-

(i) % represents the content to the dry mass of the aggregates

3.3.1 **Sample preparation, specimen compaction and curing processes**

Sample preparation

The following steps are adapted from the SANS 3001-BSM2:201X Edition 1 to prepare RCA for mixing with bitumen emulsion and foamed bitumen:

1. The content of the hygroscopic moisture in the RCA at the time the sample bags are reconstitution is measured as discussed in Section 3.2.2.
2. The reconstitution of RCA fractions is done in plastic bags and each mix design with bitumen emulsion requires 13 kg aggregates to produce 3 specimens therefore 2 bags with 13 kg are reconstituted for the mixes with bitumen emulsion. Whereas, a 26 kg bag of aggregates are reconstituted for mixes with foamed bitumen to produce 6 specimens per mix design.
3. The dry mass (M_d) of the reconstituted samples is calculated from Equation 3-3 by subtracting the mass of the hygroscopic moisture (calculated from the percentage of the hygroscopic moisture (W)) from the mass of the reconstituted air dried aggregates (M_{AD}).

$$M_d = \frac{M_{AD}}{1 + \frac{W}{100}}$$

Equation 3-3

4. The dry mass is used to calculate the following input values for the mixes: the mass of the water added (M_w) to achieve OMC, mass of active filler (M_{AF}) and mass of bitumen emulsion or foamed bitumen (M_{SA}) added based on the relative percentage to dry mass (P_A) as summarised in Table 5. The quantities for the active filler and bitumen content are calculated with Equation 3-4. The mass of water added is discussed separately in Sections 3.3.2 and 3.3.3.

$$M_{AF} = P_A x M_d$$

Equation 3-4

5. The OMC determined in Section 3.2.3 is reduced by 6% due to the difference in the applied compaction energy between the modified AASHTO and vibratory hammer. This is done because BSM specimens are compacted with the vibratory hammer.
6. In order to improve the quality of the mix and reduce potential variability that results from the sensitivity of bitumen to temperature, 1% of the dry mass of the aggregates (a fraction of the OMC calculated in step 5) is added to the aggregates in the plastic bags. The bags are sealed and placed in an oven at 25˚C overnight. The water used for mixing is also placed in the oven at 25˚C overnight.
7. The constant bitumen content added to the mixes in order to test the effect of active filler is deduced based on the final grading of the aggregates as guided by Section A1.2.2.2 in the Wirtgen cold recycling manual (Wirtgen Group, 2012). The section requires the

sum total of the percentage of the aggregates passing the 0.075 mm sieve and the sum total of the percentage of the aggregates passing the 4.75 mm sieve.

8. For the active filler effect mixes, the bitumen content is determined as 2.2% in step 7 and 3 mixes with 1% cement,1% lime and a mix with no active filler are made with bitumen emulsion and foamed bitumen.
9. For the optimum bitumen content mixes the bitumen content is varied (2%, 2.4% and 2.6%) with a constant active filler as determined in the active filler effect stage.
10. Prior to mixing, the temperature of the aggregates, water and bitumen emulsion or bitumen for foam are measured and recorded.

Compaction

The BSM specimens for ITS testing are compacted in two equal layers with the Wirtgen WLV1 vibratory hammer (Figure 3-8 A). The following steps to compact all the specimens made with bitumen emulsion and foamed bitumen are modified from SANS 3001-BSM3:201X Edition 1:

1. In order to calculate the mass of the stabilised RCA required for each layer, the mass of the compacted specimen (M_S) (with the MDD as previously determined in Section 3.2.3) is calculated with Equation 3-5.

$$Ms = \frac{(\pi\ x\ d^2)}{4x10^6}\ x\ h\ x\ (MDD\ x\ (1 + \frac{OMC}{100})$$

Equation 3-5

2. The mass of the stabilised RCA for each layer (M_L) is calculated from Equation 3-6 and it is weighed and packed in plastic bags which are sealed to prevent loss of moisture prior to compaction.

$$M_L = \frac{M_s}{2}$$

Equation 3-6

4. The samples are compacted in a steel split mould (152 mm x 120 mm) in two equal layers and a limit on the specimen height (h) is set to 95 mm on the vibratory hammer in order to achieve MDD.
5. The split mould is sprayed with spray cook to lubricate the sides to easily remove the compacted specimen from the mould.
6. A spatula is used to spread the aggregates evenly on the sides of the mould and fill the gaps between the coarse aggregates with finer aggregates.

7. An interlayer roughening device (Figure 3-8 B) is used to loosen the first layer after compaction in order to provide adhesion between the two layers.
8. The specimen is removed immediately after compaction and not after 4 hours as specified, however the removal is done with care resulting to no damage on the specimen.
9. Prior to curing, each specimen is weighed (g) and the height (mm) of the compacted specimen is measured at 3 evenly spaced spots with a calliper.

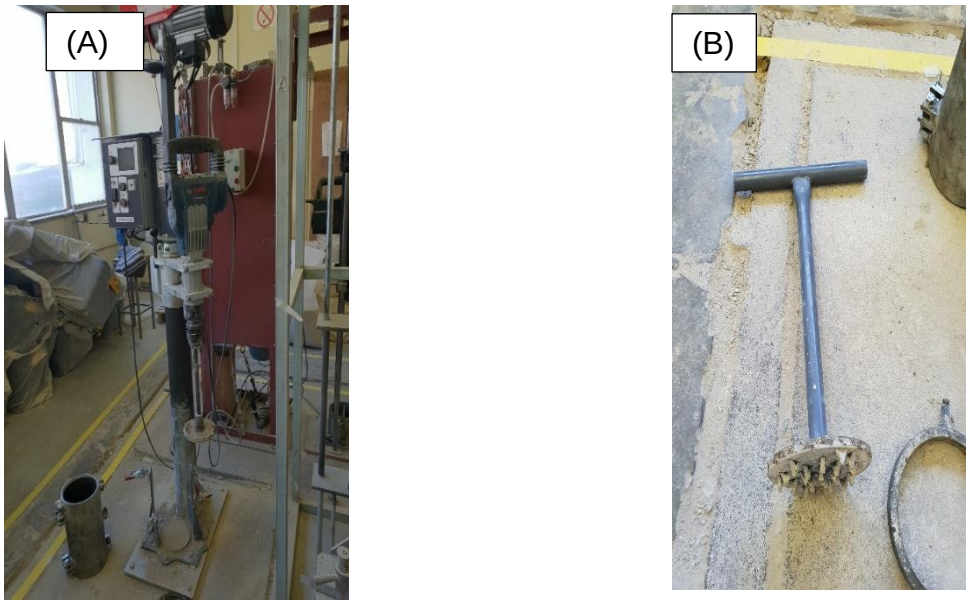

Figure 3-8: (A) Vibratory Hammer and (B) Interlayer roughening device

Curing

The curing process is done to release moisture from the specimens in order to increase adhesion between the aggregates and bitumen. The accelerated curing process specified in SANS 3001-BSM2-201X is used with modifications for all specimens produced with bitumen emulsion and foamed bitumen.

1. The specimens are placed in an oven at 40^{o}C for 72 hr (Figure 3-9 A).
2. After 72 hrs all the specimens are taken out of the oven, weighed (g) and placed in a temperature-controlled room at 25^{o}C.
3. The specimens that are tested dry are allowed to cool down to 25^{o}C for 24hrs prior to testing
4. Buckets filled with 10 l of water are placed in an oven at 25^{o}C overnight in order to increase the temperature of the water.
5. The specimens tested wet are placed in the heated water obtained from step 4 for a further 24 hrs in a temperature-controlled room at 25^{o}C as illustrated by Figure 3-9B.

Figure 3-9 (A) curing of specimen in the oven and (B) soaking in water method

3.3.2 **Bitumen emulsion mix design procedure**

Each mix is made from a 13 kg graded RCA and 3 specimens (152 mm x 95 mm) are produced. The following steps are used to produce the different mixes as summarised in Table 5 with bitumen emulsion to test the effect of active filler and to determine the optimum binder content as specified in SANS 3001-BSM 2:201X Edition 1:

1. The stability of the bitumen emulsion is checked by making a paste with 50 g cement, 17 ml water and 83 ml bitumen emulsion. The paste is stirred until the colour changes to black indicating the breaking of bitumen emulsion and the time of the process is recorded.
2. The calculated mass of the bitumen emulsion (M_{AS}) with Equation 3-4 for a specific content, taking into account that 40% of the bitumen emulsion is water and emulsifier, is weighed and heated in an oven at 60^{o}C for 3 hours prior to mixing.
3. The aggregates are spread in the pan mixer and the initial temperature of the aggregates is recorded using a laser thermal measurement device (Figure 3-10 A).
4. The active filler, calculated from Equation 3-4, M_{AF}, is evenly sprinkled on the aggregates in the mixer as required.
5. The mass of the water (M_W) determined from Equation 3-7 to achieve the optimum fluid content (OPC) is calculated and evenly sprinkled while the pan mixer rotates with the dry ingredients. The OPC is the total mass of the liquids added to the aggregates to achieve OMC. Therefore, OPC is equal to OMC, however it is made up of the mass of the bitumen emulsion (M_{AS}) plus the mass of the hygroscopic moisture(M_{AD}-M_D) plus the 1% of aggregate dry mass water added the night before (1%M_D) and the required water to reach OMC of the aggregates before mixing (M_W).

$$M_w = \frac{OFC\ x\ (M_D + M_{AF})}{100} - (M_{AD} - M_D) - M_{AS} - 1\%M_D$$

Equation 3-7

6. The heated bitumen emulsion is weighed (Figure 3-10 B) to obtain the required content percentages (Table 5) to aggregate dry mass and added to the mixer. The bitumen emulsion is mixed with the moist RCA until all the aggregates are covered with bitumen emulsion (Figure 3-10 C).
7. A sample of the stabilised RCA is taken to determine the moulding moisture content as guided by SANS 3001 GR20:2010 Edition 1.1.
8. The mass of stabilised material for each layer calculated with Equation 3-6 is weighed and sealed in plastic bags.
9. The material is compacted, specimen weighed (Mw) and cured as previously discussed in Section 3.3.1.

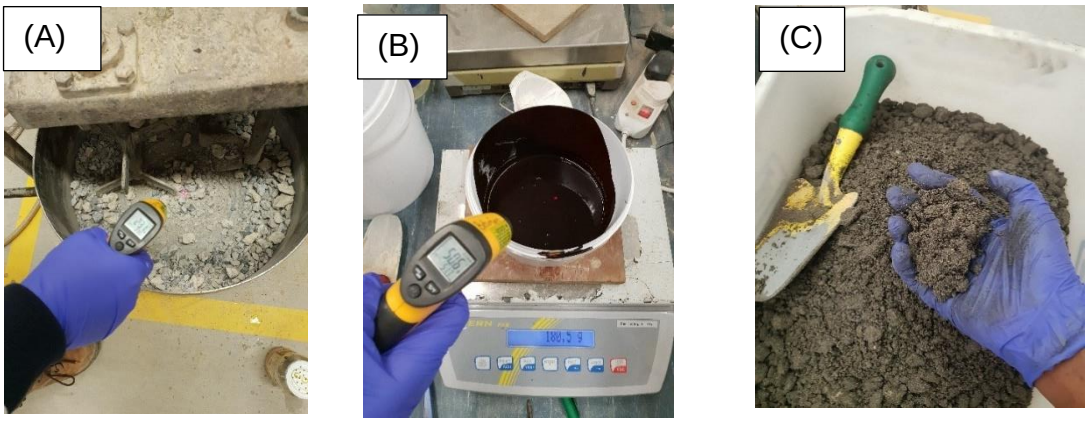

Figure 3-10: Mixing process (A) RCA in rotating pan mixer, (B) heated bitumen emulsion and (C) final stabilised RCA

3.3.3 **Foamed bitumen mix design procedure**

Each mix is made from a 26 kg graded RCA which produces 6 specimens. The mixing is done with a pug mill mixer (Figure 3-11 A) and the foamed bitumen is produced with the Wirtgen WLB 10S laboratory foaming plant (Figure 3-7). The following steps are used for both mixes with bitumen foam to test the effect of active filler and determine the optimum binder content as specified by SANS 3001-BSM 2:201X Edition 1:

1. 15 litres of 70/100 penetration grade bitumen is heated in a forced draft oven over night at 100ºC and for 3 hours at 160ºC prior to mixing.
2. The foam plant is switched on to heat up to 165ºC and the heated bitumen is poured into the bitumen kettle of the plant.

3. The bitumen spray rate is calibrated to spray 100 g/s and the air pressure is adjusted. The water spray rate is also calibrated to spray 7.2 l/hr to satisfy the required water content in the foam.
4. The foaming characteristics of the bitumen are checked by producing foamed bitumen after calibration at the target bitumen temperature of 165°C with 2% water content.
5. The aggregates are spread out uniformly along the length of the pug mill mixer and the active filler is sprinkled on top as required. These dry ingredients are mixed at medium speed for 30 secs.
6. The total mass of water (M_W) to achieve OMC is determined with Equation 3-8, where the mass of the hygroscopic moisture ($M_{AD} – M_D$) and the added 1% moisture of the dry mass of the RCA ($1\%M_D$) are subtracted.

$$M_W = \frac{OMC\ x\ (M_D + M_{AF})}{100} - (M_{AD} - M_D) - 1\%M_D$$

Equation 3-8 The water is added in two portions at different stages of the mixing process. 80% of M_w calculated in step 6 is added and mixed with the aggregates for 30 secs prior to mixing with foamed bitumen.

8. The remaining 20% of M_w is added after RCA is stabilised with foamed bitumen.
9. Two samples of the stabilised RCA are taken before packing of the layers and after packing the last layer to determine the moulding moisture content of the aggregates guided by SANS 3001 GR20:2010 Edition 1.1.
10. The stabilised RCA is weighed for each layer of the specimen and sealed in plastic bags (Figure 3-11A) Thereafter the material is compacted and the specimen is weighed (Mw) and placed in an oven for curing.

Figure 3-11: (A) pug mill mixer and (B) packed stabilised RCA for each layer

3.3.4 **Specimen Indirect Tensile strength testing**

All the specimens produced from the stabilisation of RCA with bitumen emulsion and foamed bitumen are tested for the indirect tensile strength (ITS) at 25°C with the universal testing

machine 30 (UTM 30). The following steps are used to measure the peak compressive force and deformation at failure for each of the 3 specimens tested dry and 3 specimens tested wet after soaking per mix design as specified by SANS 3001-BSM4:201X Edition 1:

1. The specimen is weighed (g) after curing (Mc) and the mass is used to calculate the bulk density (BD) of each specimen with Equation 3-9. The surface temperature of each specimen is measured with a laser thermal measurement device prior to testing.

$$BD = \frac{4x10^6 x M_c}{(\pi\ x\ d^2) x\ h}$$

Equation 3-9

2. The specimen is placed on the bottom loading strip along the height and top loading strip is placed parallel to the bottom loading strip on top of the specimen.
3. The specimen is loaded at a rate of 50 mm/min until the peak force is reached and the specimen breaks. The peak force (G) and the deformation at failure are recorded.
4. The specimen is removed and the temperature of the core is measured and recorded.
5. The moisture content of the specimens at the time of testing for both specimens tested dry and specimens tested wet are determined by placing the broken specimens in a steel dish which is weighed and placed in an oven at 110^{o}C overnight as guided by SANS 3001 GR20:2010 Edition 1.1.

3.3.5 **ITS result analysis method**

The results obtained from the ITS test are used to calculate the indirect tensile strength of the stabilised RCA, assess the moisture sensitive of the material and establish the influence varies active fillers or an increase in the bitumen content has on the strength of the mix. The steps followed are obtained from the SANS 3001-BSM4:201X, Wirtgen Cold Recycling Technology and the BSM Cold Recycling Laboratory Handbook.

1. The bulk density (BD) of each specimen in the set produced for each mix design is calculated with Equation 3-9. An outlier test is done on the set to verify consistency of the specimens by sorting the BD of each specimen in ascending order.
2. The average and standard deviations of the BD of the set are calculated and used to determine the critical outlier value for the set which is compared with the critical outlier value (T_o) of 1.822 for a set of 6 specimens. This step is done to ensure similar specimens are produced for each mix prior to further analysis of the results.
3. The ITS of each specimen is calculated from the measured peak force (G), the diameter of the specimen (d) and the height of the specimen (h) with Equation 3-10.

$$ITS = \frac{2\ x\ G}{\pi\ x\ d\ x\ h\ x\ 10^6}$$

Equation 3-10

4. The average ITS for the dry triplicate is calculated as the representative ITS for the mix tested in a dry condition. This is also done for the wet triplicate set. This calculation is done for all mixes with 1%cement, 1%lime, no active filler, and changes in bitumen content from 2% to 2.6%.
5. The moisture resilience of the mixes is quantified by the tensile strength retained (TSR) which is calculated from the average ITS for wet specimens (Ave ITS_{wet}) and the average ITS for the dry specimens (Ave ITS_{dry}) with Equation 3-11.

$$TSR = \frac{AveITS_{wet}}{AveITS_{dry}} \times 100$$ Equation 3-11

6. The relationship between the change in the average dry ITS verses the change in active filler or increase in bitumen content is plotted on the graph to determine the sensitivity of the RCA to variations in the active filler and the bitumen content.
7. The dry density (DD) for each specimen is calculated with Equation 3-12 and the dry mass of each specimen (M_D) is determined from Equation 3-13 which is an input for the dry density calculation. The average DD is calculated for the dry and wet triplicate set for each mix.

$$DD = \frac{4x10^6xM_D}{(\pi\ x\ d^2)x\ h}$$

Equation 3-12

$$M_D = \frac{100\ x\ M_w}{(100 + OMC)}$$

Equation 3-13

8. A stress verse strain graph is plotted for each specimen tested to determine the relationship between the increase in the applied force and the deformation of the specimen from each mix design.

3.4 Phase 3 – Performance Properties

The performance properties phase aims to determine the shear parameters and resilient modulus of the final two mix designs made from 2.2% bitumen emulsion and 2.2% foamed bitumen content with no active filler. These properties indicate the shear strength and stiffness of the RCA stabilised with bitumen emulsion and foamed bitumen. The steps

followed in the mixing process with bitumen emulsion and foamed bitumen are as discussed in Section 3.3.2 and 3.3.3, respectively. The compaction, curing, testing of the specimens and result analyses are done as specified by SANS 3001 BSM 5:201X Edition 1.1. A total of ten specimens (300 mm x 152 mm) are produced for each mix design. After curing, eight specimens are tested with the monotonic test in pairs for each confinement pressure (0, 50, 100, 200 kPa) to determine the shear strength of the mix. The remaining two specimens are tested after 24hrs of soaking at a confinement pressure of 100 kPa to evaluate the influence of moisture on the cohesion of the mix. The resilient modulus is determined from the dynamic loading test with the triaxial where two specimens are tested for each mix design with bitumen emulsion and foamed bitumen at varies deviator stress ratios.

3.4.1 **Triaxial specimen preparation**

Compaction

The specimens produced for this phase are 300 mm in height and 152 mm in diameter hence compaction is executed with the Wirtgen WLW1 vibratory hammer (Figure 3-6A) in five equal layers as guided by SANS 3001-BSM3:201X Edition 1.1 The following steps are followed:

1. The compacted mass of the stabilised RCA specimen is calculated with Equation 3-5 where the height input is 300 mm. The other input variables remain the same as used for the ITS specimens.
2. The mass of each layer in the specimen is calculated with Equation 3-6 and weighed off, packed and sealed in plastic bags prior to compaction.
3. The compaction is executed in a steel split mould sized 152 mm in diameter and 300 mm in height. The compaction steps followed from this point are as stated in Section 3.3.1 Compaction, step 5 to 9.

Curing

The curing method used for the triaxial specimens aims to reduce the moisture content of the specimens to 65% of the OMC. This is done to achieve an equilibrium state in the specimen to represent a typical worst case scenario for the mix in a pavement structure. The curing steps are outlined in SANS 3001-BSM5:201X and they are summarized as follows:

1. After compaction, the specimen is weighed (M_M) and placed in a force draft-drying oven at 40^{o}C for 2 hrs as shown in Figure 3-12 A and B.

2. The mass of the moisture in the specimen (M_w) prior to curing is estimated with Equation 3-14 for use in the evaluation of the remaining moisture in the specimen at each curing period.

$$M_W = M_M \times (1 - \frac{100}{100 + OMC\ or\ OFC})$$

Equation 3-14

3. After 2hrs, the specimen is weighed (M_{Ci}) to determine the loss of mass which represents the evaporated water from the specimen. The specimen is returned to the oven and kept for 3 hours prior the next weighing.
4. The moisture content in the specimen is tracked through the loss of mass after each curing period in the oven. The lost mass (M_{Li}) is calculated with Equation 3-15 as the difference between the mass of the specimen before placed in the oven (M_M) and mass of specimen at curing hour i (M_{ci}).

$$M_{Li} = M_M - M_{Ci}$$

Equation 3-15

5. The moisture content of the specimen at curing period i is calculated as a percentage to the compaction moisture (M_w) with Equation 3-16. This process is done until the moisture content of the specimen reaches 65% of the OMC.

$$W_{ci} = 100 \times (1 - \frac{M_{Li}}{M_W})$$

Equation 3-16

6. Once the moisture content in the specimen reaches 65% of OMC, the specimen is removed from the oven and placed in a plastic bag, sealed and returned to the oven at 40^{o}C for a further 48 hrs of curing (Figure 3-12C).After the 48 hrs of curing, the specimen is removed from the oven and allowed to cool for 12 hrs to 25^{o}C in a clean sealed plastic bag to prevent any loss of moisture in a temperature controlled room (Figure 3-12D). Two of the ten specimens are soaked in water at 25^{o}C for 24 hrs. Prior to testing, the specimen is weighed (M_{Pc}), the height (h) and diameter (d) are measured at 3 different points and the averages are calculated. These values are used to determine the bulk density (BD) for each specimen with Equation 3-17 and an outlier check is done as described in the BSM5 specification.

$$BD = \frac{4 \times 10^6 \times M_{PC}}{\pi \times d^2 \times h}$$

Equation 3-17

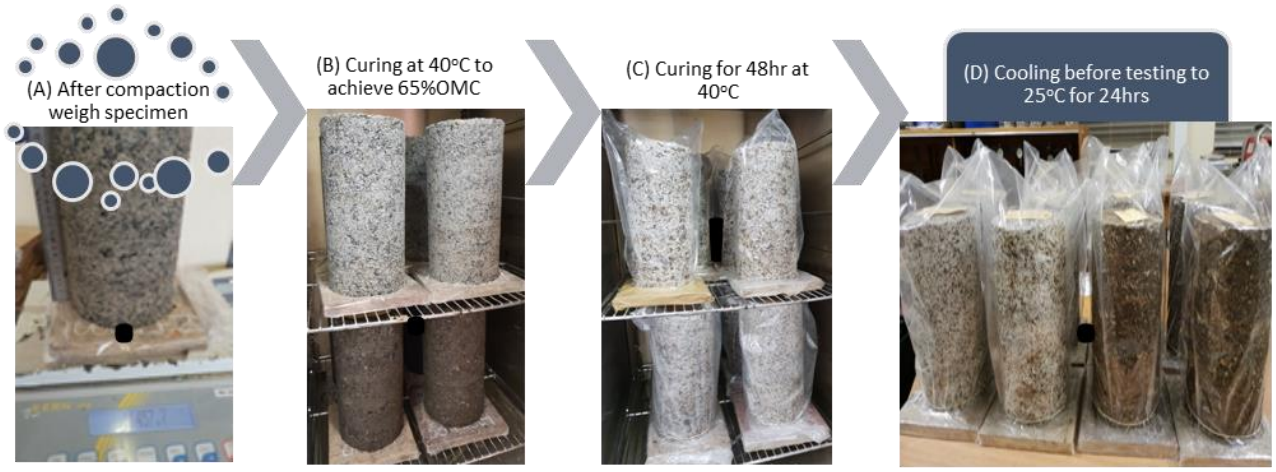

Figure 3-12: Triaxial specimen curing process prior to testing.

3.4.2 **Triaxial monotonic test setup**

In the laboratory, the shear strength of a mix design is tested with the monotonic triaxial test. The test applies a constant displacement controlled compressive force at 3 mm/min until the specimen confined at a given confinement air pressure fails in shear. A set of 2 specimens are tested at the same confinement pressure and 4 confinement pressures are applied (0 kPa, 50 kPa, 100 kPa, 200 kPa). The result from each confinement set is used to determine the shear envelop of the mix design using Mohr Coulomb model. The steps followed are guided by the SANS 3001_BSM5:201X and the BSM Cold Recycling Laboratory handbook and they are summarised as follows:

1. After the specimen is weighed prior to testing, the specimen is placed on the base plate in the MTS machine as demonstrated in Figure 3-13A.
2. A rubber bladder is placed over the specimen which is used for the confinement pressure which is regulated with the air pressure supplied through the pipe indicated in Figure 3-13B.
3. The confining grey steel cylinder is placed over the rubber bladder and bolted to the base plate to secure the setup when the specimen is loaded as illustrated in Figure 3-13C.
4. Prior to the application of air in the rubber bladder, the top plate highlighted in Figure 3-13A is placed and the loading ram (circled in Figure 3-13C) is lowered and aligned into the depression point of the top plate with a small gap in between.
5. The air valve is open to inflate the rubber bladder to apply the desired confining pressure on the specimen.

6. The loading program is set to apply the 3 mm/min constant displacement controlled compressive force and the loading ram compresses the specimen until it cannot resist the applied force which leads to bulging of the specimen in the centre as it fails in shear as demonstrated in Figure 3-13D.
7. Once the specimen has failed in shear, the confining pressure is released and the loading ram is returned to the original position.
8. The peak force (f_P) is recorded and used to determine the principal stress applied to the specimen.
9. The setup is taken apart and the specimen is broken in the centre as demonstrated in Figure 3-13E to measure the temperature and a 1000 g of the loss material is taken to determine the moisture content of the specimen after testing (W_{PS}).
10. The steps are repeated for each specimen tested at the required confinement pressure.

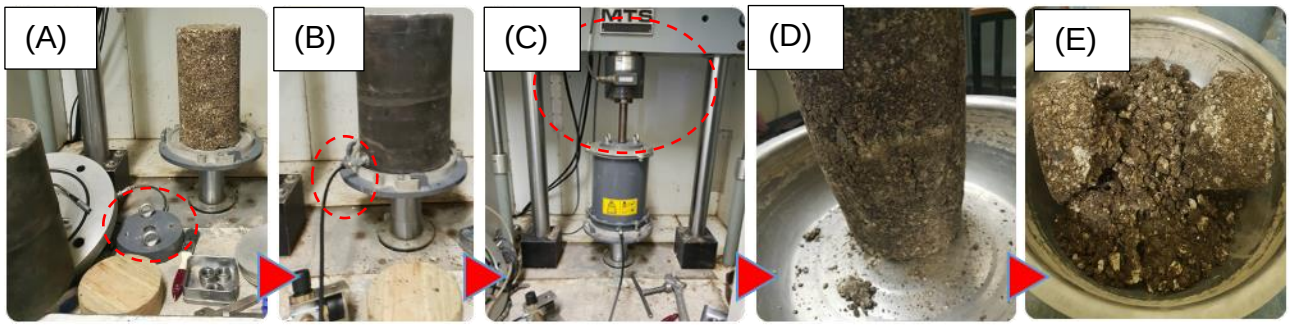

Figure 3-13: Monotonic Triaxial test setup process

3.4.3 **Shear parameters evaluation**

The shear strength of a mix design is characterised by the cohesion (C) and internal angle of friction (ϕ) determined from the failure envelop plotted from the Mohr circles obtained from each confining pressure. The evaluation of the shear parameters is guided by SANS 3001-BSM5:201X and the steps are summarised as follows:

1. The applied failure stress (σ_{1P}) for each specimen is calculated from the applied peak force (f_P) on each specimen at each confining pressure (σ_3) with Equation 3-18.

$$\sigma_{1P} = \frac{4 \times f_P \times 10^6}{(\pi \times d^2)}$$

Equation 3-18

2. The total applied failure stress (σ_{1TP}) which includes the weight of the top plate is calculated with Equation 3-19. This calculation is done for all the 8 specimens tested at the 4 confining pressures.

$$\sigma_{1TP} = \sigma_{1P} + \frac{(4 \times M_{DW} \times 9.81)}{\pi \times d^2}$$

Equation 3-19

3. An average of the σ_{1TP} for the two specimens tested at the same confinement is calculated and plotted on the y-axis against the confining pressure (σ_3) on the x-axis. A best fit line is plotted on the data and the slope (A) and the intercept (B) of the line are determined.
4. The internal angle of friction (ϕ) is calculated first from the slope as an input to Equation 3-20.

$$\phi = sin^{-1}(\frac{A-1}{A+1})$$

Equation 3-20

5. The cohesion of the mix design is calculated from the internal angle of friction and the intercept as input values in Equation 3-21.

$$C = B \times \frac{1 - \sin(\phi)}{2 \times \cos(\phi)}$$

Equation 3-21

6. The influence of moisture on the cohesion of the mix design is assessed from the calculation of the retained cohesion (c_{RET}). This parameter is calculated from the ratio of the peak total applied stress (σ_{1SBF}) resisted by the soaked specimens tested at 100 kPa confinement pressure in comparison to the unsoaked equilibrium(σ_{1USBF}) specimens tested at the same confinement pressure of 100 kPa with Equation 3-22.

$$c_{RET} = \frac{(\sigma_{1SBF} - \sigma_3) \times 100}{(\sigma_{1USBF} - \sigma_3)}$$

Equation 3-22

7. The dry density of the specimens after curing or soaking is calculated with Equation 3-23 to ensure the specimen was compacted properly and that all specimens have similar densities.

$$D_T = \frac{100 \times M_{PS} \times 4 \times 10^6}{(100 + W_{PS}) \times (\pi \times h \times d^2)}$$

Equation 3-23

3.4.4 **Triaxial dynamic test setup**

The response of a mix design to repeated loading is assessed with the dynamic load test conducted with the Triaxial material testing system 2703 (MTS) in the laboratory. The resilient modulus (M_r) i.e. stiffness, quantifies this response and it indicates the load spreading ability of the mix. The value (M_r) determined is used in the pavement design models to estimate the life of the pavement subjected to a given design load. The test setup and testing process used is guided by the proposed protocol for resilient/chord modulus and permanent deformation characteristics of unbound and bound granular materials. The protocol requires that for each test condition, two replicate samples for each mix design are tested at varying impact loads. For this project, the specimens are tested in an equilibrium state as done for the shear strength.

The test setup for evaluating the resilient modulus consists of four intricate stages, outlined in Figure 3-14, were detail is imperative for the consistency of the test. Stage one of the setup requires the determination of the forces to be applied on the specimen to achieve the desired deviator stress ratios (DSR) to determine sensitivity. Stage two of the setup consists of making the latex membrane and its placement on the specimen. Stage three of the setup consists of the attachment of the linear variable differential transducers (LVDT) used to measure the deformation of the specimen during loading. The final stage of the setup is the assembly of the pressure chamber and checking for leaks when air is supplied for the desired confinement pressure. The description of each stage will be illustrated and explained in this section.

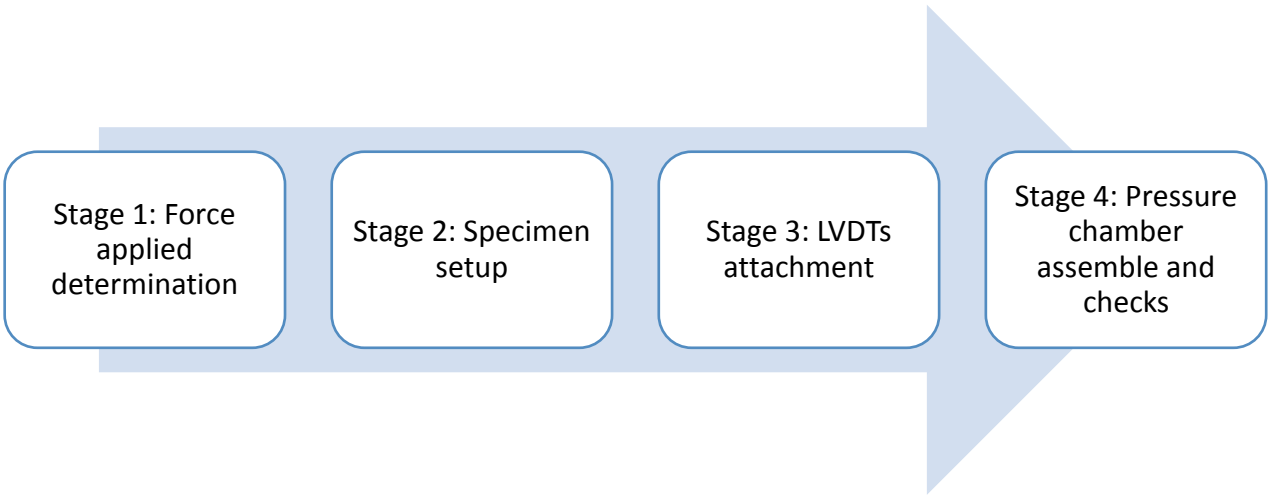

Figure 3-14: Triaxial dynamic test setup process

STAGE 1: Force applied determination

At each phase of the test, characterised by a constant confinement pressure (Figure 3-15B and C), the specimen is exposed to repeated loading at varying deviator stresses as shown in Figure 3-15G. Each load cycle is in the form of a haversine shaped pulse were the load is applied for 0.1 second followed by a 0.9 second rest period before the next load cycle is applied. In each phase, a total of a 100 load cycles are applied for each deviator stress (Figure 3-15A). Prior to testing, the specimens are subjected to a conditioning phase followed by five phases consisting of different confinement pressures (σ_3) of the specimen, which are as follows: 200kPa, 150kPa, 100kPa, 50kPa, 20kPa. At each confinement pressure, five deviator stress ratios (DSRs) as highlighted in Figure 3-15F are applied on the specimen which are as follows: 20%, 30%, 40%, 50%, 55%. The determination of the load applied to achieve each DSR is calculated from the following steps (Figure 3-15):

1. In order to determine the force applied on the specimen, the deviator stress is required. The deviator stress is determined from the principle stress at failure ($\sigma_{1,f}$) which is evaluated from the shear parameters.
2. The shear parameters include the cohesion (C) and internal angle of friction(ϕ) of the mix design computed from the monotonic test with the equation on Figure 3-15D.
3. The deviator stress (σ_d) is determined as the product of the pre-selected stress ratio and deviator stress at failure ($\sigma_{d,f}$) as demonstrated in Figure 3-15G.
4. The load applied (Figure 3-15H) on the specimen is calculated from the principle stress (σ_1) which is deduced from the deviator stress (σ_d) plus the confining pressure (σ_3) of the phase. Then the sum is multiplied by the area of the specimen base.
5. These load values highlighted in (Figure 3-15H) are manually captured in the MTS software prior to testing.

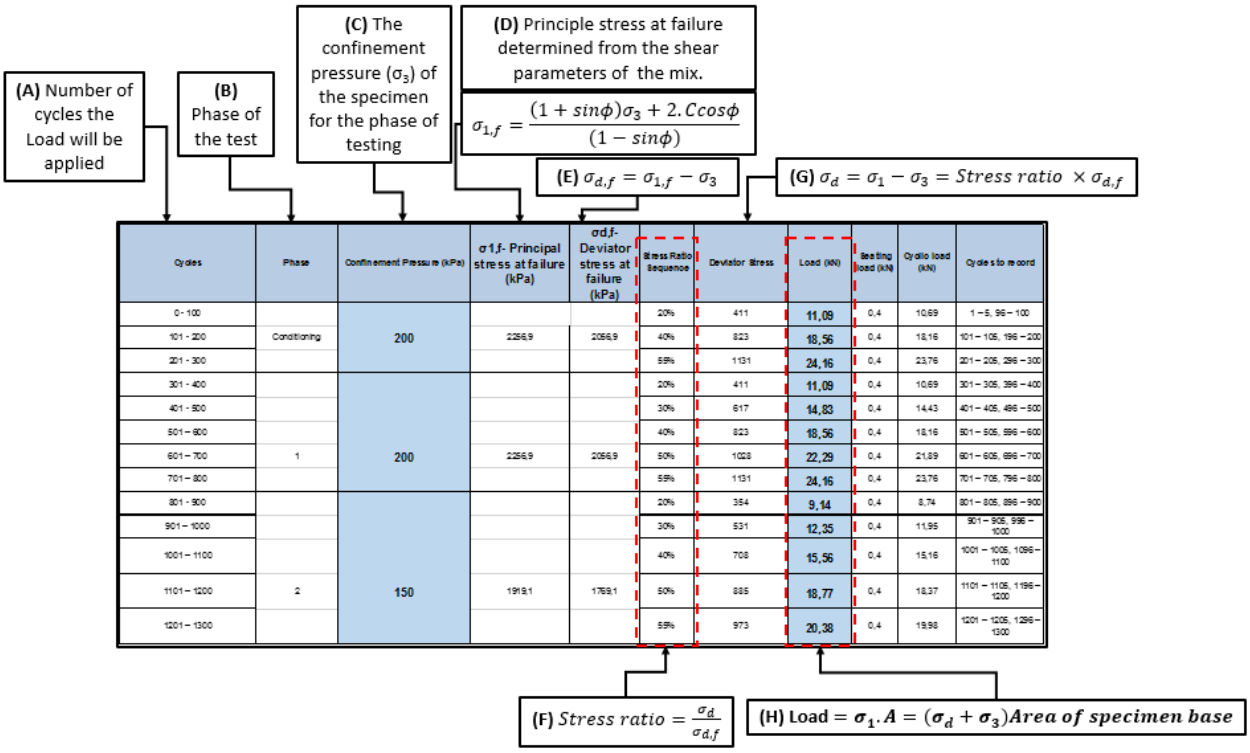

Cycles	Phase	Confinement Pressure (kPa)	σ1,f- Principal stress at failure (kPa)	σd,f- Deviator stress at failure (kPa)	Stress Ratio Sequence	Deviator Stress	Load (kN)	Seating load (kN)	Cyclic load (kN)	Cycles to record
0 - 100					20%	411	11,09	0,4	10,69	1 – 5, 96 – 100
101 - 200	Conditioning	200	2256,9	2056,9	40%	823	18,56	0,4	18,16	101 – 105, 196 – 200
201 - 300					59%	1131	24,16	0,4	23,76	201 – 205, 296 – 300
301 - 400					20%	411	11,09	0,4	10,69	301 – 305, 396 – 400
401 - 500					30%	617	14,83	0,4	14,43	401 – 405, 496 – 500
501 – 600					40%	823	18,56	0,4	18,16	501 – 505, 596 – 600
601 – 700	1	200	2256,9	2056,9	50%	1028	22,29	0,4	21,89	601 – 605, 696 – 700
701 – 800					59%	1131	24,16	0,4	23,76	701 – 705, 796 – 800
801 - 900					20%	354	9,14	0,4	8,74	801 – 805, 896 – 900
901 – 1000					30%	531	12,35	0,4	11,95	901 – 905, 996 – 1000
1001 – 1100					40%	708	15,56	0,4	15,16	1001 – 1005, 1096 – 1100
1101 – 1200	2	150	1919,1	1769,1	50%	885	18,77	0,4	18,37	1101 – 1105, 1196 – 1200
1201 – 1300					59%	973	20,38	0,4	19,98	1201 – 1205, 1296 – 1300

Figure 3-15: Dynamic loading input data

STAGE 2: Specimen setup

The process to setup the specimen consists of the manufacture of the latex membrane (400 mm x 150 mm) and it is carefully placement on the specimen. The placement of the membrane is done with care in order to avoid any damage of the membrane or the damage of the specimen. Therefore, the protocol specifies the following steps for the application of the membrane on the specimen:

1. The membrane is stretched over the steel stretcher. The air tube is used to remove the air between the stretcher and the membrane in order to stretch the membrane as demonstrated in Figure 3-16A.
2. The membrane stretcher and membrane are placed over the specimen with care. The air tube closing is released, and air is allowed to flow into the tube, the membrane returns to its original diameter, and the membrane stays on the specimen. The stretcher is removed with care and the membrane is released onto the specimen.
3. The specimen with the membrane is transferred to the Triaxial cell base pedestal onto the base disc as illustrated in Figure 3-16B.
4. The membrane is rolled down to the base disc shown in Figure 3-16B and secured with two O-rings illustrated on Figure 3-16C. The top of the specimen is covered with the loading cap which is then covered with the membrane and secured with the two O-rings to seal the membrane to prevent air going into the membrane

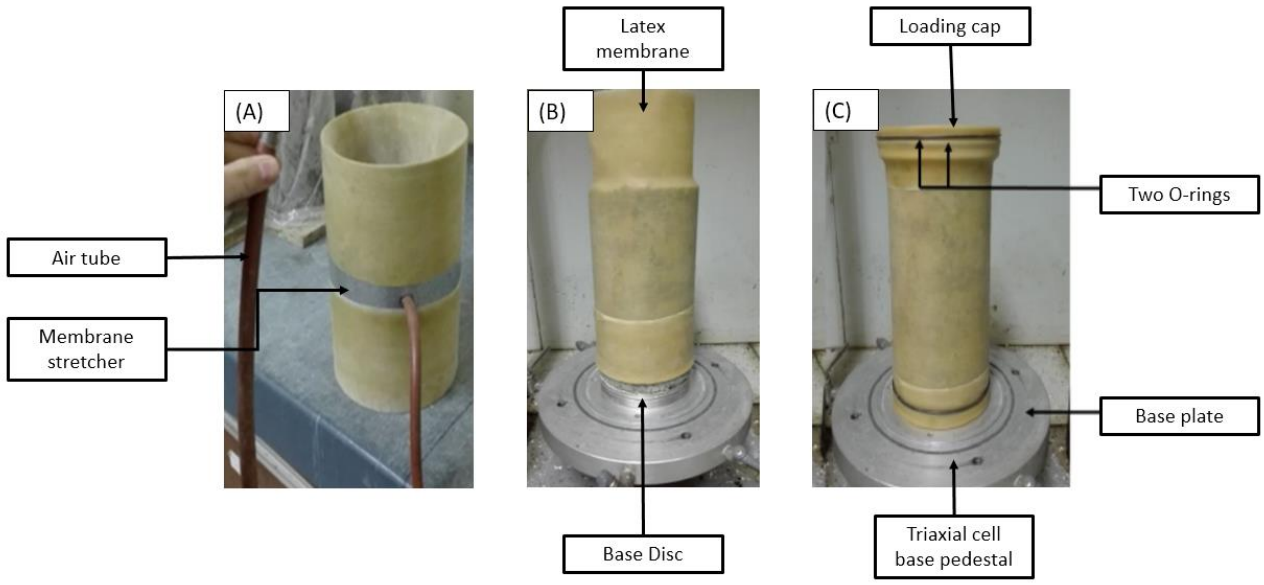

Figure 3-16: (A) Membrane stretcher (B) membrane stretcher placed over specimen (C) specimen with membrane placed on pressure cell base plate(Adapted from, Bredenkamp, 2018)

STAGE 3: LVDT attachment

The LVDTs are used to measure the change in length of the specimen induced by the repeated loading. The LVDT holder can secure three LVDT probes around the specimen and elastic bands are used to ensure the holder makes good contact with the specimen as indicated by Figure 3-17. The proposed protocol requires a 100 mm gap i.e. gauge length (L_g) between the holders. The final step to the setup is to ensure that the tips of the LVDT probes are slightly pressed and placed on the centre of the bottom holder. A few checks done prior to the assembly of the pressure chamber are as follows:

1. The LVDT holders should be parallel to each other.
2. LVDTs probes should be straight and secured by the bolts on the holder.
3. The cables for each probe should not be stuck between the holders and the LVDTs as this will impede the movement of the LVDTs.

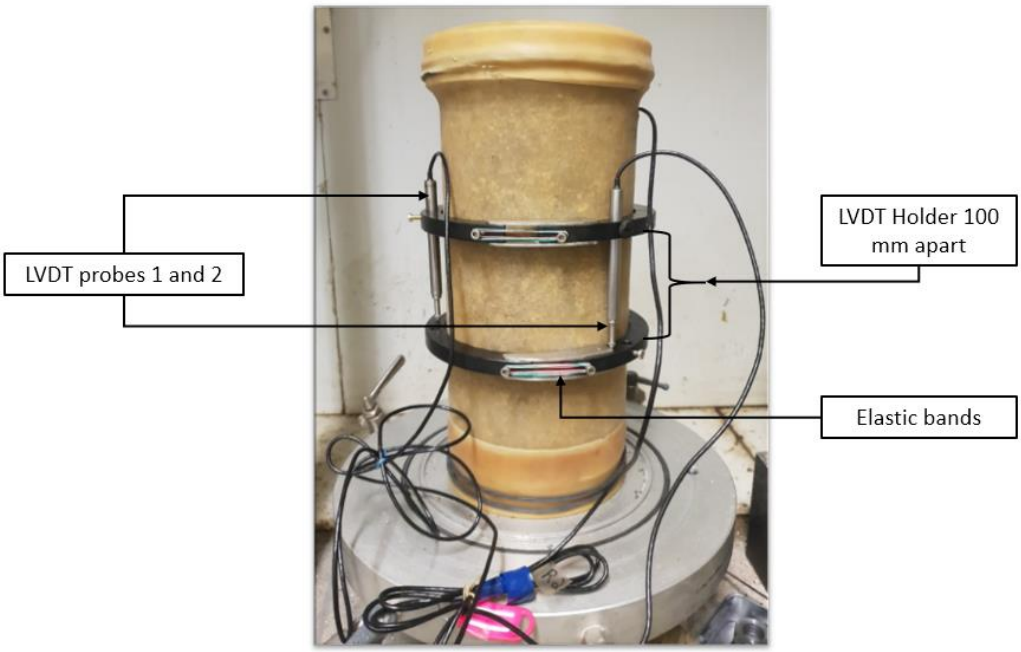

Figure 3-17: LVDT set up

STAGE 4: Pressure chamber setup

The final stage to the dynamic triaxial test setup as shown in Figure 3-14 is the assembly of the pressure chamber as depicted in Figure 3-18. The first step is to place the steel brace on the base pedestal and align the tie rod holes with the holes on the base pedestal. This step is followed by the lubrication of the bottom and top circumference of the pressure chamber to ensure the chamber is airtight. The cables on the LVDTs are connected to the corresponding cables on the chamber top cover. The top cover is then placed on the pressure chamber. A steel piston is aligned to the depression point in the loading cap shown on Figure 3-16 C. The tie rods are fastened to the base pedestal. The loading frame is lowered, and the loading ram is aligned with the steel piston in the top cover. The following checks are done prior to testing:

1. Air is supplied into the chamber to achieve a pressure of 100kPa. This is done to check for air leaks which would result in the loss of pressure in the chamber.
2. Check that the LVDTs are active on the computer monitor to ensure the cables are connected properly.

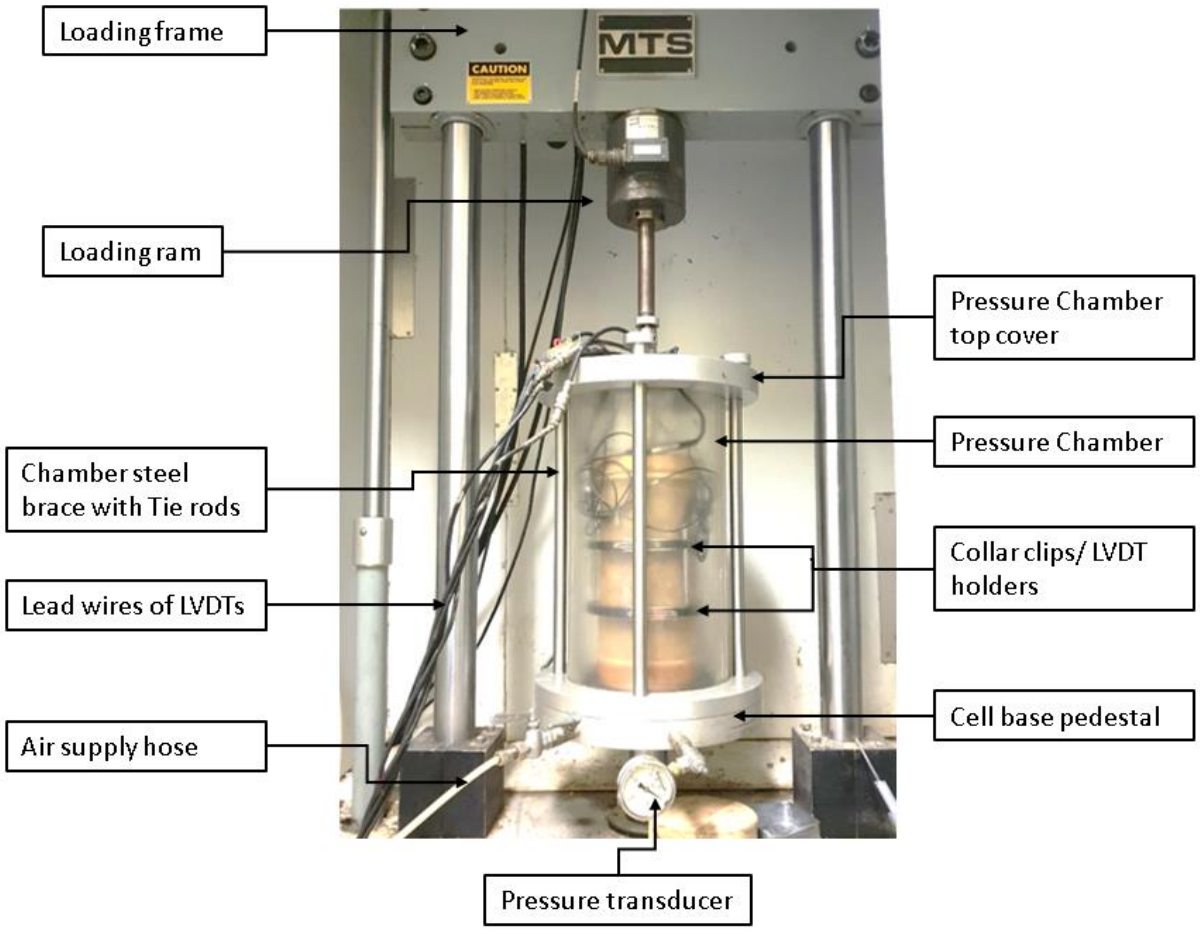

Figure 3-18: The Triaxial pressure chamber

3.4.5 **Resilient modulus data processing**

The testing and determination of the resilient modulus for each specimen is a lengthy process that requires attention to detail as illustrated by the test setup process in 3.4.4. This section aims to document the process followed to determine the relationship between the resilient modulus (M_r) and bulk stress (θ) as influenced by the variation of the deviator stress ratio (DSR). The data processing is guided by the proposed protocol for resilient/chord modulus and permanent deformation characteristics of unbound and bound granular materials. The capture system records the force and displacement for each load applied in the last five load cycles for each confinement phase. The calculation process uses the force and deformation values to determine the M_r as explained in a step by step process illustrated in Figure 3-19.

The resilient modulus (Mr) is a function of the confinement stress (σ_3) and deviator stress ratio (DSR). Each Mr determined in terms of the σ_3 and the DSR is calculated from an average of the last five load cycles for a specific confinement and DSR. In order to calculate

the M_r, the cyclic stress (σ_{cyclic}) and resilient axial strain (ε_a) for each cycle are required. The cyclic stress is calculated from the cyclic load (P_{cyclic}) and area of loading. Whereas, the resilient axial strain per cycle is calculated from the change in length ($\Delta\delta_a$) of the gauge length (L_g) measured by the LVDTs or the change in length of the specimen. An adjustment made to the protocol evaluates the M_r from different combinations of the average strains measured from the LVDTs and the main LVDT. This is done for comparative purposes in the case one LVDT was faulty and incorrectly measured the deformation. Figure 3-19 illustrates the process followed and calculations required to determine the M_r for each confinement and DSR.

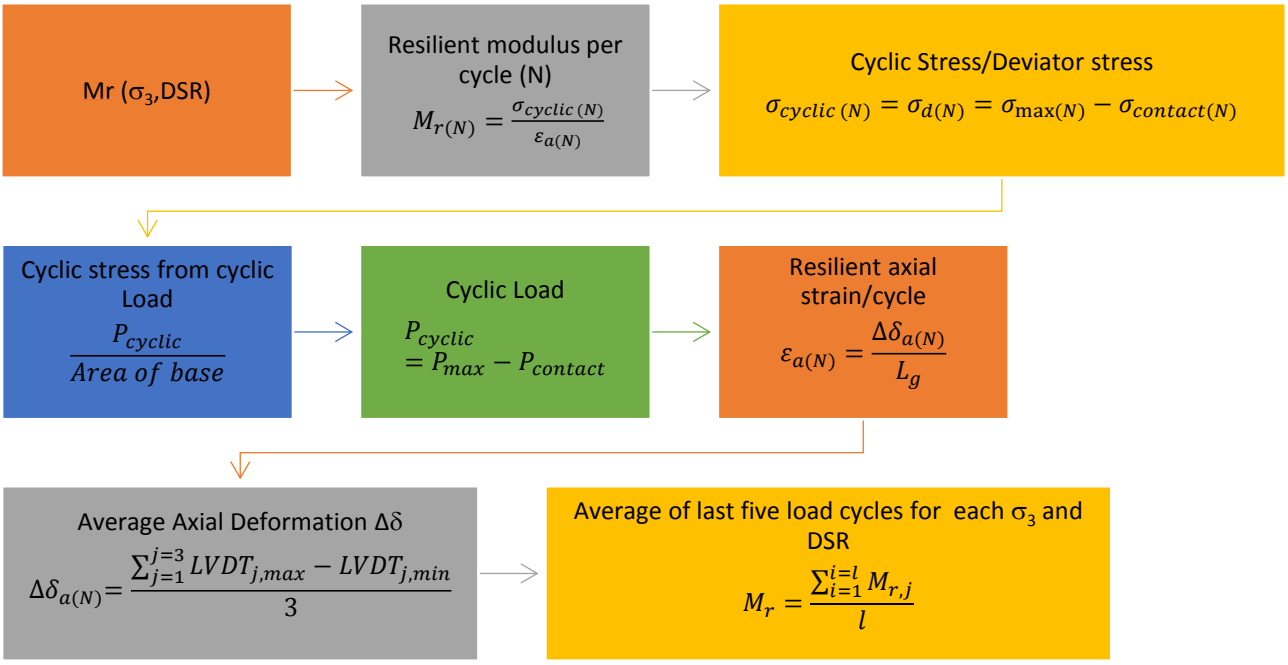

Figure 3-19: Data process to determine resilient modulus (Mr) for each confinement (σ_3) and deviator stress ratio (DSR)

3.4.6 **Resilient modulus modelling**

The model used to describe the relationship between the resilient modulus and bulk stress is done for use in the pavement design of a layer with the material. A model is developed from the data obtained from the test and material coefficients are determined. A BSM is a stress dependent material consequently models used to describe the stress dependency of the resilient modulus for granular materials are used. Seven models presented in Table 6

are used to describe the resilient modulus of the BSM_RCA with bitumen emulsion and foamed bitumen.

Table 6: Resilient modulus models for granular materials

MODEL NAME	MODEL	PARAMETERS
MR-θ	$Mr = k_1\theta^{k2}$	θ = bulk stress ($\sigma_1+\sigma_2+\sigma_3$) (kPa)
MR-σ_3-σ_D	$Mr = k_1\sigma_3^{k2}\sigma_d^{k3}$	σ_3=confinement stress (kPa)
PARABOLIC MR-σ_3-σ_D	$Mr = k_1\sigma_3^{k2}(-k_3(\sigma_d/\sigma_{d,f})^2+k_4(\sigma_d/\sigma_{d,f})+k_5$	σ_d= deviator stress (kPa)
MR-θ-σ_D/$\sigma_{D,F}$	$Mr = k_1\theta^{k2}(1-k_3(\sigma_d/\sigma_{d,f})^{k4}$	$\sigma_{d,f}$=deviator stress at failure (kPa)
MR-σ_3-σ_D/$\sigma_{D,F}$	$Mr = k_1\sigma_3^{k2}(1-k_3(\sigma_d/\sigma_{d,f})^{k4}$	σ_1=principle stress (kPa)
MR-σ_3-σ_1/$\sigma_{1.F}$	$Mr = k_1\sigma_3^{k2}(1-k_3(\sigma_1/\sigma_{1,f})^{k4}$	$\sigma_{1,f}$=principle stress at failure (kPa)
MR-θ-σ_1/$\sigma_{1.F}$	$Mr = k_1\theta^{k2}(1-k3(\sigma_1/\sigma_{1,f})^{k4}$	k_1,k_2,k_3,k_4,k_5=material coefficients

The different models are used to determine how the confinement stress, deviator stress, bulk stress, stress ratios such as the deviator stress ratio (DSR) or the principle stress ratio (PSR) would influence the resilient modulus of the mix designs. Various models are fitted to determine which model best describes the measured resilient modulus for BSM emulsion and BSM foam with RCA. A nonlinear regression analysis with the solve function in Excel was used to determine the material coefficients by reducing the difference between the measured Mr and calculated Mr from the model to as low as possible. Then the coefficient correlation R squared is calculated between the measured Mr and calculated Mr to determine the correlation. That is the modelling process for the stress dependency of the resilient modulus.

3.5 Statistical Data Analysis Methods

The analysis of the data obtained from the indirect tensile strength test, monotonic triaxial test and dynamic cyclic triaxial test was proceeds with several statistical methods. In order to describe the data, the following basic statistical methods were used: mean, standard deviation, regression analysis, analysis of variance (ANOVA). This section discusses why the methods were used, how each method works and what the result means.

3.5.1 **Mean/Average**

The calculation of the mean and variance are the most basic statistical methods used to define a distribution of the data as illustrated in Figure 3-20. A sample mean, m_x, is calculated from the sum of n observations with x_i values divided by the number of observations n as presented by Equation 3-24. Furthermore, a sample mean is used instead of a population

mean because a smaller size sample set of the specimens is used (van As, 2008). The mean/average of a set of ITS results provides a representation of the overall result for the set of the same mix design.

$$m_x = \frac{1}{n}.\sum_{i=1}^{n} x_i$$

Equation 3-24

In combination to the mean, error bars can be plotted to show the variation/dispersion of the data set about the mean to indicate if the mean is a representative value of the set as demonstrated by Figure 3-20. The error bars can represent the standard deviation or the difference between the highest and the lowest values of the set. A set of means inform the user on the influence a variable, such as the type of active filler, has on the measured property such as indirect tensile strength dry and wet. However, a further analysis of the means can be done with the use of regression analysis.

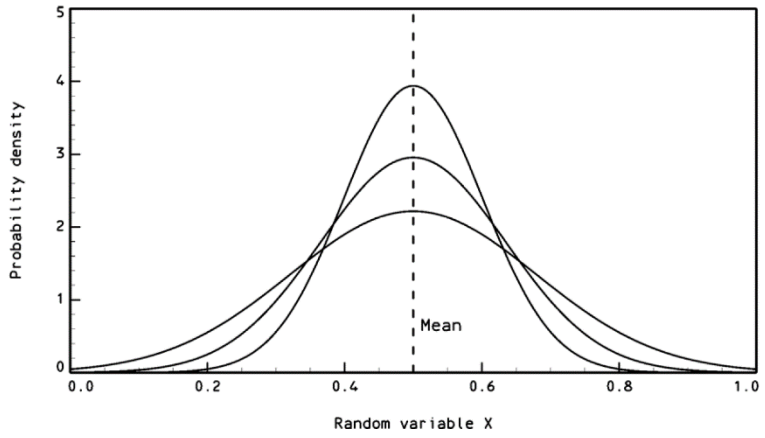

Figure 3-20: Data distribution characteristics mean and variance (van As, 2008)

3.5.2 **Regression Analysis**

Once a set of means has been determined, a regression analysis is conducted to model the data or the relationship between two variables such as type of active filler and ITS with an equation. There are numerous regression lines that can be used but for this project, a linear regression was used as it was determined to be adequate. The linear regression is a straight line with a slope coefficient which indicates the nature of the relationship between two factors. When two slope coefficients are compared, the higher and positive slope suggests that an increase in the one variable results to an increase in the other. In addition, the value of the slope coefficient indicates the rate of influence or the degree of influence one variable has on another.

In combination with the regression analysis, the fit of the data to the equation is measured with the correction coefficient, R, which ranges between -1 and 1 referred to as the R-square value (van As, 2008). The correlation coefficient represents linearity of the relationship between the dependent and independent variables. Therefore, it shows how a change in one variable affects the change in the other variable. The R-square value is determined from the data and it is commonly used because an R-square value closest to one demonstrates that the equation is a good fit for the data. Therefore, from these methods the relationship between two or more factors can be summarised and evaluated. However, for a deeper understanding of the relationship between variables, a further analysis of the data can be done with an analysis of variances of the data set.

3.5.3 **Analysis of variance**

An analysis of variances (ANOVA) method is a hypothesis test that is used to compare the means of two or more samples selected based on a specific variable such as type of active filler (van As, 2008). The ANOVA output illustrates the significance of influence of different independent variables, such as type of active filler, type of binder and increasing bitumen content, on a measured dependent variable such as ITS based on a comparison of the means. A significant level referred as the p-value, which is based on the confidence level of the data indicates how different independent variables influence the measured dependent variable. A confidence level of 95% is typically used for engineering therefore a p-value lower the 5% or 0.05 shows that the variable significantly influences the measured variable (van As, 2008). Kashaya (2013) presents the systematic process of the one-way ANOVA to determine the p-value. The analysis of data was done by setting up a table with the means obtained from each triplicate set of ITS specimens in Excel. A one way ANOVA data analysis function was used to determine the difference between the means and produces a p-value determined from the confidence level of 95% commonly used in practise (van As, 2008).

3.6 Chapter Summary

The chapter presents the experimental design of the project in order to determine the feasibility to stabilise RCA with low viscosity bitumen to produce a BSM. The experiment was divided into 4 Phases. Phase 1 focused on understanding the RCA physical properties and characteristics of the foamed bitumen. The physical properties of RCA measured included the gradation, hygroscopic moisture, moisture density relationships, atterberg limits, cement activity and CBR. The gradation was determined from crushing RCA with 3 different crushing processes to determine the suitable grading for BSM. The steps followed

and specifications used for each test are outlined in the chapter along with adjustments made.

Phase 2 of the experiment produced a variety of BSM mix designs to determine the suitable active filler or measure the influence of active filler on the ITS. Also, the influence of bitumen content was analysed in Phase 2. The chapter provides a summary of the process followed as outlined in the SANS 3001 BSM set which guides the mixing, compaction, curing and testing of the BSM ITS specimens. The different mixing methods followed for foamed bitumen and bitumen emulsion mixes is discussed and illustrated. A brief outline of the data analysis to determine the ITS is also presented in the chapter.

Phase 3 of the experiment determines the shear parameters and resilient modulus of the optimum BSM mix design with foamed bitumen and bitumen emulsion. The triaxial specimens produced to measure the performance properties were prepared as guided by SANS 3001 BSM 5. The testing of the resilient modulus was done as guided by the proposed protocol for resilient chord modulus and permanent deformation characteristics of unbound and bound granular materials. A summary and demonstration of the steps followed for the input data, specimen setup, LVDTs attachment and pressure chamber assembly to test the resilient modulus is done. The data processing of both tests is explained in the chapter along with the modelling process of the resilient modulus.

Finally, the chapter discusses the statistical methods used to process the data obtained from the tests conducted. The results obtained from the tests where described with the mean and standard deviation of the set. Then the relationship between the dependent (ITS) and independent variable (type of active filler) were modelled using a linear regression analysis. A further evaluation of the results was done with ANOVA that summarised the independent variable, which had the most significant influence on the dependent variable. Therefore, the understanding of these statistical data analysis methods was important to make sense of the data obtained from the tests. Phase 4 of the research is discussed in Chapter 6.

Chapter 4: Materials Characterisation and BSM mix design Optimisation

Phase 1 of the project investigates the grading for RCA, determines the physical properties of the aggregate and the foaming characteristics of the 70/100 penetration grade bitumen. The physical properties tested for the RCA are as follows: grading, hygroscopic moisture, maximum dry density at optimum moisture content, PI, pH and CBR. Phase 2 of the project explores the effect that active filler has on the RCA mixes when stabilised with bitumen emulsion and foamed bitumen. The optimum binder content for the RCA is also examined in this phase. The results of all the tests done in phase one and two are presented and discussed in this section.

4.1 Aggregate Grading Results and Discussion

4.1.1 RCA Grading Results

Concrete segments were crushed with a laboratory jaw crusher with three different processes that produced three samples with different types of gradations referred to as S1, S2 and S3. The particle size distributions obtained for each grading are plotted and compared to the grading limits specified in the TG2 (Asphalt Academy, 2009) for BSMs stabilised with bitumen emulsion or foamed bitumen. A comparison of these particle size distributions is done based on their grading modulus calculated with Equation 2-3. A grading modulus (GM) between 2 and 3 indicates gradings ranging from fine to continuously graded up to a coarsely graded aggregate mix. Whereas, a GM of 3 indicates no content of the particles sizes passing the 2 mm sieve resulting in a coarse grading. A grading modulus of 2 is the boundary between coarse and fine grading (SANRAL, 2014). The particle size distributions for S1, S2 and S3 were further compared to the Talbot grading curve produced with Equation 2-4 where n = 0.45 to determine the distribution of the aggregate sizes for a continuously graded aggregate mix.

The grading curve for S1 is plotted and it falls within the marginal section due to the high content of coarse aggregates, which is confirmed by the high grading modulus of 2.71 as illustrated in Figure 4-1. In addition, only 1.7% filler was obtained from the crushing process, which results in the grading to not satisfy the 2% minimum filler required for stabilisation with bitumen emulsion and the 4% minimum filler required for stabilisation with foamed bitumen

(Asphalt Academy, 2009). Therefore, a two-stage crushing process was done for S2 in an attempt to increase the filler content.

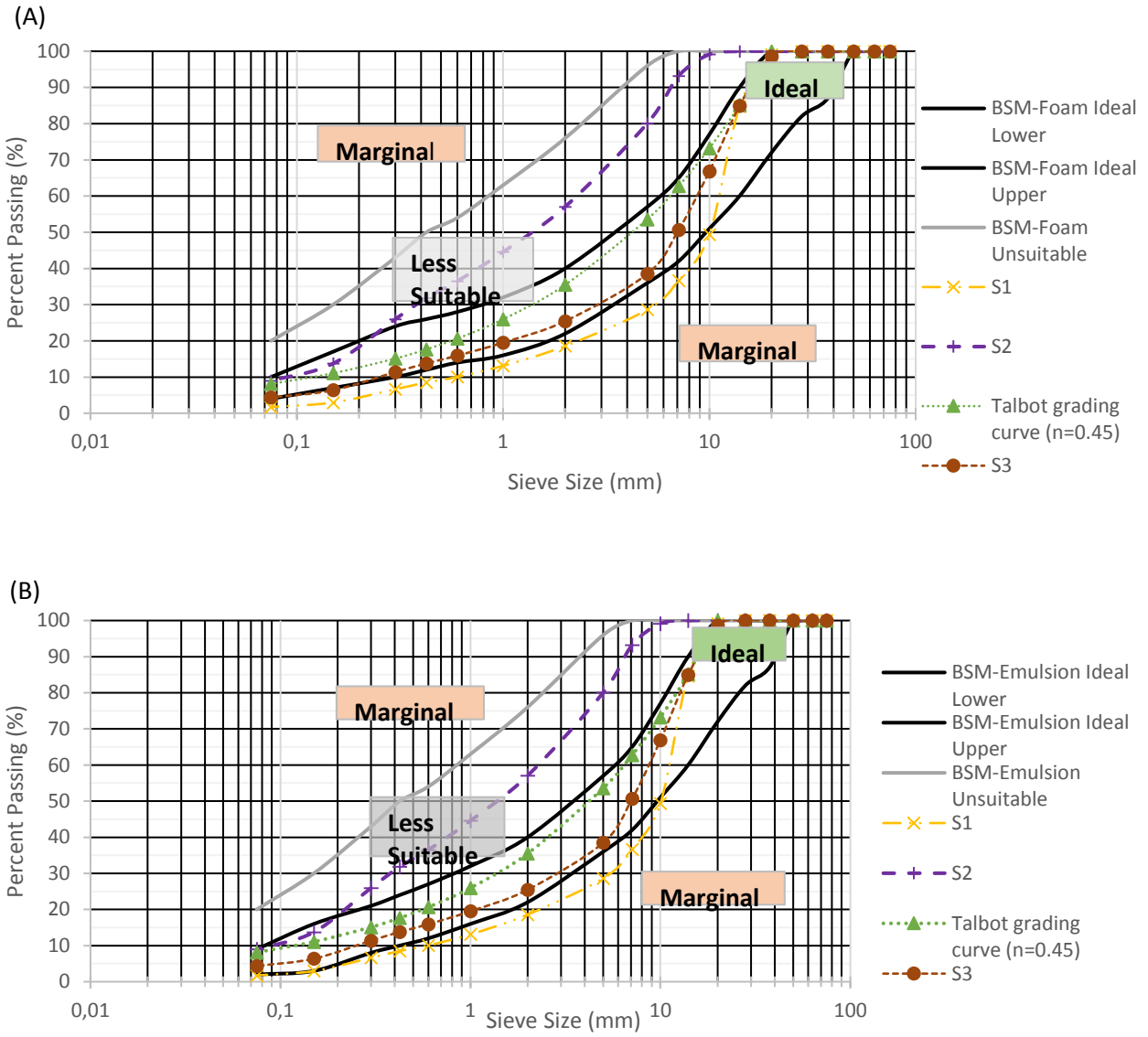

Figure 4-1: RCA grading S1, S2 and S3 compared to the specified grading for stabilisation with (A) bitumen emulsion and (B) foamed bitumen

The filler obtained from the crushing process of S2 amounted to 9% of the total mass of the sample. Furthermore, the maximum particle size obtained was 10 mm and as a result, the grading of S2 is undesirably finer as indicated by the low grading modulus of 2.02. A plot of S2 on Figure 4-1 shows that the grading falls in the less suitable range for stabilisation with bitumen emulsion and foamed bitumen therefore fails to meet the BSM grading requirement. The practical implications of the crushing process applied to generate the grading curve for S2 would be an expensive option. However, it indicates that a secondary crushing of RCA is required. As a result, a third sample (S3) was crushed with a slight adjustment to the crushing process of S2. The adjustment made was that a 50% fraction of the total sample

underwent secondary crushing through the smallest gap (2mm) of the jaw crusher to slightly increase the filler content. Consequently, S3 was produced with the adjusted crushing process and the filler content obtained amounted to 4.3% of the total mass of the crushed sample. The grading of S3 plotted on Figure 4-1 shows the curve fits in the ideal range for stabilisation with both bitumen emulsion and foamed bitumen.

The calculated grading modulus for S1 of 2.71 categorised the grading as coarser when compared to S2 with a grading modulus of 2.02. The grading modulus for S3 is calculated as 2.56, which was closer to the calculated grading modulus of 2.39 for the Talbot grading curve. As illustrated on Figure 4-1, the S3 grading curve is closer to that of the Talbot grading curve. The TG2 specifies a grading modulus less than 0.75 as unsuitable for stabilisation with bitumen. Therefore, based on the GM, all the gradations produced would be suitable for stabilisation with bitumen. However, for a higher quality layer, the grading of S3 is the most suitable because it compares well to the Fuller grading curve. Furthermore, it fits in the ideal grading boundaries for stabilisation with both bitumen emulsion and foamed bitumen.

The percentage passing and retained on each sieve for the S3 grading is presented in Table 4-1. The percentage passing of the 5 mm sieve is 38% and the percentage passing the 0.075 mm sieve is 4.3%. Subsequently, the bitumen content used for the active filler effect stage is obtained as 2.2% for both bitumen emulsion and foamed bitumen (Wirtgen Group, 2012). The retained percentage is used to determine the mass for each aggregate size for a total mass required per sample. An adjustment is made to the final reconstituted grading of S3 to produce the test specimens. The method of substitution states that the mass required for the 28 mm and 20 mm aggregate fractions are accounted for in the mass of the 14 mm as specified in SANS 3001GR30. This is done due to the restriction on the maximum aggregate size because of the mould sizes used in the laboratory.

Table 7- Final Grading of RCA percentage passing

SIEVE SIZE (MM)	S3 - PERCENTAGE PASSING (%)	RETAINED PERCENTAGE (%)
37.5	100.0	0
28	98.1	1.9
20	96.7	1.4
14	84.9	11.8
10	66.9	18.1
7,1	50.7	16.2
5	38.5	12.2
2	25.4	13.0
1	19.5	5.9
0,6	15.9	3.6
0,425	13.8	2.2
0,3	11.4	2.4
0,15	6.4	5.0
0,075	4.3	2.0
FILLER	0	4.3

4.1.2 **RCA Grading for BSM Discussion**

The result of the final grading, S3, indicates that recycled concrete can be used as an alternative aggregate and crushed with a typical crushing process to generate a continuous grading suitable for stabilisation with bitumen. A continuous graded aggregate obtained with the Talbot grading curve (Equation 2-4) ensures that the aggregates pack well when compacted. Studies show that when a higher density is achieved, an optimum performance of the graded aggregates transpires (Leite *et al.*, 2011b; Van Niekerk, 2002). However, the compressive strength of the original concrete has an effect on the particle size distribution generated when the concrete is crushed (Koper *et al.*, 2017). Therefore, the portion of the aggregates to undergo secondary crushing will vary in order to generate the continuous grading and required filler content.

The filler content improves the performance of a layer as a result of the bonds formed by the mastic/mortar between the aggregates. From this study, secondary crushing was done on 50% of the original crushed aggregates and the filler content obtained was 4.3% as given in Table 7. The filler content of 4.3% meets the minimum specified 4% filler content required for stabilisation with foamed bitumen. However, recycled concrete with higher compressive strengths may require a larger portion to undergo secondary crushing to generate the required minimum filler content because of the high crushing values as seen by Koper *et al.* (2017). Additionally, the filler content of a graded material influences the optimum densification and cohesion which then determines the performance of any unbound granular layer (Araya, 2011) including recycled aggregates (Van Niekerk, 2002).

The filler in the context of BSMs provides assistance for the dispersion of the foamed bitumen in the mix and forms bonds between the larger aggregates hence the minimum requirement of 4% is specified (Asphalt Academy, 2009). However, the type and amount of filler results in an increase in the surface area of the RCA. An increase in surface area leads to an increased moisture requirement for mixing and compaction (Poon & Chan, 2006). This result can be translated to an increase in the required bitumen content, especially for bitumen emulsion. In contrast to foamed bitumen, the bitumen emulsion contributes towards the optimum moisture content of the aggregates to achieve the required maximum dry density (Asphalt Academy, 2009). Consequently, the filler content is limited to 9% for bitumen emulsion and 10% for foamed bitumen (Asphalt Academy, 2009). Therefore, a continuous grading with the required filler content benefits the performance of the BSM (Asphalt Academy, 2009). The performance of a BSM is also dependent on the physical properties of the aggregates.

4.2 RCA Physical Properties

Prior to stabilisation of RCA, several tests were conducted to determine the physical properties of the S3 grading RCA mix. Mixes with two different 14 mm aggregates namely RCA 1 and RCA 2 were tested and compared to determine the influence of each aggregate. The tests conducted included the hygroscopic moisture, plasticity index (PI), pH, the maximum dry density at the optimum moisture content and the 4-day soaked CBR. The challenges faced when RCA 1 and RCA 2 were mixed are briefly discussed prior to the presentation of the aggregate results.

4.2.1 **The separation of the RCA 1 and RCA 2 14 mm aggregate**

The 14 mm aggregates were separated based on the differences in colour of the mortar, texture and particle shape. The separation was done due to challenges with the inconsistency of the physical properties such as the moisture density relationship, illustrated in Figure 4-2A. A difference in the required moisture content for compaction was observed when a higher content of RCA 1 14mm was present in the mix. As a result, a higher moisture content was required for an optimum packing to achieve the maximum density. On the contrary, a higher content of RCA 2 14mm required a lower moisture content during compaction for an optimum packing. Consequently, due to the varying contents of RCA 1 and RCA 2 in the specimens produced for each point plotted. The resultant moisture density curve failed to reach a unique maximum dry density at an optimum moisture content.

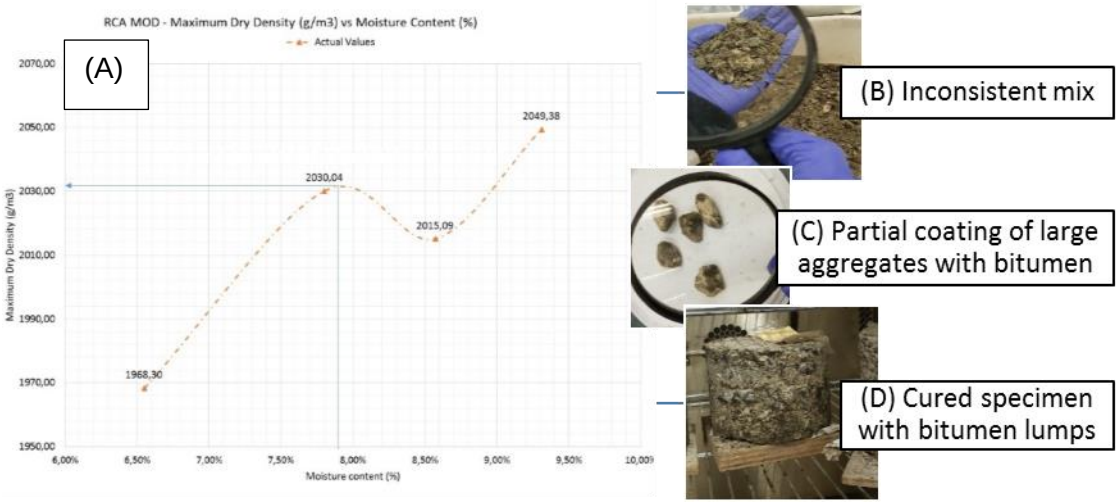

Figure 4-2: Inconsistency challenges leading to the separation of RCA 1 and RCA 2

The mixed aggregates were stabilised with bitumen emulsion at a moisture content of 7.9% based on the first peak achieved on the curve as indicated in Figure 4-2A. However, mixes made with a higher content of the porous RCA 1 resulted in a dry mix which was evident by the dry 14 mm aggregates shown on Figure 4-2B. As a result, the mix contained dry aggregates partially coated with bitumen which broke prematurely as the mortar absorbed the emulsion and water (Figure 4-2C). The specimens produced from this mix exhibited bitumen lumps on the surface after curing which is undesirable for a BSM (Figure 4-2D). Therefore, the 14 mm aggregates were separated and the mix variables were adjusted in order to improve the mix produced. The section below presents the slight difference in the physical properties of RCA 1 and RCA 2.

4.2.2 **Hygroscopic Moisture and Plasticity Index**

The hygroscopic moisture was determined prior to all mixing activities consistently throughout the experiment period. The measured hygroscopic moisture ranged from 2.3 to 2.96% of the total dry mass of the reconstituted aggregates for RCA 1 and RCA 2 as shown in Table 8. The 0.66% difference in the range was a result of the variation in the humidity in the laboratory. Hygroscopic moisture of RCA affects the required OMC of the grading presented in Table 7. The hygroscopic moisture of 2.3 to 2.96% amounts to at least 17 to 26% of the required OMC. In contrast to natural aggregates, the high hygroscopic moisture of RCA is important for stabilisation with bitumen emulsion. This is due to the sensitive of the low viscosity bitumen to the moisture in the aggregates during mixing as previously discussed in section 4.2.1. An under estimation of the hygroscopic moisture or moisture content of the aggregates prior to mixing results in the premature breaking of the bitumen

emulsion prior to compaction. This results from the porous RCA that absorb the water in the bitumen emulsion.

Table 8: Summary of the physical properties for RCA 1 and RCA 2

PHYSICAL PROPERTY	**RCA 1**	**RCA 2**
HYGROSCOPIC MOISTURE	2.3 – 2.96%	
PLASTICITY INDEX (PI)	Non-plastic	
PH	12.32	12.35
MAXIMUM DRY DENSITY	1903 kg/m^3	1933 kg/m^3
OPTIMUM MOISTURE CONTENT ACHIEVED WITH MOD HAMMER	13%	11 %
OPTIMUM MOISTURE CONTENT –USED FOR VIBRATORY HAMMER	12.2%	10.3%
4 DAY SOAKED CBR - MOD HAMMER	50 %	64%
4 DAY SOAKED CBR - VIBRATORY HAMMER	70%	60%

Another important test for stabilisation with bitumen is the determination of the plasticity index (PI) of the fine aggregates. The PI of the aggregates passing the 0.425 mm sieve was tested and the result characterised the fine RCA as non-plastic (Table 8). This result corresponds to a similar analysis done by Barisanga (2014) were the PI of a mix of RCA and Masonry was obtained as non-plastic. The non-plastic PI satisfies the required maximum PI of 7 and 10 for stabilisation with bitumen emulsion and foamed bitumen, respectively (Asphalt Academy, 2009). This means that extreme variations in the moisture content of the specimen or layer will not result to a change of the fine aggregates of the RCA from plastic to liquid form, therefore no volume changes will be experienced with this material (Christopher *et al.*, 2006). Furthermore, an increase in the moisture content leads to increased lubrication in the aggregate matric. Resulting in a reduction of the shear strength of the material due to movement or slippage of the aggregates under repeated loading (Thom, 2008). This test is important for stabilisation with bitumen emulsion as it affects the moisture requirement for mixing, compaction and sensitivity to increases in moisture content which leads to the loss of strength.

4.2.3 **Active cement**

The cement activity of the RCA is determined from the measurement of the pH of two solutions made with S3 grading with 14 mm RCA 1 and RCA 2. The pH, of the solution made from distilled water (pH of 7) mixed with graded RCA, increases when cement consumption occurs. The average pH measured was 12.32 for RCA 1 and 12.35 for RCA 2 as presented in Table 8. The measured pH indicates active cement in the aggregate mixes. Additionally,

another test to evaluate the active cement was conducted by spraying a RCA specimen that was cured for 3 days with phenolphthalein. The specimen turned pink as illustrated in Figure 4-3 which indicates active cement in the specimen. Cement activity of the RCA is an important factor to be considered in design to allow for the possibility of self-cementation of the specimen or the layer in the long term. In addition, the presence of cement is beneficial for stabilisation with bitumen as it can assist with the dispersion during mixing and improve the adhesion between the aggregates (Asphalt Academy, 2009). Therefore, RCA can potentially be more cost effective than natural aggregate because of the inherent cement present in the aggregates to improve the dispersion with the bitumen. Furthermore, due to the known fact that possible cementation will occur in RCA specimens exposed to moisture. Stabilisation with bitumen will add flexibility to what would be a layer with an increasing stiffness, which can potentially result in cracking and to an eventual loss of strength.

Figure 4-3: RCA specimen sprayed with phenolphthalein

4.2.4 **Density and moisture content of RCA 1 and RCA 2**

The S3 grading is used to determine two moisture density relationships for mixes made with the 14 mm RCA 1 and RCA 2. The relationships between the dry density and moisture content for RCA 1 and RCA 2 were determined with the Modified AASHTO compaction effort. Where each specimen is compacted with 55 blows per layer. The moisture density relationship for RCA 1 shows an increase in the density with increasing moisture content as plotted in Figure 4-4 A. This behaviour is unusual for typical granular materials and is a result of the porous mortar. The moisture was squeezed out of the aggregates during the compaction of the 13.7% moisture content RCA 1 specimen as demonstrated by Figure 4-4 B. The maximum dry density and optimum moisture content of RCA 1 is therefore deduced as 1903 kg/m^3 at 13% as presented in Table 8. Whereas, for RCA 2 a maximum dry density of 1933 kg/m^3 was achieved at a optimum moisture content of 11% (Table 8). In contrast to

RCA1, the moisture density relationship obtained for RCA 2 is similar to that of a typical relationship obtained for natural crushed aggregates. The density decreases with increasing moisture content once the optimum moisture has been achieved (Molenaar, 2010). Nevertheless, the densities of both RCA 1 and RCA 2 are similar due to the use of the same grading (S3) yet a 2% difference is obtained between the OMC values. It can be concluded that based on the moisture density relationships, there is a distinct difference between RCA 1 and RCA 2. Therefore, it is important to separate different coarse RCA aggregates for a consistent mix as seen above where a 15% underestimation or overestimation can occur in the OMC.

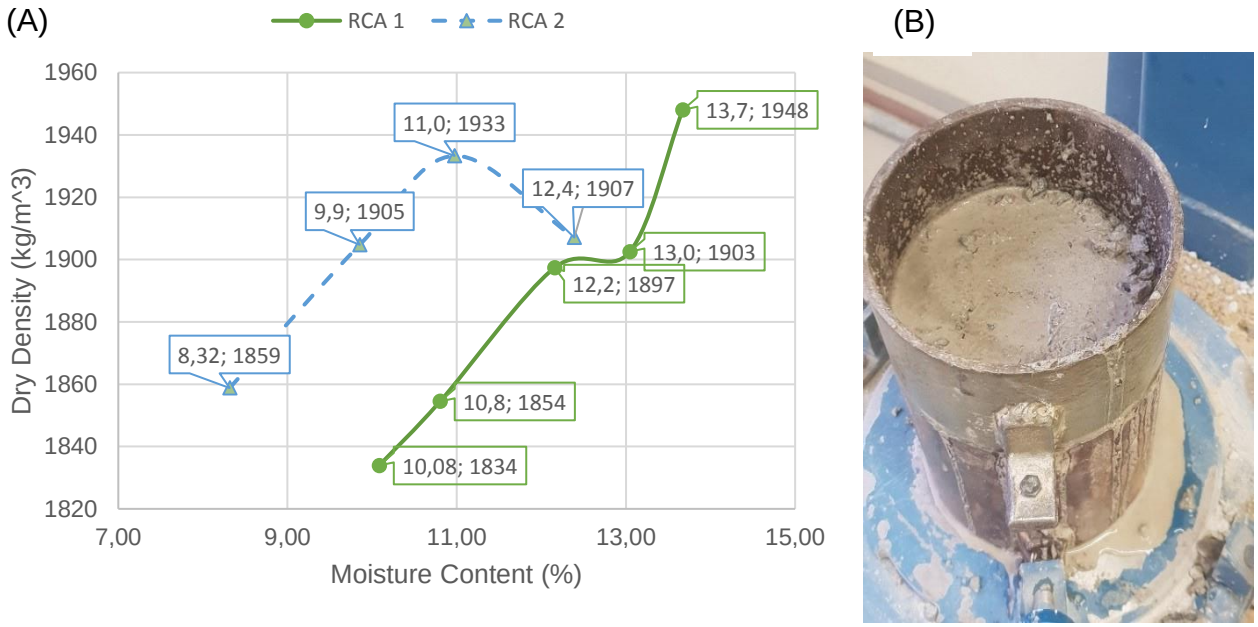

Figure 4-4: (A) Dry density vs moisture content of RCA 1 and RCA 2 and (B) RCA 1 specimen at 13.7% moisture content during compaction with the Modified AASHTO

The RCA 1 aggregate is chosen for the final aggregate mix for stabilisation with bitumen based on the moisture density relationship compared to RCA 2 indicating RCA1 to be a potentially weaker aggregate (Figure 4-4 A). The choice to use the weaker RCA is important for the assessment of the potential to stabilise RCA with bitumen. The final maximum dry density used for all the specimens is 1903 kg/m^3 obtained at 13% OMC. The density obtained at 13.7% is not used because the specimen was over saturated and water drained out of the specimen with filler during compaction (Figure 4-3 B). Based on the observation of the mix, the mortar broke down due to the excess moisture and compaction. Resulting in the aggregates packing densely increasing the density of the specimen. It is undesirable to compact the specimen at a high moisture content. Although a high moisture content increases the density, it also results in the loss of filler. This behaviour is typical for recycled

aggregates with a porous mortar such as RCA 1 due to the composition of the aggregates. A similar trend was seen in the study by Van Niekerk (2002) where the density of RCA mixed with masonry increased with moisture content.

Both the densities achieved for RCA 1 and RCA 2 are in line with densities obtained in other studies for RCA, however, notably lower due to the coarser grading (Barisanga, 2014; Van Niekerk, 2002; Poon & Chan, 2006, Breadedkamp ,2018). The OMC for both RCA 1 and RCA 2 presented in Table 8 are high, as expected for recycled materials, in comparison to OMC obtained for typical natural aggregates (Poon & Chan, 2006). The BSM specimen would be produced at the OMC to achieve the maximum dry density, therefore OMC is a critical physical property. The specification for specimen preparation of BSMs requires compaction to be done with a vibratory hammer for an effective packing of the aggregates and bitumen. For that reason, the OMC obtained with the Modified AASHTO compaction method is reduced by 6% as presented in Table 8. As a result, the final OMC for the BSM mix designs is 94% of the OMC obtained from the Modified AASHTO compaction. The reduction is done because the vibratory hammer compaction effort requires less moisture to achieve the target dry density obtained with the Modified AASHTO compaction method (Kelfkens, 2008).

4.2.5 **Soaked CBR of RCA 1 and RCA 2**

The CBR of RCA 1 and RCA 2 is evaluated to estimate the bearing capacity and illustrate the influence different types of compaction methods have on this parameter. In addition, the TG2 requires a 4 day soaked CBR of untreated marginal aggregates in order to determine the resultant BSM classification of the stabilised aggregates (Asphalt Academy, 2009). The 4 day soaked $CBR_{2.54\,mm}$ of two specimens made with RCA 1 and two specimens made with RCA 2 were measured. Each specimen was compacted with either a MOD Hammer or a vibratory hammer. The CBR obtained based on the MOD compaction for RCA 1 of 50% was 14% lower than the CBR obtained for RCA 2 of 64% (Figure 4 5). The result supports the assumption that RCA 1 is potentially the weaker aggregate of the two. The CBR values obtained for both aggregates are consistent with the findings done by Poon and Chan (2006) for RCA.

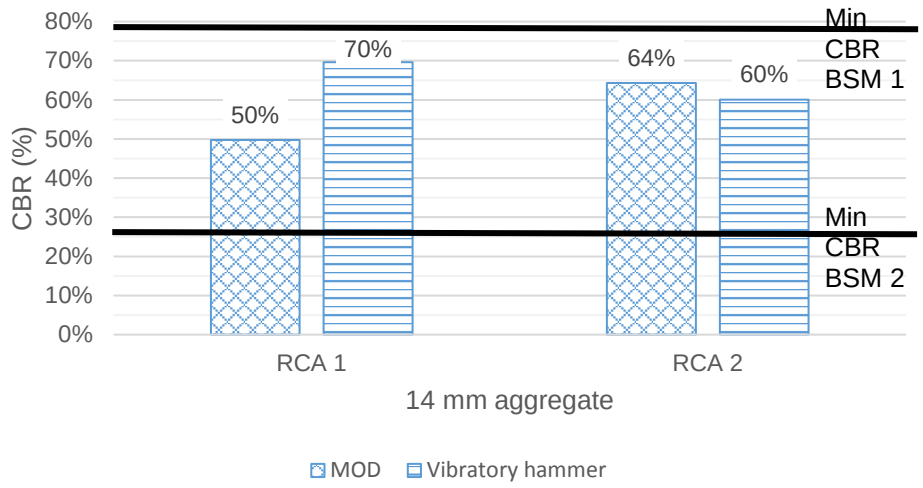

Figure 4-5: Comparison of CBR obtained for RCA 1 and RCA 2 with different compaction methods

Alternatively, the vibratory hammer provides better packing at low amplitudes in comparison to the impact force applied by the MOD hammer. As a result, a higher CBR is expected due to the higher compaction energy applied. That being the case, CBR specimens were produced with both RCA 1 and RCA 2 compacted with the vibratory hammer to evaluate the influence of the compaction method on the measured CBR. The results suggest that RCA 1 benefited from the compaction with the vibratory hammer as shown by the CBR of 70% which is a 40% increase demonstrated in Figure 4 5. This trend is not consistent for RCA 2 where a 6% decrease in the CBR occurred. Therefore, the influence of the compaction with the vibratory hammer is inconclusive for CBR. The CBR values obtained with the MOD hammer for both mixes exceed the specified minimum CBR of 25% required for a BSM 2 layer however failed to meet the required 80% CBR for a BSM 1 as illustrated in Figure 4 5.

4.3 Active Filler Influence on BSM_RCA

The influence of active fillers on RCA stabilised with foamed bitumen or bitumen emulsion was gauged from mix designs made with 1% cement, 1% lime and no active filler. A set of six bitumen emulsion specimens (BSM_E) and a set of six foamed bitumen specimens (BSM_F) were produced from each mix design. The purpose of an active filler in a BSM mix is to assist with the dispersion of the bitumen in the aggregates, improve the adhesion between binder and aggregates, and increase the curing rate and stiffness of the mix. The improvement of these aspects can be quantified based on the average ITS achieved by the triplicate set of specimens produced from each mix design with different active fillers. The specimens were tested for the dry and wet indirect tensile strength (ITS) which were then compared to the TG2 requirements for BSM classifications. The section presents the average results obtained from the addition of active fillers to mix designs prepared with 2.2% bitumen emulsion and 2.2% foamed bitumen. The influence of each active filler on the BSM_RCA made with foamed bitumen and bitumen emulsion is analysed followed by the overall influence of the active fillers.

4.3.1 Cement

The addition of 1% cement produced specimens that meets the minimum required dry and wet ITS for BSM1 as specified in the TG2. The BSM_E performed better than the BSM_F in both the dry and wet ITS as illustrated in Figure 4-6. An average dry ITS of 381 kPa was achieved by BSM_E and an average dry ITS of 333 kPa was obtained for the BSM_F. Additionally, the BSM_E retained a higher tensile strength (TSR) which is calculated as 110.5% whereas, BSM_F only retained 75.4% of the tensile strength as shown in Figure 4-6. The influence of moisture damage was seen mostly in BSM_F specimens demonstrated by the loss of tensile strength i.e. decreased TSR. It should be noted from Table 9 that only 2% bitumen was added to the foamed bitumen mixes therefore that would influence the resultant strength obtained. The TSR of 110.5% achieved by the BSM_E portrays a perception that soaking improved the ITS. Conversely, an in depth analysis of the results reveal that the BSM_E had an average core temperature of 22^{o}C while, BSM_F were tested at an average core temperature of 25.2^{o}C as presented in Table 9. Consequently, the low testing temperature clarifies the higher ITS obtained from BSM_E specimens as bitumen is a temperature dependent material. Therefore, there is no significant difference between the average dry and wet ITS of BSM_E based on the error bars shown on Figure 4-6 as a result, no increase in the ITS actually occurred.

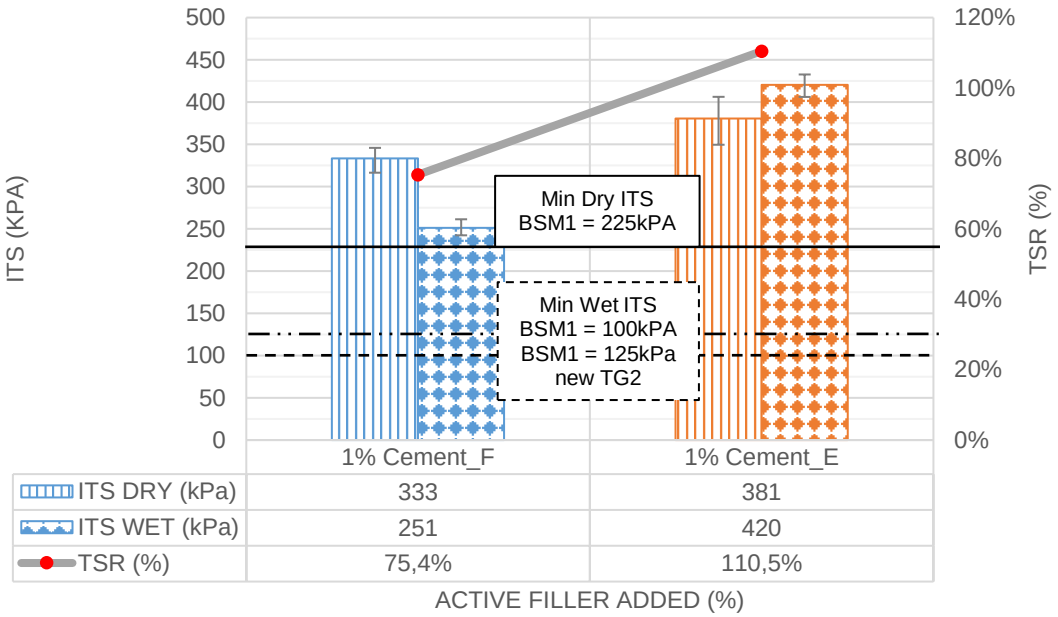

Figure 4-6: The influence of 1% cement on mixes made with 2.2% foamed bitumen (1% Cement_F) and 2.2% bitumen emulsion (1% Cement_E)

Both mix designs (BSM_F and BSM_E) with 1% cement as active filler resulted in BSMs that met the TG2 requirements to produce a BSM1 layer based on both the dry and wet ITS as indicated in Figure 4-6. The dry ITS obtained for both mix designs exceed the TG2 specified dry ITS of 225kPa. Similarly, the wet ITS obtained for both mix designs met the minimum required wet ITS of 100kPa. A further consideration of the mix with bitumen emulsion shows that the dry ITS of 381kPa is substantially high for a typical BSM mix and a rigid mix is likely to occur which is undesirable for BSM mixes (Asphalt Academy, 2009). Furthermore, these findings (Figure 4-6) are inconsistent with findings from Nwando (2013). The study found a lower dry ITS from a mix design with RAP and crushed dolerite stabilised with 2.4% bitumen content and 1% cement. An average dry ITS of 226.3kPa was obtained for BSM_E and 256.4kPa was achieved by BSM_F. The results highlight that RCA performed better than the mix design with RAP and crushed Dolerite. Alternatively, the results also suggest that the potential behaviour of the BSM made with RCA may differ from the typical non-continuous BSM previously shown by Jenkins (2000). This is a result of the inherent self-cementation or the added 1% cement. The specimens may show increases in stiffness, resulting in brittle BSMs. Therefore, the addition of cement should be reassessed when RCA is used as an aggregate for BSM due to the inherent active latent cement as shown by the preliminary pH result of 12.3. Cement might not be the best active filler for a RCA_BSM mix consequently a mix design with 1% lime as an active fillers was done.

4.3.2 Lime

The addition of 1% lime produced specimens that satisfied the minimum required dry and wet ITS specified by the TG2 for the production of a BSM1 layer, demonstrated in Figure 4-7. An average dry ITS of 385kPa is obtained for BSM_E whereas, an average of 263kPa is achieved for BSM_F. In addition, based on the error bars, which represent the maximum and minimum ITS values obtained for each triplicate set, the BSM_F mixes are the most susceptible to moisture damage. This observation is supported by the 83.8% tensile strength retained by the BSM_F specimens (Figure 4-7). In contrast, the BSM_E retained 98.4% of the tensile strength after exposure to moisture as presented in Figure 4-7. Unlike the cement specimens, the average temperature of the cores was measured as 24.6ºC for BSM_F and 23.2ºC for BSM_E that being the case, temperature did not play a role in the measured wet ITS. Nevertheless, there is no significant difference in the average ITS obtained for dry BSM_E in comparison to the wet BSM_E.

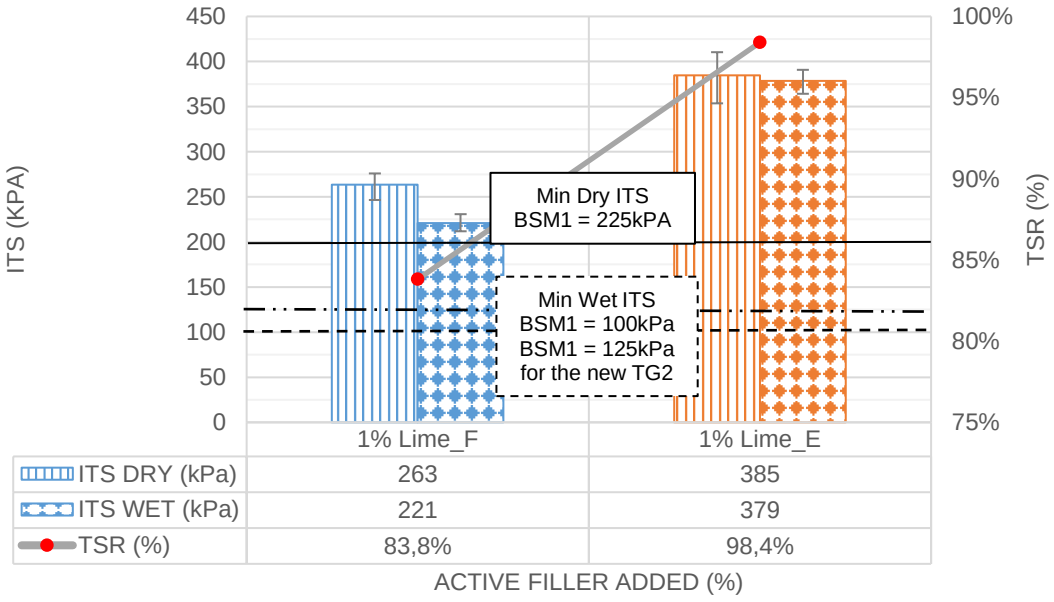

Figure 4-7: The influence of 1% lime on mix designs produced from 2.2% foamed bitumen (1%Lime_F) and 2.2% bitumen emulsion (1%Lime_E).

Both the mix designs exceeded the minimum required dry ITS of 225kPa and the wet ITS of 100kPa to potentially produce a BSM 1 mix as demonstrated on Figure 4-7. The average dry ITS measured for BSM_E with 1% lime performed better than the BSM_F similarly to cement mix designs discussed in 4.3.1. This indicates that mix designs with bitumen emulsion gain the most benefit from the addition of active filler. Although bitumen emulsion appears to be the best binder for RCA, the high dry ITS points to a potential brittle mix. Both

mixes retained the required minimum TSR of 60% indicating low sensitivity towards moisture damage.

Similar to cement mix designs, these results are inconsistent with findings by Nwando (2013). A BSM produced from 1% lime and 2.4% bitumen content, retained 76% of the tensile strength with a BSM_E specimens and for BSM_F retained 29% of the dry ITS. From this study, the BSM_F mix with lime exceeded the specified minimum TSR of 60%. This suggests that RCA is resilient against weakening induced by moisture in comparison to the mix design with RAP and crushed dolerite stabilised with BSM_F produced by Nwando (2013). In general, an increase in moisture reduces the tensile strength for BSMs with natural aggregates. There is potential of improvement for BSM mixes by adding lime to bitumen emulsion more than there is for foamed bitumen mixes. Similarly, to the 1% cement BSM, the behaviour of the specimens with lime may differ from typical BSMs. Hence mixes with no active filler were explored to further understand the interaction of bitumen with RCA.

4.3.3 **No active filler**

The stabilisation of RCA with foamed bitumen or bitumen emulsion with no active filler produced mixes, which satisfied the TG2 specified requirements as illustrated in Figure 4-8. The BSM_F obtained an average dry ITS of 271kPa whereas, BSM_E achieved an average dry ITS of 280kPa. The dry ITS obtained for BSM_F and BSM_E are similar indicating that the addition of either foamed bitumen or bitumen emulsion has a comparable effect on the RCA. The average wet ITS for BSM_F is obtained as 214kPa which represents a 79.1% retained tensile strength. Although the reduction in tensile strength is above the specified minimum of 60%, it is clear that BSM_F specimens are susceptible to a loss in strength when an increase in moisture occurs. On the other hand, BSM_E achieved an average wet ITS of 320kPa which translates to a 114.2% TSR. Similar to the cement specimens, the increased wet ITS for BSM_E is a result of the low average core testing temperature of 22.6^{o}C compared to the 25^{o}C measured for the BSM_F specimens. A potential BSM 1 layer is possible with 2.2% bitumen emulsion or 2.2% foamed bitumen with no active filler. Therefore, the results tell us that no active filler is required to stabilise RCA with low viscosity bitumen.

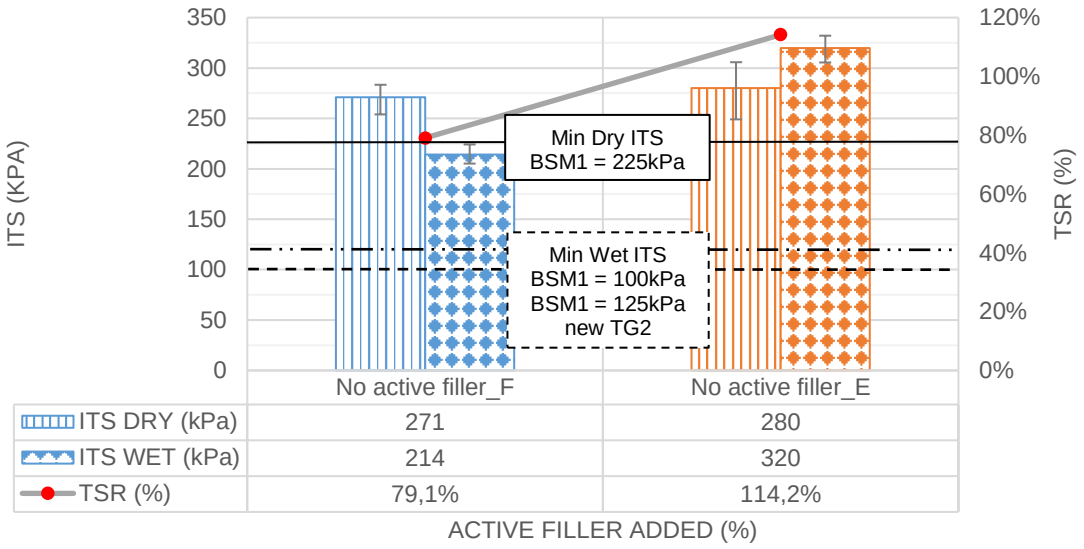

Figure 4-8: The dry and wet ITS of BSM_RCA mixes with foamed bitumen and bitumen emulsion without active filler.

4.3.4 **Overall General observations**

The BSM_E performed better than the BSM_F when active fillers were added to the mixes as demonstrated in Figure 4-9. For mixes with no active filler, the BSM_E achieved an average dry ITS that was similar to that of BSM_F. However, an increase occurs for dry and wet ITS measured for BSM_E when active fillers were added. Cement and lime had a similar effect on the dry ITS of BSM_E. On the other hand, a general loss in strength of the BSM_F specimens when soaked in water can be seen as illustrated in Figure 4-9. The cement had an impact on the dry ITS for BSM_F however the most reduction in tensile strength occurred in that mix. In general, BSM_F are prone to loss in strength when an increase in moisture occurs whereas an opposite effect occurs for BSM_E.

Overall, RCA stabilised with low viscosity bitumen retained its strength when soaked in water considering the low density of the specimens. The moisture penetration can be attributed to the coating mechanism of the aggregates as illustrated by Figure 4-10. In addition, the BSM_F mixes had high porosity that can be seen from Table 9, were the slightly higher moisture content was present at break after soaking in water for 24hrs. The lime fills the voids and less water penetrates the specimens based on the low moisture at break.

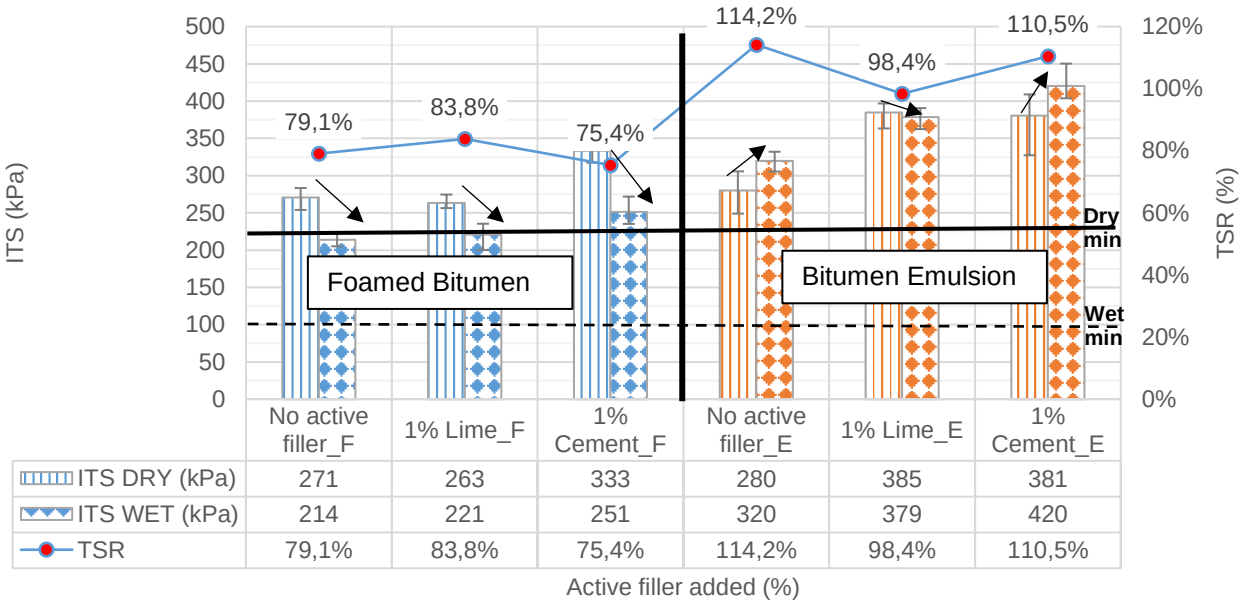

Figure 4-9: A comparison of the influence of active fillers on the mix designs with 2.2% bitumen emulsion and 2.2% foamed bitumen.

Temperature at testing of the specimen is an important variable that has an influence on the measured ITS of the specimen as seen in Table 9. This demonstrates that the active fillers contributed to the dispersion of the bitumen, which increased the tensile strength of the BSM specimens. As expected, the BSM_E specimens showed that the RCA was coated and the voids in the mortar partially filled Figure 4-10B). Whereas, in BSM_F specimens the RCA remained uncoated and porous increasing sensitivity to moisture penetration (Figure 4-10 A). Based on these results, bitumen emulsion with active filler would improve the performance properties of the BSM with RCA.

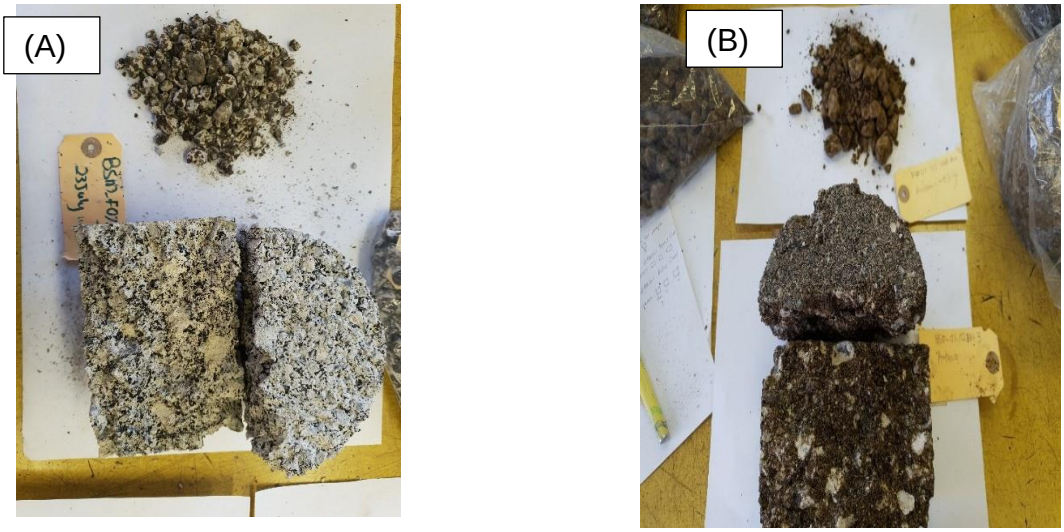

Figure 4-10: (A) Aggregate coating for Foamed bitumen specimen and (B) bitumen emulsion specimen

Table 9: Average values obtained from suitable active filler mix designs with triplicate specimens

		Foamed Bitumen mixes			Bitumen Emulsion mixes		
Bitumen Addition	**(%)**	**2.2**	**2.2**	**2**	**2.2**	**2.2**	**2.2**
Type/amount of active filler	(%)	No active filler_F	1% Lime_F	1% Cement_F	No active filler_E	1% Lime_E	1% Cement_E
Moulding moisture content	(%)	11.5%	11.9%	11.7%	9.6%	9.9%	8.9%
TEST RESULTS							
ITS $_{DRY}$	(kPa)	**271**	**263**	**333**	**280**	**385**	**381**
Moisture content at break	(%)	4.1%	4.3%	4.0%	3.6%	3.8%	3.9%
Dry Density	(kg/m^3)	1933	1925	1933	1909	1946	1975
Temperature at break	(ºC)	25.2	26.4	25.4	26.4	26.8	26.9
Displacement	(mm)	1.44	1.12	1.04	1.39	1.16	1.37
Fracture Energy		4.34	3.20	3.89	4.43	4.99	5.80
ITS $_{WET}$	(kPa)	**214**	**221**	**251**	**320**	**379**	**420**
Moisture content at break	(%)	10.1%	5.3%	9.5%	6.9%	6.4%	7.2%
Dry Density	(kg/m^3)	1918	1905.6	1916.5	1943.0	1954.0	1957.8
Temperature at break	(ºC)	25.0	24.6	25.2	22.6	23.2	22.0
Displacement	(mm)	1.379	1.146	1.239	1.443	1.449	1.649
Tensile Strength ratio		79.1%	83.8%	75.4%	114.2%	98.4%	110.5%

4.4 Active Filler Influence on “Stiffness” and Flexibility of BSM_RCA

The stiffness of a material represents the relationship between the stress and strain of the material. In this section, the stiffness is the ratio of the stress (ITS) and the strain determined from the deformation of the specimen tested with the ITS. While, the flexibility of the material gives an indication on aspects such as energy absorption and durability of the material against repeated loading i.e. how the material recovers after impact. These properties can be measured with various methods. In this project the stress and strain obtained from the ITS testing, of each mix design with the active fillers, were used to determine the stiffness and flexibility of the mixes. The analysis aims to understand how different types of active fillers influence the stiffness and flexibility of a BSM with RCA.

4.4.1 **Stiffness**

The addition of active fillers increased the stiffness and deformation of mixes stabilised with bitumen emulsion and foamed bitumen as presented in Figure 4-11. The stiffness increased from 292 kPa to 345 kPa for lime mixes and when cement was added, the stiffness increased to 484 kPa for foamed bitumen specimens. However, the deformation at break decreased from 1.44 mm to 1.04 mm with the addition of active fillers for the foamed bitumen specimens. This means that the mixes became sensitive to loading consequently failing at lower deformations. On the other hand, the stiffness for bitumen emulsion specimens also increased with the addition of active fillers from 316 kPa to 512 kPa for lime and 428kPa for cement mixes. However, unlike foamed bitumen specimens, the addition of cement increased the average deformation at break for bitumen emulsion specimens. As a result, the cement increased the resilience of the bitumen emulsion specimen against loading and failure occurred at a higher deformation.

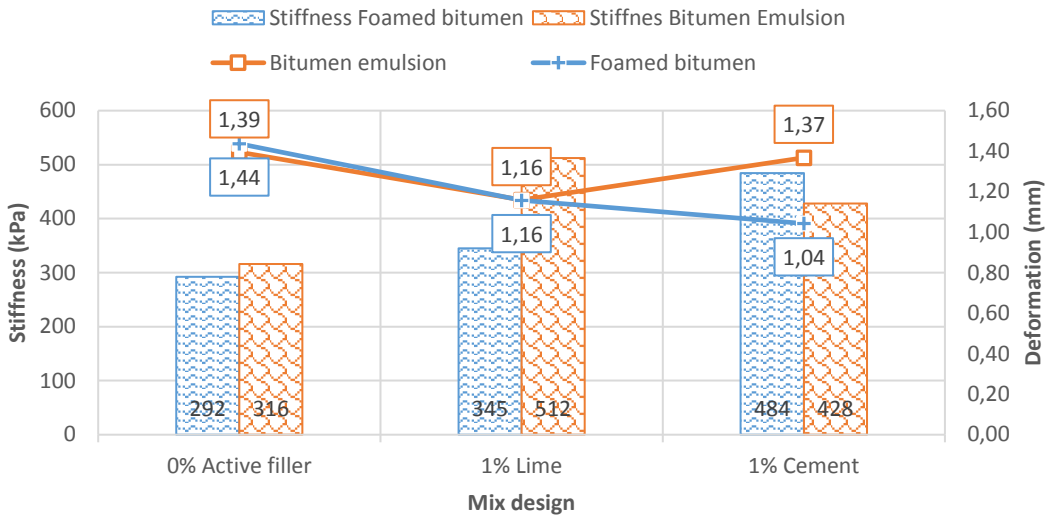

Figure 4-11: The influence of active filler on the stiffness of RCA BSM mixes with foamed bitumen and bitumen emulsion.

The addition of active fillers to the stabilised RCA improved the stiffness for both foamed and bitumen emulsion however, a reduction in the deformation occurred. As a result, active fillers results in a high stiffness mix indicating a good carrying capacity and load distribution to the supporting layers. The results are consistent with findings of a past study by Campher (2015), which shows that the addition of active filler to a BSM mix increases the stiffness and reduces the strain at break. Furthermore, the stiffness of foamed bitumen specimens is more sensitive to the addition of active fillers. Therefore, the addition of active fillers to a BSM mix increases the stiffness and reduces the strain at break.

4.4.2 **Flexibility**

The fracture energy is determined from the area under the force and deformation graph measured to the maximum deformation as demonstrated in Figure 2-35. This parameter quantifies the flexibility of a mix design and the dissipation of energy generated from the loading. The addition of active fillers decreased the fracture energy for foamed bitumen specimens from 164 kPa to 121 kPa for lime and 142 kPa for cement. Therefore, a reduction in the flexibility occurred for foamed bitumen specimens, which is emphasized by the decrease in the deformation at break as illustrated in Figure 4-12. This behaviour contradicts the results obtained by Campher (2015), where an increase in the fracture energy occurred with the increase in cement for mixes stabilised with foamed bitumen. Therefore, this indicates that the addition of active fillers can play different roles in different mixes regarding flexibility.

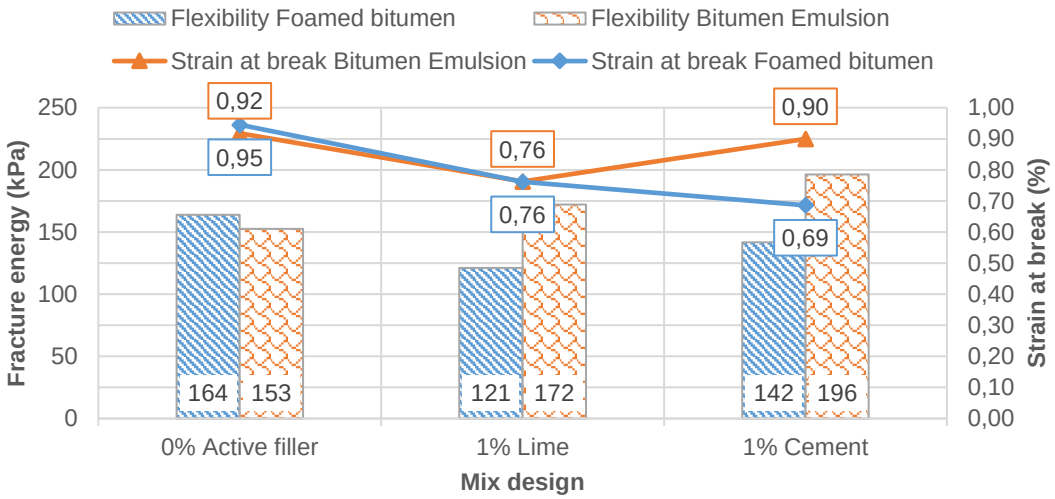

Figure 4-12: Influence of active filler on the flexiability of RCA BSM mixes with foamed bitumen and bitumen emulsion.

Alternatively, the role of active filler in RCA stabilised with bitumen emulsion corresponded to that observed by Campher (2015). The addition of active filler increased the fracture energy resulting in more flexible and ductile mixes. The fracture energy increased from 153 kPa to 172 kPa for lime and 196 kPa for cement. Consequently, the measurement of flexibility give an indication on the response of a BSM with RCA to loading. In addition, the parameter is critical for BSM_RCA specimens due to the weak mortar, which rapidly deteriorates under loading. Therefore, foamed bitumen produces brittle mixes sensitive to loading with the addition of active filler. While, bitumen emulsion produces ductile specimens with a higher resilience towards loading with the addition of active fillers.

4.5 Influence of Increasing Bitumen Content on BSM_RCA

Mixes made with no active filler at various contents of bitumen emulsion and foamed bitumen revealed that the dry ITS is sensitive to increased contents of bitumen as plotted in Figure 4-13. Each data point is a representation of the average of the triplicate set of specimens and the error bars represent the maximum and minimum values obtained for each triplicate set. A steeper increase in the dry ITS occurred for the bitumen emulsion specimens from 275 kPa with 2% bitumen to 371 kPa at 2.6% bitumen content. However, foamed bitumen mixes increased slightly from 191 kPa with 2% bitumen content to 278 kPa with 2.6% bitumen content. The bitumen emulsion mixes benefit the most from an increase in bitumen content as shown by the slope of the regression line of 17100, which is greater than the 12948 obtained for the foamed bitumen specimens regression line (Figure 4-13).

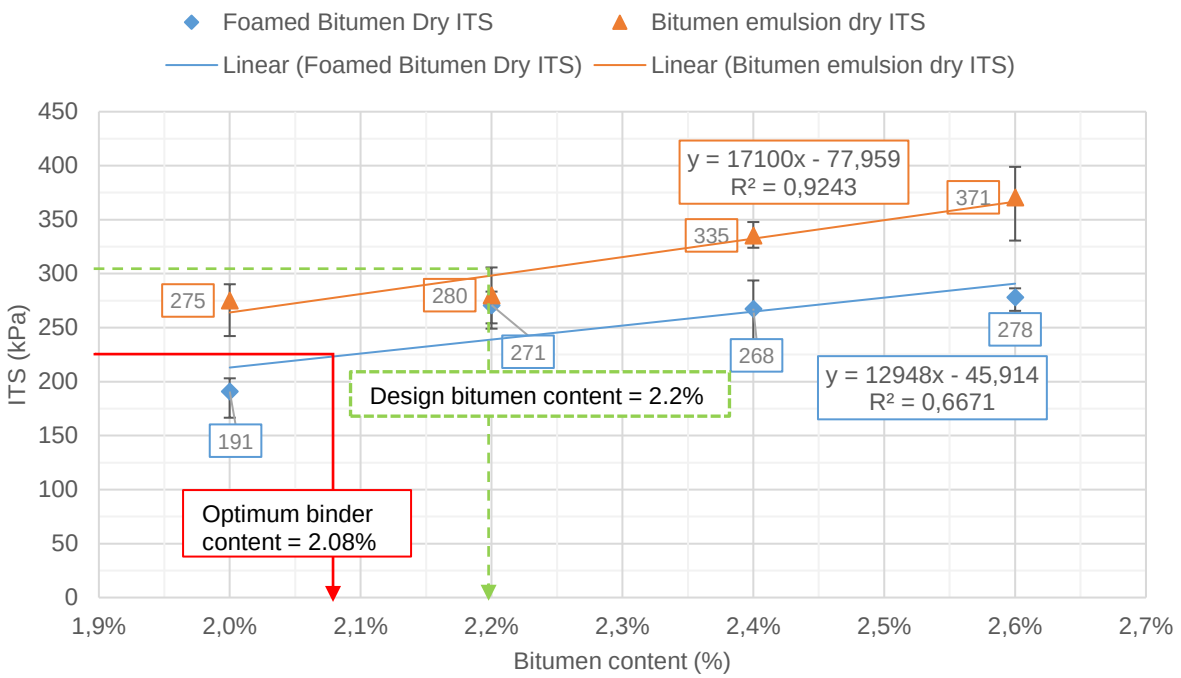

Figure 4-13: The relationship between the bitumen content and the dry ITS for specimens produced with bitumen emulsion and foamed bitumen.

An increase in the bitumen content for both foamed bitumen and bitumen emulsion mixes resulted to an increase in the resistance to moisture damage. The trend is displayed by the increase of the wet ITS when the bitumen content increases as illustrated in Figure 4-14. The degree of influence of the increased bitumen content on the wet ITS is the same for both foamed bitumen and bitumen emulsion specimens. This is based on the slope of the regression lines (13687 bitumen emulsion vs 13502 foamed bitumen). Therefore, foamed bitumen provides a similar resistance to increases in moisture as bitumen emulsion. All the mixes exceed the minimum required wet ITS of 100 kPa as specified by the TG2.

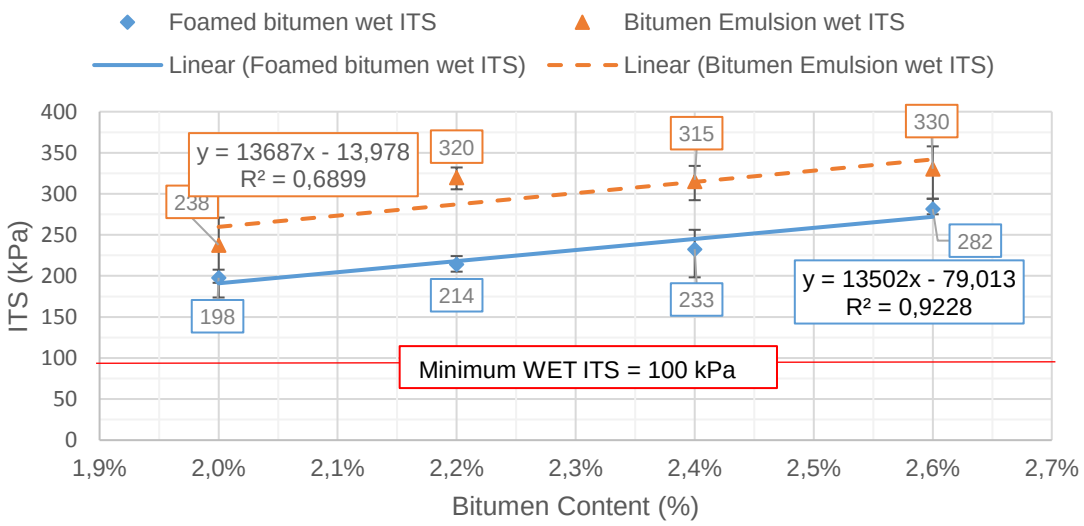

Figure 4-14: Influence of bitumen content on wet ITS of bitumen emulsion and foamed bitumen

In addition, since bitumen is a temperature dependent material, a 2ºC difference in the testing temperature of the dry and wet specimen resulted in an unrealistic TSR above 100% as demonstrated in Figure 4-15. However, it is known that the soaking of a specimen does not result in an increase in strength. For that reason, care should be taken to ensure the temperature of the specimens is within the specified tolerance prior to testing.

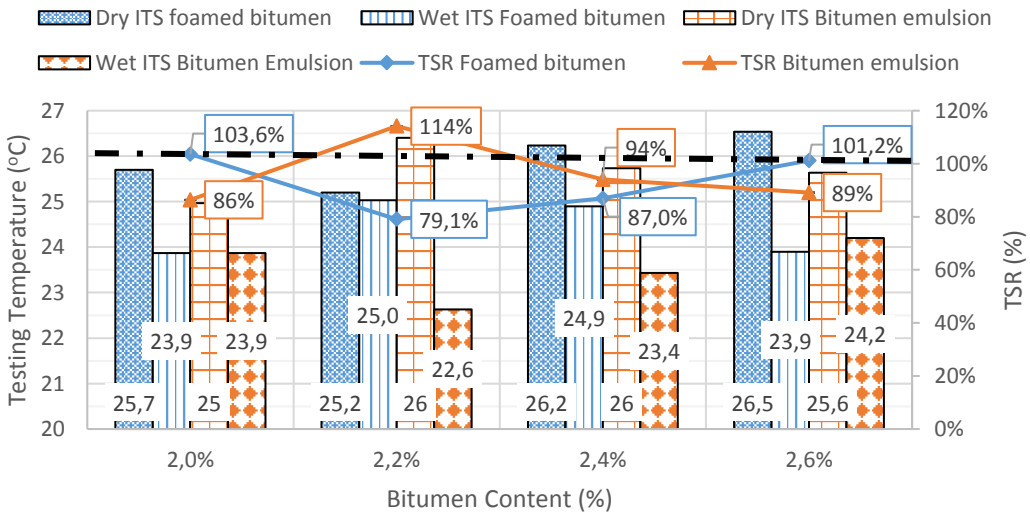

Figure 4-15: The influence of increases in bitumen content on the dry ITS, wet ITS and TSR of specimens made with foamed bitumen and bitumen emulsion

4.6 ANOVA

A one-way ANOVA is performed using the results obtained from the mix design phase of the experiment. The analysis is done to determine the significant influential factor on the

behaviour of RCA stabilised with bitumen emulsion and foamed bitumen. The independent variables include the type of active filler, type of binder and an increase in the binder content. The dependent variables measured were the wet and dry ITS, stiffness, fracture energy and strain at break of the specimens. The p-value is determined for each independent variable to determine the significance of the influence on the dependent variable. The results of the analysis are presented in this section.

4.6.1 **Influence on Dry and Wet ITS**

The one-way ANOVA is done to determine the factors which have the most significant influence on the measured wet and dry ITS. The type of binder in mixes with different types of active fillers had the most significant influence on the wet ITS as presented in Figure 4-16. A p-value of 0.01 is obtained for the wet ITS that is less the confidence level of 0.05 used for the analysis. Alternatively, the dry ITS is significantly influenced by the type of binder in mixes with increasing binder content and no active filler as demonstrated in Figure 4-16. A p-value of 0.05 was obtained for this variable, which is equal to the test confidence level. The wet ITS was insignificantly influenced by the change in the type of active filler. Moreover, the dry ITS is least influenced by the increase in binder content and change in type of active.

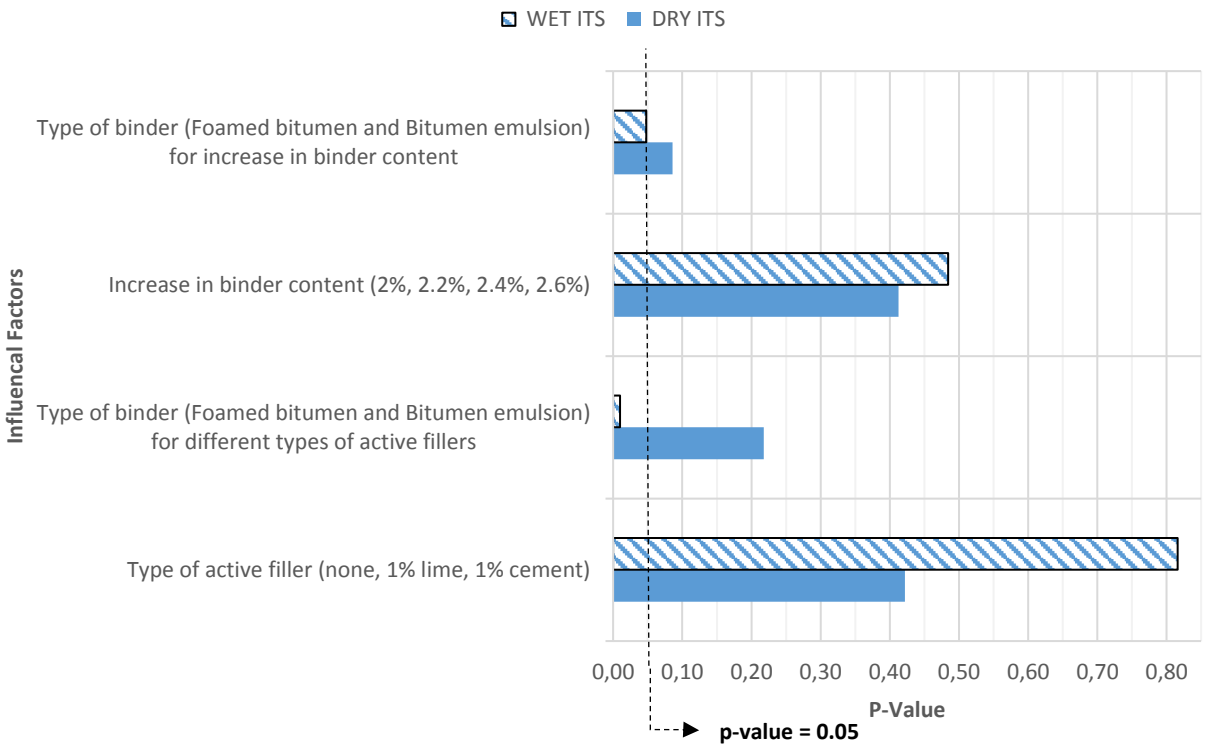

Figure 4-16 ANOVA analysis for factors which influence the dry and wet ITS of RCA-BSM

The results of the ANOVA indicate that for a moisture susceptible mix, the type of binder used to stabilise RCA is the most important variable. This is due to the difference in the

binding and coating of the aggregates provided by the foamed bitumen and bitumen emulsion. On the other hand, the dry ITS is significantly influenced by the type of binder in mixes with no active filler. However, least influenced by the increase in the bitumen content. Therefore, for a higher strength the type of binder used is an important parameter for the dry ITS. The type of active filler has the least influence on the dry and wet ITS of BSM_RCA therefore RCA might not actually need any active filler.

4.6.2 **Influence on Stiffness, Strain at break and Fracture energy**

The change in the type of binder used to stabilise RCA with no active filler has the most influence on the stiffness of the dry specimens as demonstrated in Figure 4-17. A p-value of 0.05 is obtained. Conversely, the least influence on the stiffness of the dry specimens with a p-value of 0.6 is obtained for changes in the type of binder in mixes with active filler. A further analysis of Figure 4-17 illustrates a pattern where variables such as an increase in binder content and variation in the type of active filler significantly influences the fracture energy. Moreover, variations of the type of binder and type of active filler influence the strain at break and the stiffness but inversely impacts the fracture energy.

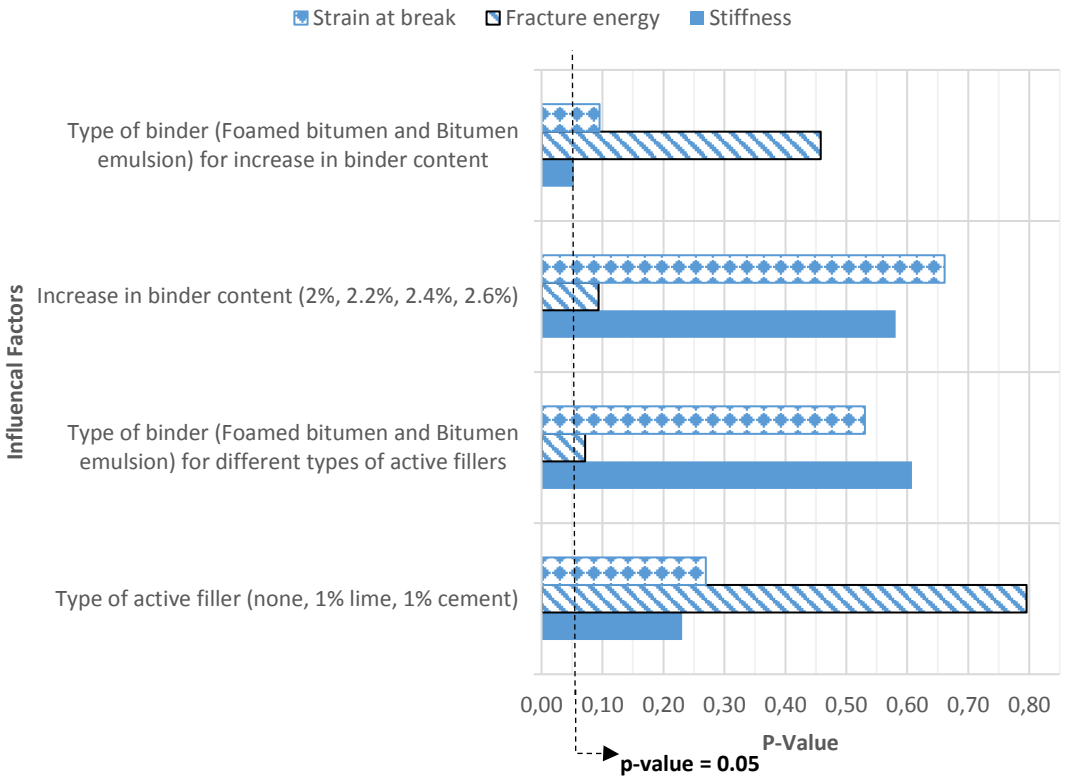

Figure 4-17: The p-Value obtained from the influence of active filler, type of binder on the strain at break, fracture energy and stiffness of dry ITS specimens.

The results of this ANOVA suggest that foamed bitumen and bitumen emulsion produce mixes with significantly different stiffnesses, which have a different strain at break. On the other hand, the fracture energy of the specimens indicating the flexibility, is significantly influenced by the increase in the binder content which is obvious i.e. the higher the bitumen content the more flexible the specimen. In addition, the type of active filler has a similar effect as the variation in binder content. Where, different active fillers bind the aggregates differently, which influences how the aggregates respond to loading. Based on the analysis, we also learn that there is a relationship between the strain at break and the stiffness of the dry ITS specimens due to the similar influential factors. Therefore, the type of binder in BSM_RCA with no active filler significantly influences the stiffness and strain at break. In addition, the fracture energy is significantly influenced by the type of binder in mixes with varying types of active fillers and an increase of the binder content.

4.7 Chapter Summary

A continuous grading is required for stabilisation with foamed bitumen and bitumen emulsion. For optimum strength, a continuous grading ensures optimum packing of the aggregates after compaction. The gradation for the RCA was obtained from a two stage crushing process to increase the filler content to meet the minimum requirement of 4%. The RCA grading achieved a grading modulus of 2.56 and fitted the specified boundaries in the TG2. Subsequent to the determination of the grading, the following physical properties were measured: hygroscopic moisture, maximum dry density, optimum moisture content, plasticity index, pH and the CBR. The tests revealed that when working with RCA, consistency of the larger aggregates such as the 14 mm, significantly influences the measured physical properties.

The hygroscopic moisture ranged between 2.3 and 2.96% which indicates the importance of the test as it will affect the OMC of the specimens in mixing and compaction. The PI was evaluated as non-plastic, which ensures that the aggregates are not highly sensitive to variations of the moisture content. Due to the self-cementation potential of RCA, the cement activity was measured with the pH which was obtained as 12.32 which indicates active latent cement. The maximum dry density for the RCA used for BSM was obtained as 1903 kg/m^3 achieved at an OMC of 13%. Lastly, the CBR was measured from specimens compacted with a MOD hammer and vibratory hammer which showed that the compaction method influences the bearing capacity of the BSM with RCA.

The CBR of 50% indicates that a BSM 2 mix design can be produced from the RCA. However, the indirect tensile strength (ITS) of specimens produced from RCA stabilised with foamed bitumen and bitumen emulsion with varying types of active filler indicates a BSM 1 mix design can be produced. The ITS results also indicated that the addition of active filler improved the dry and wet ITS of the BSM_RCA. However, mixes with no active filler meet the minimum specification for a BSM 1. An analysis of the ITS data with different active fillers shows that the addition of active filler increases the stiffness and reduces the deformation at break therefore brittle mix. Furthermore, an analysis of the flexibility of specimens shows that the foamed bitumen where the most brittle. These results were confirmed by the ANOVA.

The type of binder had the most influence on the wet ITS due to the difference in the coating and binding of aggregates. The dry ITS was mostly influenced by the type of binder in mixes with no active filler. Additionally, the type of binder and active filler influenced the stiffness and strain at break. While, the flexibility was mostly influenced by the increase in binder content and variation in active filler. Therefore, there is potential to stabilise RCA with foamed bitumen or bitumen emulsion. The performance parameters such as the shear strength and resilient modulus provide a better understanding on how the mix will respond to loading in a pavement structure under dynamic loading.

Chapter 5: Shear Parameters and Resilient Modulus

To determine the feasible use of BSM_RCA, the shear strength and resilient modulus for the bitumen emulsion specimens (BSM_E) and foamed bitumen specimens (BSM_F) are measured. The final mix design comprised of 2.2% bitumen content with no active filler as this was found to be sufficient according to the ITS results presented in Section 4.3. Furthermore, an analysis of the influence bitumen content has on the dry ITS of the BSM_F and BSM_E specimens indicates that the minimum specified dry ITS can be achieved at a bitumen content of 2.08%. However, an observation of the 2% mixes appeared to be dry. Therefore, a decision was taken to use 2.2% for both binder types, which is still a representative, economical and practical bitumen content when applied to traditional BSM mixes.

The shear strength is defined by the cohesion and internal angle of friction determined from the Mohr circles as illustrated in Figure 2-5. Whereas, the resilient modulus (Mr) is determined from the relationship between the cyclic load and the recoverable strain demonstrated in Figure 2-6. The shear parameters indicate the classification of the resultant BSM as guided by the TG2. Moreover, the relationship between the bulk stress and the Mr demonstrates the behaviour of the specimens under dynamic loading with an increase in the applied stress. These performance parameters are then used to determine the pavement life of the mix designs. The stress dependent behaviour of the mix designs is modelled and the results are presented in this chapter.

5.1 Shear Properties

The shear parameters indicate that the BSM_E and BSM_F provide the same shear resistance against loading. A cohesion of 177 kPa is measured for BSM_F and 174 kPa for BSM_E as presented in Table 10. Additionally, the internal angle of friction for BSM_F is measured as 50.4^{o} with a retained cohesion (RC) of 90%. Whereas 47.9^{o} was obtained for BSM_E with a RC of 88.2% (Table 10). The TG2 requires a minimum cohesion range between 100 and 250 kPa for a BSM2. As a result, the BSM_RCA can be classified as a BSM2 for both BSM_F and BSM_E specimens. However, the internal angles of friction and RC exceed the minimum specified angle of internal friction of 40^{o} and RC of 75% for a BSM1. Considering that RCA has an inherent latent active cement, the cohesion could potentially increase as a result of possible self-cementation of the aggregates (Poon & Chan, 2006). Furthermore, studies on the possibility of the self-cementation of BSM_RCA should be

investigated to determine whether the cohesion increases with time and exposure to moisture. Care must be taken as high cohesion values result in brittle mixes sensitive to shrinkage cracking therefore exposing the pavement structure to water damage.

Table 10: The cohesion, internal angle of friction and retained cohesion for foamed bitumen and bitumen emulsion RCA mixes.

Shear parameters/Binder	Foamed Bitumen	BSM Class	Bitumen emulsion	BSM Class
Cohesion (kPa)	177 kPa	BSM2	174 kPa	BSM2
Internal angle of friction	50.4º	BSM1	47.9º	BSM1
Retained Cohesion	90%	BSM1	88.2%	BSM1

A further comparison of the shear strength of BSM_RCA is done with the shear strength of unmodified RCA, stabilised CDW consisting mainly of RCA and BSMs with traditional granular materials. The shear parameters obtained for unstabilised RCA 1 (Bredenkamp, 2018) and RCA 2 (Rudman & Jenkins, 2015) are higher than those achieved for BSM_RCA presented in Figure 5-1 and Figure 5-2. A cohesion of 273.7 kPa is measured for RCA 1 and 252.1 kPa for RCA 2 after 1 day of curing as illustrated in Figure 5-1. The corresponding internal angle of friction for RCA 1 is obtained as 54.6º and 51º for RCA 2 as illustrated in Figure 5-2. Therefore, the shear parameters obtained for BSM_RCA are lower than those obtained for unstabilised RCA 1 and RCA 2.

Several factors related to the nature of RCA play a role in the measured shear strength, namely: pH, gradations, filler content, mortar content, quality of previous concrete and density. Based on the pH, RCA 1 and RCA 2 had a higher pH (pH = 13.4) than the current research (pH = 12.32) as a result the specimens had a higher potential to self-cement. Moreover, a high pH leads to a brittle specimen/layer and manifestation of high cohesion values (Rudman, 2019b). Furthermore, RCA 1 and RCA 2 had different gradations with higher filler contents resulting in different densities (RCA 1 and RCA 2 = 2110 kg/m3; this research = 1903 kg/m3). A significant adhesion of mortar was visually observed on the RCA used to produce the BSM_RCA, hence the CBR of 50% was achieved. The reduced internal angle of friction is a typical occurrence for BSM mixes. The additional bitumen increases the lubrication between the aggregates during loading. These findings highlight the variability that occurs with RCA as a result, an understanding of the aggregate is critical for its use. Alternative RCA materials with different gradations and pH need to be investigated.

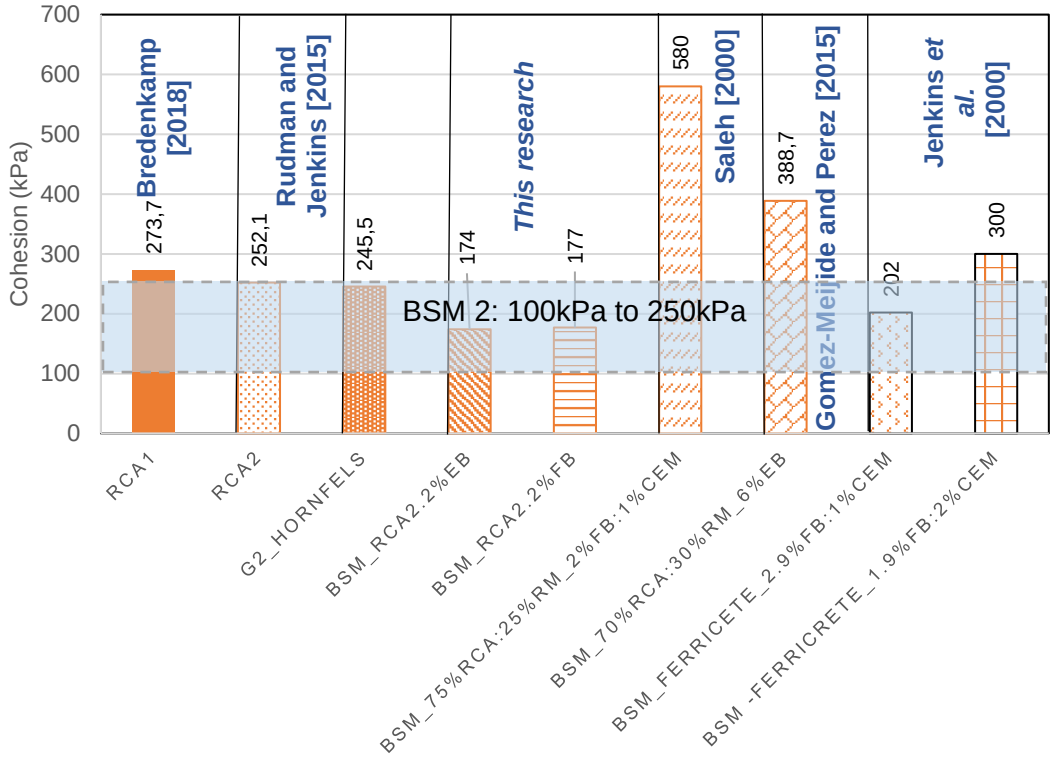

Figure 5-1: BSM_RCA Cohesion compared to other cohesion of various mixes

Previous research on bitumen stabilisation of construction demolition waste (CDW) done by Saleh (2000) and Gomez-Meijide & Perez (2015) showed potential to improve the structural capacity of such aggregates. This research shows that an economical practical mix can be produced by stabilising RCA with either foamed bitumen or bitumen emulsion. This can be seen in Figure 5-2 where a comparison is done between the internal angle of friction obtained by Saleh (2000) from a stabilised mix granulate consisting of 75% RCA and 25% masonry. The mix was made with 2% foamed bitumen and 1% cement which achieved a high cohesion of 580 kPa and an internal angle of friction of 54.27º. The mix made by Saleh (2000) resulted in an inordinately high cohesion and must have been very brittle due to the additional cement. In this case, a material that fails in fatigue cracking and not permanent deformation might behave in a similar manner to a cement stabilised material.

Furthermore, Gomez-Meijide & Perez (2015) produced a mix with CDW containing mainly 70% RCA stabilised with 6% bitumen emulsion. The mix achieved a cohesion of 388.7 kPa with an internal angle of friction of 43.5º. However, considering the high bitumen content of 6%, the mix is uneconomical. The bitumen content is similar to what is added to produce a hot asphalt mix. Therefore, the use of 100% RCA in a BSM is economical and practical but care should be taken to avoid brittle behaviour of the mix due to high cohesion as obtained by Saleh (2000).

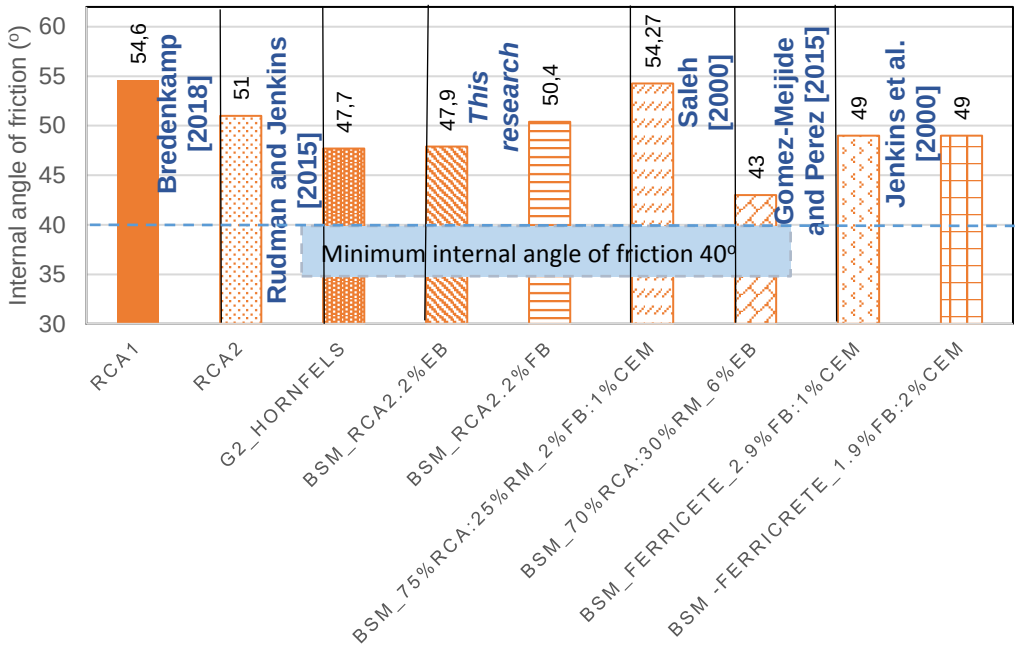

Figure 5-2: BSM_RCA Internal angle compared to other similar mixes

Finally, based on a comparison done with typical BSMs produced by Jenkins (2000), the BSM_RCA mix has potential for use to improve the benefit of the environmental sustainability of a BSM in a pavement structure. Figure 5-1 and Figure 5-2 show the cohesion of 202 kPa with an internal angle of friction of 49° achieved with a mix made with ferricrete stabilised with 2.9% foamed bitumen and 1% cement. The shear parameters obtained for BSM_RCA with both foamed and bitumen emulsion are comparable indicating similarity in the shear strength. Therefore, BSM_RCA has potential for use in the base layer, perhaps even in a high traffic roads. However, an in depth analysis of the resilience modulus is required to fully understand the behaviour of the mix under repetitive loading.

5.2 Resilient Modules

The resilient modulus of a bitumen stabilised RCA with foamed bitumen and bitumen emulsion are presented in this section. The specimens were tested with a moisture content of 65% OMC compacted to 100% Modified AASTHO. A plot of the resilient modulus versus the bulk stress illustrates the stress dependency of the material under repeated dynamic loading which is important for understanding the material's response. The typical response of a granular unbound or non-continuously bound material has been shown to be stress dependent. Where, an increase in confinement and applied stress results in an increase in the resilient modulus of the material. The modelling of the data describes the degree of the stress dependency of the material and it is used in the mechanistic empirical structural

design of the layer. Seven types of granular material models will be used to define the stress dependency of BSM-RCA in order to determine the most suitable model.

5.2.1 **Relationship between Mr and bulk stress**

The bitumen stabilised RCA with foamed bitumen and bitumen emulsion are stress dependent as shown in Figure 5-3. Where, an increase in the bulk stress results in an increase in the resilient modulus. A comparison between the results obtained for each repeat (Appendix A) shows that the results are reliable and can be used with confidence. At a deviator stress ratio (DSR) of 51%, no stress softening occurs for foamed bitumen specimens however, a slight decrease in the resilient modulus for bitumen emulsion specimens occurs (Figure 5-3). The resilient modulus for foamed bitumen specimens ranges from 376 to 660 MPa, which is slightly higher than the bitumen emulsion range of 360 to 575 MPa. In addition, the stiffness measured for foamed bitumen specimens is equally influenced by the confinement and DSR. However, a different relationship is observed for bitumen emulsion specimens. An increase in confinement has a greater increase on the resilient modulus than the increase in DSR for bitumen emulsion specimens. This can be seen based on the shallow slopes of the data points of the change in the DSR compared to the steep slope of the data points of the change in confinement pressure (Figure 5-3). Therefore, bitumen emulsion specimens are more sensitive to increases in confinement than an increase in the DSR.

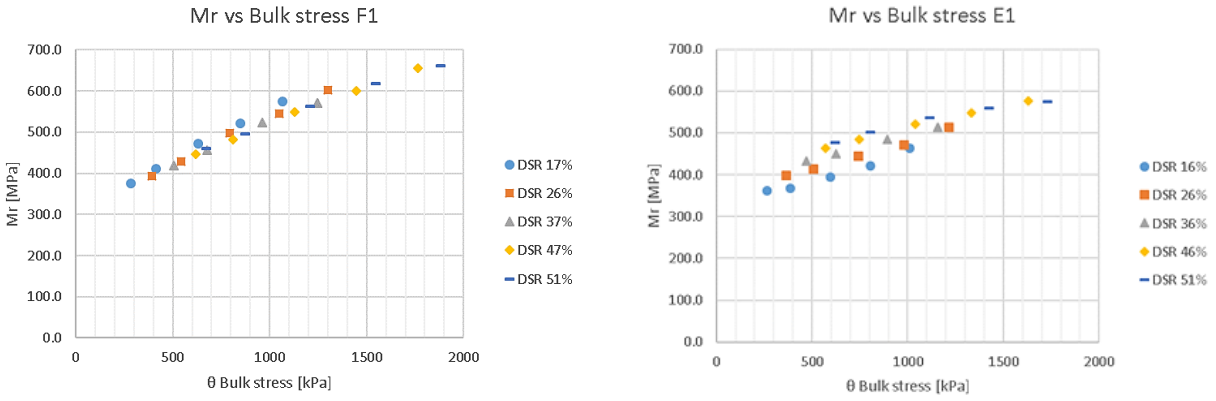

Figure 5-3: The relationship between the resilient modulus and the bulk stress obtained for a bitumen stabilised RCA with foamed bitumen (F1) and bitumen emulsion (E1).

The results show that both mixes are stress dependent in a similar manner to typical unbound granular materials and traditional BSM mixes. The foamed bitumen specimen is slightly stiffer than the bitumen emulsion. This contradicts the stiffness determined from the ITS results in Section 4.4.1 which show bitumen emulsion to be slightly stiffer. However,

considering the difference in coating of the aggregates (Figure 4-10) between foamed bitumen and bitumen emulsion, a slight difference is expected. The spot-welds of the foamed bitumen allow for the potential for self-cementation of the uncoated aggregates. Whereas, in bitumen emulsion specimens the coating reduces the friction between the aggregates resulting in higher dependency on confinement for strength.

The stiffness range for both mixes is lower when compared to the range of 600 to 1500 MPa obtained for BSMs produced from crushed stone and RAP (Ebels, 2007). However, the stiffness is significantly higher than what has been obtained for BSMs produced from G1 stabilised with 2% foamed bitumen which ranges between 150 to 300 MPa (Jenkins, 2000). Additionally, the stiffness range for BSM_RCA is higher than the stiffness ranges obtained for mixed granulate (65% RCA, 35% Masonry) as shown by Van Niekerk (2002). Therefore, it is plausible to assume that the addition of low viscosity bitumen to RCA increased the stiffness and produced a suitable BSM. The material coefficients obtained from the modelling of the data will provide more information on the response of the BSM_RCA mixes to repeated loading.

5.2.2 **Resilient modulus model Results**

The relationships between the resilient modulus and the bulk stress, confinement stress, deviator stress, deviator stress ratio (DSR) and principle stress ratio (PSR) are presented in this section. Each figure in the section presents the model coefficients along with the correlation coefficients, r^2, obtained for the BSM_RCA with bitumen emulsion and foamed bitumen. The models for each mix design correspond to the values obtained for the repeat specimen with bitumen emulsion and foamed bitumen presented in Appendix A. Therefore, this indicates that the results are repeatable and reliable for all the models fitted to the data thus can be used with confidence.

Mr-θ

The bulk stress resilient modulus model (Mr-θ) determines the resilient modulus as a function of the bulk stress and it is the most commonly used model to describe the stress dependency of a granular material because of its simplicity. As previously mentioned, the BSM with RCA is a stress dependent material as demonstrated in Figure 5-4, where the Mr-θ model fits the measured data perfectly especially for foamed bitumen. The correlation coefficient obtained for the foamed bitumen mix of 0.977 is higher than 0.864 obtained for the bitumen emulsion. This shows that the model better describes the stress dependency of the resilient modulus for foamed bitumen specimens. The foamed bitumen mix exhibits a

linear behaviour where an increase in bulk stress increases the resilient modulus. However, for the bitumen emulsion mix, the scattered data shows the slight difference between the effect of an increase in bulk stress and confinement stress on the Mr. This observation highlights the inability of the model to describe separately the influence of the confinement stress and deviator stress.

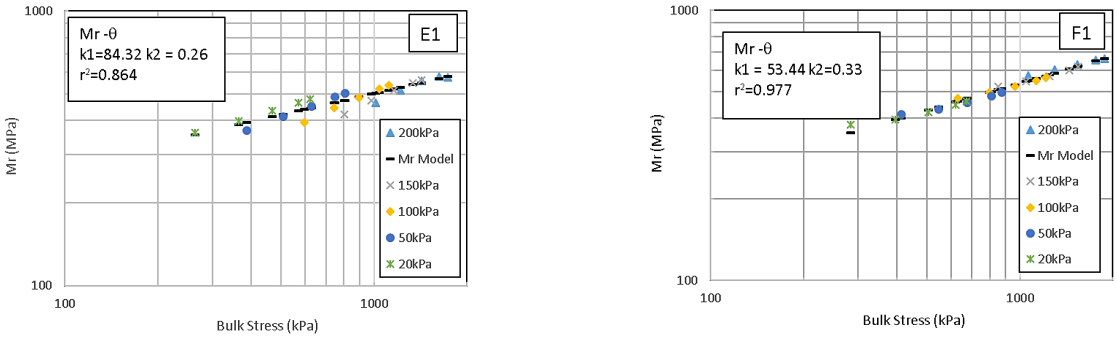

Figure 5-4: The bulk stress influenced resilient modulus model fitted for BSM_RCA with bitumen emulsion (E1) and foamed bitumen (F1)

Mr-σ3-σd

The confinement and deviator stress resilient modulus model (Mr-σ3-σd) aims to integrate the influence of an increase in confinement stress (σ3) and the deviator stress (σd) on the measured resilient modulus. As a result, the Mr-σ3-σd model determines the resilient modulus as a function of the confinement stress and deviator stress influenced separately. A correlation coefficient of 0.986 is obtained for the bitumen emulsion specimen that indicates a good fit of the data as illustrated in Figure 5-5 E1. The correlation coefficient for foamed bitumen is obtained as 0.975, which also indicates a perfect fit of the data. For this reason, this Mr-σ3-σd model best describes the stress dependency of both mixes. Noted in Section 5.2.1, the bitumen emulsion specimen appears to be influenced differently by changes in the confinement stress and deviator stress thus the model incorporates the difference. However, the model does not consider the reduction in the resilient modulus at high deviator stress ratios (DSR) that bring about failure of the specimen i.e. stress softening. Therefore, only stress stiffening is described which is physically incorrect for granular materials.

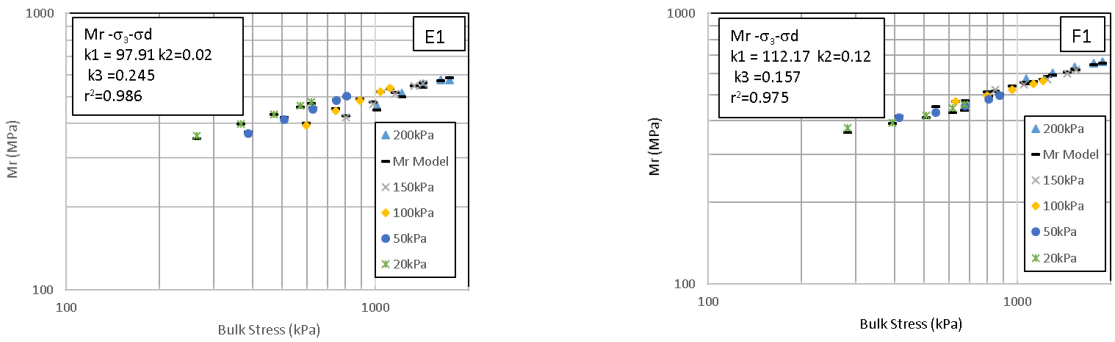

Figure 5-5: The confinement and deviator stress influenced resilient modulus model fitted for BSM_RCA with bitumen emulsion (E1) and foamed bitumen (F1).

Parabolic Mr-σ3-σd

The parabolic confinement and deviator stress resilient modulus model (Parabolic Mr-σ3-σd) aims to take account for the decrease in the resilient modulus at high stresses when the material is approaching failure. Similarly, to the Mr-σ3-σd model, it integrates the influence of the confinement stress and the deviator stress separately on the resilient modulus. The model has described the measured resilient modulus for both bitumen emulsion (E1) and foamed bitumen (F1) mixes perfectly as illustrated in Figure 5-6. The correlation coefficients obtained for bitumen emulsion of 0.963 and 0.962 for foamed bitumen indicates a perfect fit. Although, there is no stress softening of the specimens a slight reduction in the resilient modulus occurring at the high confinement and deviator stresses is described by the model.

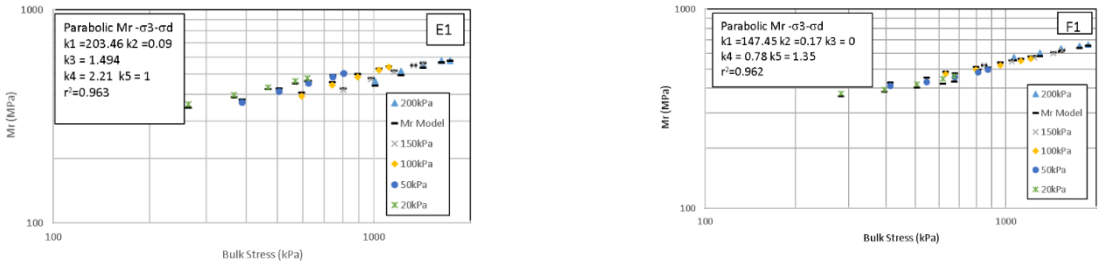

Figure 5-6: The parabolic confinement deviator stress influenced resilient modulus model fitted for the measured Mr for BSM_RCA with bitumen emulsion (E1) and foamed bitumen (F1).

Mr-σ3-σd/σd,f

The confinement stress and deviator stress ratio resilient modulus model (Mr-σ3-σd/σd,f) is fitted to describes the resilient modulus based on the confinement stress (σ3) and deviator stress ratio (DSR) instead of the deviator stress. Presented in Figure 5-7, the model is not a good fit for the bitumen emulsion data as indicated by the correlation coefficient of 0.379. However, there is a good correlation for the foamed bitumen resilient modulus shown by the

correlation coefficient of 0.801. The model aims to determine if the confinement stress has a significant influence on the resilient modulus. In addition, how the consideration of the deviator stress ratio would affect this relationship. Based on the results, there is no relationship between the two variables considered together in this manner.

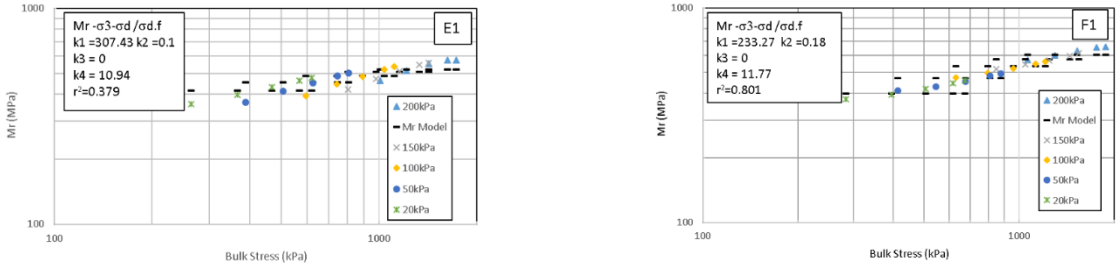

Figure 5-7: The confinement and DSR resilient modulus model fitted to the measured Mr for BSM_RCA with bitumen emulsion (E1) and foamed bitumen (F1).

Mr-θ-σd/σd,f

Furthermore, based on the previous model, the resilient modulus is determined based on the bulk stress (θ) and the deviator stress ratios (DSR). The confinement stress is removed as the main influencer to the resilient modulus and the bulk stress is used. The bulk stress deviator stress ratio model (Mr-θ-σd/σd,f) is an extension of the Mr-θ model however, it considers stress stiffening caused by the increasing DSR. Additionally, it considers stress softening that occurs at high DSR. Presented on Figure 5-8, is the fit of the model on the measured resilient modulus for bitumen emulsion (E1) and foamed bitumen (F1). The relationship between the bulk stress and the DSR provides a better description of the resilient modulus for both BSM_RCA mixes. The best fit is obtained for the foamed bitumen resilient modulus with a correction coefficient of 0.993 whereas the bitumen emulsion results fitted with a correlation coefficient of 0.864. Consequently, both mix designs are described better with the Mr-θ-σd/σd,f model than by the Mr-σ3-σd/σd,f model. Therefore, the resilient modulus for the BSM_RCA mixes is dependent on the bulk stress.

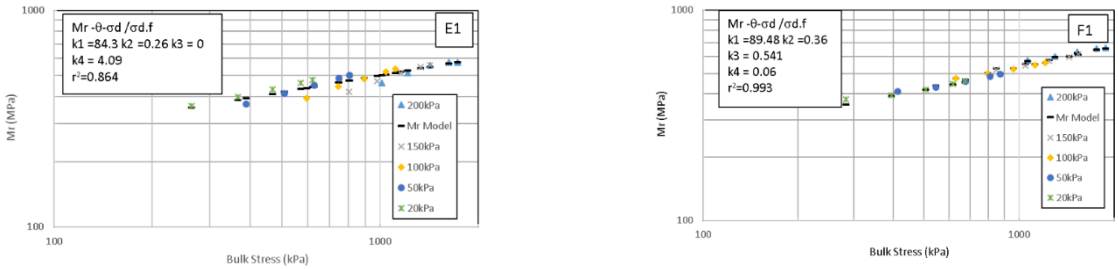

Figure 5-8: The bulk stress and deviator stress ratio influenced resilient modulus model fitted to measured Mr for BSM_RCA with bitumen emulsion (E1) and foamed bitumen (F1).

Mr-θ-σ1/σ1,f

For research purposes, an analysis is done to determine how the Mr-θ-σd/σd,f model changes if the deviator stress ratio (DSR) is replaced with the principal stress ratio (PSR). This variation removes the effect of the change in confinement stress from the stress ratio component. The results from the bulk stress and principal stress ratio resilient modulus model are presented in Figure 5-9. An exact fitted is obtained similarly to the bulk stress and deviator stress ratio model with a correlation coefficient of 0.864 for bitumen emulsion and 0.993 for foamed bitumen. Therefore, these is no significant difference obtained if the stress ratio component is used as the DSR or PSR. Both stress ratios results in the same fit of the models.

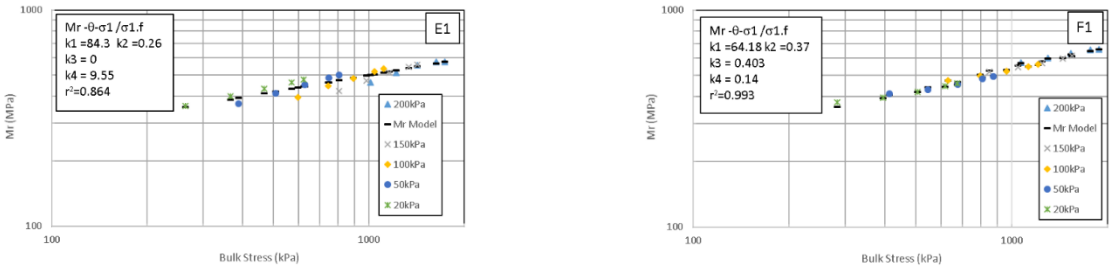

Figure 5-9: The bulk stress and principal stress ratio influenced resilient modulus model fitted for the measured Mr for BSM_RCA made with bitumen emulsion (E1) and foamed bitumen (F1).

Mr-σ3-σ1/σ1,f

Lastly, a similar analysis performed for the bulk stress DSR model is done for the confinement stress and DSR where the DSR is replaced with the PSR. As presented in Figure 5-10, a similar trend effect occurs. The replacement of the DSR with PSR does not influence the resultant model. Therefore, the resilient modulus for BSM_RCA is a function of both the confinement and deviator stresses which is best described with the bulk stress.

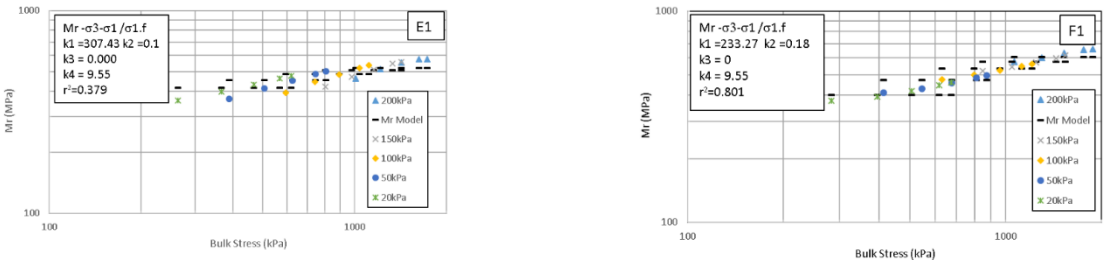

Figure 5-10: The confinement stress and principal stress ratio influenced resilient modulus model fitted to measured Mr obtained for BSM_RCA with bitumen emulsion (E1) and foamed bitumen (F1).

5.2.3 **Model coefficient sensitivity analysis**

This section aims to present the observed influence of each model coefficient on the resilient modulus based on a sensitivity analysis conducted on the foamed bitumen models. The foamed bitumen model is used because of its linear behaviour. This enables the to observation of variations without difficulty and it is assumed the same effect occurs for bitumen emulsion models.

Mr-θ (k1,k2)

By understanding the effect of the parameters, a comparison of these coefficients between the various models can be conducted. As a result, the sensitivity analysis is done to determine how changes in the k1 and k2 coefficients amend the Mr-θ model. An increase of the k1 coefficient from 53.44 to 80 while keeping the k2 coefficient constant, results to a parallel upward shift in the model as illustrated in Figure 5-11. Whereas, a reduction of the k1 coefficient to 20 results to a parallel downward shift. Therefore, this means that the higher the k1 coefficient a relatively higher resilient modulus is obtained at the same bulk stresses. This indicates the inherent strength of the material under dynamic loading.

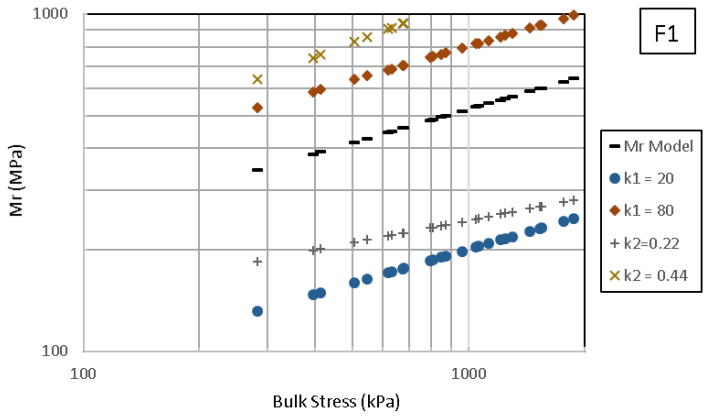

Figure 5-11: Graphical illustration of how k1 and k2 affect the Mr-θ model for Mr.

For instance, the foamed bitumen specimen obtained a k1 coefficient of 53.44, which is lower than the 84.32 achieved by the bitumen emulsion specimens. For that reason, a lower stiffness is obtained for foamed bitumen specimen at the same bulk stresses. However, a judgement on the overall stress dependency of the resilient modulus is also influenced by the k2 coefficient. A decrease of the k2 coefficient from 0.33 to 0.22 results in a downward shift and a decrease in the slope of the model as demonstrated in Figure 5-11. While, an increase of the k2 coefficient to 0.44 results in an upward shift and an increase in slope of the model. Therefore, this shows that the higher the k2 value, an increase in the bulk stress results in a higher rate of increase of the resilient modulus. The k2 coefficient describes the

sensitively of the material to increases in the bulk stress i.e. slope of the model. The higher the k2 value, the more sensitive the material is to changes in the bulk stress where a higher stiffness at a higher rate of increase occurs with an increase of the bulk stress. Therefore, in this case, F1 benefits more from an increase in the bulk stress, which is exhibited by the higher k2 of 0.33 in comparison to 0.26 achieved by bitumen emulsion specimens.

Mr-σ3-σd (k1,k2,k3)

In the confinement and deviator stress resilient modulus model (Mr-σ3-σd), changes to the k1 and k2 coefficients results to similar shifts as observed on the Mr-θ model. The higher the k1 coefficient, the higher the resilient modulus of the material as presented in Figure 5-12. The higher the k2 coefficient, the higher the resilient modulus and the rate of increase as the confinement stress increases (Figure 5-12). Furthermore, a 0.1 decrease of the k3 coefficient from 0.157 shows a decrease in the resilient modulus and a slight decrease in the rate/slope of the resilient modulus at higher deviator stresses as illustrated in Figure 5-12. On the other hand, a 0.1 increase in the k3 coefficient results in an increase of the resilient modulus and a general increase in the slope of the line. This implies that the k3 coefficient in the model takes into account that an inherently strong aggregate i.e. higher initial stiffness, stiffens further with an increased deviator stress that increases with the principle stress. Whereas, an inherently weaker aggregate i.e. lower initial stiffness, at high stress state a decrease in stiffness occurs.

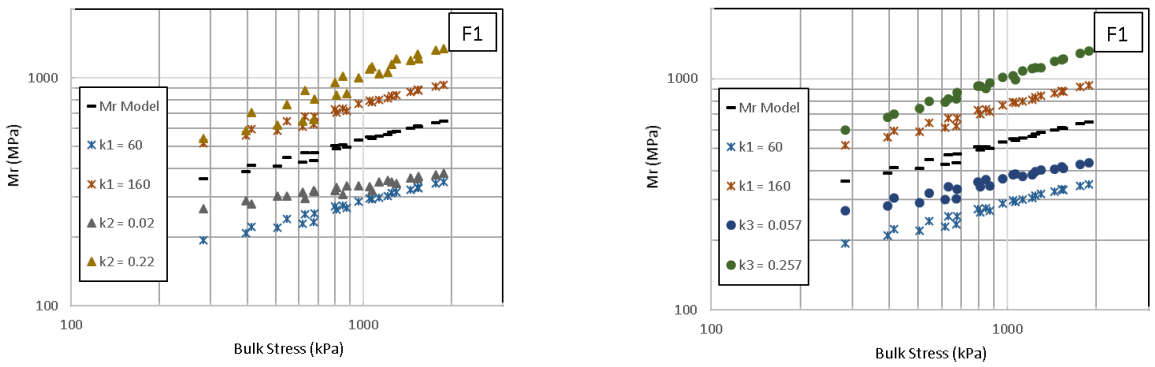

Figure 5-12: Illustration of the influence of k1, k2 and k3 on the confinement and deviator stress influenced resilient modulus model.

A comparison between the k3 coefficients obtained for the foamed bitumen and bitumen emulsion specimens' shows that the bitumen emulsion benefits from an increase of the stress state within the specimen. This is evident by the high k3 coefficient of 0.245 obtained for the bitumen emulsion compared to the lower k3 coefficient of 0.157 for foamed bitumen.

This supports the earlier statement that bitumen emulsion is highly dependent on the overall stress state of the specimen rather than solely on the confinement stress.

Parabolic Mr-σ3-σd (k1,k2,k3,k4,k5)

Similarly, to the previous models, the k1 and k2 coefficients for the parabolic Mr-σ3-σd model have the same effect as seen and discussed in the Mr-σ3-σd model coefficient analysis. Focus will be drawn to discuss how k3, k4 and k5 coefficients influence the relationship between the resilient modulus and bulk stress determined by the parabolic Mr-σ3-σd model. An increase of the k3 coefficient from 0 to 0.5 presents a scatter of the points at higher DSR values which decrease slightly as presented in Figure 5-13. Moreover, a further increase to 2 presents a wider scatter of the points especially at high DSR values leading to lower resilient modulus. However, a decrease of the k3 coefficient to -2 produces points with a slightly higher resilient modulus but a higher rate of reduction in the resilient modulus at high DSR levels as demonstrated in Figure 5-13. Therefore, the k3 coefficient describes the rate of decrease of the Mr with increasing levels of the DSR. A high positive k3 coefficient produces a wider spread of the points meaning, the higher the tolerance to increased bulk stresses prior to the occurrence of stress softening followed by a gradual decrease. On the contrary, the lower the k3 coefficient represents the sensitivity of the resilient modulus to changes in the bulk stress and DSR. Meaning, a rapid reduction of the stiffness occurs with an increase in the DSR. An analysis of the k3 coefficients obtained for the foamed bitumen mix indicates no stress softening occurs at the test DSRs. On the other hand, bitumen emulsion specimen obtained a k3 coefficient of 1.494 which indicates a wide spread of the data points with a gradual decrease in the resilient modulus at a higher DSR.

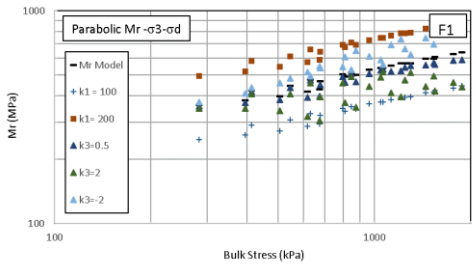

Figure 5-13: Illustration of the influence of k3 on the parabolic confinement and deviator stress influence resilient modulus model.

Subsequently, a study of the k4 and k5 coefficients is presented in Figure 5-14 compared to the effect of the k1 coefficient on the model. A decrease of the k4 coefficient from 0.78 to 0.25 results in a slight decrease in the resilient modulus however, at high DSR and bulk stresses. While, an increase of the k4 coefficient from 0.78 to 1.25 results to an increased

resilient modulus at higher bulk stresses or DSR. For that reason, a comparison of the k4 coefficients obtained for foamed bitumen and bitumen emulsion indicates the following: the k4 coefficient obtained for bitumen emulsion of 2.21, which is high, illustrates that the high DSR results in an increase of the resilient modulus. While, the low k4 coefficient of 0.78 obtained for foamed bitumen indicates a lower influence of the DSR on the resilient modulus therefore less decrease in the resilient modulus at a higher DSR.

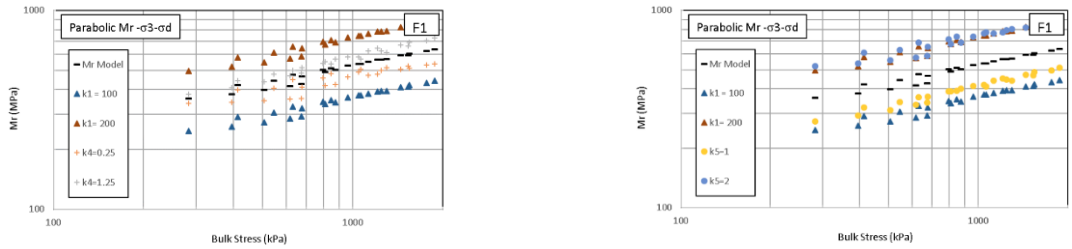

Figure 5-14: Illustration of k4 and k5 coefficients for the parabolic confinement and deviator stress influenced resilient modulus model.

On the other hand, an increase of the k5 coefficient from 1.35 to 2 presents an increase in the Mr similar to the effect of the k1 coefficient as presented in Figure 5-14. While, a decrease of the k5 coefficient from 1.35 to 1 result in a parallel downward shift of the resilient modulus model similar to the effect of k1. Therefore, the higher the k5 coefficient the higher the resilient modulus. The foamed bitumen specimens achieved a k5 coefficient of 1.35, which is higher than the 1 achieved by bitumen emulsion. This indicates and supports the initial statement that foamed bitumen achieved a higher resilient modulus overall.

Mr-σ3-σd/σd,f (k1,k2,k3,k4)

A sensitivity analysis of the k1 and k2 coefficients of the adjusted confinement and deviator stress resilient modulus model (Mr-σ3-σd/σd,f) also showed similar effects on the resilient modulus as observed in the Mr-θ model. Presented in Figure 5-15 is the effect of the k3 and k4 coefficients on the resilient modulus determined from the Mr-σ3-σd/σd,f model compared to the changes introduced by the k1 coefficient. An increase or decrease of the k3 and k4 coefficients for the foamed bitumen specimen results to no changes in the resilient modulus. Therefore, the deviator stress ratios and confinement stresses have no relationship with the resilient modulus based on this model. A similar conclusion can be made for the bitumen emulsion specimens, which obtained a k3 coefficient of 0.

Figure 5-15: The effect of k3 and k4 on the resilient modulus influenced by the confinement stress and DSR.

Mr-θ-σd/σd,f (k1,k2,k3,k4)

However, an adjustment of the previous model with the bulk stress presents a different relationship. An increase of the k3 coefficient from 0.541 to 0.75, results to a parallel downward shift of the resilient modulus model as illustrated in Figure 5-16. Whereas, a decrease of the k3 coefficient to 0.25 results in an increase/upward parallel shift of the resilient modulus model. Thus, the lower the k3 the higher the resilient modulus with increasing bulk stress. Whereas, a high k3 coefficient indicates a reduced resilient modulus. As a result, the k3 coefficient of this model represents the power of the DSR on reducing the resilient modulus as it increases. The k3 coefficient of 0 obtained for the bitumen emulsion specimens indicates that the DSR has no influence on the resilient modulus which is incorrect because based on observations of the bitumen emulsion resilient modulus, the DSR has a significant influence. On the other hand, a k3 coefficient of 0.541 is obtained for foamed bitumen resilient modulus model indicating a reduction of the resilient modulus occurs when the DSR increases. However, based on the observation of the data no stress softening occurs as the DSR and bulk stress increases

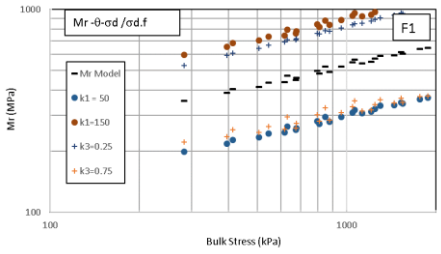

Figure 5-16: The effect of the k3 coefficient on the bulk stress and deviator stress ratio resilient modulus model of foamed bitumen.

Meanwhile, an increase of the k4 coefficient from 0.06 to 0.2 results in a slight increase of the resilient modulus however, a scatter of the date points occurs as presented in Figure 5-17. In contrast, a decrease of the k4 coefficient to 0 results in a slight however tightly pack of the data points. The k4 coefficient indicates the sensitivity of the material to changes in the DSR. Where, a high k4 value means a slight increase in the resilient modulus paired

with reduced sensitivity to changes in the DSR. While, a low k4 coefficient indicates a slight decrease in the resilient modulus paired with an increase in the sensitivity of the material to changes of the DSR.

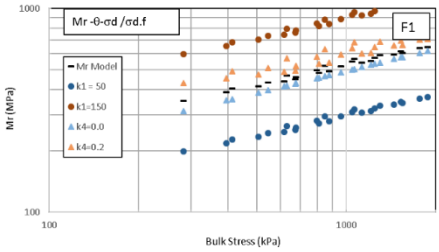

Figure 5-17: Influence k4 coefficient on the resilient modulus determined from the bulk stress and DSR model.

Mr-θ-σ1/σ1,f (k1, k2,k3,k4)

When the stress ratio of the Mr-θ-σd/σd,f model is replaced with the principal stress ratio (PSR), the k1 and k2 coefficients have the same effect as presented with all the previous models and it is illustrated in Figure 5-18. A high k1 coefficient results in a higher resilient modulus while, a high k2 coefficient results in a high resilient modulus with a higher rate of increase with the increase in the bulk stress. Conversely, an increase of the k3 coefficient from 0.403 to 0.6 presents a reduction of the resilient modulus with increases of the bulk stress as demonstrated in Figure 5-18. Whereas, a decrease of the k3 to 0.2 a slight increase of the slope of the resilient modulus model occurs therefore resulting in higher resilient modulus at high bulk stresses. A comparison of the k3 coefficient for bitumen emulsion and foamed bitumen obtained as 0 and 0.403 respectively, indicate foamed bitumen is influenced by the stress ratio.

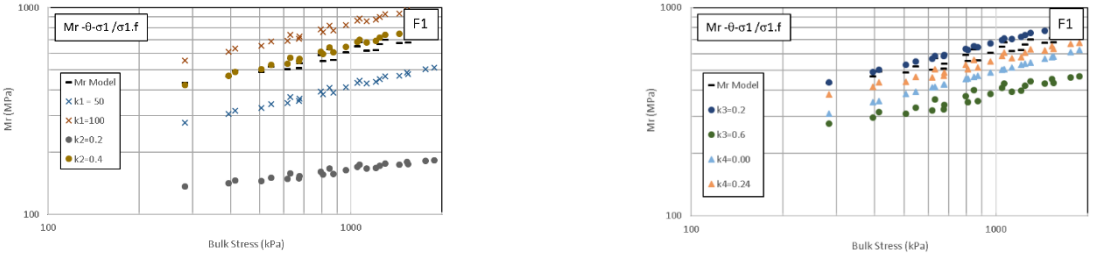

Figure 5-18: Influence of the k1, k2, k3 and k4 coefficients on the bulk stress and PSR resilient modulus model.

An analysis of the variation of the k4 coefficient indicates that a decrease from 0.14 to 0 or an increase from 0.14 to 0.24 results in a reduction of the resilient modulus. The bitumen emulsion presents a k4 coefficient of 0 which removes the influence of the stress ratio on the model. This is not accurate because the bitumen emulsion has been shown to be highly

stress dependent. On the other hand, the foamed bitumen model obtained a k4 coefficient of 0.14 which indicates a reduction occurs when the bulk stress and PSR increases. However, this contradicts previous finds of the stress dependency of the foamed bitumen specimen.

Mr-σ3-σ1/σ1,f

The replacement of the bulk stress in the previous model with the confinement stress presents no effect of the k3 and k4 coefficients on the resilient modulus as presented in Figure 5-19. While, the k1 and k2 have the same effect has observed from the previous model. This model does not describe the stress dependency of the resilient modulus obtained for both BSM_RCA mixes with regards the PSR as shown by the k3 of 0 obtained for both mixes.

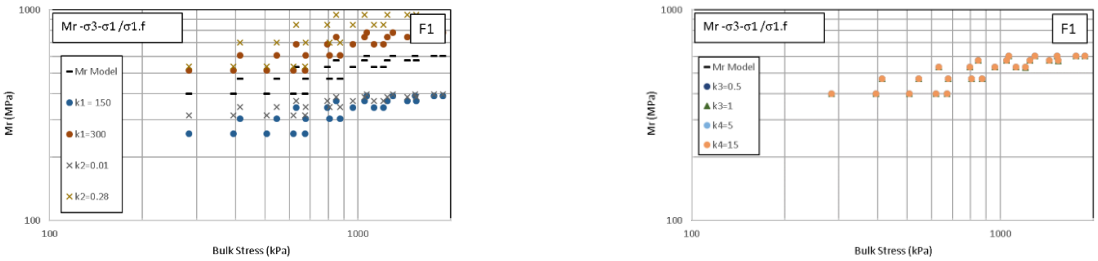

Figure 5-19: Influence of k1, k2,k3 and k4 coefficients on the resilient modulus model determined from the confinement stress and PSR.

5.2.4 Resilient Modulus Model Discussion

The discussion of the results obtained from the modelling of the measured resilient modulus for BSM_RCA with bitumen emulsion and foamed bitumen is done in this section. The aim is to conduct a comparison with results obtained for typical granular materials, mixed granulates, BSM of a mixed granulate and typical BSMs.

Mr-θ

For the resilient modulus determined from the bulk stress model, a comparison of the k1 and k2 coefficients obtained for the BSM_RCA with foamed bitumen and bitumen emulsion is done with a wide variety of aggregate mixes presented in Table 11 . This is due to the simplicity of the model that a large number of researchers previously used the model. The BSM_RCA achieved a higher resilient modulus relationship when compared to unbound aggregates such as mixed granulates composed with 70% RCA, 65%RCA, crushed stone and sand gravel as indicated in Table 11. This is based on the k1 coefficients of 8.96 obtained for the 70%RCA (Barisanga, 2014), 5.7 for 65%RCA (Van Niekerk, 2002), 49.7 for

crushed stone, 29.9 for the sand aggregate blend and 30.8 for sand gravel (Huang, 2003). These values indicated that 100% RCA stabilised with bitumen achieved a higher resilient modulus overall.

However, an analysis of the k2 coefficients of the same materials shows that the unbound aggregates are more sensitive to increases in the bulk stress. Meaning, the higher the bulk stress the higher the resilient modulus and the rate it increases. This observation is made from the k2 coefficients of 0.61, 0.626, 0.45, 0.59 and 0.53, respectively. These k2 coefficients are higher than the k2 coefficients obtained for BSM_RCA which indicate that the unbound aggregates are dependent on the bulk stress for stiffness at a higher degree than the BSM_RCA.

On the other hand, when a non-continuously bound mix is produced from crushed stone, RAP and mixed granulate with foamed bitumen a similar sensitivity to bulk stress is observed for BSM_RCA based on the k2 coefficients of the mixes presented in Table 11 (Ebels & Jenkins, 2007a; Jenkins, 2000; Saleh, 2000). However, the k1 coefficients ranges significantly, which illustrates that the resilient modulus of the mixes is primarily dependent on the type of aggregate used in the mix. The analysis indicates that BSM with RCA produces specimens that behave similarly to other BSMs. The Mr-θ model does not consider the influence of confinement stress and deviator stress separately. Therefore, other models derived from this model are analysed.

Table 11: Comparison of Mr – theta model coefficients obtained for other mixes

Mr-θ				
Mix Designs	**k1**	**k2**	**r^2**	**References**
BSM_RCA-E1	84.32	0.26	0.864	
BSM_RCA-F1	53.44	0.33	0.977	
70C:30M-100%DOC(70%RCA)	8.96	0.61	0.897	Barisanga (2014)
AL-65%RCA 4 day Curing	5.70	0.63	0.955	Van Niekerk (2002)
MGtud$_2$ (78%RCA,2% Fbitumen)	132.50	0.32	0.940	Saleh (2000)
G2van$_{1.5}$ (23% Hornfels and 77% RAP with 1.5% Foamed bitumen + 2% Cement)	48.00	0.33	0.860	Jenkins (2000)
75C-0 (75%Crushed stone and RAP with 3.6% Bitumen Emulsion)	132.79	0.36	0.940	Ebels (2008)
75C-0 (75%Crushed stone and RAP with 3.6% Foamed Bitumen)	134.34	0.30	0.750	
Crushed Stone	49.70	0.45		Huang (1993)
Sand-aggregate blend	29.90	0.59		
Sand-gravel	30.80	0.53		

Mr-σ3-σd and Parabolic Mr-σ3-σd

The confinement and deviator stress resilient modulus models describes the resilient modulus of a material holistically by incorporating the influence of the stress state in its separate components. The results are discussed based on a study conducted by Van Niekerk, (2002) on a mixed granulate with 65% RCA and 35% masonry presented in Table 12. BSM_RCA outperforms the mixed granulates based on the k1 coefficients which reflects the enhancement introduced by the low viscosity bitumen. Additionally, the bitumen has also reduced the degree of dependency of the aggregates on the confinement stress as highlighted by the lower k2 coefficients obtained for BSM_RCA. However, the k3 coefficient reveals the degree of influence of the deviator stress on the resilient modulus. This shows that the bitumen emulsion mix is dependent on the overall stress state within the specimen similarly to the unbound mix granulate which obtained a k3 coefficient of 0.24 and 0.27 respectively. Similar conclusions can be stated for both models (Mr-σ3-σd and Parabolic Mr-σ3-σd).

Table 12: Comparison of the model coefficients obtained for BSM_RCA and a mix granulate for the Mr-σ3-σd and Parabolic Mr-σ3-σd models

Mix designs	k1	k2	k3	k4	k5	r^2	References
Mr-σ3-σd							
BSM_RCA-E1	97.91	0.02	0.24			0.986	
BSM_RCA-F1	112.17	0.12	0.16			0.975	
AL-65%RCA 4 day Curing	11.83	0.38	0.27	-	-	0.984	Van Niekerk (2002)
Parabolic Mr-σ3-σd							
BSM_RCA-E1	203.46	0.09	1.49	2.21	1.00	0.963	
BSM_RCA-F1	147.45	0.17	0.00	0.78	1.35	0.962	
AL-65%RCA 4 day Curing	28.47	0.26	1.24	2.18	2.74	0.947	Van Niekerk (2002)

An analysis of the k4 coefficients obtained for the parabolic Mr-σ3-σd model highlights the degree of stress softening that occurs in the specimen as the DSR increases. A similar rate is obtained for the bitumen emulsion BSM_RCA (E1) and unbound mixed granulates of 2.21 and 2.18, respectively. This shows that BSM_RCA mix with bitumen emulsion behaves similarly to typical granular materials, which are dependent on the stress state for resilience. The excellent correlation of the data to both models indicate that the addition of the bitumen enhanced the performance properties of the RCA, produced a response that is understood and described by existing resilient modulus models.

Mr-θ-σd/σd,f and Mr-σ3-σd/σd,f

The resilient modulus determined from the bulk stress and DSR model has been used to model the resilient modulus for an unbound mixed granulate by Barisanga (2014) and Van Niekerk (2002) and a BSM mixed granulate by Saleh (2000). The k1 coefficients for BSM_RCA (84.3 and 89.48) indicate that a higher resilient modulus is obtained in comparison to the unbound mixed granulate (22.55 and 24.19) as presented in Table 13. Moreover, they are higher than the BSM with mixed granulate, where the k1 coefficient of 48MPa is achieved. This shows that 100% RCA is a stronger aggregate and benefits from the addition of low viscosity bitumen.

Table 13: Model coefficients obtained for BSM_RCA compared to those obtained for a mixed granulate and stabilised mixed granulate for the Mr-σ3-σd/σd,f and Mr-θ-σd/σd,f models.

Mix designs	k1	k2	k3	k4	r^2	References
Mr-θ-σd/σd.f						
BSM_RCA-E1	84.30	0.26	0.00	4.09	0.864	
BSM_RCA-F1	89.48	0.36	0.54	0.06	0.993	
AL-65%RCA 4-day Curing	22.55	0.43	0.87	5.14	0.948	Van Niekerk (2002)
70C:30M-100%DOC (70%RCA)	24.19	0.77	0.90	0.02	0.973	Barisanga (2014)
$MGtud_2$ (78%RCA,2% Fbitumen)	48.00	0.50	0.50	1.20	0.900	Sahel (2000)
Mr-σ3-σd/σd.f						
BSM_RCA-E1	307.43	0.10	0.00	10.94	0.379	
BSM_RCA-F1	233.27	0.18	0.00	11.77	0.801	

A high k2 coefficient indicates a higher sensitivity of a mix to changes in the bulk stress. Consequently, mixed granulates are highly influenced by an increase of the bulk stress illustrated by the high k2 coefficients of 0.43, 0.77 and 0.5 as presented in Table 13. In addition, the k3 coefficients indicate the degree of influence of the DSR on the resilient modulus. The higher the k3 coefficient, a lower resilient modulus is obtained as the bulk stress increases. On the other hand, a high k4 coefficient indicates the sensitivity of the material to changes of the DSR. Where, less sensitivity occurs for the BSM_RCA E1 and mixed granulate of 65%RCA. The model coefficients obtained for BSM with RCA show that the addition of bitumen improved the resilient response of the recycled aggregate in comparison to its unbound and mixed form. The confinement stress has no influence on the resilient modulus as seen from the k3 coefficient of 0 and the low correlation obtained for the measured data.

Mr-θ-σ1/σ1,f and Mr-σ3-σ1/σ1,f

The DSR replaced with the PSR produces similar outcomes as obtained from the DSR confinement or bulk stress resilient modulus model previously discussed. The Mr-σ3-σ1/σ1,f model has been used to model the resilient modulus for a BSMs with 77% RAP and G1 aggregates by Jenkins, (2000) and a BSM with mixed granulate by Saleh (2000). The model coefficients presented in Table 14, show that although G1 is tougher aggregate based on the density and other physical properties when stabilised with foamed bitumen it obtains a lower resilient modulus than 100% RCA. This is based on a comparison of the k1 coefficients of 307,43 for E1, 233.27 F1 and 125.4MPa obtained for $G1gau_2$. Interestingly, the BSM with mixed granulate ($MGtud_2$) obtained a higher k1 coefficient of 531.5 MPa which indicates a higher resilient modulus than all the other mixes presented in Table 14.

Table 14: Model coefficients obtained BSM_RCA compared to those obtained for typical BSM and mixed granulate BSM from Mr-θ-σ1/σ1,f and Mr-σ3-σ1/σ1,f models.

Mix designs	k1	k2	k3	k4	r^2	References
Mr-σ3-σ1/σ1.f						
BSM_RCA-E1	307.43	0.10	0.00	9.55	0.379	
BSM_RCA-F1	233.27	0.18	0.00	9.55	0.801	
$G2van_{1.5}$ (23% hornfels and 77% RAP with 1.5% Foamed bitumen + 2% Cement)	273.20	-0.04	-2.80	0.92	0.990	Jenkins (2000)
$G1gau_2$ (quartzite with 2% foamed bitumen)	125.4	0.139	-4.391	6.217	0.91	
$MGtud_2$ (78%RCA,2% Foamed bitumen)	531.50	0.04	-2.24	1.11	0.970	Sahel (2000)
Mr-θ-σ1/σ1.f						
BSM_RCA-E1	84.30	0.26	0.00	9.55	0.864	
BSM_RCA-F1	64.18	0.37	0.40	0.14	0.993	

The analysis of the k2 coefficient highlights the degree of influence the confinement stress (σ3) and bulk stress (θ) has on the resilient modulus. The k2 coefficients obtained for BSM_RCA with foamed bitumen of 0.18 and $G1gau_2$ of 0.139 indicates that these mixes are highly dependent on the confinement stress for stiffness. While, the $G2van_{1.5}$ and $MGtud_2$ obtained the lowest k2 coefficients of -0.04 and 0.04, respectively. Which highlights the low dependency on the confinement. An observation of the k3 coefficient, suggests no stress softening occurs for the BSM specimens tested at the stress states evident by the k3 coefficient of 0 for BSM_RCA, -2.8 for $G2van_{1.5}$, -4.391 for $G1gau_2$ and -2.24 for $MGtud_2$. Therefore, the BSM_RCA results agrees relatively well with results for typical BMSs and BSM with mixed granulates.

5.2.5 **Best fit models for BSM_RCA**

This section presents the resilient modulus model that best describes the stress dependency of BSM_RCA with bitumen emulsion and foamed bitumen. Two different models are selected based on the highest correlation coefficient, squared difference between the measured and calculated resilient modulus and physically accuracy. The two different models highlight the slight difference in behaviour of the RCA stabilised with bitumen emulsion and foamed bitumen under repeated loading. It should be noted that the other models presented in the chapter represented the results accurately. The final best-fit models are used to determine the pavement life (N) of the material conducted in Chapter 6.

Bitumen Emulsion

The parabolic confinement and deviator stress resilient modulus model (Parabolic Mr-σ3-σd) describes the stress dependency of the BSM_RCA mix with bitumen emulsion the best with a correlation coefficient of 0.963. This model also describes the behaviour of the mix correctly. This result is the same for the repeat specimen. Although the square of the difference between the measured and calculated resilient modulus is obtained as 3508, which is higher than the lowest of 1371 obtained from the Mr-σ3-σd model. The parabolic version of the model is physically correct as stated by Van Niekerk (2002) as it takes into account the influence of high DSRs which result to stress softening. The final model is presented by Equation 5-1.

$$Mr = 203.46\sigma_3^{0.09}(-1.494(\sigma d/\sigma d.f)^2+2.21(\sigma d/\sigma d.f)+1)$$

Equation 5-1

Foamed bitumen

The bulk stress and DSR resilient modulus model (Mr-θ-σd/σd.f) described the stress dependency of the foamed bitumen BSM_RCA accurately with a correlation coefficient of 0.993 obtained for both tested specimens. The model incorporates the influence the deviator stress thus it is physically accurate. The bulk stress dominates the resilient modulus obtained for foamed bitumen BSM_RCA and there is a linear relationship between the bulk stress and the resilient modulus. The bulk stress model with the principal stress ratio also describes the stress dependency of the resilient modulus in the same way. The final model with the coefficients is presented by Equation 5-2.

$$Mr = 89.48\theta^{0.36}(1-0.541(\sigma d/\sigma d.f)^{0.06})$$

Equation 5-2

5.3 Chapter Summary

The monotonic triaxial testing of BSM_RCA revealed that mixes produced from foamed bitumen and bitumen emulsion provide the same shear resistance. In addition, both mixes exceeded the minimum required 40^{o} internal angle of friction for a BSM 1. On the other hand, the cohesion achieved by both mixes fell in the BSM 2 range. Due to the self-cementation potential of RCA, the cohesion will increase. However, the study did not determine the curing period required to increase the cohesion. The retained cohesion of both mixes exceeded the specified 75% therefore both mixes are resistant to damage induced by moisture when soaked for 24 hours.

The BSM_RCA shear parameters were compared with those of an unbound RCA, stabilised CDW and a typical South African BSM. The evaluation shows that the BSM_RCA shear strength decreased in comparison to the shear parameters achieved by unbound RCA. This is attributed to the different grading, pH, maximum dry density and type of RCA. Furthermore, a comparison between the stabilised CDW (70%RCA and 30% masonry) showed that BSM_RCA requires a lower bitumen content and works perfectly with no active filler. Additionally, the comparison to the typical BSM produced with the TG2 indicates that the BSM_RCA to be similar in terms of shear strength. Therefore, based on the shear parameters there is potential in stabilising RCA with bitumen. However, the resilient modulus will provide a better understanding of the mix when subjected to dynamic repeated loading.

The resilient modulus for both foamed and bitumen emulsion mixes are stress dependent. This is evident from the increase in resilient modulus as the bulk stress increases. However, the stress dependency of these mixes is slightly different. For the foamed bitumen, a linear relationship is obtained while a non-linear relationship occurs for the bitumen emulsion. As a result, different models fitted the data obtained for each mix design to define the resilient modulus. The measured data was fitted to seven granular material resilient modulus models where the foamed bitumen data was described accurately by all the models. The correlation coefficients obtained ranging between 0.801 to 0.993. While, only five of the models fitted the bitumen emulsion measured resilient modulus. The BSM_RCA is a stress dependent mix, which is comparable to other typical BSMs.

Chapter 6: Pavement Design and Analysis

The structural capacity of a BSM with RCA is determined in this chapter as part of two types of typical flexible pavement structures that can be used for a Category B road in South Africa. This analysis aims to estimate how functional the mix design would be placed in the base layer of these various pavement systems. The chapter presents a brief overview of the different types of pavement design methods used in South Africa for the design of a flexible pavement. In addition, the transfer functions used to model the damage endured by each pavement layer are presented followed by the design process used to estimate the structural capacity. Furthermore, the iterative process used to determine the resilient modulus of the BSM_RCA is presented. Finally, the results of the analysis are presented and discussed.

6.1 Flexible Pavement Design Brief Literature Review

6.1.1 Overview of flexible pavement design

The design of a pavement structure aims to provide a balanced economical platform to protect the subgrade (Asphalt Academy, 2009). Different pavement structures and the types of layers are extensively discussed in Section 2-1. The design of a flexible pavement structure incorporates the holistic behaviour of each layer in the structure and the response to loading to determine the structural capacity of the pavement (SAPEM, 2014). The typical flexible pavement structures analysed in this chapter aim to determine the structural capacity of a BSM_RCA for use in a flexible pavement structure built in South Africa. There are eight methods (listed in Table 15) outlined in SAPEM Chapter 10 that can be used to evaluate the structural capacity of a flexible pavement structure. The design methods can be categorized as empirical (based on experience) or analytical empirical (combination of experience and material mechanics fundamentals) (Wirtgen Group, 2012).

Table 15: Types of flexible pavement design methods (SAPEM, 2014)

Flexible pavement design method	**Abbreviation**
1. South African mechanistic-empirical design method	SAMDM
2. Pavement number	PN
3. Dynamic cone penetratrometer	DCP
4. AASHTO structural Number	SN
5. FWD Deflection bowl parameter method	-
6. FWD structural number	SN
7. TRRL surface deflection	
8. Asphalt institute surface deflection	

The pavement number method specified in the TG2 is an example of an empirical design method due to the calibration conducted which incorporates the performance of BSMs built and currently in service in South Africa. However, for new materials such as BSM_RCA, an analytical and empirical method, based on the critical parameters of a layer, is required to determine the structural capacity of each layer. Consequently, the SAMDM method is the most appropriate method for the design of BSM_RCA as a new pavement material (SAPEM, 2014; Wirtgen Group, 2012). In addition, the SAMDM method allows for the consideration of the material properties obtained from laboratory tests and determines the stresses and strains induced in the material (SAPEM, 2014). Transfer functions developed for unbound, bound and non-continuously bound materials translate the static stresses and strains in the layer into damage accumulated from repeated traffic loading. This enables the pavement life to be estimated for a specific terminal condition (Theyse & Muthen, 1994). Therefore, the SAMDM method will be used for the design of the pavement structures analysed in this chapter.

6.1.2 **South African Mechanistic- Empirical Design method (SAMDM)**

The use of the SAMDM is an iterative process where a multilayer linear elastic analysis is conducted to determine the stresses and strains in each pavement layer (Long & Theyse, 2004). The main input components for the process include the pavement structure, material characteristics and loading conditions as outlined in Figure 6-1 (Theyse *et al.*, 1996). The loading conditions are composed of the tyre pressure, wheel configuration and climate conditions. Whereas, the material characteristics include the type of layer, layer thickness, resilient modulus and Poisson's ratio (Theyse & Muthen, 1994). Moreover, the outputs of

the analysis are stresses and strains at the critical positions for each type of layer which serve as input to the transfer function.

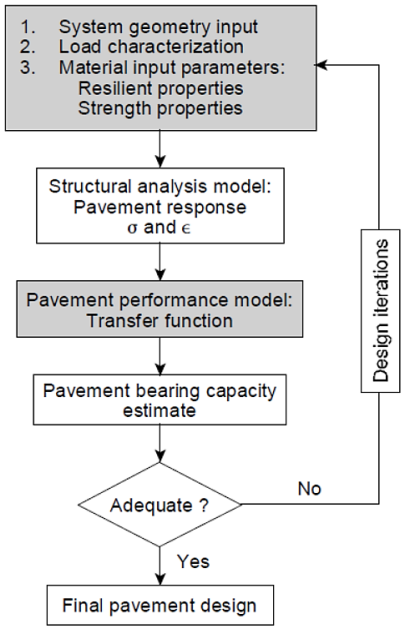

Figure 6-1: Iterative process for mechanistic-empirical design (Theyse & Muthen, 1994)

A transfer function, referred to as a damage model or failure criteria, estimates the structural capacity of a layer based on the critical parameter that is likely to induce failure in the layer (SAPEM, 2014). In essence, a transfer function is developed from the performance of the layer in service and takes into account material strength properties, the conditions where the layer will be constructed (wet or dry climate) and the road category (SAPEM, 2014). The critical parameters used in the transfer functions are determined at specified locations in each layer, as illustrated in Figure 6-2.

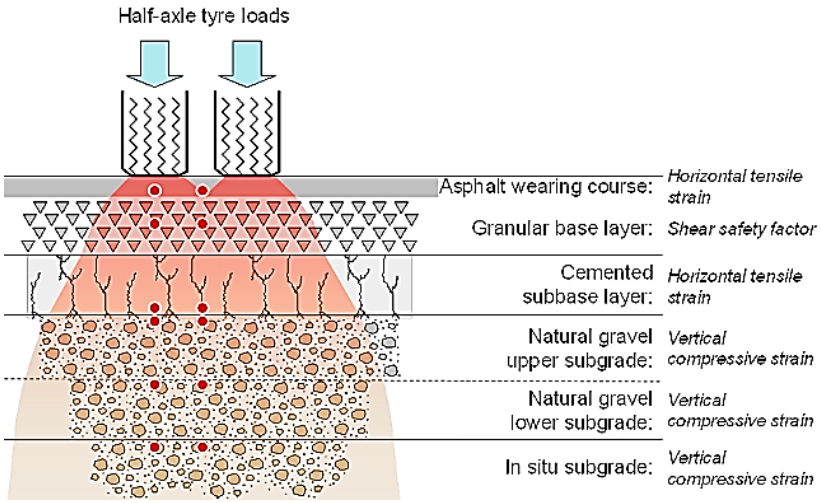

Figure 6-2: The critical parameters and locations for unbound and bound layers used in a flexible pavement structure. (SAPEM, 2014)

Unbound granular layers used in the base or subbase resist loading by shear stress. Hence, the critical parameter for such a layer is the stress state determined in the middle of the layer (Figure 6-2) defined by the principle (σ_1) and confinement stresses (σ_3). The transfer function used to determine the pavement life of an unbound granular layer is presented by

Equation 6-1. The transfer function is used to determine the pavement life of unbound granular materials with classifications ranging from G1 to G6 and equivalent granular materials from severely cracked cement-stabilised layers (EG4 to EG6). The shear parameters of the material are used to determine the stress ratio, F, an input for the transfer function. The F parameter considers weakening that occurs due to increased moisture with the K constant or the use of φterm and C term adjusted for increased moisture. The constants α and β consider the reliability of the design required for each road category and suggested values are obtained from SAPME Chapter 10.

$$N = 10^{\alpha F + \beta}$$

Equation 6-1

where

$$F = \frac{\sigma_3 \varphi_{term} + C_{term}}{(\sigma_1 - \sigma_3)} \text{ Or}$$

$$F = \frac{\sigma_3 (K\left(tan^2\left(45 + \frac{\varphi}{2}\right) - 1\right)) + 2KCtan(45 + \frac{\varphi}{2})}{(\sigma_1 - \sigma_3)}$$

- α and β constants for road category
- σ1 and σ3 = major and minor principle stresses
- φterm and C term
- C = cohesion (kPa)
- φ = angle of internal friction
- K= constant (0.65 saturated conditions, 0.8 moderate moisture conditions and 0.95 normal moisture conditions)

On the other hand, the subgrade failure mode is permanent deformation quantified by the vertical compressive strain (εv) determined at the top of the layer. The transfer function used to determine the pavement life of a subgrade layer is presented by Equation 6-2. The function requires two inputs namely: reliability constant “a” and the vertical compressive strain (εv) obtained from the multilayer analysis.

$$N_{PD} = 10^{(a-10log\varepsilon_v)}$$

Equation 6-2

where:

a = constant for road category given in SAPME Chapter 10

ε_v= vertical compressive stain

Bound layers such as asphalt and cement stabilised layers resist loading by bending. For that reason, the critical parameter for these layers is located at the bottom of the layer defined as the horizontal tensile strain (ε_t) as demonstrated in Figure 6-2. However, a cement stabilised layer is analysed in two phases. Therefore, two transfer functions are used for the pavement life analysis and the sum of the lives determines the pavement life of the cement stabilised layer. Phase 1 determines the pavement life that can be obtained as a result of bending of the layer evaluated with Equation 6-3.

$$N_{eff} = SF10^{c(1-\frac{\varepsilon}{d\varepsilon_b})}$$

Equation 6-3

where:

SF = shift factor for crack propagation

c, d = constants for road category

ε_t= horizontal tensile strain at bottom of layer (μstrain)

ε_b= stain at break

Phase 2 of the cement stabilised layer assumes extensive cracking of the layer has occurred. As a result, the layer is assumed to be an equivalent granular layer and it is analysed as a granular layer with Equation 6-1. When a cement stabilised layer is used in the subbase of the pavement structure, no crushing at the top of the layer is assumed due to the low stresses that occur in the subbase. Therefore, no crushing is analysed as guided by SAPME Chapter 10.

A BSM layer failure mode is permanent deformation, however due to its non-continuously bound nature the pavement life is determined differently from an unbound granular layer. The critical parameters are the stress state of the layer similar to those of an unbound granular layer. However, the critical position is located at a depth a quarter of the layer thickness measured from the top of the layer (Asphalt Academy unpublished, 2020). The pavement life of a BSM layer is determined with the recently developed Stellenbosch BSM

function presented by Equation 6-4. The transfer function assumes that 10mm of the total pavement rutting occurs in the base layer. The critical input parameters include the compaction density (Pmod) and the retained cohesion (RT) of the specimens measured in the laboratory. The Stellenbosch BSM function is slightly different from the Louden function currently operating in Rubicon.

$$N = 10^{(A-57.286(DSR)^3+0.0009159(Pmod.RetC)+0.86753}$$

Equation 6-4

where:

A - Constant for road category

: DSR – Deviator stress ratio

: Pmod - Density from Mod AASHTO (%)

: RetC – Retained Cohesion (%)

These transfer functions will be used in the pavement analysis of the BSM_RCA in different pavement structures.

6.2 Estimation of the Structural Capacity of a BSM_RCA layer

6.2.1 **Pavement structures, material properties and pavement life determination**

The structural capacity of the BSM_RCA will be compared to the structural capacity obtained for a reference pavement structure with a typical BSM produced in a study by Nwando (2013). Two types of typical flexible pavement structures referred to as pavement Structure A and pavement Structure B are analysed for a Category B road with a 10 mm seal surfacing. A Category B road is designed with a reliability of 90% and is expected to carry traffic that ranges between 0.3 to 10 million E80s over the design period (SAPEM, 2014). The loading conditions assume a standard 80 kN super single axle for a simplified analysis. Furthermore, a tyre pressure of 720 kPa is used based on the advancement of technology that allows high tyre pressures for trucks (Bredenkamp, 2018).

Pavement Structure A

In order to determine the response of the BSM supported by a relatively weaker subbase made with a G5, pavement Structure A is used. It is previously shown in Section 5.2 that BSM_RCA is a stress dependent material. Therefore, the stiffness of the layer will be dependent on the support provided by the supporting layer. Figure 6-3 presents the setup

and critical positions for the layers in pavement Structure A with BSM_RCA foamed bitumen (A) and bitumen emulsion (B). In addition, the figure presents the assumed input variables such as the Poisson's ratio and resilient modulus. The critical parameters for each layer are determined at the critical positions located directly under the wheel for a super single loading configuration. The critical position for the BSM_RCA is located at 47.5 mm which is a quarter of the layer thickness measured from the top of the pavement structure (Asphalt Academy unpublished, 2020). The Poisson's ratio for the G5 and G7 are used a 0.35 as indicated in Figure 6-3 (Theyse & Muthen, 1994). Furthermore, the Poisson's ratio for BSM_RCA is assumed as 0.35 as used for typical BSM layers (Jenkins *et al.*, 2000). The final resilient modulus presented in the figure is obtained from the resilient modulus iteration discussed in section 6.2.2.

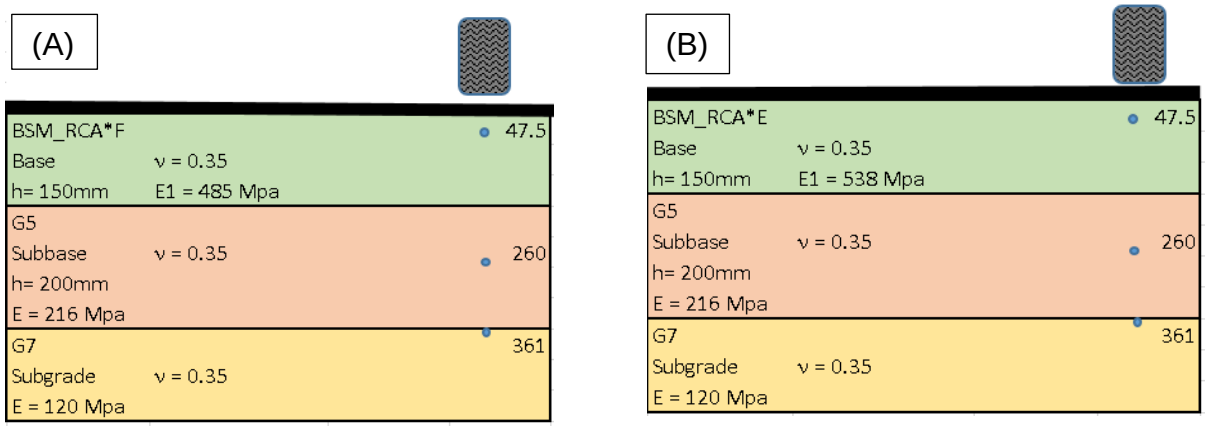

Figure 6-3: Pavement Structure A foamed bitumen (A) and bitumen emulsion (B).

The reference pavement Structure A determines the pavement life that can be obtained from a typical BSM stabilised with foamed bitumen and bitumen emulsion supported by a weak subbase. Figure 6-4 presents the setup of the reference pavement structure A, which includes the material properties and locations of the critical positions for each layer. The typical BSM is composed of 20% RAP and 80% dolerite (Nwando, 2013). Additionally, the BSM is stabilised with 2.4% bitumen content and 1% cement. The same assumptions made for Figure 6-3 are applicable for this pavement structure. The only difference is the material properties used as inputs for the transfer functions. No sublayers are used for the analysis of the resilient modulus due to the limit on the sublayer thickness as suggested by the unpublished TG2. This is further discussed in Section 6.2.2.

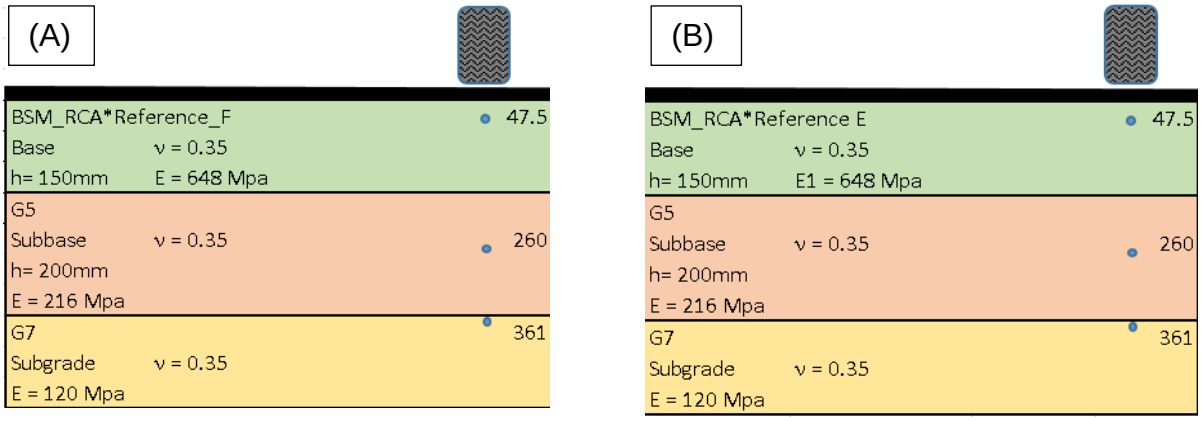

Figure 6-4: Reference pavement Structure A foamed bitumen (A) and bitumen emulsion (B)

The lowest pavement life dictates the overall pavement life for each of the four pavement structures presented in Figure 6-3 and Figure 6-4. The inputs for the BSM transfer function are obtained from laboratory test results, which include the relative density obtained from the MOD ASSTHO and the retained cohesion. For the BSM with RCA, the density is used as a 100% and the retained cohesion was obtained as 90% for the foamed bitumen and 88.2% for the bitumen emulsion mix. For the typical BSM in the reference pavement structure, the relative density was obtained as 99.7% for the foamed bitumen and 98.6% for bitumen emulsion mixes (Nwando, 2013). The retained cohesion was not analysed from the typical BSM therefore based on the dry and wet ITS of the mixes a retained cohesion is assumed as 75% (Asphalt Academy unpublished, 2020). The shear parameters for each mix used to determine the deviator stress ratio are presented in Table 16.

Table 16: Shear parameters for BSM mix designs

BSM Mix/Variable	**Internal angle of friction (º)**	**Cohesion (kPa)**
BSM_RCA_Foam	50.4	177
BSM_RCA_Emulsion	47.9	174
BSM_RAP+Dolerite_Foam	19.9	495.8
BSM_RAP+Dolerite_Emulsion	28	392.8

The pavement life for the G5 layer is determined from Equation 6-1 with the principle stress ($\sigma 1$) and confinement stress ($\sigma 3$) as the critical inputs parameters. The climate conditions analysed include the dry, moderate and wet conditions with input variables for φterm and Cterm presented in Table 17 (SAPEM, 2014). Furthermore, the constants that considers the road category are obtained as $\alpha = 2.6$ and $\beta=3.7$ (SAPME, 2012). The pavement life of the

subgrade is determined from the vertical compressive strain and a constant a = 36.38 for a Category B road.

Table 17: G5 transfer function input variables

Variable/Material-Climate	Wet	Moderate	Dry
φterm	3.6	3.3	3.2
Cterm	143	115	83

Pavement Structure B

The pavement life of the BSM layers supported by a relatively stiffer support is analysed from pavement Structure B with a subbase made from a cement-stabilised material. Due to the stress dependency of a BSM layer, a stiffer support would increase the life of the layer. The pavement structures used for the analysis are presented in Figure 6-5 and Figure 6-6. Moreover, the Poisson's ratio, resilient modulus and positions of the critical parameters for each layer are indicated on the figures. The critical positions, material inputs and assumptions for the BSM and G7 subgrade are the same as discussed for pavement Structure A. The cement stabilised layer is assumed to have a Poisson's ratio of 0.35 as suggested by Theyse *et al.* (1996). The critical parameter for Phase 1 of the pavement analysis for the C3 subbase is the horizontal tensile strain. This parameter is measured at the bottom of the layer at a depth of 360 mm in the pavement structure as indicated on Figure 6-5. While, the critical parameter for the Phase 2 pavement life analysis is determined at the middle of the layer as done for unbound granular layers located at a depth of 260 mm in the pavement structure.

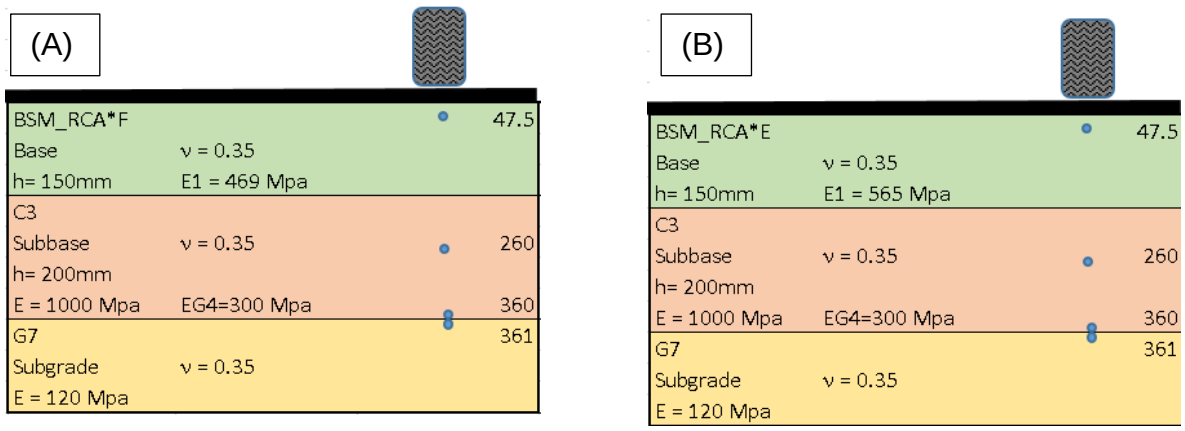

Figure 6-5: Pavement Structure B with foamed bitumen (A) and bitumen emulsion (B)

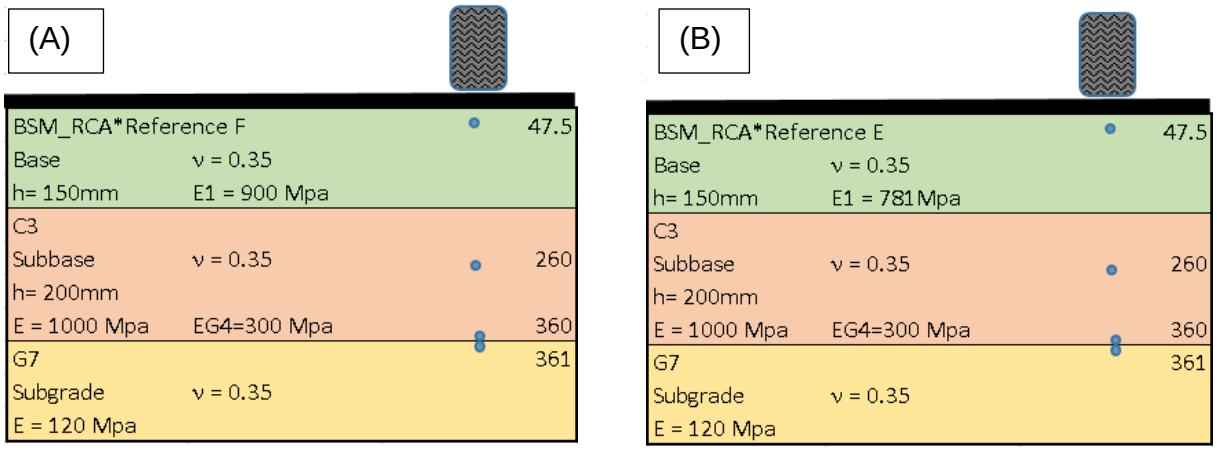

Figure 6-6: Reference pavement Structure B with foamed bitumen (A) and bitumen emulsion (B)

Due to no laboratory results for the C3 mix, a suggested unconfined compressive strength (UCS) of 2250 kPa is used for the pavement life analysis (SAPME, Chapter 10). Similarly, with the strain at break, a recommended value of 125 microstrain is used for the design of the C3 layer. The other input variables for the Phase 1 transfer function given by Equation 6-3 are obtained from SAPME Chapter 10 presented in Table 18. On the other hand, in Phase 2, the pavement life analysis considers the layer as an equivalent granular layer (EG4) and Equation 6-1 is used with the input parameters presented in Table 19.

Table 18: Input variables for Phase one pavement analysis for C3 subbase

SF =	1.9
c=	6.8
d=	7.6
εb=	125.0
t	200.0

Table 19: EG4 transfer function input variables

Variable/Material-Climate	Wet	Moderate	Dry
φterm	4.0	3.5	3.1
Cterm	140.0	120.0	100.0

6.2.2 **Resilient modulus iteration**

The resilient modulus is another critical input parameter into the mechanistic empirical design method. This parameter indicates the stiffness that can be reached by a specific layer depending on the supporting layer. Therefore, the resilient modulus of the stress dependent layers differs in each pavement structure analysed. The stiffness indicates the load spreading ability of the layers with the aim to reduce the stresses and strains in the

subgrade. Since BSM_RCA has been shown to be a stress dependent layer, the resilient modulus is therefore dependent on the supporting layer. BSM_RCA is a relatively new material and two different resilient modulus models as presented in Section 5.2.5 describes the resilient modulus of the mixes with foamed bitumen and bitumen emulsion. Therefore, the final resilient modulus that serves as input in each pavement structure is determined in an iterative process.

There are three methods used to evaluate the final resilient modulus for each BSM mix design namely; resilient modulus models, modular ratio and maximum stiffness limit. The use of the resilient modulus models is iterative. The process requires the calculation of the principal and confinement stresses that occur in the layer with the multilayer linear elastic analysis of pavement Structure A and B. The stresses are used as inputs into the models presented in Table 20 to determine the resilient modulus for each BSM mix design. Subsequently, the resilient modulus calculated from the model is used as input into the multilayer analysis and new stresses and strains are calculate. Once the resilient modulus converges and no change occurs it is compared to the maximum resilient modulus that can be provided by the layer depending on the supporting layer and the resilient modulus obtained from the modular ratio (Asphalt Academy unpublished, 2020).

Table 20: Resilient modulus models for the BSM mixes

BSM Mix	**Model**	**k1**	**k2**	**k3**	**k4**	**K5**
BSM_RCA_Foam	$Mr = k1\theta^{k2}(1-k3(\sigma d/\sigma d,f)^{k4}$	89.48	0.36	0.54	0.06	-
BSM_RCA_Emulsion	$Mr = k1\sigma_3^{k2}(-k3(\sigma_{d/}\ \sigma_{d,f})^2+k4(\sigma_d/\ \sigma_{d,f})+k5$	203.46	0.09	1.494	2.21	1
BSM_RAP+Dolerite_Foam	$Mr = k1\theta^{k2}$	199.59	0.21	-	-	-
BSM_RAP+Dolerite_Emulsion	$Mr = k1\theta^{k2}$	71.18	0.33	-	-	-

All the BSM mix designs exceed the specified BSM 1 requirements therefore, the maximum resilient modulus that can be achieved by the mixes is specified as 1200 MPa if the subbase is a cement-stabilised layer. While, in the case the layer is supported by an unbound granular subbase layer the maximum stiffness is recommended as 1000 MPa (Asphalt Academy unpublished, 2020). Furthermore, the modular ratio aims to limit the resilient modulus of a layer based on the stiffness of the supporting layer. As a result, the modular ratio is the ratio between the stiffness of the top layer and the bottom layer (Asphalt Academy, 2009). In the case of a BSM in the base, the modular ratio is specified as a maximum of 3 which will be used to determine the maximum stiffness that can be achieved by the BSM given the stiffness of the subbase (Asphalt Academy, 2009). The modular ratio is not applicable when

a cement-stabilised layer is used due to the high stiffness achieved by the layer. No sublayers are used in the analysis of a BSM due to the discrepancy that occurs with BSM layer thickness less than 100 mm which produce unrealistic results (Asphalt Academy unpublished, 2020). In addition, the second sublayer attracts a large amount of stress, which results in premature failure based on the analysis. As a result, for BSM analysis with sublayers requires a minimum sublayer thickness of 100 mm.

The final comparison of the resilient modulus indicates that the stresses in the BSM_RCA result in a resilient modulus lower than the resilient modulus determined from the modular ratio and the maximum stiffness limit set for BSMs depending on the supporting subbase. This is true for both pavement Structure A and pavement Structure B as presented in Table 21. Whereas, with the typical BSMs in pavement Structure A the resilient modulus obtained from the modular ratio dictates the final resilient modulus as highlighted in Table 21. In addition, the typical BSMs in pavement Structure A can resist higher stresses and strains than the BSM_RCA therefore the models assume high stiffnesses. While in pavement Structure B, the resilient modulus for the typical BSMs used for the pavement analysis are obtained from the models which are less than the maximum specified resilient modulus for a BSM 1 supported by a cement stabilised subbase. The final resilient moduli used to determine the pavement life for each BSM layer are highlighted in Table 21. This exercise is important for the determination of a realistic resilient modulus for the analysis of the pavement life of a BSM layer in a specific pavement structure.

Table 21: The resilient modulus obtained for pavement Structure A and pavement Structure B for each BSM mix design analysed.

BSM Mix_Pavement Structure	**Mr_Modular ratio (MPa)**	**Mr_Maximum stiffness (MPa)**	**Mr_Model (MPa)**
BSM_RCA_Foam_A	648	1000	484.8
BSM_RCA_Foam_B	-	1200	468.8
BSM_RCA_Emulsion_A	648	1000	538.2
BSM_RCA_Emulsion_B	-	1200	564.7
BSM_RAP+Dolerite_Foam_A	648	1000	927.4
BSM_RAP+Dolerite_Foam_B	-	1200	900
BSM_RAP+Dolerite_Emulsion_A	648	1000	791.3
BSM_RAP+Dolerite_Emulsion_B	-	1200	781.4

The typical BSMs achieved higher stiffness due to the high cohesion resulting from the 1% cement. However, an interesting observation is made regarding the anticipated increase of the stiffness of the BSM mixes when constructed on a stiff subbase. Only the BSM_RCA with bitumen emulsion increases slightly while all the other mixes stiffnesses slightly decreases when built on a stiff subbase. This can be attributed to the increase in the stresses in the base as an increase in the stiffness distribution or loading spreading of the pavement structure occurs with a stiffer subbase.

6.3 Pavement Life Results and Discussion

This section presents the stress and strain distribution in pavement Structure A and pavement Structure B as obtained from MEPADs. Followed by a presentation of the pavement life obtained for each pavement structure with the different BSM mixes in the base layer. Thereafter, a comparison of the pavement life obtained for each BSM mix is done. Finally, an overall comparison of the pavement life obtained for the base, subbase and subgrade for each type of pavement structure is analysed.

6.3.1 Stress and strain distribution in the pavement structures

The inverted pavement structure with a reducing stiffness from the top to the bottom aims to reduce the stresses and strains resisted by the subgrade. Hence, the stresses and strains distributions in the pavement structures show how the applied load induces stresses and strains at different locations in the pavement. The stress and strain distributions also show how the different BSM base layers influence the stresses in the supporting layers.

Pavement Structure A

In pavement Structure A, a weak subbase layer supports the base. The BSM bases distribute the horizontal and vertical stresses in a similar manner as illustrated in Figure 6-7. The vertical compressive stress (σ_v) is maximum at the top of the layer at the applied 720 kPa tyre pressure and reduces to 80 kPa at the top of the subgrade. While, the horizontal compressive stress (σ_h) is a maximum at the top and a parabolic reduction occurs into the pavement structure. Furthermore, tensile stresses occur in the subbase; however, this is an error made by the linear analysis program. The base layers provide the same stress distribution in the layer horizontally and vertically.

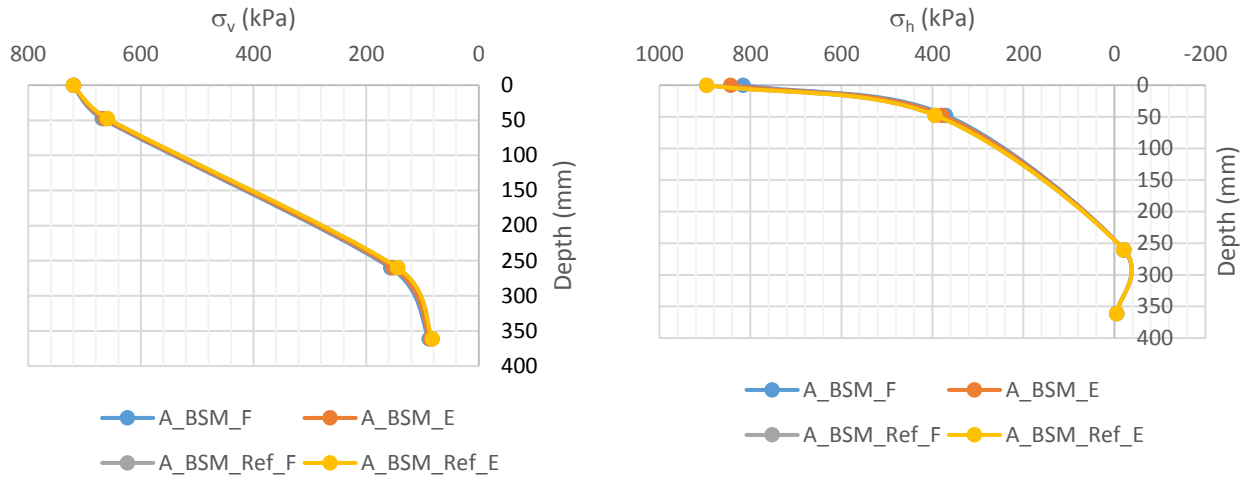

Figure 6-7: Vertical and horizontal Stress distributions in pavement Structure A

On the other hand, a slight difference is observed for the vertical and horizontal strains distributions in pavement Structure A as illustrated in Figure 6-8. The highest vertical compressive strain (ε_v) of 880 micro strain occurs in the BSM_RCA base with foamed bitumen (BSM_F). This is attributed to the lower stiffness of 484 MPa in comparison to the other BSM mixes. However, the vertical compressive strain distribution in the reference structures is the same for both mix designs with foamed bitumen and bitumen emulsion due to the same stiffness of 648 MPa used for the analysis as highlighted in Table 21. The vertical compressive strain is an important parameter for the subgrade pavement life. Therefore, the distribution indicates that the higher the stiffness the better the distribution of the strain in the pavement structure. All the BSM base layers reduce the vertical compressive strain in the subgrade significantly as illustrated Figure 6-8.

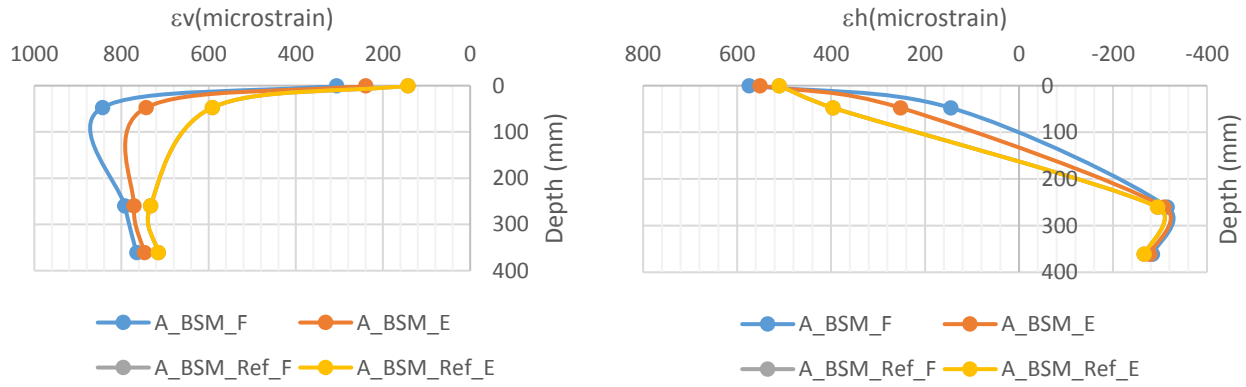

Figure 6-8: Vertical and horizontal strain distribution in pavement Structure A

The horizontal compressive strain (ε_h) in the pavement structures decreases from the maximum at the top of the layer to a tensile strain at the top of the subgrade as demonstrated

in Figure 6-8. Moreover, slightly different rates of reduction can be observed, were a linear reduction occurs for the high stiffness reference BSM layers and a parabolic reduction occurs for the BSM_RCA mixes. Therefore, higher horizontal strains are induced in the supporting layers of the BSM_RCA.

Pavement Structure B

In pavement Structure B, a stiffer support is provided for the BSM base layers. However, a similar vertical and horizontal stress distribution occurs for all the pavement structures as presented in Figure 6-9. Therefore, the stress distribution is not influenced by the different BSM mix designs as the mixes provide similar distributions of the stresses in the pavement structure.

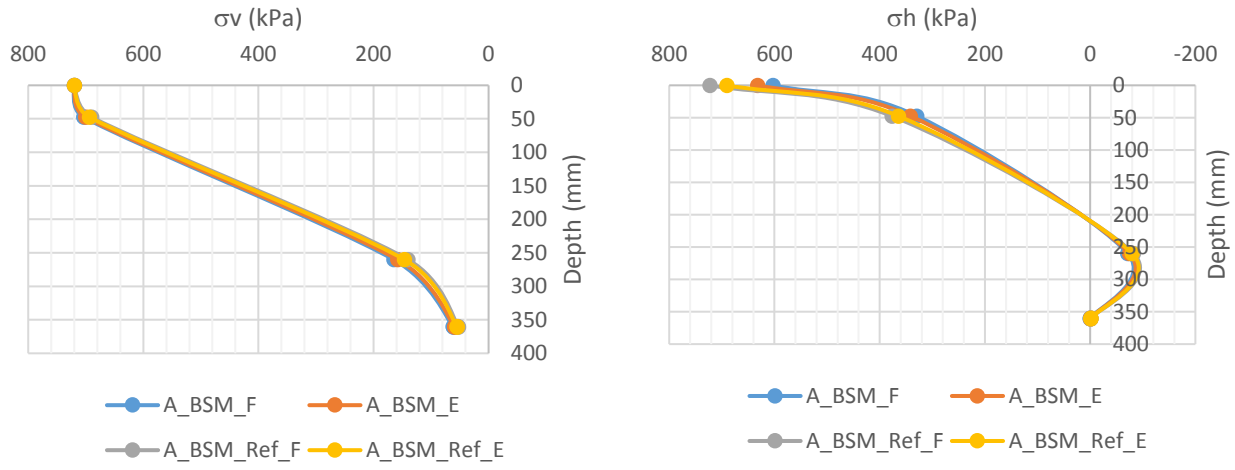

Figure 6-9: Vertical and horizontal stress distribution in pavement Structure B

The vertical and horizontal strain distribution in pavement Structure B is presented in Figure 6-10. The majority of the vertical compressive strain (ε_v) is induced in the base layers and varies due to the difference in the stiffness of the base layers. However, a similar vertical compressive strain occurs at the top of the subgrade, which is used to determine the pavement life of the layer. On the other hand, the distribution of the horizontal strain differs between the BSM_RCA base and the typical BSM mix. Large compressive horizontal strains occur in the reference base layers. While, tensile horizontal strains occur in the BSM_RCA base layers. Therefore, the stiff subbase results to a slightly different distribution of the horizontal strain in the pavement structure.

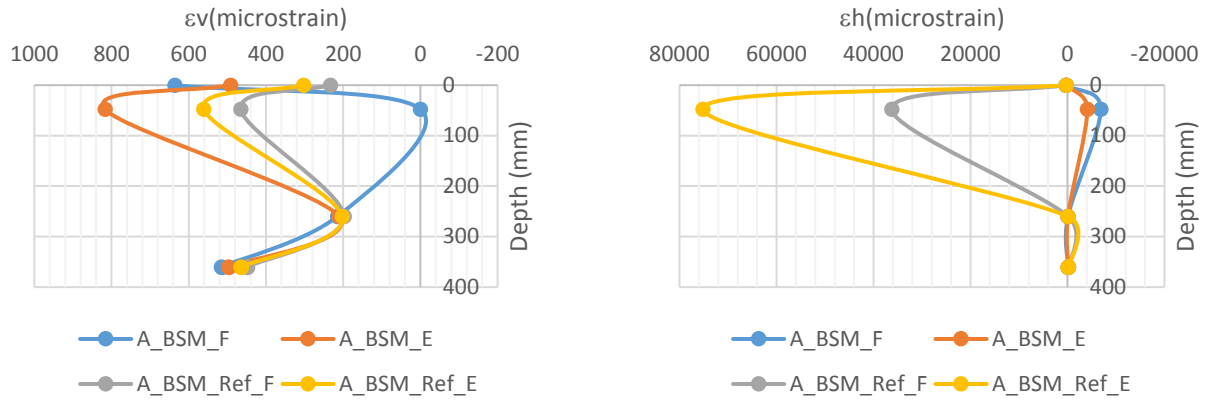

Figure 6-10: Vertical and horizontal strain distribution in pavement Structure B

6.3.2 **Pavement Structure analysis**

This section presents the critical parameters obtained for each pavement layer in pavement Structure A and B with a base layer from the varying BSM mix designs. The pavement life obtained for each layer in each pavement structure is presented. The minimum pavement life for a Category B road is 300000 E80s therefore that is the lowest required pavement life.

The pavement analysis for pavement Structure A with a base made from BSM_RCA stabilised with foamed bitumen resulted in the G5 subbase as the weakest layer as highlighted in Table 22. A summary of the critical parameters obtained for each layer are presented in Table 22 with the layer thicknesses and final resilient modulus used for the design. In a wet climate, the G5 subbase layer can carry 84500 E80s, which is lower than the required 300 000. However, if the pavement structure is built for a dry climate the layer can support 644 000 E80s. To improve the performance of the pavement structure a thicker base of 200 mm can be constructed, or an improvement of the subgrade can be done. Pavement Structure A is not a well-balanced pavement hence the failure of the subbase layer in wet climates.

Table 22: Pavement lives obtained for pavement Structure A with BSM_RCA foamed bitumen

Pavement Structure A_BSM_F						
Layer	**Mr**	**Thickness**	**Critical parameter**	**Pavement life**		
				Dry	**Moderate**	**Wet**
Base - BSM_RCA*F	485	150	σ1 = 669 (kPa) σ3 = 371 (kPa)	2,81E+08		
Subbase - G5	216	200	σ1 = 177 (kPa) σ3 = 0 (kPa)	6,44E+05	2,50E+05	8,45E+04
Subgrade -G7	120	-	ev = 765.4 (με)	3,48E+07		

An improved subbase to C3 analysed for pavement Structure B with a base constructed from a BSM_RCA stabilised with foamed bitumen, the pavement life is obtained as 7 620 000 E80s for the base as presented in Table 23. Therefore, an improvement of the subbase results in a pavement structure deemed suitable for a Category B road. As a result, there is benefit to a stiffer subbase even though there is no increase in the resilient modulus of the base layer. However, in comparison to pavement Structure A, the pavement life for the base layer reduced due to the increase of the critical parameters. This means that an increase of the stiffness distribution in the pavement structure results in increased stresses in the base layer.

Table 23: Pavement lives obtained for pavement Structure B with BSM_RCA foamed bitumen

Pavement Structure B_BSM_F						
Layer	**Mr**	**Thickness**	**Critical parameter**	**Pavement life**		
				Dry	**Moderate**	**Wet**
Base - BSM_RCA*F	469	150	σ1 =704 (kPa) σ3 = 329 (kPa)	7,62E+06		
Subbase - C3	1000		eh = 182 (με)	6,53E+05		
Subbase - EG4	300	200	σ1 = 193 (kPa) σ3 = 0 (kPa)	1,65E+08 1,65E+08	1,05E+08 1,05E+08	6,70E+07 6,70E+07
Subgrade -G7	120	-	ev = 765.4 (με)	1,85E+09		

Due to the slightly different response to loading obtained for a BSM_RCA stabilised with foamed bitumen or bitumen emulsions, separate pavement analysis are conducted. The pavement life for pavement Structure A with a bitumen emulsion BSM_RCA is obtained as 91000 E80s as presented in Table 24. Therefore, the use of the pavement structure in a wet climate is not suitable for a Category B road that requires a minimum of 300 000 E80s.This result is similar to that obtained for the pavement Structure A with foamed bitumen BSM_RCA. This is an interesting outcome considering the significantly higher stiffness obtained for the BSM_RCA_E of 539 MPa presented in Table 24. Furthermore, the BSM_RCA_F base layer achieves a pavement life of 281 million E80s compared to the 114 million E80s achieved by the BSM_RCA_E. However, the higher stiffness BSM_RCA_E protects the subgrade better with a reduced vertical strain of 747.8 micro stain from 765.5 micro strain. This difference increased the life of the subgrade from 34.8 million E80s to 43.9 million E80s. Therefore, there is a slight benefit obtained from stabilisation of RCA with bitumen emulsion over foamed bitumen.

Table 24: Pavement lives obtained for pavement Structure A with BSM_RCA bitumen emulsion

Pavement Structure A_BSM_E						
Layer	**Mr**	**Thickness**	**Critical parameter**	**Pavement life**		
				Dry	**Moderate**	**Wet**
Base - BSM_RCA*E	538	150	σ1 = 666 (kPa) σ3 = 379 (kPa)	1,14E+08		
Subbase - G5	216	200	σ1 = 173 (kPa) σ3 = 0 (kPa)	7,31E+05	2,76E+05	9,10E+04
Subgrade -G7	120	-	ev = 747.8 (με)	4,39E+07		

The improvement of the subbase from G5 to a C3 cement stabilised layer has the same effect on the pavement life of pavement Structure B with a bitumen emulsion stabilised RCA base as presented in Table 25. The pavement life is obtained as 1.97 million E80s, which exceeds the minimum pavement life required for a Category B road. The pavement life is significantly lower than the 7.62 million E80s that can be supported by the foamed bitumen RCA base. This is an unexpected outcome however it is a result of the higher shear parameters of the foamed bitumen RCA BSM mix design.

Table 25: Pavement lives obtained for pavement Structure B with BSM_RCA bitumen emulsion

Pavement Structure B_BSM_E						
Layer	**Mr**	**Thickness**	**Critical parameter**	**Pavement life**		
				Dry	**Moderate**	**Wet**
Base - BSM_RCA*F	565	150	σ1 = 700 (kPa) σ3 = 342 (kPa)	1,97E+06		
Subbase - C3	1000	200	eh = 176 (με)	7,12E+05		
Subbase - EG4	300		σ1 = 185 (kPa) σ3 = 0 (kPa)	1,86E+08 1,86E+08	1,16E+08 1,17E+08	7,25E+07 7,32E+07
Subgrade -G7	120	-	ev = 495.9 (με)	2,67E+09		

The reference pavement Structure A with a base layer constructed with a typical BSM obtained a pavement life of 105000 E80s as presented in Table 26. The pavement life is also dictated by the G5 subbase built for wet climates. Therefore, this pavement structure is not suitable for a Category B road as obtained with the base layer from stabilised RCA. The table presents the final resilient modulus, layer thickness and critical parameters for each pavement layer. The pavement structure is however, suitable if built for a dry or moderate climate Category B road.

Table 26: Pavement lives obtained for reference pavement Structure A with BSM_RAP and Dolerite foamed bitumen

Pavement Structure A_BSM_Reference F						
Layer	**Mr**	**Thickness**	**Critical parameter**	**Pavement life**		
				Dry	**Moderate**	**Wet**
Base - BSM_RCA*F	648	150	σ1 = 660 (kPa) σ3 = 395 (kPa)	1,86E+08		
Subbase - G5	216	200	σ1 = 165 (kPa) σ3 = 0 (kPa)	9,38E+05	3,38E+05	1,05E+05
Subgrade -G7	120	-	ev = 716 (με)	6,77E+07		

Interestingly, with an improved subbase the pavement life for pavement Structure B with a typical BSM is dictated by the subbase built for wet climates as presented in Table 27. A pavement life of 97.4 million E80s is obtained as the lowest pavement life. This outcome is surprisingly different from the BSM with RCA pavement structures with an improved subbase. The minimum pavement life exceeds the required pavement life for a Category B road. This performance is attributed to the 2.4% bitumen content and 1% cement in the BSM mix which results in higher cohesion values used in the transfer function.

Table 27: Pavement lives obtained for reference pavement Structure B with BSM_RAP and Dolerite foamed bitumen

Pavement Structure B_BSM_Reference F						
Layer	**Mr**	**Thickness**	**Critical parameter**	**Pavement life**		
				Dry	**Moderate**	**Wet**
Base - BSM_RCA*F	920	150	σ1 = 690 (kPa) σ3 = 377 (kPa)	1,06E+08		
Subbase - C3	1000	200	eh = 162 (με)	9,00E+05		
Subbase - EG4	300		σ1 = 165 (kPa)	2,81E+08	1,65E+08	9,74E+07
			σ3 = 0 (kPa)	2,81E+08	1,66E+08	9,83E+07
Subgrade -G7	120	-	ev = 447.6 (με)	7,43E+09		

In the case the typical BSM is stabilised with bitumen emulsion and the base is supported by a G5 subbase, a similar pavement life as obtained for the typical BSM with foamed bitumen as presented in Table 28. The pavement life is obtained as 105 000 E80s similarly to that of the foamed bitumen mix design. This outcome is a result of the same stiffness used for the base layer as obtained from the resilient modulus analysis. Therefore, the exact same stress distribution occurs in the pavement Structure. A slight difference is obtained for the individual pavement lives for the base layers due to the different shear parameters.

Table 28: Pavement lives obtained for reference pavement Structure A with BSM_RAP and Dolerite bitumen emulsion

Pavement Structure A_BSM_Reference E						
Layer	**Mr**	**Thickness**	**Critical parameter**	**Pavement life**		
				Dry	**Moderate**	**Wet**
Base - BSM_RCA*Ref E	648	150	σ1 = 660 (kPa) σ3 = 395 (kPa)	1,24E+08		
Subbase - G5	216	200	σ1 = 165 (kPa) σ3 = 0 (kPa)	9,38E+05	3,38E+05	1,05E+05
Subgrade -G7	120	-	ev = 716 (με)	6,77E+07		

However, an improved subbase results to the pavement life dictated by the base layer with bitumen emulsion as indicated in Table 29. The pavement life is obtained as 45.4 million E80s for the pavement Structure B with a stiff subbase. This outcome is attributed to the high stress state in the base as a result of the high stiffness based on the distribution into the pavement structure. The pavement structure is suitable for use in a Category B road.

Table 29: Pavement lives obtained for reference pavement Structure B with BSM_RAP and Dolerite bitumen emulsion

Pavement Structure B_BSM_Reference E						
Layer	**Mr**	**Thickness**	**Critical parameter**	**Pavement life**		
				Dry	**Moderate**	**Wet**
Base - BSM_RCA*F	781	150	σ1 = 694 (kPa) σ3 = 365 (kPa)	4,54E+07		
Subbase - C3	1000	200	eh = 167 (με)	8,33E+05		
Subbase - EG4	300		σ1 = 172 (kPa)	2,40E+08	1,45E+08	8,73E+07
			σ3 = 0 (kPa)	2,41E+08	1,46E+08	8,81E+07
Subgrade -G7	120	-	ev = 463.4 (με)	5,25E+09		

6.3.3 **Base layer pavement life comparison**

All the BSM base layers achieve a pavement life that is suitable for a Category B road as presented in Figure 6-11. The base layer with the highest life is surprisingly obtained from pavement Structure A RCA stabilised with foamed bitumen. A pavement life of 281 million ESALs is determined at a DSR of 30%. This is interesting because the layer provided the lowest resilient modulus. However, the mix has the highest shear parameters therefore has a higher shear strength. The weakest base was obtained from pavement Structure B with RCA stabilised with bitumen emulsion. This is due to the high stresses attracted to the layer as displayed by the highest DSR of 40%. Therefore, the higher the DSR the shorter the pavement life of a BSM. However, shear parameters also influence the pavement life

obtained for the layer. The BSM_RCA base layers are comparable to the typical BSMs. The pavement life can be improved with a reduction of the DSR. Furthermore, the DSR can be improved with either increased bitumen content, addition of cement or thicker pavement layer.

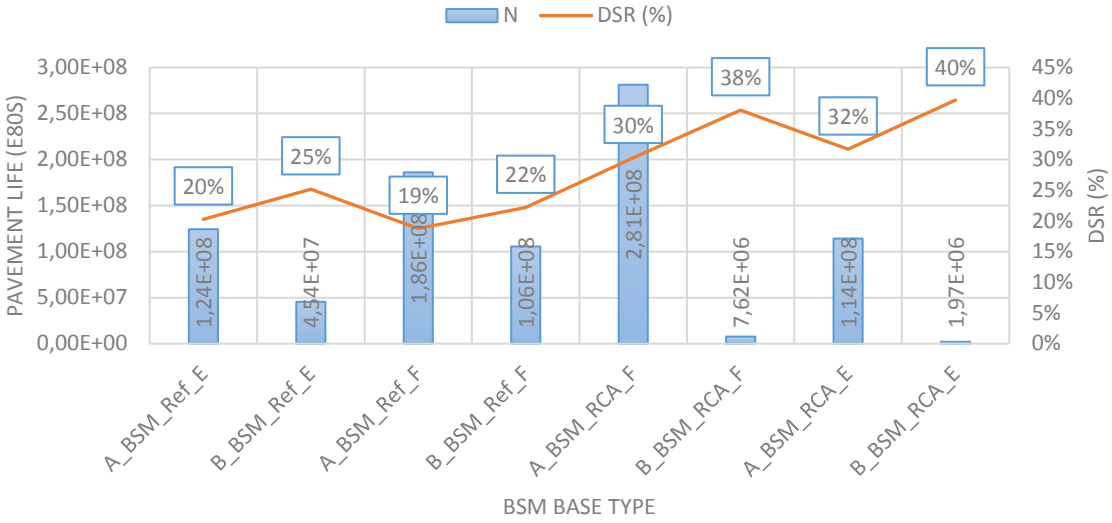

Figure 6-11: Pavement lives obtained for BSM_RCA_F, BSM_RCA_E, BSM_Ref_F and BSM_Ref_E

6.3.4 **Overall pavement life comparison**

Pavement A

The overall performance of the four different pavement structures with a G5 subbase indicates that the subbase is the weakest layer in Figure 6-12. The foamed bitumen BSM bases both with RCA and 20% RAP and dolerite outperform the bitumen emulsion counterparts. This is due to the difference in the coating provided by the types of bitumen stabilisation agents. The spot welds observed from foamed bitumen mixes result to higher shear parameters as presented in Table 16. In addition, the high shear parameters provide a higher shear strength from the same aggregates. The reference BSM base provide a better protection of the subgrade as shown by the higher pavement life obtained from the pavement as demonstrated in Figure 6-12. However, BSM_RCA performs similarly to a typical BSM.

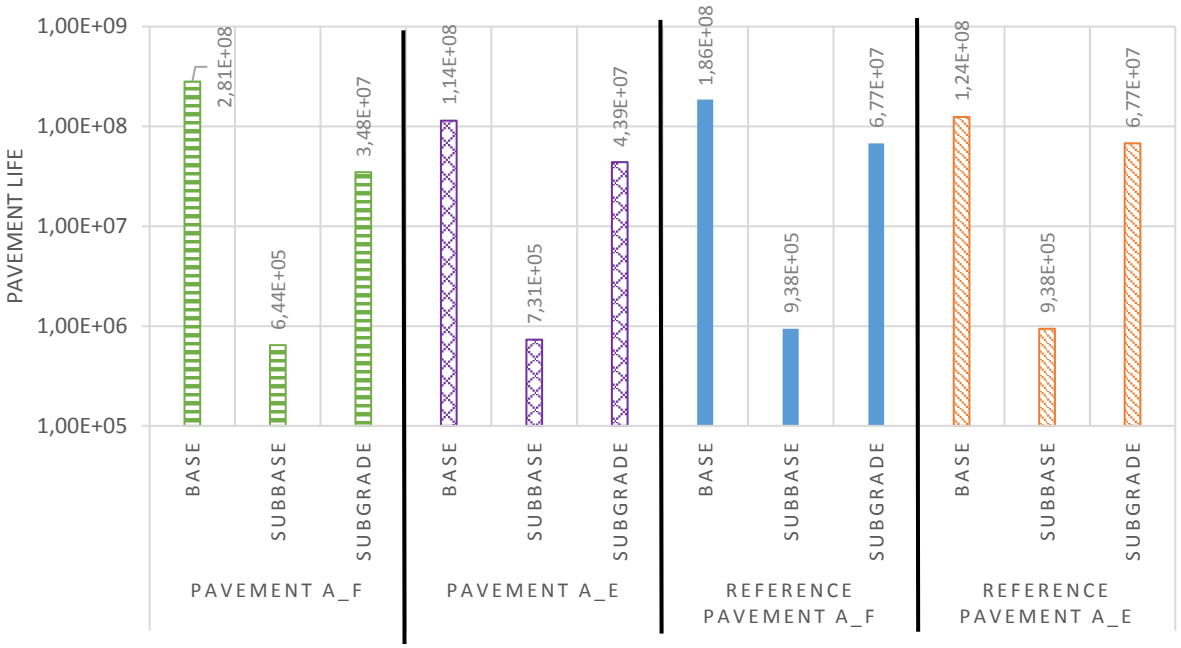

Figure 6-12: Pavement lives obtained for dry climate for Pavement Structures A

Pavement B

An overall analysis of the four pavement Structures with a C3 subbase show the importance of a good support for the BSM base as illustrated in Figure 6-13. All the pavement layers exceed the minimum and maximum required traffic loading for a Category B road. The subgrade is well protected as shown by the long pavement life that can be sustained by the layer demonstrated in Figure 6-13. The typical BSM bases as presented in the strain distribution provide a better protection of the subgrade due to the high strength obtained from the high bitumen content and added cement. Therefore, great benefit can be obtained from providing a good support for the BSM layer. Moreover, BSM_RCA is a comparable alternative to other typical BSMs used in the base layer.

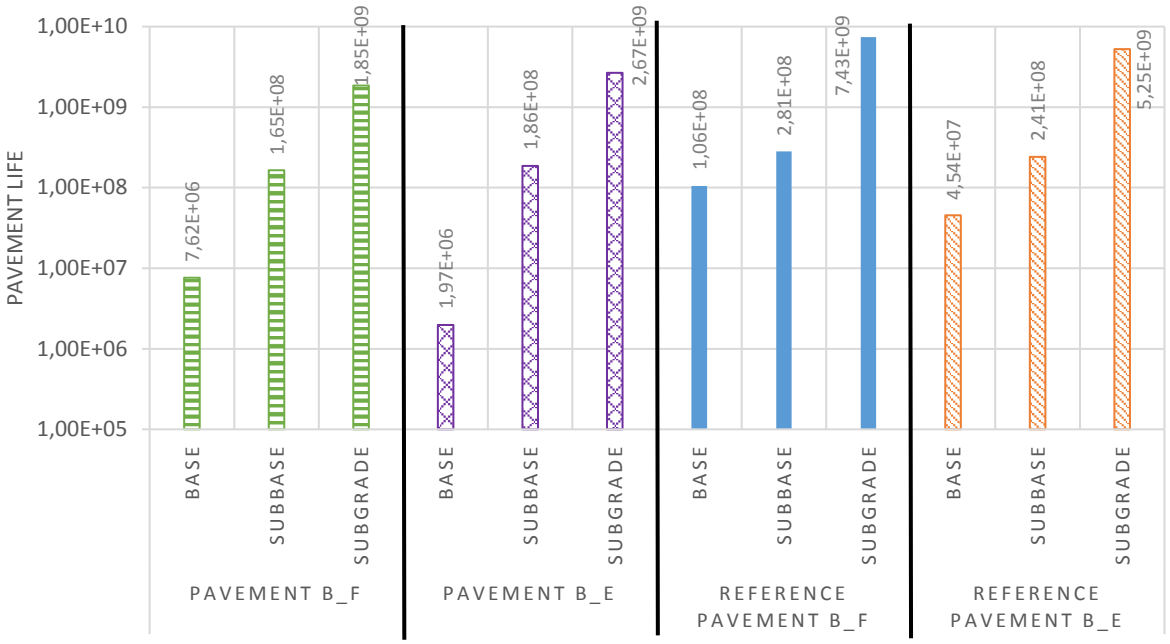

Figure 6-13: Pavement lives obtained for dry climate for Pavement Structures B

6.4 Practical Considerations

The use of RCA in a bitumen-stabilised material requires a good understanding of material mechanics. Although RCA has been shown to respond similarly to natural unbound granular materials, there are numerous considerations to be cognitive regarding its use. In the production of the BSM_RCA, preliminary challenges faced stemmed from the variability of the RCA from the source. A slight variation of the RCA mortar or contamination has an influence on the required optimum moisture content. Consequently, a variation in the moisture content leads to a variation in the bitumen content more especially bitumen emulsion and subsequently influences the quality of the mix.

Bitumen stabilised materials are reliant on the dispersion of the bitumen droplets provided by the filler content or active filler. However, the moisture content of the aggregate mix assists the filler or active filler to disperse the bitumen to the coarse aggregates. Therefore, control over the variation of the RCA aggregate contributes to a consistent mix with well-understood properties. The handling of RCA is well explained in Rudman (2019). The document outlines the required additional tests for RCA for a better understanding of the aggregate on site.

Once the preliminary physical properties of RCA are consistent, the application of the TG2 and SANS 3001 to produce a BSM mix are straightforward. However, pre-soaking is required to reduce the absorptivity of the aggregate during mixing with bitumen especially for mixes with bitumen emulsions. In addition, the specified minimum temperature of the

aggregates as required in the TG2 is applicable for RCA. The testing and structural capacity determination can be done in the same way as for typical BSMs though the mechanistic empirical method is a better option for the pavement life analysis.

6.5 Chapter Summary

The pavement life analysis of RCA stabilised with foamed bitumen and bitumen emulsion is presented in this chapter. The analysis aims to determine the structural capacity that can be achieved with the BSM_RCA used in a base layer of a Category B flexible pavement. The pavement lives obtained are compared to the pavement lives that can be achieved with a typical BSM mix composed of 20%RAP and 80% dolerite. The South African mechanistic empirical design method is used to conduct the analysis as guided by SAPME Chapter 10. The design method was used due to its flexibility to determine the pavement life of new pavement materials such as BSM_RCA. The chapter presents the transfer functions used to design unbound, bound and non-continuously bound pavement layers. The transfer functions for unbound and bound pavement layers are obtained from SAPME Chapter 10. Whereas, the transfer function used for the design of the non-continuously bound pavement layers is obtained from the new unpublished TG2. The Stellenbosch BSM function is used to determine the pavement lives of the BSM layers.

The process followed to determine the pavement lives required the definition of the pavement structures to be analysed, material properties of the layers within the pavement structure and the loading conditions. An 80 kN super single axles with 720 kPa tyre pressure is used for the analysis. Two types of pavement structures were analysed referred to as pavement Structure A and pavement Structure B. Structure A was selected to determine the pavement life that could be obtained for a system with a BSM base supported by G5 subbase. Pavement B enables a structure to be analysed with a BSM base supported by a cemented C3 subbase. The resilient modulus used for each of the four base layers from the different BSM mix designs was determined with three methods and the lowest resilient modulus was used in the analysis. The method used include the resilient modulus models for each mix design, the modular ratio concept and maximum allowable stiffness specified depending on the supporting subbase.

The pavement analysis shows that in general a BSM base requires a good supporting subbase. This conclusion is based on the pavement lives obtained for pavement Structure A that were dictated by the subbase designed for wet climate conditions. Pavement Structure B is most suitable for all BSM base layers. Although the typical BSM mixes

outperformed the BSM_RCA, comparable results were obtained. The practical consideration highlights the importance for understanding how to manage the variability that is inherent in the use of RCA. In addition, pre-soaking of the aggregates prior to stabilisation was critical for a good quality BSM mix with RCA. Therefore, RCA is suitable for use as BSM in a base layer for Category B road.

Chapter 7: Conclusion and Recommendations

The purpose of the current study was to determine the potential to stabilise recycled concrete aggregate (RCA) with foamed bitumen and bitumen emulsion to produce a bitumen stabilised material (BSM). A four-Phase process was followed to achieve the goal of the study.

- Phase 1: determined whether the preliminary physical properties of the RCA were suitable for stabilisation with bitumen as guided by the TG2.
- Phase 2: determined the optimum mix design from BSM mix designs produced to determine the suitable active filler and optimum binder content required and tested for the indirect tensile strength (ITS)
- Phase 3: measured the performance properties of the optimum mix design with the monotonic triaxial and dynamic triaxial tests. The performance properties measured include the shear parameters and the resilient modulus of optimum mix design. Additionally, resilient modulus models to describe the resilient modulus of the mixes were evaluated.
- Phase 4: determined the structural capacity of the optimum mix designs compared to that of a typical BSM supported by an unbound natural gravel and bound subbase.

The following conclusions can be drawn from the present study:

Preliminary physical properties outcomes

- A continuous grading was obtained with a two-stage crushing process. The grading meets the specified gradations required for a BSM with a filler content of 4.3% and a grading modulus of 2.56. Therefore, a simple crushing process can be used on RCA to obtain the required grading for a BSM mix.
- The RCA PI indicates the fine aggregates are non-plastic for a potential BSM 1 mix design.
- The maximum dry density of 1903 kg/m^3 and soaked CBR of 50% indicated a BSM 2 mix design could be produced. However, the shear parameters of the mix showed otherwise. Therefore, the aggregate performance properties are a better indicator of the potential BSM classification of the RCA.
- The pH of 12.32 and hygroscopic moisture content ranging between 2.3 and 2.96% have been found to be important factors in the mixing process of the aggregate.

Therefore, these properties should be tested prior to the production of a BSM for a good quality mix.

Recycle concrete was found to be a suitable aggregate for stabilisation with foamed bitumen and bitumen emulsion based on the preliminary aggregate physical properties required by the TG2.

Active filler and bitumen content outcomes

- The study has shown that no active filler is required to produce a potential BSM 1 mix design with either foamed bitumen or bitumen emulsion, when RCA aggregates are stabilised with bitumen.
- The suitable active filler results show that the addition of lime or cement increase the measured dry ITS and reduce the moisture susceptibility of the BSM mixes. Therefore, the BSM_RCA mix can benefit from the addition of active filler when required.
- A surprising finding from the study was the required bitumen content of 2.08% to produce a BSM 1 mix design. Therefore, this shows that the RCA does not absorb the bitumen added to the aggregates whilst still providing desired performance. This conclusion is based on the increase in ITS with an increase in the bitumen content.
- An increase of the bitumen content increases the flexibility of the BSM mix, which increases durability. This was observed from the increase in the strain at break and wet ITS of the mixes.

The production of a BSM with RCA guided by the SANS 3001 specification was suitable however, the sourcing and processing of RCA should be done as guided by Rudman (2019).

Performance properties and pavement life

- The measured shear parameters for the foamed bitumen and bitumen emulsion mix designs indicate that a potential BSM 1 can be produced from BSM_RCA mixes. Therefore, the addition of low viscosity bitumen improved the performance properties of the RCA and produced a comparable BSM to other typical BSMs.
- Two different resilient modulus models best fitted the resilient modulus obtained for the mixes with either foamed bitumen or bitumen emulsion. Therefore, this indicates that there is a difference in the response of each mix design to repeated loading.
- The pavement life analysis shows that the shear parameters have the greatest influence on the resultant pavement life. The foamed bitumen mix design

outperformed even the typical BSM placed in the base layer of a pavement structure placed on a stiff support.

- The pavement life analysis shows that the most benefit is obtained from a BSM if it is built on a stiff support in order to provide a holistic protection of the supporting layers. Therefore, the BSM_RCA produced in this research can be placed in a base layer for a Category B flexible pavement structure.

Recommendations

It is recommended that further research be undertaken in the following areas:

- The influence of an improved gradation on the performance of the BSM mix design, for example a higher filler content.
- Produce BSM mixes designs from different RCA sources and compositions with masonry to determine the required active filler and optimum bitumen content.
- Produce a BSM with RCA and natural granular material to determine feasibility of the mix composition.
- Determine the influence of the aggregate's pH on the resultant BSM classification or requirement for suitable active filler.
- Mixes with varying active filler should be produced to determine the influence of increasing the active filler on the measured dry and wet ITS.
- Determine if there is a relationship between the increases of filler content and the required bitumen content for this aggregate.
- Produce a BSM from a cationic slow setting bitumen emulsion to determine feasibility.
- The effect of the self-cementation should be measured to determine how long the BSM mix would self-cement and increase the cohesion of the mix.
- The permanent deformation of the BSM_RCA would provide a further understanding of the behaviour of the material under long term loading.

There is potential for versatile uses of recycled concrete aggregate in the pavement structure.

Bibliography

Addis, B. 1998. *Fundamentals of concrete*. G. Owens (ed.). Midrand, South Africa: Cement and Concrete Institute.

Alexander, M., Beushausen, H.-D., Amtsbuchler, R., Cairns, J. & Ballim, Y. 2009. *Fulton's Concrete Technology*. Ninth ed. G. Owens (ed.). Midrand, South Africa: Cement and Concrete Institute.

Araya, A.A. 2011. Characterization of Unbound Granular Materials for Pavements. IHE/TUDelft.

Ardalan, N., Wilson, D.J. & Larkin, T.J. 2016. AN EVALUATION OF RESEARCHE UNDERTAKEN ON RECYCLED CONCRETE AGGREGATES IN ROAD CONSTRUCTION. In Auckland *IPENZ Transportation Group Conference*. 8.

Arnold, G. & Arnold, D. 2008. Rut depth prediction of granular pavements using the repeated load triaxial apparatus and application in New Zealand specifications for granular materials. In N.T. Ed Ellis, Hai-Sui Yu, Glenn McDowell, Andrew R. Dawson (ed.). Nottingham, UK *Advances in Transportation Geotechnics*. 65–71.

Arnold, G.A., Dawson, A.R., Hughes, D.A.B. & Robinson, D. 2002. Serviceability design of granular pavement materials. In Lisbon, Portugal *Proc., 6th Int. Conf …*. 1–18. [Online], Available: http://www.repeatedloadtriaxial.co.nz/cms/uploads/RLTT/ARNOLD and DAWSON BCRA 2002.pdf.

Arshad, M. & Ahmed, M.F. 2017. Potential use of reclaimed asphalt pavement and recycled concrete aggregate in base / subbase layers of flexible pavements. *Construction and Building Materials*. 151:83–97.

van As, S.C. 2008. *Applied statistics for Civil Engineers*.

Asphalt Academy. 2009. *Technical Guideline:A guideline for the Design and Construction of Bitumen Emulsion and Foamed bitumen stabilised Materials.* Second Edi ed. D. Collings, J. Grobler, M. Hughes, K. Jenkins, F. Jooste, F. Long, & H. Thompson (eds.). Pretoria: Asphalt Academy.

Asphalt Academy unpublished. 2020. *Technical Guideline: Bitumen Stabilised materials*. Third Edit ed. D. Collings, J. Grobler, M. Hughes, K. Jenkins, F. Jooste, F. Long, & H. Thompson (eds.). Pretoria, South Africa: Asphalt Academy.

Van Aswegen, E. 2013. Effect of density and moisture content on the resilient modulus of

unbound granular material.

Barisanga, F. 2014. Material Characterisation and Response Modelling of Recycled Concrete and Masonry in Pavements. Stellenbosch University.

Barksdale, R.D. & Itani, S.Y. 1989. Influence of aggregate shape on base behaviour. *Transportation Research Board*. (1227):171–182.

Barksdale, R.D., ALBA, J., Khosla, N.P., Kim, R., Lambe, P.C. & Rahman, M.S. 1997. *LABORATORY DETERMINATION OF RESILIENT MODULUS FOR FLEXIBLE PAVEMENT DESIGN*. [Online], Available: https://trid.trb.org/view/488108 [2018, August 05].

Barnes, K. & Rudman, C. 2016. IN BUILDERS ' RUBBLE THROUGH UPTAKE IN ROAD REHABILITATION AND CONSTRUCTION. In *80th IMESA Conference East London*. 110–114.

Behiry, A. & El-Maaty, E.A. 2013. Utilization of cement treated recycled concrete aggregates as base or subbase layer in Egypt. *Ain Shams Engineering Journal*. 4(4):661–673.

Boateng, J.A., Paige-Green, P. & Mgangira, M. 2009. Evaluation of Test methods for estimating resilient modulus of pavement Geomaterials. *Proceedings of the 28th southern African Transference*. (ISBN : 978-1-920017-39-2).

Boudlal, O. & Melbouci, B. 2009. Study of the behaviour of aggregates demolition by the Proctor and CBR tests. In *GeoHunan International Conference*. 75–80.

Bredenkamp, Z. 2018. The performance properties of recycled concrete in road pavement materials. Stellenbosch Univeristy.

Brown, R.H. & Marek, C.R. 1996. *Effect of crusher operation on coarse aggregate shape*. United States.

Brown, S.F. & Chan, F.W.. 1996. Reduced rutting in unbound granular pavement layers through improved grading design. *Proceedings of the institution of civil engineers: Transport*. 117:315.

Campher, L. 2015. SHRINKAGE AND FLEXIBILITY BEHAVIOUR OF BITUMEN STABILISED MATERIALS. Stellenbosch University.

Cary, C.E. & Zapata, C.E. 2011. Resilient Modulus for Unsaturated Unbound Materials. *Road Materials and Pavement Design*. 12(3):615–638.

Christopher, B.R., Schwartz, C.P.E. & Boudreau, R. 2006. *Geotechnical aspects of*

pavements. US Woodbury. [Online], Available: http://scholar.google.com/scholar?hl=en&btnG=Search&q=intitle:Geotechnical+Aspects+of+Pavements#1.

Cleghorn, A. 2015. The Self-Cementing Performance Properties of Recycled Concrete Aggregates in Road Pavements. Stellenbosch University.

Collings, D. & Jenkins, K. 2011. The Long-term Behaviour of Bitumen Stabilised Materials (BSMs). In *10th Conference on Asphalt Pavements for Southern Africa*. 1–14.

Collings, D.C. & Jenkins, K.J. 2009. Key characteristics of materials stabilised with foamed bitumen. *Advanced Testing and Characterisation of Bituminous Materials, Vols 1 and 2*. 1161–1168.

Cook, C. 2015. Effects of Particle Shape on Performance and Durability of Aggregates Used in Road Construction. George Mason University. [Online], Available: http://digilib.gmu.edu/jspui/bitstream/handle/1920/9933/CookCl_thesis_2015.pdf?sequence=1&isAllowed=y.

Craig, R.F. 2013. *Craig's Soil Mechanics*. Vol. 53.

Croney, D. & Croney, P. 1998. *The design and performance of road pavements*. 3rd ed. ed. New York, N.Y.: McGraw-Hill.

DalBen, M.D. & Jenkins, K.J. 2014. Performance of cold recycling materials with foamed bitumen and increasing percentage of reclaimed asphalt pavement. *Road Materials and Pavement Design*. 15(2):348–371.

Van Dam, T., Smith, K., Truschke, C. & Vitton, S. 2011. *Using Recycled Concrete in MDOT ' s Transportation Infrastructure — Manual of Practice*. Houghon.

Dr Rudman, C. & Prof Jenkins, K. 2019. *Granular Materials- Graded Crushed Stone Transportation Science 434*.

Ebels, L. 2008. CHARACTERISATION OF MATERIAL PROPERTIES AND BEHAVIOUR OF COLD BITUMINOUS MIXTURES. (March).

Ebels, L.J. 2007. Characterization of bitumen stabilised granular pavement material properties using tri-axial testing. *Africa*. (June):607–618.

Ebels, L.-J. & Jenkins, K. 2007a. Characterization of Bitumen Stabilised Granular Pavement Material using Tri-axial Testing.

Ebels, L.-J. & Jenkins, K.J. 2007b. Mix design of bitumen stabilised materials: Best practice

and considerations for classification. *Proceedings of the 9th Conference on ….* (September):213–232. [Online], Available: http://www.researchgate.net/profile/Lucas_Jan_Ebels/publication/268395132_MIX_DESIGN_OF_BITUMEN_STABILISED_MATERIALS_BEST_PRACTICE_AND_CONSIDERATIONS_FOR_CLASSIFICATION/links/5536290f0cf268fd001612a7.pdf.

Ebels, L.-J. & Jenkins, K.J. 2007c. Mix design of bitumen stabilised materials: Best practice and considerations for classification. In Gaborone, Botswana *Proceedings of the 9th Conference on Asphalt Pavements for Southern Africa (CAPSA'07)*. 213–232.

Ebels, L.J. & Jenkins, K.J. 2006. Determination of Material Properties of Bitumen Stabilised Materials using Tri-axial Testing. In Québec City, Canada *10th International Conference on Asphalt Pavements*. 12–17.

Fatemi, S. & Imaninasab, R. 2016. Performance evaluation of recycled asphalt mixtures by construction and demolition waste materials.

Fazhou, W., Yumpeng, L. & Shuguang, H. 2013. Effect of early cement hydration on the chemical stability of asphalt emulsion. *Construction and Building Materials*. 42:146–151.

Fenton, M. 2013. FLEXIBILITY ASSESSMENT OF BITUMEN STABILISED MATERIALS. Stellenbosch University.

Gomez-Meijide, B. & Perez, I. 2015. Nonlinear elastic behavior of bitumen emulsion-stabilized materials with C & D waste aggregates. *Construction and Building materials*. 98:853–863.

Gomez-Meijide, B. & Perez, I. 2016. Binder-aggregate adhesion and resistance to permanent deformation of bitumen-emulsion-stabilized materials made with construction and demolition waste aggregates. *Journal of Cleaner Production*.

Gomez-Meijide, B., Perez, I. & Pasandín, A.R. 2016. Recycled construction and demolition waste in Cold Asphalt Mixtures: evolutionary properties. *Journal of Cleaner Production*. 112:588–598.

Gómez-Meijide, B. & Pérez, I. 2013. Effects of the use of construction and demolition waste aggregates in cold asphalt mixtures. *Construction and Building Materials*. 51:267–277.

Gómez-Meijide, B. & Pérez, I. 2015. Nonlinear elastic behavior of bitumen emulsion-stabilized materials with C&D waste aggregates. *Construction and Building Materials*.

Gómez-Meijide, B., Pérez, I., Airey, G. & Thom, N. 2015. Stiffness of cold asphalt mixtures with recycled aggregates from construction and demolition waste. *Construction and Building Materials*. 77:168–178.

Hoff, I., Bakløkk, L.J. & Aurstad, J. 2004. Influence of laboratory compaction method on unbound granular materials. In A.R. Dawson (ed.). Nottingham: Leiden *6th International Symposium on Pavements Unbound*. 1–11.

Huang, Y.H. 2003. Pavement Analysis and Design. *Pearson*. 792.

Hunter, R.N. 1994. *Bituminous Mixtures in road construction*. 1st ed. R.N. Hunter (ed.). London: Thomas Telford Services Ltd.

Iwański, M. & Chomicz-Kowalska, A. 2013a. Laboratory study on mechanical parameters of foamed bitumen mixtures in the cold recycling technology. *Procedia Engineering*. 57:433–442.

Iwański, M. & Chomicz-Kowalska, A. 2013b. Laboratory study on mechanical parameters of foamed bitumen mixtures in the cold recycling technology. *Procedia Engineering*. 57:433–442.

Janoo, V.C. 1998. *Quantification of shape, angularity, and surface texture of base course materials*. Hanover NH.

Jenkins, K. 2000. Mix design considerations for cold and half-warm bituminous mixes with emphasis on foamed bitumen. Stellenbosch University.

Jenkins, K.J. & Collings, D.C. 2017. Mix design of bitumen-stabilised materials – South Africa and abroad. *Road Materials and Pavement Design*. 18(2):331–349.

Jenkins, K.J. & Yu, M. 2009a. Cold-Recycling Techniques Using Bitumen Stabilization: Where Is This Technology Going? In Reston, VA: American Society of Civil Engineers *Road Pavement Material Characterization and Rehabilitation*. 191–200.

Jenkins, K.J. & Yu, M. 2009b. Cold-Recycling Techniques using Bitumen Stabilisation: Where is this technology going? In Changsha, China *GeoHunan International Conference*.

Jenkins, K.J., Molenaar, A.A.A., De Groot, J.L.A. & Van De Ven, M.F.C. 2000. Developments in the uses of foamed bitumen in road pavements. *Heron*. 45(3):167–176.

Jenkins, K.J., van de Ven, M., Molenaar, A.A.A. & de Groot, J. 2002. Performance Prediction

of Cold Foamed Bitumen Mixes. In Copenhagen, Denmark *Ninth International Conference on Asphalt Pavements*. 1–16.

Jenkins, K.J., Long, F.M. & Ebels, L.J. 2007. Foamed bitumen mixes = Shear performance? *International Journal of Pavement Engineering*. 8(2):85–98.

Jenkins, K.J., Twagira, M.E., Kelfkens, R.W. & Mulusa, W.K. 2012. New laboratory testing procedures for mix design and classification of bitumen-stabilised materials. *Road Materials and Pavement Design*. 0629(November).

Jordaan, G. & Kilian, A. 2016. the Cost-Effective Upgrading , Preservation and Rehabilitation of Roads – Optimising the Use of Available Technologies. (Satc):61–76.

Kashaya, A.A. 2013. SURFACE RUN-OFF BEHAVIOUR OF BITUMEN EMULSIONS USED FOR THE CONSTRUCTION OF SEALS. Stellenbosch.

Kelfkens, R.W.C. 2008. VIBRATORY HAMMER COMPACTION OF BITUMIN STABILIZED MATERIALS. Stellenbosch University.

Kendall, M., Baker, B., Evans, P., Ramanujam, J. & Ntroduction, I. 1999. Foamed Bitumen Stabilisation. In Queenlands *Symposium A Quarterly Journal In Modern Foreign Literatures*. 1–18.

Kisku, N., Joshi, H., Ansari, M., Panda, S.K., Nayak, S. & Dutta, S.C. 2017. A critical review and assessment for usage of recycled aggregate as sustainable construction material. *Construction and Building Materials*. 131:721–740.

Koper, A., Koper, W. & Koper, M. 2017. Influence of raw concrete material quality on selected properties of recycled concrete aggregates. *Procedia Engineering*. 172:536–543.

Leite, C., Motta, S., Vasconcelos, K.L. & Bernucci, L. 2011a. Laboratory evaluation of recycled construction and demolition waste for pavements. *Construction and Building Materials*. 25:2972–2979.

Leite, F.D.C., Motta, R.D.S., Vasconcelos, K.L. & Bernucci, L. 2011b. Laboratory evaluation of recycled construction and demolition waste for pavements. *Construction and Building Materials*. 25(6):2972–2979.

Lekarp, F., Isacsson, Ui. & Dawson, A. 2000. State of the Art. I: Resilient Response of unbound aggregates. *Journal of Tr*. 3(1):3–46.

Lewis, T., Myburgh, P., Paige-Green, P., Perrie, B., Wright, D. & van Zyl, G. 2013. South

African Pavement Engineering Manual: Chapter 3 Materials Testing. In 2nd ed. D.F. Johns (ed.) *SAPEM*. 1–100.

Limbachiya, M.C., Marrocchino, E. & Koulouris, A. 2007. Chemical-mineralogical characterisation of coarse recycled concrete aggregate. *Waste Management*. 27(2):201–208.

Loizos, A. 2007. In-situ characterization of foamed bitumen treated layer mixes for heavy-duty pavements. *International Journal of Pavement Engineering*. 8(2):123–135.

Long, F. & Theyse, H. 2004. Mechanistic-Empirical Structural Design Models for Foamed and Emulsified bitumen treated materials. In Vol. 1. Pretoria *8th Conference on asphalt pavements for Southern Africa*. 1–19.

mahdi, zaid. 2017. Evaluation of Using the Crushed Concrete Aggregate as Unbound Pavement Layer. *Journal of Babylon University/Engineering Sciences/ No*. 25(4).

Marais, C.P. & Tait, M.I. 1989. PAVEMENTS WITH BITUMEN EMULSION TREATED BASES: PROPOSED MATERIAL SPECIFICATIONS, MIX DESIGN CRITERIA AND STRUCTURAL DESIGN PROCEDURES FOR SOUTHERN AFRICAN CONDITIONS. In Swaziland: CAPSA *5TH CONFERENCE ON ASPHALT PAVEMENTS FOR SOUTHERN AFRICA*. 26–35.

Marradi, A. & Lancieri, F. 2008. Performance of Cement Stabilized Recycled Crushed Concrete. In Beijing *4th International Conference Bituminous Mixtures and Pavements*. 1–10.

Meyer, M.D. 1999. *Bitumen emulsion Technical Bulletin*. [Online], Available: https://sc.akzonobel.com/en/asphalt/Documents/AN_Asphalt_Emulsion_TB_eng.pdf.

Molenaar, A.A.A. 2007. Design of flexible pavement, lecture note CT 4860 structural pavement design. *Delft University of Technology, Delft the Netherlands*. (March).

Molenaar, A.A.A. 2010. *Cohesive and non-cohesive soils and unbound granular materials for bases and sub-bases in roads*.

Mollenhauer, K., Simnofske, D., Valentin, J., Čížková, Z. & Suda, J. 2016. Mix designs for cold recycled pavement materials considering local weather and traffic conditions. In Prague, Czech Republic *6th Eurasphalt and Eurobitume Congress*.

Moloto, P. 2010. Accelerated curing protocol for bitumen stabilized materials. Stellenbosch University.

Mulusa, W.K. 2009. Development of a Simple Triaxial Test for Characterising Bitumen Stabilised Materials.

Nataatmadja, A. & Tan, Y.. 2001a. Resilient response of Recycled Concrete Road Aggregates. *Journal of Transportation engineering*. (September October):450–453.

Nataatmadja, A. & Tan, Y.. 2001b. Resilient response of recycled concrete road aggregates. *Journal of Transportation engineering*. 127(October):450–453.

Van Niekerk, A.A. 2002. Mechanical Behaviour and Performance of Granular Bases and Subbases in Pavements. Delft University of Technology.

Nwando, A. 2013. Flexibility and Performance Properties of Bitumen Stabilised materials. Stellenbosch University.

Oikonomou, N.D. 2005. Recycled concrete aggregates. *Cement and Concrete Composites*. 27(2):315–318.

Paige-Green, P. 1999. A comparative study of the grading coefficient , a new particle size distribution. *Bulletin of Engineering Geology and the Environment*. 57(3):215–223.

Paige-Green, P. 2010. A Preliminary Evaluation of the Reuse of Cementitious Materials. *29th Southern African Transport Conference (SATC 2010)*. 0001(August):520–529.

Pasandín, A.R. & Pérez, I. 2015. Overview of bituminous mixtures made with recycled concrete aggregates. *Construction and Building Materials*. 74:151–161.

Pickel, D. 2014. Recycled concrete aggregate: influence of aggregate pre-saturation and curing conditions on the hardened properties of concrete. 189.

Polat, R., Yadollahi, M.M., Sagsoz, A.E. & Arasan, S. 2013. The Correlation between Aggregate Shape and Compressive Strength of Concrete. *International Journal of Structural and Civil Engineering Research*. 2(3):62–80.

Poon, C.S. & Chan, D. 2006. Feasible use of recycled concrete aggregates and crushed clay brick as unbound road sub-base. *Construction and Building Materials*. 20(8):578–585.

Richardson, D.N. 2005. *Aggregate Gradation Optimization - Literature Search*. Missouri. [Online], Available: http://library.modot.mo.gov/RDT/reports/Ri98035/RDT05001.pdf.

Ronald, W., Thomas, H. & Kennedy, W. 1968. *An indirect tensile test for stabilized materials*. Texas. [Online], Available: https://library.ctr.utexas.edu/digitized/texasarchive/phase1/98-1-chr.pdf [2019, January

10].

Rudman, C.E. 2019a. Aspects of Self-cementing when applied in Roads (draft thesis). Stellenbosch University.

Rudman, C.E. 2019b. Aspects of Self - Cementation of Recycled Concrete Aggregate When Applied in Roads. Stellenbosch University.

Rudman, C.E. & Jenkins, K.. 2015. Self-Cementing Mechanisms of Recycled Concrete and Masonry Aggregate. In Durban *Conference on Asphalt Pavements for Southern Africa*.

Saeed, A. & Hammons, M. 2008. Use of Recycled concrete as unbound base aggregate in airfield and highway pavements to enhance sustainability. *Airfield and highway Pavements*. 497–508.

Saleh, A.H. 2000. Stabilisation of Mix Granulate by using foamed Bitumen for use in Road pavements.pdf. International institute for infrastructural hydraulic and environmental engineering.

Saleh, M.F. 2006. Effect of aggregate gradation, mineral fillers, bitumen grade, and source an mechanical properties of foamed bitumen-stabilized mixes. *Geomaterials 2006*. 1952(1952):90–100.

Sánchez De Juan, M. & Gutierrez, A.P. 2009. INFLUENCE OF ATTACHED MORTAR CONTENT ON THE PROPERTIES OF RECYCLED CONCRETE AGGREGATE. *Construction and building materials*. 23:872–877. [Online], Available: http://congress.cimne.upc.es/rilem04/admin/Files/FilePaper/p346.pdf [2017, June 19].

SANRAL. 2014. *Chapter 3: Materials Testing*.

SAPEM, C. 2014. *South Afican Pavement Engineering Manaul - Chapter 10*.

Schultz, R. 2015. *What Do "Sustainable Construction" and "Green Building" Really Mean?* [Online], Available: http://blog.winkbuild.com/blog/what-do-sustainable-construction-and-green-building-really-mean [2018, April 12].

Sharma, G., Vaishnav, G., Khanna, I. & Jaiman, M. 2016. A Review on use of industrial waste in sub base of flexible pavement. *SSRG International Journal of Civil Engineering (SSRG-IJCE)*. 3(5):256–261.

Strauss, P.J. & Van der Walt, N. 1989. STRESS ABSORBING MEMBRANES AND FLEXIBLE ASPHALT OVERLAYS TO PREVENT REFLECTION CRACKING AT JOINTS OR CRACKS IN STIFF PAVEMENTS. In Swaziland: Executive Committee

CAPSA ’89 *5th Conference on Asphalt Pavements for Southern Africa*. [Online], Available: https://trid.trb.org/view.aspx?id=354476 [2018, August 21].

Sweere, G.T.. 1990. Unbound granular bases for roads. Technical University of Delft.

Talbot, A. & Richart, F.K. 1923. *The strength of concrete its relation to the cement aggregates and water*.

Theyse, H.L. 2002. *Stiffness, Strength, and Performance of Unbound Aggregate Materials: Application of South African HVS and Laboratory Results to California Flexible Pavements. Report produced under the auspices of the California Partnered Pavement Research Program for the*. Pretoria, South Africa.

Theyse, H.. & Muthen, M. 1994. *PAVEMENT ANALYSIS AND DESIGN SOFTWARE (PADS) BASED ON THE SOUTH AFRICAN MECHANISTIC-EMPIRICAL DESIGN METHOD H L THEYSE and M MUTHEN*. Pretoria, South Africa.

Theyse, H.., De Beer, M. & Rust, F.. 1996. Overview of South African Mechanistic Pavement Design method. *Transportation Research Record*. (1):6–17.

Thom, N. 2008. *Principles of pavement engineering*. 1st Editio ed. London: Thomas Telford.

Thorn, N.. & Brown, S.. 1989. The mechanical properties of unbound aggregates from various sources. In *International Symposium on Unbound Aggregates in Roads*. 130–142.

Twagira, E.M. 2010. Influence of Durability Properties on Performance of Bitumen Stabilized Materials. University of Stellenbosch.

Twagira, M.E. & Jenkins, K.J. 2009. Moisture damage on bituminous stabilized materials using a MIST device. In Rhodes, Greece *7th International RILEM Symposium ATCBM09*. 1–10.

Valentin, J., Suda, J., Batista, F., Mollenhauer, K. & Simnofske, D. 2016. Stiffness characterization of cold recycled mixtures. 14:758–767.

Weinert, H.H. 1980. *The natural road construction materials of southern africa*. Pretoria: National institute for transport and road research.

Wirtgen Group. 2012. *Wirtgen Cold Recycling Technology Manual*. 1st Editio ed. Windhagen, Germany.

Wirtgen Group. 2017. *BSM Cold Recycling Laboratory Handbook*. 1st Editon ed. Windhagen, Germany: Wirtgen.

Yan, J., Ni, F., Yang, M. & Li, J. 2010. An experimental study on fatigue properties of emulsion and foam cold recycled mixes. *Construction and Building Materials*. 24(11):2151–2156.

Yang, N.C. 1972. *Design of functional pavements.* New York, N.Y.: McGraw-Hill.

Yang, D., Hao, Y. & Wang, T. 2010. Experimental research on recycled aggregate concrete for highway pavement. In H. Wei, Y. Wang, J. Rong, & J. Weng (eds.). Beijing, China: American Society of Civil Engineers *10th International Conference of Chinese Transportation Professionals (ICCTP)*. 2913–2919.

Yoder, E.J. (Eldon J. 1975. *Principles of pavement design*. 2nd ed. ed. New York, N.Y.: John Wiley and Sons.

Zhang, J., Shi, C., Li, Y., Pan, X., Poon, C.S. & Xie, Z. 2015. Influence of carbonated recycled concrete aggregate on properties of cement mortar. *Construction and Building Materials*. 98(August):1–7.

Zhao, Z., Remond, S., Damidot, D. & Xu, W. 2013. Influence of hardened cement paste content on the water absorption of fine recycled concrete aggregates. *Journal of Sustainable Cement-Based Materials*. 2(3–4):186–203.

Van Zyl, E.B. 2015. Influence of Specimen Geometry and Grading Curve on the Performance of an Unbound Granular Material. University of Stellenbosch.

Appendix A

Resilient modulus vs Bulk stress for repeat specimen

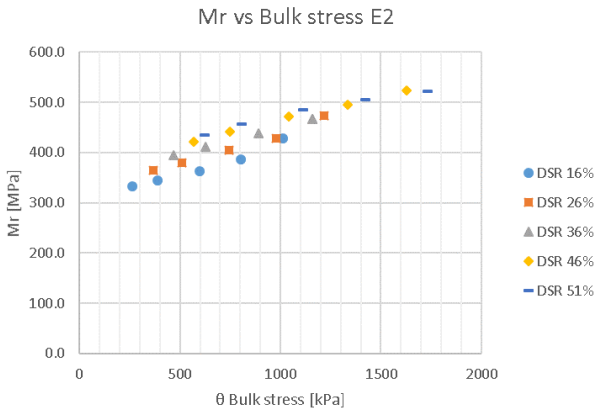

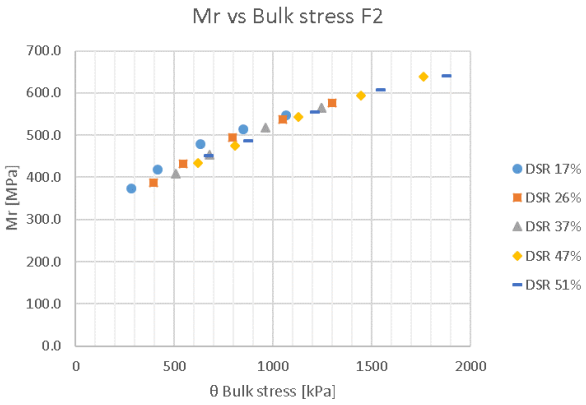

Resilient modules models of the repeat specimen